Minor planet astrophotometry

Thesis

The Open University

Minor Planet Astrophotometry

Gareth Vaughan Williams

A Thesis Submitted for the Degree of
Doctor of Philosophy

September 2012

Department of Physical Sciences
The Open University, UK

Date of Submission: 28 August 2012
Date of Award: 22 May 2013.

Abstract

Historically, the Minor Planet Center (MPC) has concentrated on improving the quality of the astrometric observations and the resulting orbits of minor planets. In light of long-standing complaints in the literature about the quality of the photometric parameters for the minor planets, there has been a need to improve the quality of the absolute magnitudes, H, and slope parameters, G. However, this task is complex, as the bulk of the minor-planet magnitude estimates are supplied by the astrometric observers. These observations are not made through standard filters and are made with respect to the (indifferent) magnitudes in numerous astrometric reference catalogues. Such magnitude estimates are labelled "astrophotometry", to reflect their low quality.

This thesis describes a method for correcting the catalogue- and observer-specific errors present in the astrophotometry. This method was applied to more than 70 million astrometric observations with magnitude estimates.

New H determinations have been made for 322 607 numbered minor planets, while new G determinations have been made for 64 348 numbered minor planets. New assumed G values have been determined for 258 259 numbered minor planets. Analysis of the results shows that the problems identified in the literature have been removed, particularly the –0.5 magnitude offset at $H \approx 14$ that is present in the current MPC HG data set. Implications of the new H magnitudes on the albedos determined by the WISE space mission and on the differential H distributions of various types of solar-system object are discussed.

Acknowledgements

When I first became interested in astronomy in the early 1970s, the study of minor planets was very much a backwater of solar-system research and there was very little information on these bodies in the popular literature. In primary school, my interest in minor planets lay in nomenclature issues, principally their names. I collected a large number of names from various astronomical books and wrote them in a note book, along with dates of discovery and names of discoverers. Even at that young age, I recall noting differences in the dates of discovery and spelling of names between different sources. In secondary school, my principal interest shifted to minor-planet (and comet) dynamics, initially ephemeris computations, then orbit computations. Shortly after joining the British Astronomical Association (BAA) in 1979, I ran across a famous name for the first time: Brian Marsden. I was intrigued by his remark on *BAA Circular* 601 (taken from *IAU Circular* 3440) regarding the suggestion by David Herald that the recently-discovered comet C/1979 M1 (Bradfield) = 1979 X = 1979l was identical to comet C/1771 A1 (Great Comet) = 1770 II. Brian did not think that the identification was correct, a supposition that was confirmed on *BAA Circular* 602 (taken from *IAU Circular* 3442) when he wrote "identity with 1770 II does not seem possible". I wanted to understand the process that had led him to this conclusion. I had learned to calculate ephemerides and compute orbits and perturbations using a calculator, pen and paper. (I may be the youngest person in the world whose *first* orbital integration was undertaken manually, writing out the difference tables on large sheets of paper!) The obvious next step was to take advantage of the blossoming microcomputer revolution that was underway in the U.K. at that time and write computer programs to do the calculations. My first computer was a BBC Model B with 32K main RAM and 16K "sideways" RAM. I wrote an orbit integration program (in BBC BASIC with some 6502 assembler handling the reading of the planetary coordinates from the sideways RAM) for that machine that could integrate an orbit from one epoch to another, including the perturbing effects of Jupiter, Saturn, Mars and Earth. The program *and* the planetary coordinates fit in the 48K RAM. Descendants of that program, re-written (and expanded) in Fortran at college, allowed me to undertake a final-year project entitled "Identification of Minor Planets", which I sent, following the suggestion of my adviser, to Brian for comment. His response was quick and positive, and I had the opportunity to meet with him briefly a month or so later at a BAA meeting. Our exchange of letters over the next two years made Brian think that I might be a good candidate for a vacancy at the Minor Planet Center that arose at the end of 1989 following the retirement of Conrad Bardwell. I am honoured by the trust that Brian placed in my abilities in orbital matters and computer programming, and I am humbled that I was able to work with him for almost 21 years.

For my thesis work, I wanted to avoid a dynamical investigation, as these tend to be very theoretical, with little practical application to my work at the Minor Planet Center. Since I would have to juggle a very demanding job with my thesis work, it was important that the work be of practical use to me (and the Minor Planet Center). The idea of working with and improving the photometry reported with the astrometry had obvious practical implications for my professional work and was thus an obvious avenue for a research topic. I am gratified that the Open University agreed to allow me to undertake this graduate work, and that I was permitted to do it remotely.

It would not have been possible to complete the work presented in this thesis while working full-time without the easy-going support offered by my advisers: Simon Green, Neil McBride and Stephen Wolters for the Open University; and Brian Marsden and Timothy Spahr as my local advisers.

Thanks are also due to the following individuals (in no particular order and with my sincere apologies for any inadvertent omissions): Will Graves, Michael Blake and Maria McEachern in the Wolbach Library for assistance in tracking down old publications and external theses; Donna Coletti, former head of the Wolbach Library, who entrusted me with a key to the locked book stacks containing the fragile observatory publications; José Luis Galache, for critiquing drafts of this document; Michael Rudenko, for advice about MySQL implementations and Ruby; Maik Meyer, who produced excellent English translations of numerous important historical German-language papers; Brian D. Warner, for supplying a gratis copy of his Canopus software; Herbert Raab, for a gratis copy of his Astrometrica software; Claes-Ingvar Lagerkvist, Uppsala Observatory, for supplying a CD-ROM of the raw data files from the Asteroid Photometric Catalogue; Carolyn Stern-Grant, for enabling early access to the raw OCRed text of articles from the Astrophysics Data System Bibliographic Services; Jessica Mink, for enabling access to astrometric catalogues removed from the servers at the Center for Astrophysics (CfA); J. Scott Stuart, Jim Scotti, Jeff Larsen and Ed Beshore for supplying information on the magnitude-reduction procedures used by their respective surveys; and William Wyatt, for maintaining the CfA's local copy of the Sloan Digital Sky Survey's databases.

This research has made extensive use of the following data sources:

- The Astrophysics Data System Bibliographic Services (ADS) (`http://adsabs.harvard.edu`)
- The Sloan Digital Sky Survey (SDSS)

"Funding for the SDSS and SDSS-II has been provided by the Alfred P. Sloan Foundation, the Participating Institutions, the National Science Foundation, the U.S. Department of Energy, the National Aeronautics and Space Administration, the Japanese Monbukagakusho, the Max Planck Society, and the Higher Education Funding Council for England. The SDSS Web Site is `http://www.sdss.org/`.

The SDSS is managed by the Astrophysical Research Consortium for the Participating Institutions. The Participating Institutions are the American Museum of Natural History, Astrophysical Institute Potsdam, University of Basel, University of Cambridge, Case Western Reserve University, University of Chicago, Drexel University, Fermilab, the Institute for Advanced Study, the Japan Participation Group, Johns Hopkins University, the Joint Institute for Nuclear Astrophysics, the Kavli Institute for Particle Astrophysics and Cosmology, the Korean Scientist Group, the Chinese Academy of Sciences (LAMOST), Los Alamos National Laboratory, the Max-Planck-Institute for Astronomy (MPIA), the Max-Planck-Institute for Astrophysics (MPA), New Mexico State University, Ohio State University, University of Pittsburgh, University of Portsmouth, Princeton University, the United States Naval Observatory, and the University of Washington."

- The Two Micron All-Sky Survey (2MASS)

  "This publication makes use of data products from the Two Micron All Sky Survey, which is a joint project of the University of Massachusetts and the Infrared Processing and Analysis Center/ California Institute of Technology, funded by the National Aeronautics and Space Administration and the National Science Foundation."

- SIMBAD

  "This publication has made use of the SIMBAD database, operated at CDS, Strasbourg, France"

- The Wide-field Infrared Survey Explorer (WISE)

  "This publication makes use of data products from the Wide-field Infrared Survey Explorer, which is a joint project of the University of California, Los Angeles, and the Jet Propulsion Laboratory/California Institute of Technology, funded by the National Aeronautics and Space Administration."

- NEOWISE

  "This publication also makes use of data products from NEOWISE, which is a project of the Jet Propulsion Laboratory/California Institute of Technology, funded by the Planetary Science Division of the National Aeronautics and Space Administration."

- VizieR (Ochsenbein *et al.*, 2000)
- The Asteroid Photometric Catalogue (APC)
- Babelfish
- Google Earth and Google Sky

Finally, the love and support of my wife, Cynthia, who cajoled me into finally undertaking this research, was essential in maintaining my sanity while juggling work and thesis. She also assisted with various data-entry jobs, assisted with my little observing program, proofread the thesis and served as a sounding-board to ensure that what I was writing didn't sound ridiculous.

What started as a four-year plan for completion turned into a seven-year odyssey, due to circumstances (some happy, some sad) beyond my control. But that is life...

It would be naive to think that there are no errors in this thesis. Any errors (either typographic or factual) are hopefully minor and are the sole responsibility of the undersigned.

Gareth Williams

2012 August 31

As you set out for Ithaca
hope that your journey is a long one,
full of adventure, full of discovery.

May there be many summer mornings when,
with what pleasure, what joy,
you come into harbours seen for the first time;
and may you visit many Egyptian cities
to learn and learn again from those who know.

Keep Ithaca always in your mind.
Arriving there is what you're destined for.

But do not hurry the journey at all.
Better if it lasts for years,
so that you are old by the time you reach the island,
wealthy with all you have gained on the way,
not expecting Ithaca to make you rich.

Ithaca gave you the marvellous journey.
Without her, you would not have set out.
She has nothing left to give you now.
And if you find her poor, Ithaca won't have fooled you.
Wise as you will have become, so full of experience,
you will have understood by then what these Ithacas mean.

Ithaca, music by Vangelis, excerpt of lyrics from the poem by Constantinos P. Cavafy
(translation from the original Greek)

Contents

List of Figures

List of Tables

1: Introduction

as·trom·e·try *n.* The scientific measurement of the positions and motions of celestial bodies. — **as′tro·met′ric** *adj.*
pho·tom·e·try *n. Physics.* The measurement of the properties of light, esp. of luminous intensity. — **pho′to·met′ric** *adj.* — **pho·tom′e·trist** *n.*

The American Heritage Dictionary, Second College Edition, 1982
Published by Houghton Mifflin Company

This thesis presents research work undertaken to understand the photometric estimates that are supplied with many of the astrometric observations of minor planets reported to the International Astronomical Union's Minor Planet Center, with the principal aim of improving our knowledge of the absolute magnitudes of the minor planets. The quality of this astrophotometry (a term used to distinguish it from the higher-quality traditional photometric observations) is rather poor, but it is possible to improve the quality by removing systematic catalogue-related and observer-related errors from the observations. Since the absolute magnitudes of most of the observed population of minor planets are derived solely from the astrophotometry, it is important to understand the biases and errors that are present in the astrophotometry. The results obtained are applied to a redetermination of the geometric albedos obtained by the NEOWISE mission.

Minor planets are minor members of the solar system, including asteroids and comets, as well as intermediate objects such as Trans-Neptunian Objects. The majority of known minor planets reside in the Main Belt (also known at the Asteroid Belt), which lies between the orbits of Mars and Jupiter, and are primarily rocky objects, although ices are present in objects in the outer belt (see, e.g., Hsieh and Jewitt, 2007). Another belt, the Kuiper Belt, containing a large population of icy minor bodies lies beyond the orbit of Neptune. Other populations of minor planets may be found orbiting in the same orbit as Mars, Jupiter or Neptune, or on planet-crossing orbits throughout the solar system. The minor planets were formed by the same processes that created the major planets (gradual accretion of larger particles from smaller particles via non-destructive collisions) but were prevented from growing to planetary size as a result of destructive collisions with other minor bodies. In the early solar system, the Asteroid Belt is believed to have contained about one Earth mass of material. The present-day Belt contains only ~ 5×10^{-4} Earth masses of material (Bottke *et al.*, 2005); much of the primordial mass present—believed to be one Earth mass or more (Bottke *et al.*, 2005)—in the Belt has been removed by gravitational perturbations from embryonic planetary bodies and Jupiter (Bottke *et al.*, 2005).

A good knowledge of the absolute magnitude of individual objects is important because, when combined with a measured or assumed albedo (reflectivity of the surface), the diameters of the objects may be obtained. Therefore, knowledge of the absolute magnitudes of a large set of objects leads to an observed size distribution, which can be debiased to remove observational selection effects (e.g., Spahr, 1998) to obtain the true size distribution. Knowledge of the true size distribution is important for understanding the formation and subsequent collisional and dynamical evolution of the minor planets. As the population of the Near-Earth Asteroids seems to be derived principally from the Main Belt population (e.g., Binzel, 1991), a knowledge of the latter's size distribution has implications for the size-frequency of earth impacts. With the increasing number of space missions to minor planets, we can now compare *in situ* diameter measurements to earth-bound measurements or estimates.

1.1: Thesis Contents Summary

A summary of each chapter's contents follows.

Chapter 1 provides some introductory remarks, a summary of the contents of the other chapters, a brief description of relevant organizations and my associations with them, and a list of symbols used in the thesis.

Chapter 2 [p. 11] introduces the topic that is being studied in the thesis, as well as giving relevant background. A basic knowledge of minor planets is assumed. The current *HG* system for predicting minor-planet magnitudes is described, along with a mention of historical magnitude systems. There is a brief discussion of alternative modern systems. A historical review of magnitude and phase effect studies, and the taxonomic classification of minor planets, is given.

Chapter 3 [p. 47] examines the procedures that will be used in this thesis. It describes how the catalogue systematic errors will be removed from the astrophotometry, how observer-specific systematic reduction errors will be handled, how the Minor Planet Center records which catalogues were used to reduce which observations, offers a brief review of relevant astrometric catalogues and details the default colour corrections and taxonomic classifications that will be applied.

Chapter 4 [p. 73] details the steps undertaken to prepare the special photometric catalogues of comparison stars that are needed to correct the systematic catalogue errors in the astrophotometry.

Chapter 5 [p. 93] examines the various sources of photometric data on minor planets: the astrophotometry associated with the seven big professional CCD minor-planet surveys, each of which is described briefly; the traditional photometric observations; and the observations derived from lightcurve observations.

Chapter 6 [p. 117] details the reduction procedures that are used to reduce the photometric observations. Details of the specific procedures used by some of the big professional CCD surveys to process their magnitude estimates are given.

Chapter 7 [p. 151] describes the steps involved in the iterative process that produces the corrected *HG* values, including the determination of the observer-specific corrections.

Chapter 8 [p. 161] presents summaries of the new *HG* determinations, along with a number of phase plots showing the general quality of the astrophotometric observations.

Chapter 9 [p. 167] analyses the *HG* results, comparing them to previous MPC values, noting historical "problem cases" and comparing some of the new *HG* determinations to values found in the recent literature. Application of the new *HG* values to the determination of new albedos for minor planets observed by the Wide-field Infrared Survey Explorer space mission is discussed.

Chapter 10 [p. 195] contains the summary of the research, the possibilities for further work and the concluding remarks.

The appendices [p. 211] contain a number of sections describing the designation systems for minor planets as well as various terms and historical journals referenced in this document. Also given are brief details on the data files that are accessible on the thesis website. Additional supporting material requested by the viva panel is also included.

The references [p. 251] document the papers examined during this research.

Where quotations have been given from foreign-language papers, the original language text is given first; the English translation is then given parenthetically.

1.2: Relevant Institutions

In this section I describe various institutions that are relevant to this thesis and/or me. Descriptions are correct as of 2012 January 1. The organizational structure of the International Astronomical Union (IAU) has changed since this date.

The IAU was founded in 1919 and exists to promote international cooperation and standardization among professional astronomers. The IAU operates through its 12 scientific Divisions and their 40 Commissions and 75 Working and Program groups. The official languages of the IAU are English and French[1]. The scientific Division relevant to this thesis is Division III (Planetary Systems Sciences/ Sciences des Systèmes Planètaires). Relevant Commissions are Commission 20 (Positions and Motions of Minor Planets, Comets and Satellites/Positions et Mouvements des Petites Planètes, des Comètes et des Satellites) and Commission 15 (Physical Studies of Comets and Minor Planets/L'Etude Physique des Comètes et des Petites Planètes). The IAU has 10143 Individual Members located in 90 countries (64 of which are National Members). I am an IAU member, a member of Commissions 6 (Astronomical Telegrams) and 20 (Positions and Motions of Minor Planets, Comets and Satellites), a member and secretary of the Committee for Small-Body Nomenclature (CSBN), a member of and CSBN representative on the Working Group on Planetary System Nomenclature, a member of the Working Group on Planetary Satellites and a member of the Organizing Committee of Commission 6.

The Smithsonian Institution[2] was founded in 1846 as a result of a bequest made ten years earlier by the estate of a British scientist, James Smithson (1765–1829) to the "United States of America, to found at Washington, under the name of the Smithsonian Institution, an establishment for the increase and diffusion of knowledge among men." Legally a body of the U.S. Federal Government, the Smithsonian Institution operates nineteen museums and nine research institutes, and is governed by a seventeen-member Board of Regents, which includes among its members the Vice President of the United States,

1 http://www.iau.org/
2 http://www.si.edu

the Chief Justice of the United States and six members of Congress (three members from the Senate and three members from the House of Representatives). The Smithsonian Astrophysical Observatory[3], SAO, was founded in 1890. Originally located in Washington, D.C., SAO moved to Cambridge, MA, in 1955 under the directorship of Fred Whipple. Some 300 Smithsonian and Harvard scientists undertake research on almost every major topic in astronomy and are organized into six research divisions. I have been an astronomer in the Solar, Stellar and Planetary Sciences division (formerly the Planetary Sciences division) since 1990. The Harvard-Smithsonian Center for Astrophysics[4] (CfA) was formed in 1973 as the result of a formal agreement between SAO and the Harvard College Observatory (HCO). HCO, founded in 1839, is a research institution of Harvard University and supports the teaching activities of the university's Department of Astronomy.

1.2.1: The Minor Planet Center

The Minor Planet Center (MPC) is a service of Division III (previously Commission 20) of the International Astronomical Union (IAU) and is responsible for cataloguing minor bodies of the solar system (minor planets, comets and outer irregular satellites of the giant planets). This responsibility involves collecting observations from observers and from the literature, checking the observations for correctness, computing orbits and making the observations, orbits and ephemerides available to the scientific community, in a referenced form, via both printed and electronic media. The published journals are the *Minor Planet Circulars*, the *Minor Planet Circulars Orbit Supplement* and the *Minor Planet Circulars Observation Supplement.* The *Minor Planet Electronic Circulars* are used primarily for the rapid announcement of newly-discovered near-Earth objects (NEOs) and are issued only in electronic form. The MPC assigns provisional designations to new discoveries of minor planets and assigns numbers to minor planets that have been well observed at (typically) four or more oppositions. The MPC maintains data sets of astrometric observations of numbered and unnumbered minor planets, comets and outer irregular natural satellites of the outer planets. The number of observations stored is over 90 million and increasing at a rate of about eight million a year.

Prior to and during World War II, the tracking of minor planets was handled at the Astronomisches Rechen-Institut in Berlin-Dahlem. Understandably, the system had collapsed by mid-1945.

3 http://www.cfa.harvard.edu/sao/
4 http://www.cfa.harvard.edu

Following World War II, the IAU undertook a reorganization of responsibility for handling minor planets. The numbered minor planets were to be handled by the Institute of Theoretical Astronomy (Leningrad/St. Petersburg), while the unnumbered minor planets were to be dealt with by the MPC. The MPC was founded in 1947 at the Cincinnati Observatory and moved to the Smithsonian Astrophysical Observatory, Cambridge MA, in 1978. Histories of and descriptions of the work undertaken by the MPC have been given by Herget (1971), Marsden (1980) and Spahr and Williams (2009). For most of its history, the MPC typically had only two or three staff members.

The Minor Planet Center was a pioneer in the use of computers for scientific studies and a history of such use over the first ten years is given by Herget (1956). The earliest automated computations were performed on the Cincinnati Observatory's IBM 601 Calculating Punch. Later computations used an IBM 604 Electronic Calculator, belonging to the local Proctor and Gamble company office, and IBM 607 and 701 Electronic Calculators at the General Electric Company. In 1956, Herget managed to obtain time on the IBM Naval Ordnance Research Calculator (NORC), a one-off system considered to be the first supercomputer, which was some fifty times faster (up to 15 000 floating-point operations/second) than the contemporary mass-produced IBM 650. In ten hours, the NORC completed a 5000-year integration of the motion of a minor planet, including perturbations by Venus through Neptune. The identity of the minor planet and the step-size of the integration are not mentioned, although Herget remarked that the computation "represented about one fourth of a billion separate operations".

From its inception the MPC relied on user subscriptions for its financial support, along with a small annual subvention from the IAU. This funding model worked well for almost 50 years, but the rise of the Internet and the expectation of many that material on the web is/should be free eroded the MPC's funding stream, as some subscribers abused the service, pirated the MPC's subscription data sets and made them freely available. In 2008 the MPC received a three-year funding commitment from NASA. The subscription charges were removed a year later and all data sets and published journals were made freely available on the MPC's website[5]. In 2011, the MPC was funded by NASA for a further five years.

5 http://www.minorplanetcenter.net/iau/mpc.html

I have worked at the MPC as Associate Director since 1990 and have been responsible for upgrading most of the internal procedures for processing observations and computing orbits that have allowed the small staff to handle a more-than-two orders of magnitude increase in the number of reported observations. In 1990 the Minor Planet Center processed some 68 000 observations in the *whole year*: at the present time, during the periods around northern-hemisphere autumn/winter New Moon, the MPC can receive *more* observations in a *single day*!

1.3: Typographic Conventions

This thesis was prepared in TechWriter versions 7.3–9.02 running on native and emulated versions of RISC OS, versions 3.50 to 4.39. The document was "typeset" in 10-point Trinity Medium, which is the RISC OS version of Times New Roman. Non-English characters are "set" in 10-point Common Latin2. Diagrams were generated using the RISC OS application `Draw`, while graphs were generated using `Tau` (edited if necessary with `Draw`). Names of computer programs, data files, command-line flags and URLs are set in `10-point Corpus Medium`, which is the RISC OS version of Courier. Conversion of the document to PDF was accomplished using the RISC OS `PrintPDF` application.

1.4: Origin of Software

Unless specifically indicated otherwise, all the software used in the thesis was written by me, either for personal use, for use in my job at the Minor Planet Center over the past twenty years, or especially for this thesis.

1.5: Computing Resources

All of the computations for this thesis were performed on machines housed at the Center for Astrophysics. New source code was written in Fortran 95 on my home OpenVMS systems, then tested and debugged on the clustered OpenVMS systems used at the Minor Planet Center. All of the data files associated with the project, including the photometric catalogues, were stored on disks purchased by me for use in the thesis and which are hosted on the work OpenVMS systems. These disks, totalling about 1.8 TB of storage, were arranged as two three-member triple-hosted shadow sets to ensure data availability and backup even if two of the hosting computers were unavailable or two of the disks in any

one shadow set failed. Useable disk space amounted to about 600 GB. Once programs were debugged, they were ported to Linux on my home Linux laptop using a free version of the Linux Fortran 95 compiler, which has good source-code compatibility with the OpenVMS Fortran 95 compiler. As a result of this compatibility, most of the ports took under 15 minutes. The photometric catalogues were built using data generated on both the work OpenVMS systems and the public Linux systems operated by the CfA's Computation Facility. The programs that corrected the observations and determined the *HG* parameters were run on the Minor Planet Center's 128-logical-core (64-physical-core) Linux system (consisting of eight dual-processor hyperthreaded quad-core machines) running the Rocks Cluster software. The Minor Planet Center computers are part of the Tamkin Computer Network, purchased using funding donated by the Tamkin Foundation.

1.6: List of Symbols

We give here a listing of symbols used in this thesis. Definitions listed here may be repeated in the body of the text. Other symbols are defined as needed in the body of the text.

AU	Astronomical Unit (see Appendix 3.2 [p. 219] for definition)
a	Semimajor axis (in AU)
e	Orbital eccentricity
i	Inclination (in degrees), referred to the ecliptic in the J2000.0 system
q	Perihelion distance (in AU): $q = a\,(1-e)$ [p. 219]
Q	Aphelion distance (in AU): $Q = a\,(1+e)$ [p. 219]
r	Heliocentric distance (in AU), distance from the sun to an object
R	Earth's heliocentric distance (in AU)
Δ	Geocentric distance (in AU), distance from the earth to an object
β	Phase angle (in degrees), the angle Sun–Object–Earth [p. 222], it is common to see α for the phase angle in other publications
α	Right ascension
δ	Declination
U	U band magnitude
V	V band magnitude, also used to indicate a visual magnitude

B	*B* band magnitude, also used historically to indicate a photographic measurement from a blue-sensitive plate
R	*R* band magnitude
I	*I* band magnitude
U–B	*U–B* colour, the difference between an object's *U* and *B* magnitudes
B–V	*B–V* colour, the difference between an object's *B* and *V* magnitudes
V–R	*V–R* colour, the difference between an object's *V* and *R* magnitudes
R–I	*R–I* colour, the difference between an object's *R* and *I* magnitudes

2: Background

2.1: Introduction

There are two fundamental questions that observers have about minor planets:

- Where is a particular object at any given moment?
- How bright will it be?

The first question is a well-studied dynamical problem—see, for example, Gauss (1809)— that is answered by considering the orbital elements of an object and the topocentric location of the observer at the time of observation.

The second question is a part-dynamical and part-physical problem. The dynamical portion is as described above. The physical portion depends on two parameters (H, the absolute magnitude, and G, the slope parameter) and on an IAU-approved procedure (Bowell *et al.*, 1989) for determining the apparent magnitude of minor planets. This procedure for determining apparent magnitudes is well established and although formally it is a two-parameter system, for poorly-studied objects the slope parameter is fixed to a standard value ($G = 0.15$). The absolute magnitude for each minor planet is determined from magnitude estimates made by a number of different techniques by many different observers over many years. These estimates vary in quality, so for many objects the absolute magnitude is not well determined. For most objects, the slope parameter is unknown.

Historically, astrometric observers have been the main source of magnitude estimates. For the most part, these are not of photometric quality and I use the term "astrophotometry" to reflect this. The astrophotometry is numerous, amounting to tens of millions of magnitude estimates for the numbered minor planets, but is of varying quality. One major advantage of the astrophotometry is that it is accessible, in its entirety, in a standardised format via the astrometric observation database maintained by the Minor Planet Center. Traditional photometric observations of minor planets are much less numerous than the astrophotometry, but are of much higher quality. Two major disadvantages of these data are that they are not collected together and that they are stored in a bewildering array of different formats.

The Minor Planet Center has long used an internal set of observer-specific adjustments that are used to try to adjust different observers' magnitudes onto a "standard system". A partial investigation of the problem of poorly determined absolute magnitude parameters by Petr Pravec (Ondřejov Observatory, Czech Republic), reported in the Minor Planet Mailing List[1], not only confirmed that the MPC's approach was valid, but agreed that there was some consistency in the astrophotometric magnitude estimates supplied by different observers and that it was possible to determine adjustments for each observer that would correct their *V*-band observations to a standard system. A weight could then be assigned to each observer's magnitudes depending on the amount of scatter in their magnitude estimates once this adjustment had been applied. It is important to note that the IAU magnitude system is a visual system. Most astrophotometric magnitude estimates have been made in bands other than *V*. If known for specific objects, colour indices may be used to correct the reported magnitude to *V*. However, in the absence of specific colours for individual objects (which is the norm), default corrections are applied to convert non-*V* magnitudes to *V*. These standard corrections are listed in Table 3.10 [p. 67].

In recent years, two major sources of reliable photometry of minor planets have become available: the moving-object catalogues from the Sloan Digital Sky Survey (SDSS) and 2 Micron All-Sky Survey (2MASS). The SDSS Moving-Object Catalogue (Ivezić *et al.*, 2002) supplies *B* and *V* magnitudes for each object, enabling *B–V* colour information to be determined and thus improving the reduction of non-*V* magnitudes to *V*. The 2MASS Asteroid and Comet Survey (Sykes *et al.*, 2000) supplies *H*, *J* and *K* magnitudes for each object. Additional new surveys expected to begin operation or ramp up activity in the next few years, such as Pan-STARRS (Kaiser *et al.*, 2002) and LSST (Tyson, 2002), are expected to produce large quantities of reliable photometry. Additional sources of reliable photometry may include data from light-curve studies—some initial contacts with the light-curve community have been made in order to exploit this data source—and even visual magnitude estimates by experienced variable-star observers.

With all these new data becoming available, it seemed appropriate to attempt a full investigation of the correction of the astrophotometry. This thesis attempts to expand on earlier work, by determining not only the observer-dependent corrections advocated by Pravec, but also by considering (and attempting to

1 MPML: `http://tech.groups.yahoo.com/group/mpml/` It is not currently possible to assign an accurate date or reference to Pravec's message. The MPML was hosted originally by egroups, but this site's poor service and suspect privacy policy led to the MPML moving to YahooGroups in 2000. The MPML's egroups postings used to be archived on a site called Astro Archive, but that site no longer exists.

remove) catalogue-dependent corrections. This research will attempt to utilise the existing large body of astrophotometry to improve our knowledge of the absolute magnitudes of the minor planets by:

- determining catalogue corrections to reduce magnitude estimates made with a variety of astrometric catalogues to a consistent system;
- determining time-dependent and/or brightness-dependent observer corrections and weights to remove observer biases from their astrophotometry;
- determining a new set of absolute magnitudes for the numbered minor planets; and by;
- applying these new data to a redetermination of the NEOWISE albedos.

The procedures developed in this thesis will also be used in routine work at the Minor Planet Center, where the absolute magnitudes of minor planets are recalculated anew each time new observations arrive and a new orbit is computed and published. I had already demonstrated working with the astrophotometry as I was responsible for the bulk of the absolute magnitude determinations of the numbered minor planets in the last two rounds of improvements of these values (Tedesco *et al.*, 1990, 1996).

It is also worth making an explicit statement of what this thesis is not. It is not an investigation of the surface properties of minor planets. I am interested only in the light after it is reflected from the minor planet and how I can make accurate predictions of brightness.

2.2: The *HG* Magnitude System

The visual brightness, V, of a minor planet at a given time can, in principle, be predicted using the two-parameter *HG* system (Bowell *et al.*, 1989):

$$V = H + 5 \log(r\Delta) + \Phi(\beta, G) \qquad (2.1)$$

where H is the absolute magnitude, G is the slope parameter, Φ is a phase function, β is the phase angle, and r and Δ are, respectively, the heliocentric and geocentric distance of the minor planet (in astronomical units) at the desired time. The absolute magnitude is the magnitude that an object would have if it were at 0° phase angle at a distance of 1 AU from both Earth and Sun (this is a physically-impossible situation, but a useful computational concept). The $5 \log(r\Delta)$ term compensates for the

varying helio- and geocentric distances (see Appendix 7.1 [p. 228] for a derivation). The phase function, Φ, includes a correction for the defect of illumination (an observer sees the full disk of the minor planet illuminated by the sun only when the phase angle is 0°) as well as a phase-dependent correction that is dependent on the surface properties of the minor planet. When given without a subscript, H is understood to be in the Johnson visual system. Subscripts indicate absolute magnitudes in other systems; e.g., H_R for an absolute magnitude in the Johnson-Cousins R_c system.

Equation 2.1 [p. 13] can model quite accurately the observed phase function (i.e., a plot of observed magnitude reduced to unit distance vs. phase angle) of most minor planets. Specifically, at phase angles greater than 7° the phase function declines at an essentially linear rate of ~ 0.03 mag/degree. At phase angles below 7° there is an "opposition effect" or "opposition spike", which is a non-linear brightening of ~ 0.4 mag over that expected from an extrapolation of the linear phase function. Figure 2.1 shows the value of the phase function Φ for various values of the slope parameter, G. The slope of the phase function increases as the slope parameter decreases.

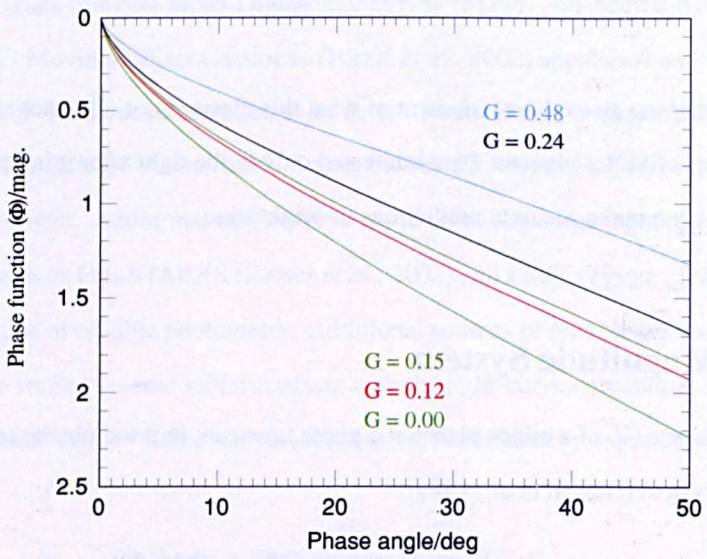

Figure 2.1: Effect of the phase function, Φ, for various values of the slope parameter, G

Equation 2.1 [p. 13] does not consider effects such as rotational variations (due to non-spherical shape or albedo features) and eclipses/occultations (due to one or more satellites). Rotational variations (see Section 6.3.7 [p. 121]), which average a mean amplitude of 0.31 mag and a median amplitude of 0.25 mag (derived from Harris *et al.*, 2007) for 2247 minor planets with known light curves, are averaged out

over the course of one rotation period. It should be noted that the Harris *et al.* listing is not an unbiased sample: there are strong observational biases against observing objects with small amplitudes and/or long rotation periods (Warner *et al.*, 2009).

For objects that are non-spherical, the values of H and G are not constants, but are dependent on the viewing angle. For small deviations from sphericity, the variation in H and G will be minimal. For a highly-elongated object, such as (216) Kleopatra (Dunham *et al.*, 1991), the difference may be substantial. The *HG* system does not handle such situations.

The phase function, Φ, has two different forms. The simpler form shown in Equation 2.2 is used in the calculation of ephemerides and is valid over the range $0 \leq G \leq 1$ and $0° \leq \beta \leq 120°$:

$$\left.\begin{aligned} \Phi(\beta, G) &= -2.5 \log \Phi \\ \Phi &= (1 - G)\Phi_1 + G\Phi_2 \\ \Phi i &= \exp[-A_i (\tan(\beta/2))^{B_i}]\,;\; i = 1,\ 2 \\ A_1 &= 3.33 \quad A_2 = 1.87 \\ B_1 &= 0.63 \quad B_2 = 1.22 \end{aligned}\right\} \tag{2.2}$$

The more rigorous form shown in Equation 2.3 is used in the determination of magnitude parameters and is valid over the range $0 \leq G \leq 1$ and $0° \leq \beta \leq 120°$:

$$\left.\begin{aligned} \Phi(\beta, G) &= -2.5 \log \Phi \\ \Phi &= (1 - G)\,\Phi_1 + G\,\Phi_2 \\ \Phi_i &= W\,\Phi_{iS} + (1 - W)\Phi_{iL}\,;\; i = 1,2 \\ W &= \exp(-90.56 \tan^2(\beta/2)) \\ \Phi_{iS} &= 1 - \frac{C_i \sin\beta}{0.119 + 1.341 \sin\beta - 0.754 \sin^2\beta} \\ \Phi_{iL} &= \exp[-A_i (\tan(\beta/2))^{B_i}] \\ A_1 &= 3.332 \quad A_2 = 1.862 \\ B_1 &= 0.631 \quad B_2 = 1.218 \\ C_1 &= 0.986 \quad C_2 = 0.238 \end{aligned}\right\} \tag{2.3}$$

Although Equations 2.2 and 2.3 are defined only for $0 \leq G \leq 1$, they are used for six numbered minor planets that have negative G values in the current MPC catalogue (Tedesco *et al.*, 1996): (163) Erigone, $G = -0.04$; (236) Honoria, $G = -0.02$; (505) Cava, $G = -0.03$; (521) Brixia, $G = -0.06$; (704) Interamnia, $G = -0.02$; and (887) Alinda, $G = -0.12$.

The difference between predictions made using the simple and rigorous phase-function (Equations 2.2 and 2.3, respectively) is shown in Figure 2.2 for various values of G. The difference is less than 0.03 mag. for $\beta < 170°$.

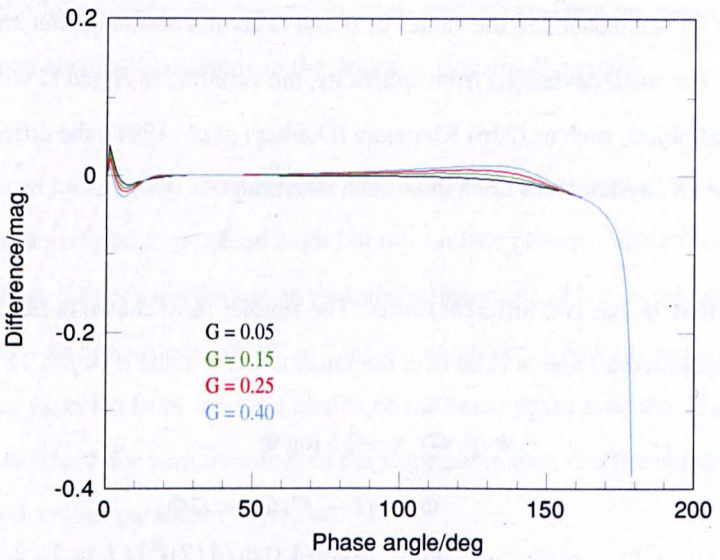

Figure 2.2: Magnitude differences between simple and rigorous phase functions

Both the absolute magnitude and slope parameter depend on whether the data being fit from light-curve studies are for maximum light, minimum light or mean magnitude. An example is provided in Baker *et al.* (2011) who observed (1082) Pirola and determined $H = 10.507 \pm 0.014$, $G = 0.080 \pm 0.016$ when considering mean magnitudes and $H = 10.320 \pm 0.013$, $G = 0.107 \pm 0.016$ when considering maximum light. Since a primary aim of this thesis is to provide accurate magnitude predictions, I will use mean magnitudes, as this will average out the effects of the light curve on the prediction.

Prior to the adoption of the *HG* system, a number of different schemes were used to predict minor-planet magnitudes. In the 19th century, the *Berliner Astronomisches Jahrbuch (BAJ)* used:

$$m = g + 5 \log(r\Delta) \tag{2.4}$$

where m was the magnitude in the system of the day, g would be the observed magnitude if the minor planet were fully illuminated and simultaneously at 1 AU from both Sun and Earth (a physical impossibility but a useful computational concept) and r and Δ are as defined in Equation 2.1 [p. 13]. The mean opposition magnitude, m_0, was defined as:

$$m_0 = g + 5 \log (a^2 - a) \tag{2.5}$$

where a is the semimajor axis of the minor planet's orbit.

In the mid-20th century, the following expression was used:

$$B = B(1,0) + 5 \log(r\Delta) + F(\beta) \tag{2.6}$$

where B is the blue-sensitive photographic magnitude, $B(1,0)$ is the magnitude at $r = \Delta = 1$ AU and $\beta = 0°$, F is a phase function, and r, Δ and β are as defined in Equation 2.1 [p. 13]. The mean opposition magnitude, $B(a,0)$, was defined as:

$$B(a,0) = B(1,0) + 5 \log (a^2 - a) \tag{2.7}$$

Before the opposition spike was described by Gehrels (1956), the phase function was:

$$F(\beta) = p\beta \tag{2.8}$$

where p is the phase coefficient (or phase factor). In the absence of a measured phase coefficient, a default value would be used. Typical default values of p were 0.023 (Gehrels, 1967a, also used in the *Efemeridy Malykh Planet*), 0.029 (Bowell and Lumme, 1979), 0.033, 0.036 and 0.039 (Gehrels and Tedesco, 1979). After the recognition of the opposition spike, Equation 2.8 was used for $\beta > 7°$, while for smaller values of β the value of $F(\beta)$ was taken from a table (Gehrels, 1967b, Gehrels and Gehrels, 1978) or read off a plot (Gehrels and Taylor, 1977).

2.3: A (Very) Brief History of Minor Planets

The first minor planet, later designated (1) Ceres, was discovered on 1801 January 1 by Giuseppe Piazzi, a Sicilian astronomer-monk, at the Palermo Observatory. Piazzi wrote a number of letters announcing his discovery to other astronomers in the following weeks but, by the time any of the letters were received, the new object had become lost. Piazzi had followed the object only until 1801 February 11, his observations then being interrupted by illness and twilight. Piazzi's observations were not made available to orbit computers until late March. Various computers obtained circular, elliptical and parabolic orbits from these observations. Ephemerides for late 1801, based on the various computed orbits, were published, but the predictions for the next opposition ranged over 5° of sky. The problem of the discordant predictions was solved by the German mathematician Carl Friedrich Gauss, who used

Piazzi's observations of Ceres to develop his general method of orbit determination. As a direct result of Gauss' calculations, Ceres was recovered by a number of observers in the period 1801 December to 1802 January. A very detailed chronology of the discovery and recovery of Ceres is given by Cunningham (2002). Although by 1807 three more minor planets had been discovered, the fifth was not discovered until 1845. Initially, minor planets were identified by name or symbol, but the practice of assigning numbers in order of discovery began in 1852 (Gould, 1852). Numbers were assigned to new objects immediately upon announcement of the discovery. This rash practice, coupled with the poor quality of many orbits, the (by necessity) haphazard way that planetary perturbations were allowed for and the consequent uncertainty in ephemerides, led to a number of incidents in which previously known objects received new numbers (e.g., Patry, 1958). By 1900, over four hundred minor planets were known. The increasing rate of discovery following the first photographic discovery of a minor planet (Wolf, 1892) prompted the introduction in 1892 of a system of provisional designations (Kreuger, 1892) that would be assigned to new discoveries. The idea was that new objects would receive numbers only when they had "good" orbits. However, many numbered objects continued to become lost in the decades after discovery. The provisional designation system was revamped at the start of 1925 (Bower, 1924) and that system is still in use today. By 1945, 1564 objects had been numbered, yet about 200 of them were effectively lost (Marsden, 1980). The count of numbered objects reached 4300 by 1990, 13 000 by 2000 and is currently over 333 000. Interesting summaries of the history of the various terms that have been used to describe the small bodies between the orbits of Mars and Jupiter are given by Hilton (2007) and by Hughes and Marsden (2007).

At its 2006 General Assembly in Prague, the International Astronomical Union adopted a resolution defining solar-system "planet", removing Pluto from the list of major planets. The Minor Planet Center assigned Pluto the number (134340) in the 2006 Aug. 8 batch of *Minor Planet Circulars*, the first batch of circulars issued after the reclassification. In addition to the solar-system planet definition, the IAU introduced the terms "dwarf planet", to cover objects such as Pluto and Ceres, and "small solar system body", to cover anything in orbit about the sun that was not a planet or dwarf planet. The resolution (see Appendix 3.1 [p. 218]) allows the term "minor planet" to continue to be used, so no change has been necessary in the names Minor Planet Center and *Minor Planet Circulars*, and both Ceres and Pluto retain their minor-planet designations.

2.4: Magnitudes in the National Ephemeris Almanacs

The early work on minor planets was concerned primarily with obtaining astrometric observations and calculating orbits to try to ensure that newly discovered objects would not be lost. Early photometric studies were both an afterthought and limited to visual comparisons with stars. Upon its discovery, Piazzi described Ceres as appearing as a magnitude eight or nine star (Zach, 1801a). When ephemerides began to be published for the minor planets in the journals of the day, it was normal practice for there to be only positional information and no information on brightness, e.g., an 1830 opposition ephemeris for Ceres by Heiligenstein (1829). Ephemerides were also published in various national almanacs, although the number of objects included and the type of data included varied both between different almanacs and within the same almanac series over time.

Ephemerides for the first four minor planets, described in the introductory remarks as "the four newly-discovered planets" and in the preface as "minor Planets", started appearing in the British *Nautical Almanac and Astronomical Ephemeris* in the 1834 edition, without any magnitude predictions. Elements and ephemerides for most known minor planets appeared in a separate *Supplement* to the 1862 edition. Magnitude predictions, specifically the predicted magnitude on the first day of each month, began appearing in the 1863 *Supplement* and continued to appear until 1869. Starting with the 1870 edition, elements and ephemerides, but no magnitudes, were published for the first five minor planets as an appendix. From 1876, the listing was restricted to the first four minor planets. Beginning with the 1960 edition, the publication was merged with the *American Ephemeris and Nautical Almanac* and renamed the *Astronomical Ephemeris*. A further change in title, to the *Astronomical Almanac*, occurred with the 1981 edition. Magnitude predictions were first included with the ephemerides in the 2003 edition of the *Astronomical Almanac*.

The German *Berliner Astronomisches Jahrbuch (BAJ)* listed ephemerides for minor planets starting with the 1805 edition. The known minor planets were listed with their planetary symbol alongside the classical planets. Starting with the 1851 edition, the fifth and subsequent minor planets were listed in a special section at the end of the volume. From 1854, these later discoveries were listed by number—in the 1854 edition the numberings began with (1) Astraea; later editions adopted the modern usage (5) Astraea, although the first four discoveries were not listed by number until the 1861 edition. Limited information on the brightness of the listed minor planets (specifically, the luminosity at the time of opposition) appears in the explanatory section of the 1844 edition and with the ephemerides in the 1853

edition, although not for the first four minor planets until the 1854 edition. Opposition magnitudes appear alongside the opposition luminosity in the 1859 edition. From the 1886 edition onwards, the opposition luminosity was dropped. The extended ephemerides for selected objects did not include magnitudes for each ephemeris date. In the tabulations of orbital elements, the mean opposition magnitude, m_0, and the absolute magnitude, g, were published beginning with the 1883 edition.

The French *Connaissance des Temps* first included minor planets as recently as 1965, but has never included magnitude information.

The German *Kleine Planeten* (*Minor Planets*) listed a single magnitude for the time of opposition. Starting in 1930, magnitudes were given for specific ephemeris dates on the extended ephemerides. The tabulation of orbital elements of all numbered minor planets in each volume included values for both m_0, the mean opposition magnitude, and g, the absolute magnitude.

The Soviet/Russian *Efemeridy Malykh Planet* (*EMP*, *Ephemerides of Minor Planets*) has given only a single magnitude for the time of opposition since the first (1947) edition. Extended ephemerides of selected objects, generally Near-Earth Asteroids, first appeared in the 1953 edition and have a magnitude for each ephemeris date. The tabulations of orbital elements included both the mean opposition magnitude (as m_0 or $B(a,0)$) and absolute magnitude (as g or $B(1,0)$) through the 1987 edition. Beginning with the 1988 edition, only the *HG* absolute magnitude parameters are given.

2.5: Dates of Publication and Date Confusion

When trying to place published papers in their proper historical context, one is faced with a dilemma: the dates of publication as recorded in on-line bibliographic services, such as the Astrophysical Data Systems Bibliographic Services (ADS), are often not correct in a modern sense. This problem is particularly acute in observatory publications where a single volume contains a number of (not necessarily related) papers. Those papers may have been published over a significant period of time, sometimes more than a decade, but the volume title page bears only a single date, which is usually the year of publication of the last paper. In many cases, there is no date associated with the individual papers. ADS references all the papers within the volume using the title-page date of publication. Within a single journal series, the dates of publication are usually valid (or, at least, consistent), although readers

of early *Astronomisches Nachrichtens* [p. 215] are warned that issues were sometimes published out of sequence and some of the printed dates of publication are incorrect. An example of date confusion can be seen in Section 2.6.1 in which Müller (1888) criticizes Parkhurst (1890)! The Müller date is probably correct (publication occurred in the last quarter of 1888 or, less likely, the first few months of 1889), while the Parkhurst date is erroneous. The Parkhurst paper appears in a volume containing miscellaneous reports published between 1886 and 1890. It is the latter date that is used in the ADS reference. The original publication of Parkhurst's paper occurred sometime between April and the last quarter of 1888. Such problems show that blind reliance on the accuracy of the current generation of on-line bibliographic services is unwise and, particularly when dealing with the old literature, that reference should be made, whenever possible, to the original printed sources.

2.6: Magnitude and Phase Effect Studies

In this section I review published work on magnitudes and phase effects.

2.6.1: Early Studies (19th Century–1970)

Zach (1801b) considered the problem of how bright Ceres would appear at the 1802 recovery opposition. He assumed that the observed brightness, L, of a minor planet was defined to be $L = 1$ at some specific time (generally the instant when the object was discovered or was at its brightest) and that the luminosity at some other time could be determined using:

$$L = \frac{r_0^2 \Delta_0^2}{r^2 \Delta^2} \tag{2.9}$$

where r is the heliocentric distance in AU, Δ is the geocentric distance in AU and the subscript zero indicates values to be taken for the moment when $L = 1$. Zach assumed $L = 1$ on 1801 Jan. 1 (the date of Ceres' discovery) and determined that $L = 0.625$ when Ceres was last observed on Feb. 11. Zach gave an ephemeris that indicated that $L = 0.429$ on Nov. 1 and that L would exceed 0.625 around Dec. 10.

A number of terms were used for L in early 19th century publications: "luminosity"; "light"; and "brilliance". In German publications, the most common term used is "lichtstärke". In addition, the definition of $L = 1$ was rather fluid; at times it referred either to the brightness at the moment of

discovery, to the brightness at the moment of maximum brightness or to the mean opposition brightness.

Until the middle of the 19th century, there was no standard magnitude scale. The difference in brightness corresponding to a difference of one magnitude was not the same in the magnitude systems used by different observers. In some scales, this brightness difference was not a constant across the entire magnitude range. An instructive table (adapted here as Table 2.1) which shows the extent of the problem was given by Pogson (1856), who compared his scale to the magnitude scales of four contemporary observers: Friedrich Struve; William Cranch Bond; Sir John Herschel; and Admiral William Smyth. All the magnitudes in the table are visual magnitudes.

Table 2.1: Correspondence of early 19th century magnitude scales

Pogson	Struve	Bond	J. Herschel	Smyth
6.0	6.0	6.0	6.0	6.0
7.0	6.6	7.0	7.3	7.0
8.0	7.3	8.0	8.6	8.0
9.0	8.0	9.0	10.0	9.6
10.0	8.6	10.0	11.3	11.2
11.0	9.3	11.6	12.6	12.8
12.0	10.0	12.9	13.9	14.4
13.0	10.6	15.2	15.2	16.0
14.0	11.3	17.5	16.6	
15.0	11.9	19.8	17.9	

This lack of standardisation complicated the observation of minor-planet magnitudes, particularly with combining estimates made by different observers using different techniques and different magnitude scales.

Argelander (1855a) remarked that when attempting to observe faint minor planets it was desirable to have information on the expected brightness of the objects. He expressed pleasure that the *BAJ* was publishing the opposition luminosity, but noted that the data provided were incomplete as no information was provided as to what magnitude was equivalent to a luminosity of one. Argelander adopted the ratio 2.56 for a one-magnitude brightness difference, this value being a computationally convenient approximation to the ratio 2.519 that had been found by Stampfer (1851) on the basis of the photometric comparison of 132 stars from the 4th to 10th magnitudes. Adopting the brightness at

a mean opposition to correspond to $L = 1$, Argelander then showed that if one knew the magnitude, M, corresponding to $L = 1$, the magnitude, m, at some other time could be computed using:

$$\left.\begin{aligned} h &= \frac{a^2(a-1)^2}{r^2\Delta^2} \\ H &= \frac{\log h}{0.4082} \\ M &= m + H \end{aligned}\right\} \qquad (2.10)$$

where a is the semimajor axis of the minor planet's orbit in astronomical units. In Equation 2.10, h is the luminosity and the expression for h is equivalent to Equation 2.9 [p. 21], replacing r_0 with a, and Δ_0 with $a-1$ (since Argelander's $L = 1$ is for a mean opposition, where $r = a$ and $\Delta = a-1$). Argelander derived values of M for 26 of the 35 then-known minor planets using his own estimates of m obtained with the meridian circle of the Bonn Observatory and values of m determined by Ferguson (1851, 1852) at the U.S. Naval Observatory, Washington. Argelander noted that the method used by Ferguson to determine magnitudes was somewhat suspect, as the comparisons were made either to catalogue stars that had been observed only once or to the components of double stars catalogued by Struve (1837). Argelander took into account the known differences between his own measures and those listed in these other catalogues and applied corrections to Ferguson's measures.

In a later paper, Argelander (1855b) made suggestions to help observers with their magnitude estimates. He argued that since the minor planets shared a common origin, suggesting that their albedos were nearly similar, the determination of the apparent brightness of minor planets would provide information on their relative sizes and, if the real diameter of any one of them was found, their true sizes. Although his belief that all minor planets have similar albedos was incorrect, his stated goal remained valid. He remarked that the magnitude scale was still not well understood and suggested that repeated measurements of stars near the north celestial pole (since they would be at an almost constant altitude in the observer's sky and not subject to gross changes in the amount of atmospheric extinction) might enable the scale to be pinned down. Argelander also suggested that frequent, accurate photometric observations might confirm that the brightness of minor planets changed over short time spans as a result of rotation. He had suspected earlier that (2) Pallas varied in brightness (Argelander, 1837) but was concerned that the variations had been caused by fluctuations in the earth's atmosphere.

Pogson (1856) presented a listing for the first 36 known minor planets of the mean opposition magnitudes and predicted magnitudes on the first day of each month from 1857 Jan. through 1858 Jan. He derived the mean opposition magnitudes, M, from magnitude estimates he obtained near opposition, which were then reduced to mean distance. The predicted magnitudes, m, were obtained using:

$$m = M - 5 \log (a^2 - a) + 5 \log (r\Delta) \qquad (2.11)$$

Equation 2.11 retains Pogson's terminology: his M was later referred to as m_0. It is unclear why Pogson did not take the conceptual leap to introduce an "absolute magnitude" at this time, thus removing the need to evaluate $M - 5 \log (a^2 - a)$ repeatedly and thereby simplifying the calculation of m. Pogson assumed the ratio 2.512 for a one-magnitude difference in brightness. He chose this value because it was the fifth root of 100 and because of its proximity to the value 2.519 obtained by Stampfer. (Pogson makes the erroneous claim that Argelander endorsed Stampfer's ratio by adopting it as the basis for his formulae for predicting minor planet magnitudes.) Before adopting the value 2.512, Pogson had considered using other ratios: 4, as proposed by Dawes (1851); 2.43, as proposed by Johnson (1853); and 2.4, as determined from his own observations. Tabulations of predicted magnitudes appeared in several subsequent years (Pogson, 1857, 1859), before the listings were adopted for inclusion in the Supplements to the *Nautical Almanac and Astronomical Ephemeris.*

The concept of minor-planet absolute magnitudes (although that term does not appear in his paper) is due to Pogson (1860), who replaced the first two terms in Equation 2.11 with N, allowing magnitudes to be predicted using:

$$m = N + 5 \log (r\Delta) \qquad (2.12)$$

Pogson supplied a list of mean opposition magnitudes, M, and absolute magnitudes, N, for 57 minor planets. His values for N are mostly within $\pm$ 0.5 mag of the modern values for H (both N and H are in the visual system, although H incorporates the opposition phase effect that is absent from N), with the notable exceptions of (1) Ceres and (4) Vesta, both of which have values of N that are ~1 mag. fainter than H.

The adoption of Pogson's magnitude scale did not fix all the problems immediately. Pickering (1879) noted that, although the various scales then in use agreed rather well for the brighter stars, there were still differences of three or four magnitudes for the fainter stars. He proposed that observers make photometric observations of a number of stars near the north celestial pole. These measures would then be compared to photometric observations made by Pickering at the Harvard College Observatory. An international committee (Pickering *et al.*, 1881, 1885) was formed and tasked with defining a standard magnitude scale. The observations proposed by Pickering (1879) formed the basis for the North Polar Sequence, a collection of visual and photographic magnitude determinations for over one thousand stars within 1° of the north celestial pole (Pickering, 1909).

An investigation of the effect of phase angle on the brightness of minor planets was undertaken by Müller (1886). Müller assumed that the luminosity was proportional to the size of the illuminated disk. If this was a correct assumption, with the luminosity at opposition being $L = 1$, then at phase angle β the luminosity would be $L_\beta = (1 + \cos\ \beta)/2$. For main-belt minor planets the maximum possible value of β is about 30°, for which $L_\beta = 0.933$, so the maximum correction for the illuminated-disk phase effect would be only 0.08 mag. In order to confirm that minor planets behaved as predicted by this equation, Müller made extensive observations of seventeen minor planets using a photometer attached to a 0.135-m refractor and a 0.207-m refractor. For each minor planet, the entire set of observations was reduced with respect to one or two comparison stars, for which Müller measured magnitudes. Müller restricted his analysis to the seven minor planets with the most observations. The observed magnitudes of the minor planets were corrected to the zenith, then reduced to mean opposition magnitudes. The defect of illumination correction was not applied. Müller observed that the reduced magnitudes were not constant, but were brightest near opposition and got progressively fainter as the phase angle increased. He plotted the reduced magnitude against the phase angle for each object, thereby producing phase curves, and noted that the seven observed objects fell into two groups: in the first group the changes in reduced brightness far from opposition were slight and the changes were quite pronounced near opposition; while for the second group the variations were much more uniform and the shape of the plotted points approached a straight line. Müller noted that the photometric behaviour of the first group was similar to that of Mars and suggested that the physical compositions were comparable, while the second group had similarities with the moon or Mercury and suggested a similar composition. Plots for two of the objects in the second group are shown in Figure 2.3 [p. 26].

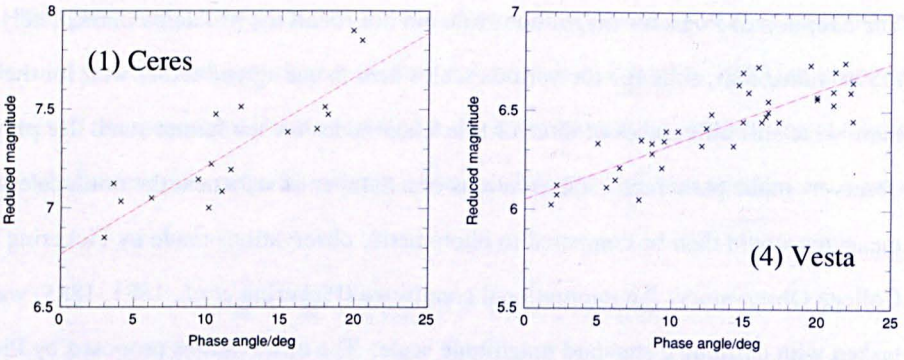

Figure 2.3: Phase dependence of reduced magnitudes from Müller (1886)

Müller does not give an explicit statement that the observed phase effect is proportional to the phase angle, but this can be inferred from his statement about the straight-line nature of the plots and from an examination of the tables showing the magnitude differences at one-degree intervals of phase. Müller also does not give explicit values for the phase coefficients. Rather, he indicates that between phase angles, β, of 3° and 21° Ceres fades by 0.73 mag. while Vesta fades by only 0.53 mag. I derived values for the absolute magnitude, g, and the phase coefficient, p, in mag/deg from the phase angles and reduced magnitudes given in Müller's table of observations. These values are given in Table 2.2. For each object, two sets of values are given: the first is derived from considering all the listed observations; the second is from those observations made at $\beta > 7°$.

Table 2.2: g and p values derived from Müller (1886)

Object	Full Phase Range		Phase > 7°	
	g	p	g	p
(1) Ceres	6.78	0.044	6.62	0.054
(2) Pallas	7.45	0.045	7.31	0.052
(4) Vesta	6.05	0.028	6.09	0.026
(7) Iris	8.50	0.017	8.54	0.015
(14) Irene	9.48	0.034	9.48	0.034
(20) Massalia	9.02	0.030	9.24	0.014
(29) Amphitrite	8.84	0.025	9.06	0.013

Although Müller remarks that some of the observed objects show greater changes in brightness near opposition than when far from opposition, this observation is not examined further and is mentioned in the summary only in passing. Since quite a number of observations were made at $\beta < 7°$, an obvious question arises: could the opposition spike be detected in Müller's data? The phase curves

of two objects with a large number of observations near opposition are shown in Figure 2.4. The plots for both (20) Massalia and, particularly, (29) Amphitrite are suggestive that Müller observed the opposition spike but failed to appreciate it fully.

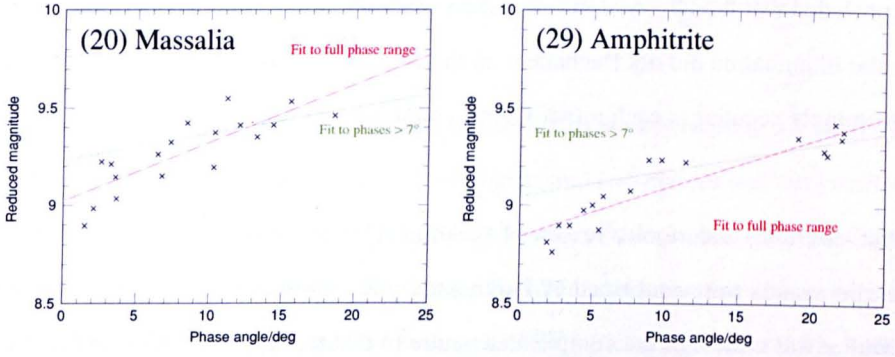

Figure 2.4: Suggestions of the opposition spike?

This opposition effect was noticed in Müller's data by other authors, including Searle (1889), who wrote: "Müller has shown that in the majority of asteroids observed by him the change of brightness was more rapid in the neighbourhood of opposition and slower at some distance from it." It would be almost 70 years before the unequivocal detection of the opposition spike was made.

Parkhurst (1890) reported his photometric observations of 18 minor planets obtained during 1887–8. He was aware that the observed magnitude of a minor planet was dependent on both the heliocentric and geocentric distances of the object, as well as on the defect of illumination, for which he supplied a table of corrections for phase angles up to ~35°. He was also aware that there was an additional phase-related effect[2], of unknown origin, that was of the form $p\beta$, where p, the phase factor, was determined from observation for each object. It is unclear where this latter piece of knowledge came from, or whether it was derived independently. Parkhurst wrote: "For reasons as yet unknown, there is usually a large additional correction for phase. Assuming this additional phase correction to be proportional to the [phase] (see Vol. XIV page 491)..." There is no reference to the earlier work of Müller (there is also no reference in Parkhurst, 1889) and the quoted reference is not relevant to either the proportionality of the phase correction or to the definition of the phase angle (a literature search for a published correction to this reference was not successful). In addition to reporting

2 Parkhurst considered this latter effect after removing the correction due to the defect of illumination, whereas Müller combined it with the defect of illumination effect. As a result of this differing analysis (only!), there would be a difference of 0.08/30 = ~ 0.003 mag/deg in the phase coefficient derived by each author for a specific object.

values of g (referred to as $G°$) for all 18 objects, Parkhurst was able to determine p for 14 objects, the values found being in the range 0.012–0.12 mag/deg. Using weights proportional to the range of β covered by the observations, the mean value of p was determined to be 0.033 mag/deg. Parkhurst recommended that this value be used as a default when observing new minor planets. Parkhurst also concluded that the observed minor planets were not appreciably self-luminous, that the amount of solar illumination did not fluctuate over the course of a year and that the phase-related effect, seemingly peculiar to each minor planet, could not be neglected.

Müller (1888) undertook a review of Parkhurst (1890). While expressing satisfaction that his earlier results were confirmed by Parkhurst's study using an entirely different observing technique, Müller was critical of the complicated nature of that technique. Müller wrote, "Das ganze Verfahlen ist im höchsten Grade umständlich und complicirt, dabei die Darstellungsweise so unübersichtlich, dass das Studium der Abhandlung dadurch ungemein erschwert wirt." ("The whole procedure is extremely cumbersome and complicated, and the kind of presentation so confusing that the study of the paper is greatly hampered.") As an example of unnecessary complication, Müller highlighted Parkhurst's computation of the phase angle. Parkhurst produced tables from which certain supplementary values could be determined, using the known values of r, Δ and R. Several further calculations were then necessary to derive an accurate value for β. By contrast, Müller gave a single simple expression for the direct calculation of β. He also questioned whether Parkhurst's observational data were sufficient for answering the question of whether the sun's light varied. Müller expressed the belief that his 1886 paper was unknown to Parkhurst, so that a comparison of the phase coefficients determined in the two studies would be instructive. The phase coefficients for the four objects common to both studies are shown in Table 2.3.

Table 2.3: Comparison of Müller and Parkhurst's phase coefficients

Object	Phase coefficient, p	
	Müller	Parkhurst
(1) Ceres	0.041	0.043
(2) Pallas	0.040	0.033
(4) Vesta	0.031	0.020
(7) Iris	0.020	0.013

Pickering (1893), comparing the results obtained by Müller and Parkhurst, remarks that "each has independently reached the conclusion that the effect of the phases of an asteroid upon its magnitude is sensibly proportional to the angle determining the phase". Pickering concluded that the mean difference between the values obtained by the two observers was 0.18 mag in g and 0.001 mag/deg. in p, a rather different conclusion than Müller's.

Reporting additional results for all seventeen of the minor planets mentioned in his 1886 paper, Müller (1893) decided that his previous division of objects into two classes was not justified. Although he determined that there were differences in the size of the phase effect, the general form of the effect was the same for all objects. He discussed each of the seventeen objects separately, comparing his results with those obtained by Parkhurst (1890), Pickering *et al.* (1884), Pickering and Wendell (1890) and Harrington (1883). Müller criticised Harrington's claim that he had observed rotational variation for (4) Vesta as the available observations were sparse and discordant, and Müller's observations much more numerous and accurate observations had shown no such variation. Müller used the example of Vesta to protest the increasing tendency of observers to claim results of great importance on the basis of sparse observational material. He also dismissed Parkhurst's measurement of $p = 0.09$ for (37) Fides as illusory, as the observations covered only a 3.5° range in phase angle. Müller also took issue with Parkhurst's explanation of the discordant nature of his observations of (40) Harmonia as being due to rotation or some unknown effect, rather than simply being bad measurements. Müller repeated his earlier observation that the straight line he fitted to the phase curve did not fit well for (29) Amphitrite and that the brightness changed more rapidly close to opposition than far from opposition. The phase coefficients found by Müller ranged from 0.018 to 0.042.

Expanding on his previous work, Parkhurst (1893) observed 28 minor planets photometrically in 1888–9, some of which he had observed in 1887–8. Combining the two data sets, he reported values of g for 36 objects and values of p for 34. The values of p ranged from 0.00–0.12 mag/deg, with a mean value (weighted as before) of 0.030 mag/deg. Since several objects had been observed in both 1887 and 1889, Parkhurst claimed that his observations demonstrated that there was no appreciable difference in the output of light by opposite sides of the sun.

Müller (1897) reported values for the phase factor, p, for 34 bright minor planets, obtaining a mean value of 0.03 mag/degree. The values of p for individual objects varied from 0.016 mag/degree to 0.053 mag/degree. Objects were observed at low phase angles and over large ranges of phase angle (often more than 20°). Müller reiterated the greater brightening near opposition observed for some objects, then noted that for simplification a straight line would be assumed for all phase curves.

Pickering (1911), claiming that the study of the variability of minor planets was "[o]ne of the most important problems in Astronomical Photometry", commented that "[t]he problem is a very complicated one, since the light varies not only with the distance from the Sun and Earth, but also with the phase angle, according to a curious law. Several observers have shown that this variation is proportional to the phase angle, a law for which no physical explanation has been offered." Pickering compared the magnitude estimates of forty-three minor planets obtained by five observers (including himself). Four of the observers used photometers, the fifth used a wedge of shaded glass to determine the limit of visibility. Interested in relating the visual photometric system to the magnitude system used in the annual *Berliner Astronomisches Jahrbuch* (*BAJ*), Pickering determined that the two magnitude systems were in agreement at $V = 9.0$, with the *BAJ* system 0.4 mag. fainter at $V = 7.0$ and 0.8 mag brighter at $V = 13.0$.

An early investigation of the quality of minor-planet photometry undertaken by Deutsch (1935) noted that the magnitude scale used in the annual *Kleine Planeten* was an assumed scale. It was unknown whether it was a visual or photographic system and how accurate it was. Deutsch argued that the minor-planet magnitude scale was visual, even though estimates were derived from photographic plates, since the magnitudes of the new minor planets were determined by comparison to the earlier-discovered minor planets and the magnitudes of those had been determined by visual comparison to stars from the *Bonner Durchmusterung*. He compared magnitude estimates of minor planets obtained at a number of active sites to the magnitudes predicted by the annual *Kleine Planeten* ephemerides, finding differences of more than two magnitudes between observation and theory.

In an editorial notice in the *Minor Planet Circulars*, Herget (1951) called attention to a serious systematic error in the magnitude estimates produced by most observers. He noted that the magnitudes reported in the *MPC*s were typically one magnitude too bright, with the exception of

observations made at the Goethe Link Observatory (Edmondson, 1952), which were calibrated using the North Polar Sequence, or by H. M. Jeffers at Lick Observatory.

Gehrels (1956) produced the first definitive description of the opposition effect from his observations of (20) Massalia. Noting that the phase function is linear at phase angles above 7°, Gehrels proposed that the absolute magnitude be defined as the value of the extrapolation of the linear section of the phase function to $\beta = 0°$.

Kuiper *et al.* (1958) reported on a systematic survey of minor planets down to $B = 16.5$, using a 0.25-m (10-inch) telescope at the McDonald Observatory, that was undertaken between 1950 and 1952. The magnitude estimates for 1167 numbered objects from this survey were combined with contemporary photoelectric observations and older data reduced to the survey system. The list of 1622 absolute magnitudes so determined was also published in the Commission 20 report in the 1958 *IAU Transactions* and the values therein were in use in ephemerides until 1970.

In a general survey of minor-planet magnitudes, Gehrels (1957) commented that "systematic differences between results published by different observatories may attain 3 mag". He examined magnitude estimates from a number of observers, compared them with the McDonald results, and derived values for the systematic differences between each observer and the McDonald survey. For some observers, such as those at Algiers and Uccle, the systematic differences were constant for the examined range of observed magnitudes; for others, such as those at Nice and Simeïs, the systematic differences were magnitude dependent. These differences are summarised in Table 2.4. Gehrels also supplied a table of phase corrections for phase angles less than 8°.

Table 2.4: Systematic differences in magnitude estimates, based on Gehrels (1957)

Observatory	Systematic difference from McDonald survey		
	Mag. Range	Diff. (Observatory – McDonald)	Av. Dev.
008 Algiers	12.0–16.5	–1.40	0.31
024 Heidelberg	12.5–16.5	–1.60	0.32
760 Indiana	13.0–16.5	+0.04	0.46
078 Johannesburg	11.5–16.0	–1.58	0.44
839 La Plata	12.0–16.0	–1.49	0.46
085 Kiev	11.0–14.0	–0.30 – 0.48 (Mag.–10.0)	0.40
020 Nice	10.0–13.0	–1.08 – 0.16 (Mag.–10.0)	0.30

020 Nice	13.0–16.5	−1.56	0.30
094 Simeïs	10.0–16.0	−1.72 − 0.22 (Mag.−14.0)	0.32
388 Tokyo	11.0–15.5	−1.68	0.37
012 Uccle	14.0–16.5	−1.61	0.33

Gehrels (1967b) considered 1500 photographic observations of minor planets obtained at Goethe Link Observatory between 1958 and 1965, combined them with the McDonald Observatory survey results, and produced absolute magnitudes for 1651 of the 1715 then-numbered minor planets. The list of absolute magnitudes appeared in the 1967 *IAU Transactions* and also appeared (in an extended listing to number 1735), in Gehrels (1970). The values in the latter publication were adopted for use in ephemerides at the 1970 IAU General Assembly.

2.6.2: Recent Studies (1971–Present)

Gehrels and Taylor (1977) undertook an investigation of the phase function of (6) Hebe. They produced a plot of the magnitude-phase relation of five minor planets within 8° of opposition.

With the availability of more photoelectric observations, Gehrels and Gehrels (1978), building on previous results, determined absolute magnitudes for 2082 numbered minor planets. At the 1979 IAU General Assembly these values were adopted for use in ephemerides until 1982. This date was extended to 1985 at the 1982 IAU General Assembly. The listing of absolute magnitudes was extended by Gehrels and Tedesco (1979) to 2101 numbered minor planets, including the 23 objects then listed as "lost". In addition, a table of phase coefficients for 60 of the objects was given.

The 1985 IAU General Assembly adopted the use of the two-parameter *HG* system (Bowell *et al.*, 1989) for predicting magnitudes. In the *HG* system the opposition effect is handled analytically, as opposed to via a table of corrections as in previous schemes. Practicalities of the new system were described by Marsden (1985) and a new listing of absolute magnitudes and slope parameters was published by Tedesco and Marsden (1986). Tedesco combined photoelectric observations with albedo and diameter determinations (Matson *et al.*, 1986) from the Infra-Red Astronomical Satellite to derive magnitude parameters for the bulk of the then-known numbered minor planets. Marsden extended the list to the remainder using uncorrected astrophotometry. Updated listings of magnitude parameters were given by Tedesco *et al.* (1990, 1996). Most of the magnitude

parameters for objects numbered since previous versions of the list were determined by the orbit computer who published the orbit when the object was numbered. In recent years, all orbits for new numberings have been computed at the Minor Planet Center, so they are being computed in a consistent fashion.

Lumme *et al.* (1993) proposed a three-parameter magnitude system for minor planets, intended to cope with problem cases such as (44) Nysa and (64) Angelina, which show very strong opposition effects ("spikes") at phase angles under 1° (Harris *et al.*, 1989b), and (419) Aurelia, which shows almost no opposition effect (Harris and Young, 1989). This proposal, which seems to have appeared only in an American Astronomical Society's Division on Dynamical Astronomy meeting abstract volume, is poorly documented in the historical record. No information on the magnitude system is provided in the abstract, other than the provisional name for the scheme: "the H, G1, G2 system".

Arguing that the *HG* system did not accurately model (at the 0.1-magnitude level) the opposition effect for a wide range of objects, Shevchenko (1997) proposed a three-parameter empirical phase function (see Equation 2.13), derived from his examination of the phase curves of 32 main-belt minor planets of various taxonomic classes:

$$V = V(1,0) - \frac{a}{1+\beta} + b\beta + 5\log(r\Delta) \qquad (2.13)$$

where $V(1,0)$ is the magnitude at zero phase angle and unit geocentric distance, β is the phase angle, a is a parameter that characterises the opposition effect, b is a parameter related to the linear part of the phase curve, and r and Δ are the helio- and geocentric distances in AU. Shevchenko indicated that there was a strong correlation of the parameter a with the IRAS-derived albedos.

In an analysis of early observations of minor planets from the Sloan Digital Sky Survey (SDSS), Jurić *et al.* (2002) compared positions and magnitudes obtained in the survey to the known minor-planet population. For reasons described in the paper, the authors decided to do the bulk of the comparisons to the ASTORB orbit catalogue (Bowell *et al.*, 1994), rather than to the MPC's MPCORB orbit catalogue (Marsden *et al.*, 1994). They found that the magnitude discrepancy between the observed SDSS magnitudes and the magnitudes predicted from ASTORB was ~ +0.4 mag. (i.e., the ASTORB predictions were too bright). They also computed the discrepancy between SDSS and MPCORB predictions as ~ +0.2 mag., about half the ASTORB value. This difference

between ASTORB and MPCORB was explained by reference to Jedicke *et al.* (2002), where it was noted that MPCORB H values are derived using weighted astrophotometry (with the weights based loosely on historical photometric performance by each site) whereas ASTORB used unweighted astrophotometry.

The start-up of the many professional CCD minor-planet surveys in the late 1990s led many amateur observers to switch their observing programs from astrometry to photometry of minor planets in the following years. This photometric work has been directed primarily at deriving light-curve parameters (on a relative, rather than absolute scale), but has also provided some colour information. The bulk of recently published light-curve papers are based solely (or mostly) on amateur observations (see, e.g., Warner *et al.*, 2009).

Parker *et al.* (2008), in a study of size distributions within minor-planet families, compared determinations of absolute magnitudes derived from SDSS observations with the values listed in the ASTORB catalogue (Bowell *et al.*, 1994). They determined the difference $H_{SDSS} - H_{ASTORB}$ as 0.23 ± 0.30 mag.

Until quite recently, the Minor Planet Center maintained the *HG* parameters for the numbered minor planets as a separate list, which was added to as objects were newly numbered. Entries for existing objects were only updated on the infrequent occasions when complete *HG* lists were published. This policy was changed in September 2008, when new H determinations (with assumed $G = 0.15$) were included with new orbit determinations for old-numbered minor planets. The list values, though, are still maintained for those objects with non-default G values or H values determined to two decimal places.

Galád *et al.* (2009) attempted to use astrophotometric observations to derive light curves for a number of minor planets with long rotation periods. They did not attempt to correct the astrophotometry before combining their own photometric observations with the astrophotometry. Amateur observers are also reporting H, and sometimes G, determinations from their lightcurve observations: recent examples include H determinations of 12.50 for (1700) Zvezdara (Baker *et al.*, 2010) and 15.4 for (159402) 1999 AP_{10} (Franco *et al.*, 2010), values that differ from the then-current MPC H values by +0.03 mag. and –0.6 mag., respectively. It should be remarked that the MPC

value for (1700) was not derived at the MPC, but rather was supplied by Tedesco *et al.* (1990). Studies such as those mentioned above typically consider observations made over a period of a few months at most, but do serve to highlight gross errors, particularly in the determination of H.

Gladman *et al.* (2009) derived absolute magnitudes for 1277 objects detected in the Sub-Kilometer Asteroid Diameter Survey and commented on the wide discordances (up to ± 1 magnitude) between their H determinations for the 135 previously-known objects detected and the then-current set of HG parameters from the MPC. This was interpreted as being due to real systematic errors in the MPC H determinations.

Concern about the poor quality of many HG determinations led IAU Commission 15 to set up a Task Group in 2006 to investigate the issue (Cellino, 2006). The Task Group reported at the 2009 IAU General Assembly (Cellino, 2009). They noted the fundamental role that the absolute magnitude played in many areas of physical research (such as albedo determinations) and created an alternate phase function to replace the current HG system. The three-parameter magnitude system for minor planets was proposed by Muinonen *et al.* (2010). As with the Lumme *et al.* (1993) proposal, the new proposal uses H, G_1 and G_2 (see Equations 2.14 and 2.15).

$$V = H + 5 \log(r\Delta) + \Phi(\beta, G_1, G_2) \tag{2.14}$$

where:

$$\left.\begin{aligned} \Phi(\beta, G_1, G_2) &= G_1\Phi_1(\beta) + G_2\Phi_2(\beta) + (1 - G_1 - G_2)\Phi_3(\beta) \\ \Phi_1(\beta) &= 1 - \frac{6\beta}{\pi} \\ \Phi_2(\beta) &= 1 - \frac{9\beta}{5\pi} \\ \ln \Phi_3(\beta) &= -4\pi(\tan(\beta/2))^{2/3} \end{aligned}\right\} \tag{2.15}$$

The functions Φ_1 and Φ_2 describe the linear portion of the phase curve and Φ_3 describes the opposition effect. Muinonen's Figures 2, 3, 4 and 5 show comparisons between fits using the HG and the HG_1G_2 systems for various classes of minor planets. For the C-type (24) Themis, E-type (44) Nysa, SR-class (133) Cyrene and Q-type (1862) Apollo, the r.m.s. of the HG_1G_2 fits are about half those of the HG fits. For the F-class (419) Aurelia, the HG_1G_2 fit r.m.s. are 20% of the HG fit. However, the fits for the M-class (69) Hesperia and S-class (82) Alkmene are only comparable. For

sparsely-observed objects, the two slope parameters are replaced with a single slope parameter, G_{12}. (see Equations 2.16 and 2.17).

$$V = H + 5 \log(r\Delta) + \Phi(\beta, G_{12}) \tag{2.16}$$

where:

$$\left.\begin{aligned} \Phi(\beta, G_{12}) &= G_1\Phi_1(\beta) + G_2\Phi_2(\beta) + (1 - G_1 - G_2)\Phi_3(\beta) \\ G_1 &= 0.7527G_{12} + 0.06164, G_{12} < 0.2 \\ &= 0.9529G_{12} + 0.02162, G_{12} \geq 0.2 \\ G_2 &= -0.9612G_{12} + 0.6270, G_{12} < 0.2 \\ &= -0.6125G_{12} + 0.5572, G_{12} \geq 0.2 \end{aligned}\right\} \tag{2.17}$$

An abstract (Williams, 2012b), summarizing the status of the work undertaken in this thesis, was submitted to the Asteroids, Comets, Meteors 2012 meeting in Niigata (Japan).

A recent paper submitted by Pravec *et al.* (2012) discussed *HG* determinations based on observations of 583 minor planets obtained at Ondřejov (Czech Republic) and the Table Mountain Observatory (CA) from 1978 to 2011. Their *HG* values were compared to, amongst other data sources, the MPCORB database. They found that the absolute difference between their H values and the MPC H values reached a maximum value of about 0.5 mag. around $H \sim 14$, with the MPC H values being too bright.

2.7: Taxonomy and Colours

Minor planets are not self-luminous. They are visible only by the reflection of light received from the sun. Minor planets are not smooth, spherical mirrors, so the reflected light is modified by the surface properties of the minor planet. Taxonomy is classification by one or more observables. A full discussion of the literature relating to taxonomic classification is beyond the scope of and not relevant to this thesis. The discussion here will be restricted to the most important work. Many authors have attempted to relate the observables to the surface properties of the objects being observed, often by comparison of observed spectra to laboratory-obtained spectra of meteorites and minerals. The 1970s literature on taxonomic classification can be described politely as "confusing", with the same class name used in different publications for different types of object, as well as instances of class names being introduced

then dropped. Useful chronologies are given by Tholen (1984) and Britt and Lebofsky (1997). The use of taxonomic classifications in this study will be restricted to use of an object's taxonomic class to adjust default values for unmeasured parameters (such as colours or slope parameters).

The first observable that was used for taxonomic classification of minor planets was colour differences. Herschel (1802) reported his visual observations of (1) Ceres and (2) Pallas. From an observation made on 1802 Feb. 13, he reported that "[t]he colour of Ceres is ruddy, but not very deep". His observations on Apr. 21 compared the two minor planets: "Ceres is much more ruddy than Pallas". The next night, he observed that "Pallas is of a dusky whitish colour". Zach (1802) reported observations on Jan. 13 by Harding stating that "sie nicht von einem Sterne 9 Grösse unterscheiden konnte" ("[Harding] could not differentiate it from a magnitude 9 star"), but that the light seemed "etwas matt und röthlich" ("somewhat pale and reddish").

The first attempt to obtain a spectrum of a minor planet was made by Vogel (1874). His visual observation of the spectrum of (4) Vesta on 1872 Feb. 13 showed Hβ and two bands at 577 and 518 nm, which he interpreted (erroneously) as indicating that Vesta had an atmosphere. He also observed (8) Flora on several nights around the time of the 1873 opposition (Oct. 30), but apart from a weak continuum whose colours were almost invisible, nothing could be seen[3].

Barnard (1895) reported his measurements of the observed diameters of the first four minor planets using the 36-inch (0.9-m) Lick refractor. He combined his diameters with photometric measures from a number of other observers and derived albedos. Barnard noted that Vesta's albedo was four times that of Ceres, explaining why previous researchers had assumed that Vesta was the largest minor planet on account of its greater brightness. Barnard stated that it was clear that Ceres was by far the largest minor planet. Barnard's values of 485 miles for the diameter of Ceres, 304 miles for Pallas, 118 miles for Juno and 243 miles for Vesta, are in tolerable agreement with modern values and a vast improvement over earlier attempts, made with much smaller telescopes, at direct measurement of the diameters.

Early colour measurements were reported by Bobrovnikoff (1929), who observed twelve bright minor planets using the 0.9-m (36-inch) Lick refractor and a one-prism spectrograph. Spectra were also

3 A number of authors (e.g., Tholen, 1984) have written that Vogel could see nothing in his spectrum of (8) Flora. This may be due to a mistranslation of the original text or to a different interpretation of "nothing".

obtained of a number of G0-type stars. Photographs of each spectrum were obtained and microphotometric measures were obtained at 470, 430, 400 and 394.5 nm. The minor-planet spectra did not show any new lines or bands when compared with a lunar spectrum, although the intensity distribution was different. In addition, the intensity distributions differed among the observed minor planets. Bobrovnikoff concluded that the light of the minor planets was due wholly to reflection and that the violet and ultra-violet regions of their spectra were very weak in comparison to G0-type stars.

Various early attempts to derive colour indices were not very successful, owing to limitations inherent in the use of photographic plates. Recht (1934) observed 36 minor planets and obtained $B–V$ colours for 34 of them. He came to the erroneous conclusion that many minor planets were bluer than the sun (i.e., a $B–V$ colour numerically smaller than the sun's $B–V = 0.63$). Johnson (1939) observed three minor planets, and concluded that they showed a considerable range in spectral reflectivity. Non-standard colours were obtained and Johnson suggested that the colours of (4) Vesta and (17) Thetis showed rotational variation. Watson (1940), noting that very few natural terrestrial materials have higher reflectivity of blue light than yellow light, observed seven minor planets and found none to have significantly bluer colours than the sun. He also determined absolute magnitudes for the observed objects and found a systematic difference of +0.16 mag. between six of his values and those listed in the *Kleine Planeten*. Watson noted that for the seventh object, (4) Vesta, the *Kleine Planeten* listed $g = 4.0$ but used $g = 3.3$ for the magnitude prediction listed with the ephemeris and that $g = 3.3$ was also used in *The Handbook of the British Astronomical Association*. Fischer (1941) obtained $B–R$ colour indices for 33 minor planets and most of his values differ from modern determinations by several tenths of a magnitude. In addition, the mean of Fischer's determinations is offset by –0.26 magnitudes from modern values.

Zellner (1973), noting from a study of 16 minor planets that there was a positive correlation between the $U–V$ colour, the albedo, and the presence and strength of an infra-red absorption band, suggested that there were two distinct compositional classes, which he labelled "stony" and "carbonaceous". This study confirmed earlier work by, amongst others, Groeneveld and Kuiper (1954) and Wood and Kuiper (1963), whose plots of $U–B$ vs. $B–V$ colours showed clumps in the distribution of the minor planets that each observed. Figure 2.5, showing the distribution for 44 minor planets, is adapted from Wood and Kuiper (1963). Some of the labels present in the original diagram have been omitted for clarity. The four red dots indicate stars of the stated spectral class.

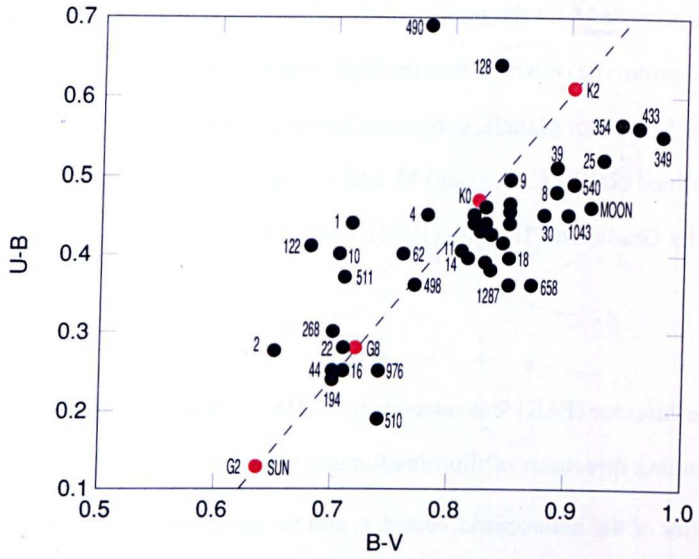

Figure 2.5: U–B vs. B–V colours, adapted from Wood and Kuiper (1963)

McCord and Chapman (1975a, 1975b) presented spectrophotometric observations for 66 minor planets and combined them with observations of 32 other minor planets observed by Chapman *et al.* (1973a, 1973b). Observations were made at wavelengths from 300 nm to 950 nm and taxonomic classification was made on the basis of nine spectral parameters, including the ratio of the reflectance at 700 nm divided by that at 400 nm and the measure of the positive curvature of the visible portion of the spectrum. The number of different classes recognised was 34[4].

Chapman *et al.* (1975) analysed published data on 110 minor planets and found that 90% of the objects observed fell into the two broad classes described by Zellner (1973). The classes were named as C and S, corresponding to the carbonaceous and stony classes of Zellner. In addition, it was noted that (4) Vesta had a unique spectrum and that three other objects, (16) Psyche, (21) Lutetia and (22) Kalliope, had spectra similar to nickel-iron meteorites: no class name was assigned to either. C classifications were common among observed objects in the outer Main Belt and among the larger minor planets. The fraction of C-type objects rose from ~ 0.5 at the inner edge of the Main Belt to ~ 0.9 at the outer edge. Objects that could not be fitted into either class C or S were assigned to class U.

4 Although Chapman *et al.* (1976) gives the number of different types as 34, a reading of McCord and Chapman (1975b) suggests that it should be 36, although no explicit figure is given in that paper.

Zellner and Gradie (1976), on the basis of their polarimetric observations of 94 minor planets, introduced the class name M for the presumed-metallic objects discussed by Chapman *et al.* (1975) and added class E, the prototype of which was the high-albedo (44) Nysa. Bowell *et al.* (1978), on the basis of observations of 523 minor planets, determined precise definitions of seven observable parameters for the previously defined classes C, S, E and M, and introduced a new class, R. Two more classes, F and P, were introduced by Gradie and Tedesco (1982); P types had spectra identical to M types, but had much lower albedos.

The Phase Angle Bisector (PAB) was introduced by Harris *et al.* (1984a) as a quantity useful in studying the effect of changing directions of illumination and viewing on the brightness of a minor planet. The PAB is the bisector of the heliocentric vector, $\bar{r}$, and the geocentric vector, $\bar{\Delta}$, to the minor planet and is a vector defined as:

$$PAB = \frac{\bar{r}/r + \bar{\Delta}/\Delta}{\left|\bar{r}/r + \bar{\Delta}/\Delta\right|} \tag{2.18}$$

For main-belt minor planets with moderate orbital eccentricities and inclinations, the PAB is essentially constant one month either side of opposition. Harris *et al.* note that, because of this constancy, a single quoted value of the PAB at an apparition serves as a compact way to specify the position of the minor planet during that apparition.

The Tholen taxonomy (Tholen, 1984) extended the classification system to 14 classes and was derived primarily from broad-band spectrophotometric colours for 589 minor planets obtained from the Eight-Color Asteroid Survey (Zellner *et al.*, 1985). Tholen identified six new groups, labelling them A, B, D, F, G and T. The previously defined classes E, M and P could not be distinguished using the ECAS data and were lumped together into class X.

Initially intending to apply the Tholen taxonomy to the 1447 minor planets observed in the second phase of the Small Main-Belt Asteroid Spectroscopic Survey (SMASSII), Bus and Binzel (2002) found that they could not reconcile the data for many of the objects they observed with the Tholen taxonomic scheme. They produced their own taxonomic system which comprised 26 classes, 12 of which could be found in the Tholen taxonomy. The classes adopted from Tholen were A, B, C, D, K, O, Q, R, S, T, V and X. The new classes were L, Cb, Cg, Cgh, Ch, Ld, Sa, Sk, Sl, Sq, Sr, Xc, Xe and Xk, where multi-

letter classes refer to objects with intermediate spectral characteristics. The mean reflectance spectra of various taxonomic classes are shown in Figure 2.6.

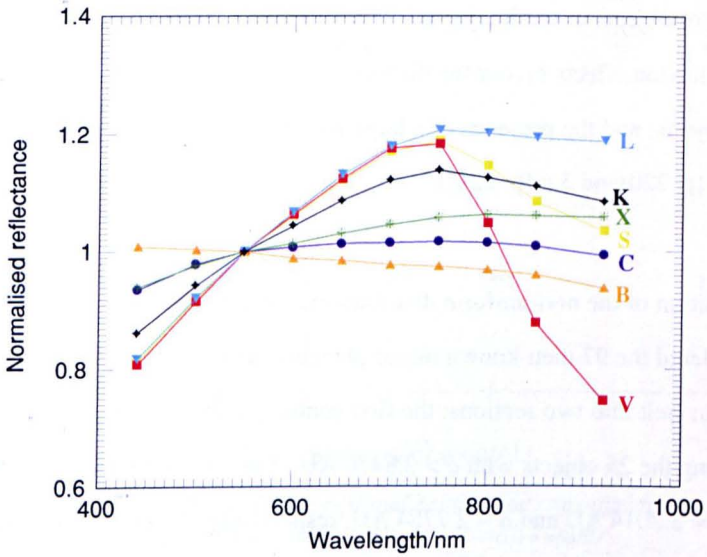

Figure 2.6: Mean reflectance spectra for various taxonomic classes, from Bus and Binzel (2002)

Summaries of the distinguishing features by which the various taxonomic classes are classified are given by Tholen and Barucci (1989) and by Bus *et al.* (2002).

DeMeo *et al.* (2009) extended the Bus-Binzel taxonomy using ground-based reflectance spectra over the range 0.45 to 2.45 μm. This wavelength range covers the 1.05-μm olivine and 0.9-μm/2-μm pyroxene absorptions (Gaffey *et al.*, 1989), spectral features that allow additional discrimination between the taxonomic classes. The number of classes in the DeMeo scheme is 24: the members of the Bus Ld class were divided into the existing D and L classes; and the Bus Sa, Sl and Sk classes were reclassified as class S. One new class, Sv, was introduced as a link between classes S and V.

2.8: Spatial Distribution of the Minor Planets

The bulk of the known minor planets (93.4% of the 599 045 objects with orbits as of 2012 June 12) are found in the Main Belt, which is located between the orbits of Mars and Jupiter. The Main Belt is the volume of space extending from 2.15 to 3.28 Astronomical Units (AU) in heliocentric distance from the ecliptic plane to a height of approximately ± 1.1 AU at the inner edge to ± 1.9 AU at the outer edge.

Main Belt minor planets (more commonly called Main Belt Asteroids, or MBAs) are those objects with semimajor axes in the range 2.15 to 3.28 AU that are in orbits that are not planet-crossing.

The distribution of objects in semimajor axis is not uniform. There are two primary reasons for this: observational selection effects favour the discovery of larger and higher-albedo objects over smaller and lower-albedo objects; and the presence of a large number of mean-motion and secular resonances (see Appendices 3.5 [p. 220]and 3.6 [p. 221]).

The first recognition of the non-uniform distribution of minor planets in the Main Belt was by Kirkwood (1869), who ordered the 97 then-known minor planets in order of increasing semimajor axis, a. He divided the Main Belt into two sections: the first containing the 72 objects with $a < 2.8470$ AU; the second containing the 25 objects with $a > 2.8470$ AU. Since the innermost and outermost objects in the inner list had $a = 2.2014$ AU and $a = 2.7784$ AU, respectively, the average separation between two consecutive entries was 0.0081 AU. With semimajor axes ranging from $a = 2.8563$ AU to 3.4927 AU, the average separation in the outer list was 0.0265 AU. Kirkwood noticed that gaps between consecutive entries that were much larger (up to eight times larger) than the relevant mean occurred around 2.50, 2.82, 2.96 and 3.28 AU. He explained this observation as follows: "A planetary particle at the distance 2.5 — in the interval between Thetis and Hestia — would make precisely three revolutions while Jupiter completes one; coming always into conjunction with that planet in the same parts of its orbit. Consequently, its orbit would become more and more eccentric ... the action of Jupiter would ultimately change its mean distance, and thus destroy the commensurability of the periodic times. ... the primitive orbit of the particle would be left destitute of matter. The same reasoning is, of course, applicable to the other intervals."

Figure 2.7 shows the distribution of objects by semimajor axis, a, and includes the 448 811 multiple-opposition objects (as of 2012 June 12) with $1.5 < a < 6$ AU. The presence of a number of mean-motion resonances with Jupiter are revealed by the lack of objects at certain heliocentric distances: the 2:1 at 3.28 AU; the 7:3 at 2.96 AU; the 5:2 at 2.82 AU; and the 3:1 at 2.50 AU. The gap around 2.1 AU is close to the 4:1 mean-motion resonance at 2.06 AU, but the effect of this resonance is overwhelmed by the much stronger ν_6 and ν_{16} secular resonances that lie in the vicinity of the 4:1 (Moons and Morbidelli, 1995). Other mean-motion resonances are marked by the presence of groups of minor planets: the Hildas at the 3:2 at 3.96 AU; and the Jupiter Trojans at the 1:1 at 5.2 AU.

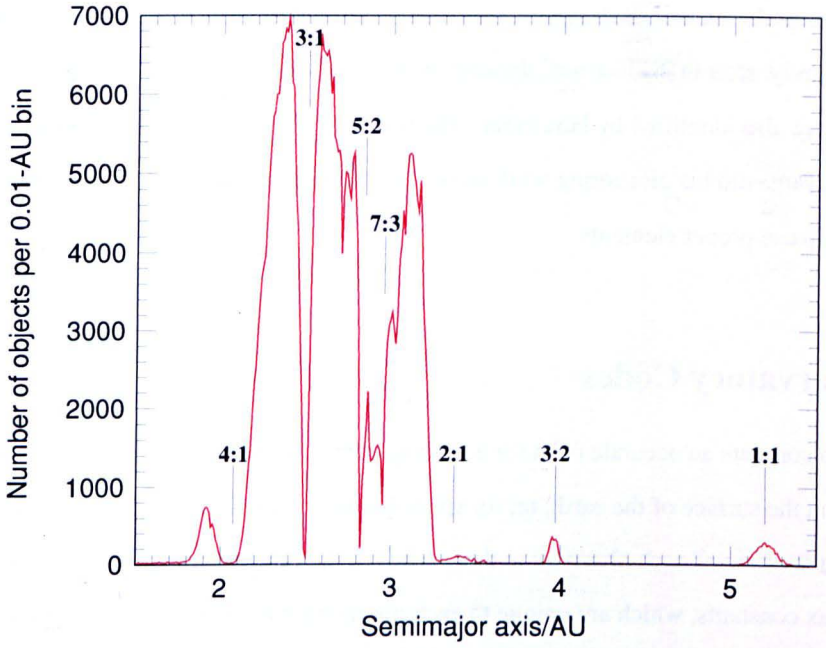

Figure 2.7: Distribution of minor-planet semimajor axes and locations of major mean-motion resonances with Jupiter

2.9: Families and Orbital Groups

A family is a set of minor planets that may share a common origin, the members of the family being the remnants of a collision of a large parent body. An orbital group is a set of minor planets that have similar osculating orbital elements. "Group" is a rather nebulous term, the definition of which has varied between different authors. Brouwer (1951) used the term "group" for sets of minor planets with similar proper elements, several of his groups are listed as families by Williams (1979, 1989). Warner *et al.* (2009) use the term "group" to refer to objects with similar osculating elements. I avoid any confusion here by using the term "orbital group", in preference to "group", to mean objects with similar osculating orbital elements.

Hirayama (1918), from an examination of the orbital elements of the first 790 numbered minor planets, noted that there were clumps in the distribution of the orbital elements (principally the mean motion, the inclination and the eccentricity) that were statistically unlikely to occur by chance. Of the 37 objects with mean motions between 720″ and 740″ per day, 16 of them had inclinations under 4°. In addition, Hirayama noted that a plot of the poles of the orbital planes of those 16 minor planets showed that 15 of the poles lay on a circle, the centre of which very nearly coincided with the pole of Jupiter's orbit. He explained this observation as a consequence of the disruption of a larger parent body and the subsequent

long-term perturbations of the fragments by Jupiter. Hirayama named this group of minor planets the Koronis Family, after (158) Koronis, the first member to be discovered. Two other families, Eos and Themis, were also identified by Hirayama. The listing by Williams (1979) includes over 100 families. While Hirayama did his pioneering work using osculating elements, modern determinations of family membership use proper elements.

2.10: Observatory Codes

In order to compute an accurate orbit for a solar system body, it is necessary to know the location of the observer on the surface of the earth, or, for space-borne observations, the observing platform's location in space at the time of each observation that is used in the orbit computation. This location is expressed via parallax constants, which are unique to each observing site. In either case, the observing location needs to be known in the fixed J2000.0 equatorial frame. One possible approach is to record a location's geographical longitude, latitude and altitude above the reference geoid on every observation. Another is to record the site's geographical longitude and the products of the site's distance from the geocentre (in Earth radii) and the sine and cosine, respectively, of the site's geocentric latitude. The first approach is simple in that the site coordinates can be read from a map, but some calculation is required to convert the given quantities for use in orbit calculations. The second approach is convenient in that the stored quantities can be used in orbital computations without further calculations. However, both of these approaches require a lot of unnecessary repetition of data for those sites where many observations are obtained.

A more compact solution to the problem is to assign each observing site a short unique code, which can be coded compactly on each observation record. This is the approach that the Minor Planet Center adopted for its archive of astrometric observations (Brouwer, 1949), which was stored originally on punched cards. The unique code adopted was a three-digit code, later extended to a three-character code when the number of observing sites neared one thousand. Given the limited RAM and disk space present in early computers, compactness was very desirable. The parallax constants stored for each code are the geographical longitude and the products of the site's distance from the geocentre (in Earth radii) and the sine and cosine, respectively, of the site's geocentric latitude.

The requirements for obtaining an observatory code are documented on the Minor Planet Center's

website[5], along with the current list[6] of assigned observatory codes (giving each site's geographical longitude and the products of the distance from the geocentre, in Earth radii, and the sine and cosine, respectively, of the geocentric latitude).

5 http://www.minorplanetcenter.net/iau/info/Astrometry.html#HowObsCode
6 http://www.minorplanetcenter.net/iau/lists/ObsCodesF.html

3: Procedures

3.1: Introduction

In this chapter, I examine the procedures that will be used to remove the various systematic errors that affect astrophotometric observations. I will consider systematic errors that arise from the use of comparison-star magnitudes from astrometric reference catalogues as well as from the reduction methods peculiar to each observer. I also review briefly the astrometric catalogues that have been used by minor-planet observers in recent decades. I discuss the collection of taxonomic classifications and colours from the published literature and describe the procedures I will use when I have to adopt a classification or colour. The assignment of adopted slope parameters for various taxonomic classes is also discussed. Finally, I discuss how I will manage the physical data that I collect and how it will be arranged for easy use by the computer programs that will correct the astrophotometry and produce the new *HG* values.

3.2: Catalogue Systematics

The astrophotometric observations are (mostly) derived from comparison of an object with the magnitudes for the comparison stars that are listed in whatever reference catalogue was used for the astrometric reduction. It is well known (e.g., Monet *et al.*, 2003) that the magnitudes listed in astrometric reference catalogues are, at best, of indifferent quality. This is partly due to the fact that the *raison d'être* of astrometric reference catalogues is simply to provide accurate positions for the included objects, and partly due to the inhomogeneous nature of the photographic plates that were scanned during the preparation of most of the astrometric catalogues used in recent decades.

The bulk of the photographic plates scanned for catalogue fields above $\delta = -30°$ come from the First (POSS-I) and Second (POSS-II) Palomar Observatory Sky Surveys (Morgan *et al.*, 1992). POSS-I used photographic emulsions 103a-O (sensitive in the range 350–500 nm) and 103a-E (620–670 nm). POSS-II used emulsions IIIa-J (385–540 nm), IIIa-F (610–690 nm) and IV-N (730–900 nm). Plates for southern-hemisphere fields came from the Anglo-Australian Observatory and the European Southern Observatory, and the plate emulsions used were IIIa-J, IIIa-F and IV-N.

From an analysis of a comparison of Sloan Digital Sky Survey photometric data with the magnitudes in the USNO-B1.0 catalogue, Monet *et al.* (2003) concluded that while there was little systematic variation in the differences between SDSS and B1.0 magnitudes across a single plate, there were systematic variations in the differences on different plates. This confirms a primary assumption underlying my research: that it is possible to derive magnitude-dependent catalogue corrections to remove the catalogue-dependent systematic errors in the astrophotometry. An example of the agreement, or lack thereof, between the USNO-A2.0 catalogue and data from the Sloan Digital Sky Survey is shown in Figure 3.1: the centre coordinates, which are positions of (70069) 1999 JT_{49} observed by LINEAR (see Section 5.2.1 [p. 94]) in 2002 April, for each plot are shown in the top-left corner and the catalogue stars plotted were extracted in a 5′ radius around those coordinates.

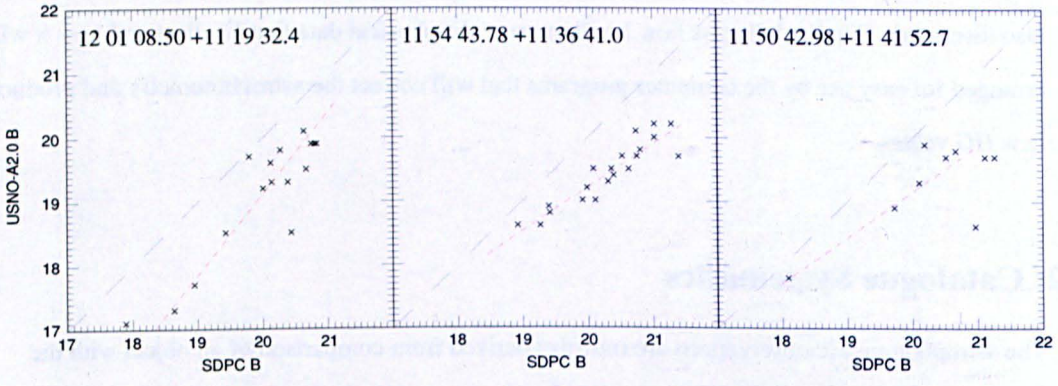

Figure 3.1: Examples of poor quality of astrometric-catalogue magnitudes

The method for correcting the catalogue systematic errors present in astrophotometric measures is as follows:

1 To correct an observed magnitude of a minor planet with position α, δ and magnitude m in band b and reduced with respect to reference catalogue C, extract stars from a photometric catalogue, P, in a radius r around α, δ.

2 Compare catalogue P's magnitudes in band b to the magnitudes of the same stars extracted from catalogue C.

3 Derive transformation equations relating the magnitudes of the stars as given in P to those as given in C.

4 With the transformation in hand, convert the observed magnitude of the minor planet.

5 Apply an observer-specific correction to the transformed magnitude.

The catalogues *C* are described in Section 3.7 [p. 55], while the steps necessary to produce *P*, the photometric catalogue and the associated combined photometric–astrophotometric catalogue, are described in Chapter 4 [p. 73]. The reduction procedures for both the catalogue and observer-specific corrections are discussed in Chapter 6 [p. 117]. In order to be able to apply the correction described above, it is necessary to know which astrometric reference catalogue was used for each astrophotometric observation. This is addressed in Section 3.6 [p. 54].

3.3: Observer Systematics

Even a cursory examination of the astrophotometry of a handful of randomly chosen minor planets will show that there are many examples in which there are differences of one magnitude or more between observations of the same minor planet observed on the same night by different observers using the same astrometric reference catalogues. Table 3.1 illustrates one such example, (67496) 2000 RK_{31}, chosen at random[1]. All the observations listed are taken from *MPS* 124439.

Table 3.1: Example of inconsistent magnitude estimates

Date of observation (UTC)	Magnitude	Observing site
2005 01 13.36322	17.6 R	703, Catalina
2005 01 13.36837	18.5 R	683, Goodricke-Pigott Observatory, Tucson
2005 01 13.37257	17.7 R	703
2005 01 13.38171	18.9 R	683
2005 01 13.38193	18.0 R	703
2005 01 13.39130	18.6 R	703
2005 01 13.39512	20.5 R	683

The obvious conclusion is that these differences are, at least partly, due to differences in the way the various observers derive their astrophotometry. The reduction techniques used by some of the major professional minor-planet surveys are discussed in Section 5.2 [p. 93].

The observer-specific systematic errors cannot be considered until the catalogue systematic errors are removed. As noted in Section 3.5 [p. 54], for most observers, the relationship between the magnitude system of their astrophotometry and standard photometric systems is unknown. The typical observer's CCD-based magnitude system will usually be "nearly" *R*, since most CCDs have peak sensitivity in or

1 Strictly speaking, a pseudo-random fashion: I simply asked my wife to choose a number between 20000 and 180000!

near the *R* band. The observer-specific corrections are an attempt to correct the observer's magnitude system onto the standard Johnson-Cousins system.

Another observer-specific effect is an incorrect aperture-size selection during the measurement process. The choice of a correct aperture size is critical for high-precision photometry. For the astrophotometry, the aperture size used for determining each magnitude is unavailable. In most cases, the aperture size used is dependent on the reduction program used for the astrometry. Within each survey, any aperture-size-selection effect is likely to be unchanging with time, subject to there being no substantial change in the observational procedure, although there may be a magnitude-dependent component. As such, this effect can be considered to be part of the observer-specific correction applied for each observer.

3.4: Standard Photometric Systems

In order to be able to intercompare magnitude estimates made by different observers with different equipment at different times, it is necessary to know what wavelengths of light are transmitted by any filters used and how the detectors respond to different wavelengths of light. Numerous different standard photometric systems have been developed. The Asiago Database on Photometric Systems (Moro and Munari, 2000) lists the parameters that describe 167 photometric systems developed between 1940 and 1999. Many of these photometric systems are poorly defined, and Moro and Munari only included information that was present in the article that introduced the new photometric system.

3.4.1: Johnson *UBVRI*

The first standardized photometric system based on photoelectric observations was the Johnson-Morgan *UBV* (usually referred to as simply Johnson *UBV*) broad-band system (Johnson and Morgan, 1951, 1953). The Johnson system is defined such that α Lyrae (Vega) has $V = 0.03$, with $U-B = B-V = 0$. The three defined bands (see Figure 3.2) were *U* (ultraviolet, peak response at ~ 350 nm, with FWHM 70 nm), *B* (blue, ~ 440 nm, 99 nm) and *V* (visual, ~ 550 nm, 87 nm). The *U* and *B* bands approximated the photographic systems then in use, while the *V* band approximated the visual response of the human eye. The major problem with the Johnson *UBV* system is that the short-wavelength cut-off of the *U* filter is determined by the transmission of the terrestrial atmosphere at those wavelengths, rather than by the filter itself. As a result *U*-band magnitudes can vary with the local weather conditions and altitude of the observing site. The *UBV* magnitudes were

to be reported for an airmass of zero (i.e., exoatmospheric, as measured outside the earth's atmosphere). The Johnson-Morgan bands were defined using a 1P21 photomultiplier and various Corning filters (*U*, Corning 9863; *B*, Corning 5030 + Schott GG13; *V*, Corning 3384). Johnson (1965) extended the system towards the red using an ITT FW-118 photoelectric detector with an S-1 photocathode and defined two bands (included in Figure 3.2): *R*, peak response at ~700 nm, with FWHM ~210 nm; and *I*, ~900 nm, ~220 nm.

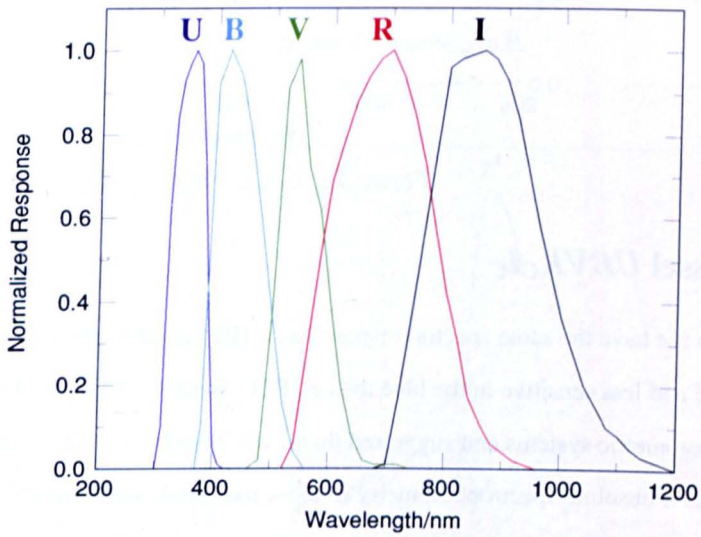

Figure 3.2: Johnson UBVRI bands

3.4.2: Cousins R_CI_C

Noting that the S-1 photocathode used in the definition of the Johnson *RI* system had poor efficiency in the (near) infrared, Cousins (1976) devised a new *RI* system defined using a GaAs photocathode, which was far more sensitive in the infrared. To distinguish the new system from the Johnson *RI* system, the Cousins bands are denoted R_C and I_C. The Cousins bands have peak responses and FWHMs as follows (see Figure 3.3 [p. 52]): R_C, ~ 600 nm, 152 nm; I_C, ~ 765 nm, 109 nm. A photographic version of the Cousins R_CI_C system was defined by Bessel (1990). The combination of Johnson *UBV* and Cousins R_CI_C is known as the Johnson-Cousins system.

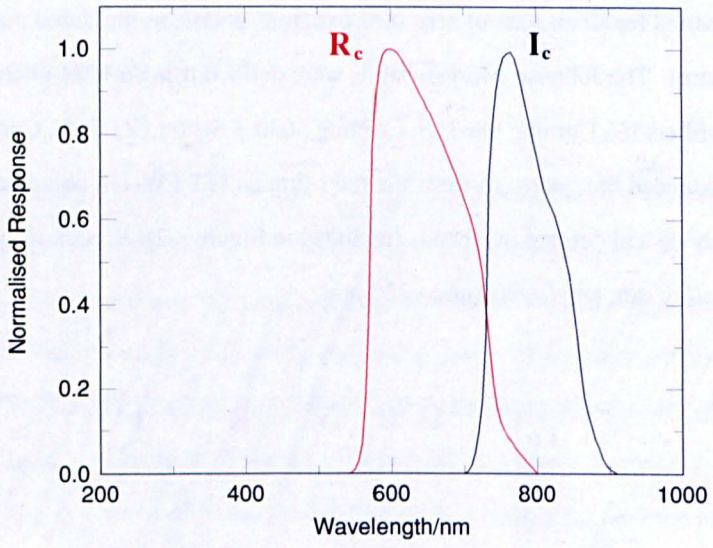

Figure 3.3: Cousins R_CI_C bands

3.4.3: Bessel *UBVR$_C$I$_C$*

CCDs do not have the same spectral response as a 1P21 photomultiplier. CCDs are more sensitive in the red and less sensitive in the blue than a 1P21. Bessel (1990) noted the poor definition of many photometric systems and suggested that it was possible to recover information on unknown passbands if absolute spectrophotometry in those passbands was available for standard stars, at least for stars with non-extreme colours. Applying his method to the Johnson-Cousins system, Bessel made recommendations for various filter combinations that allow various detectors to match the Johnson-Cousins *UBVR$_C$I$_C$* system, as shown in Figure 3.4.

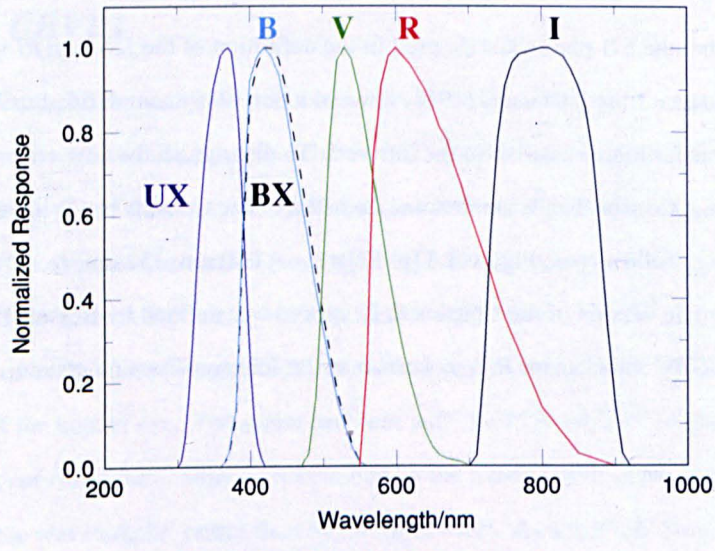

Figure 3.4: Bessel UBVR$_C$I$_C$ bands

3.4.4: Sloan *u′g′r′i′z′*

The photometric system for the Sloan Digital Sky Survey (Fukugita *et al.*, 1996) comprised five colour bands (u', g', r', i', z') that covered the entire wavelength range that is observable by silicon CCDs. The centre wavelengths and FWHMs (in nm) of the five filters (see Figure 3.5) are: u', 350, 60; g', 480, 140; r', 625, 140; i', 770, 150; and z', 910, 120. The filters are broader than the Johnson-Cousins filters, to allow greater efficiency in detecting faint sources. Sloan magnitudes are in the AB system (Oke, 1974), which is defined such that $m_{AB} = -2.5 \log(f) - 48.60$, where the flux f is measured in erg sec^{-1} cm^{-2} Hz^{-1} and the constant defines $m_{AB} = V$.

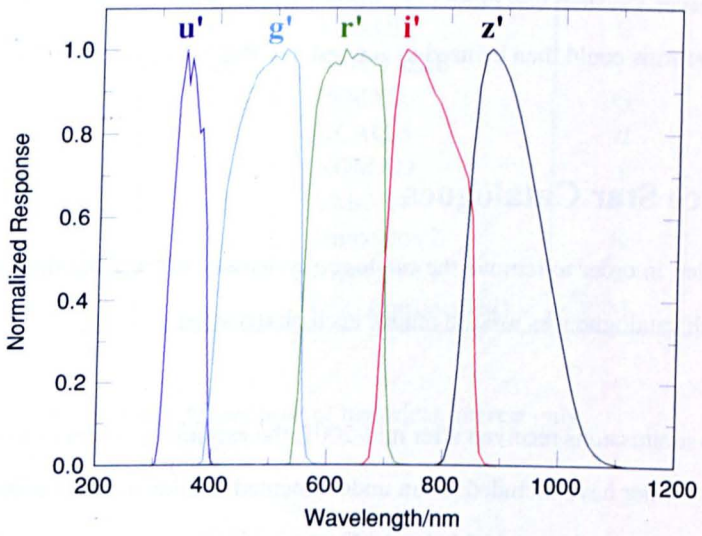

Figure 3.5: Sloan photometric bands

3.4.5: Conversions between AB and Johnson-Cousins Magnitudes

Conversions between AB and Johnson-Cousins magnitudes are given by Frei and Gunn (1994):

$$\left.\begin{aligned} V &= V_{AB} + 0.044 \\ B &= B_{AB} + 0.163 \\ R_C &= R_{C\,AB} - 0.117 \\ I_C &= I_{C\,AB} - 0.342 \end{aligned}\right\} \qquad (3.1)$$

These conversion values are implicitly included in Equations 4.1 [p. 76] and 4.2 [p. 76] and in the empirical filter corrections given by Equation 3.2 [p. 68].

3.5: Astrophotometric Systems

In practice, the astrophotometric systems are ill-defined. Although magnitudes reported to the MPC on the astrometric observation records are labelled (primarily) *R* or *V*, these labels are only approximations. No astrometric observer, to my knowledge, places their astrophotometric observations on to standard systems. Each observer's photometric system is different, defined by the make of the CCD, the optical properties of their telescope and the reduction technique used by the program that processes the images. Ideally, all observers would determine transformations between their single-passband magnitude system and standard photometric systems by observing a number of Landolt standard fields. Such transformations would relate the observer's magnitude to a standard magnitude and a standard colour: e.g., if an observer's system was close to *R*, the transforms would relate R_{OBSERVER} to *R* and either *V–R* or *R–I*. The transforms could then be used to convert any R_{OBSERVER} magnitude to *R*.

3.6: Reference Star Catalogues

As noted earlier, in order to remove the catalogue systematic errors from the astrophotometry, one needs to know which catalogue was used to reduce each observation.

Starting with submissions received after mid-2001, the astrometric observation records archived by the Minor Planet Center have included, as an undocumented feature and only if the observer reported the information in a form understandable by the Center's automated processing routines, the reference catalogue used to reduce the observations. I added the catalogue information to earlier-reported observations by scanning (manually) the observatory code headers published in the *Minor Planet Circulars*; while not complete, this effort extended substantially the availability of this useful information. The catalogue information is encoded in a single alphabetic character stored in column 72 on each observation record. The initial rationalisation for including this information was that the small differences between the reference systems used by different catalogues could be removed by the application of zonal corrections. Although studied intensively in the early twentieth century, the use of zonal corrections has fallen out of fashion in recent years. The recording of the astrometric catalogue used in the reduction also has uses in the thesis, as it allows me to know which catalogue was used to derive each astrophotometric observation.

The column-72 characters used on the astrometric observation records are shown in Table 3.2. The inclusion of Table 3.2 in this thesis is the first full and correct documentation of this encoded character, although a partially-incorrect (and unexpected) documentation of this column was given in Chesley *et al.* (2010), which was based on information I supplied to the lead author.

Table 3.2: Catalogue codes used on MPC astrometric observation records

Char	Catalogue	Char	Catalogue	Char	Catalogue
a	USNO-A1.0	n	SDSS-DR8	A	AC
b	USNO-SA1.0	o	USNO-B1.0	B	SAO 1984
c	USNO-A2.0	p	PPM	C	SAO
d	USNO-SA2.0	q	UCAC-4	D	AGK3
e	UCAC-1	r	UCAC-2	E	FK4
f	Tycho-1	s	USNO-B2.0	F	ACRS
g	Tycho-2	t	PPMXL	G	Lick Gaspra
h	GSC-1.0	u	UCAC-3	H	Ida93
i	GSC-1.1	v	NOMAD	I	Perth 70
j	GSC-1.2	w	CMC-14	J	COSMOS
k	GSC-2.2	x	Hipparcos 2	K	Yale
l	ACT	y	Hipparcos 1	L	2MASS
m	GSC-ACT	z	GSC (unspecified)	M	GSC-2.3

Many of the catalogues listed in Table 3.2 are now of historical interest only.

3.7: Review of Relevant Astrometric Catalogues

A large number of different astrometric catalogues have been used by astrometric observers over the past two hundred years. Some recent catalogues, those used for the majority of reductions of minor-body astrometric observations over the past twenty years, are described briefly below. The GSC and USNO catalogues are derived from measurements of digitized photographic plates, taken primarily at Palomar (the first and second Palomar Sky Surveys), Siding Spring (the AAO and SERC surveys) and the European Southern Observatory. Unfortunately, published descriptions of some of these catalogues are limited to popular reviews or brief abstracts in publications such as the *Bulletin of the American Astronomical Society.*

3.7.1: Guide Star Catalogue 1/2

The Guide Star Catalogue, as its name suggests, was created to support operations of the Hubble Space Telescope (HST). In order to find and track a target, HST had to locate two guide stars (with known positions) near to the target. HST's small field of view required a star catalogue with a sky density of ~100 stars per square degree. In 1979, when the HST guidance system was being designed, there was no such catalogue. The Space Telescope Science Institute decided to produce an all-sky catalogue from scans of 1477 photographic plates (Lasker *et al.*, 1990). The resulting V1.0 catalogue contained 18819291 objects (both stellar and non-stellar) as faint as 15th magnitude, reduced with respect to SAO and AGK3 reference stars. The astrometric positions were good to ± 0″.5, although there were significant astrometric problems with objects near the edges of the plates, sometimes amounting to more than 2″. The GSC-1 reported a single photographic magnitude for each detection, along with a flag that indicated which band was used. In the GSC 1 literature (Russell *et al.*, 1990) and associated data files, these bands are denoted by numeric codes. Bands 0, 3, 7, 11 and 18 are treated as *B*, bands 4, 6, 10 and 16 as *V*, and bands 1, 5, and 8 as *R*.

There are several later (and larger) versions of the GSC: the GSC-2.2 contains 455851237 objects and the GSC-2.3 contains 945592683 objects. Both catalogues are based on the same data, but the GSC-2.2 limited entries to objects brighter than $R = 18.5$ and $B = 19.5$, whereas GSC-2.3 had limits $R = 20.5$ and $B = 21.5$. Both catalogues were reduced with respect to the ACT and Tycho 2 catalogues and the astrometric positions are good to ± 0″.3, with the plate-edge problems reduced to ± 0″.75. Up to five magnitudes are reported for each entry, in bands denoted as V_{12}/V_{495}, B, B_J, R_F and I_N. Figure 1 of Lasker *et al.* (2008) compares the GSC-2 bands to standard photometric bands. The V_{12}/V_{495} bands approximate the Johnson *V* band. The B_J band is a wide band that overlaps the Johnson *B* band and about half the Johnson *V* band. The R_F band is a much narrower band than the Cousins R_c band and peaks about 70 nm further into the red. The I_N band is a good match for the Cousins I_c band. Objects with GSC-2 *B*-band magnitudes are either bright stars inserted from the Tycho catalogue or measurements taken from blue-sensitive plates. As a result of an oversight during preparation of the photometric catalogues (see Chapter 4 [p. 73]), the GSC-2 *B* magnitudes were omitted from the photometric catalogues described in Section 4.7 [p. 87]. In retrospect, this has not turned out to be a major issue, as very few observations have been reduced with respect to the GSC-2 to date (see Table 4.1 [p. 74]) and it is unlikely that this catalogue will get much usage in the future.

3.7.2: Tycho-1/2

The Tycho catalogues are based on observations with the Hipparcos astrometric satellite, which operated from 1989 to 1993. The Tycho-2 catalogue (Høg *et al.*, 2000) contains 2539913 stars down to a limiting magnitude $V_T \sim 12.5$, with a positional accuracy of ± 0".06, a proper-motion accuracy of ± 0".0025/yr and a photometric accuracy of ± 0.10 magnitudes in a photometric system that approximates Johnson *V*. The data in both catalogues are based on the same observational data, but the Tycho-2 catalogue contains more objects and is slightly more accurate owing to more advanced reduction techniques.

3.7.3: ACT

The USNO ACT catalogue (Urban *et al.*, 1997) contains 988758 stars. It was prepared by combining new reductions of the Astrographic Catalogue with the Tycho-1 catalogue.

Although not used directly by modern astrometric observers, it is worth making note of the Astrographic Catalogue (AC). The AC was part of the international Carte du Ciel project, formulated at a meeting held at the Paris Observatory in 1887. The plan was to photograph the entire sky, measure the positions of every star down to 11th magnitude and produce charts showing every star down to 14th magnitude. Such a project was beyond the capability of any one observatory, so the sky was split up into declination bands of varying widths, each of which was assigned to a participating observatory. The bulk of the photograph plates were exposed between 1892 and 1920, but measurement of the plates took, in some cases, decades. In all, some 4.6 million stars, many as faint as 13th magnitude, were measured. The positions were published as rectangular coordinates along with the plate constants required to produce right ascensions and declinations. In recent years the published rectangular coordinates have been re-reduced by the US Naval Observatory. The resulting catalogue has been very useful in providing early-epoch positions for determining proper motions.

3.7.4: GSC-ACT

The GSC-ACT (Gray, 1999) is based on GSC-1.1, astrometrically recalibrated using the Tycho-1 catalogue and higher-order fits. The recalibration reduced the systematic errors present in the

GSC-1.1 to essentially zero, and while the uncertainty in the positions of individual stars in GSC-ACT (± 0″.3, almost completely random error) is not improved much over that in GSC-1.1, the use of many GSC-ACT stars in astrometric solutions allows positions to be determined with an uncertainty of ± 0″.1. The catalogue contains 25 541 952 stars.

3.7.5: USNO-(S)A1.0/2.0

The USNO-A1.0 (Monet *et al.*, 1996) contains 488 006 860 objects with typical astrometric accuracy of ± 0″.25 and photometric accuracy of ± 0.25 mag. The astrometric calibration was performed using GSC-1.1 stars. The only requirement for inclusion in the catalogues was that a source be coincident (within 2″) on both a red-sensitive and a blue-sensitive photographic plate. Two magnitudes are reported for each entry: *B*, taken from the blue-sensitive plate; and *R*, taken from the red-sensitive plate.

The SA1.0 catalogue contains 54 787 624 objects, extracted from the A1.0 catalogue, intended to be distributed uniformly across the sky in the magnitude range 16 to 19.

The USNO-A2.0 catalogue (Monet *et al.*, 1998) was an extension to A1.0 and contains 526 230 881 objects. The astrometric calibration is in the ICRF system as utilised in the USNO ACT (Urban *et al.*, 1997) catalogue, using the same plate measurements that were used for A1.0. The only requirement for inclusion in the catalogues was that a source be coincident (within 2″) on both a red-sensitive and a blue-sensitive photographic plate. Two magnitudes are reported for each entry: *B*, taken from the blue-sensitive plate; and *R*, taken from the red-sensitive plate.

The SA2.0 catalogue contains 55 368 239 objects, extracted from the A2.0 catalogue in a similar fashion to the SA1.0 extraction.

3.7.6: USNO-B1.0

The third-generation digitized-photographic USNO catalogue, the USNO-B1.0 (Monet *et al.*, 2003) contains 1 042 618 261 objects measured from scans of 7435 plates. It claims to "provide all-sky coverage, completeness down to $V \sim 21$, ± 0″.2 astrometric uncertainty at J2000.0, ± 0.3-mag

photometric uncertainty in up to five colors and 85% accuracy for distinguishing stars from nonstellar objects". The astrometric accuracy of the B1.0 is a significant improvement over that of the A-1.0 and A-2.0 catalogues. Up to five magnitudes are reported: one or two *B* magnitudes from blue-sensitive plates; one or two *R* magnitudes from red-sensitive plates; and up to one I_N magnitude.

3.7.7: UCAC-1/2/3

The USNO CCD Astrograph Catalogues are based on measures of CCD frames taken with the U.S. Naval Observatory's 0.2-m f/10 twin astrograph. The catalogues have a limiting magnitude of $R \sim 16$. The current-epoch CCD observations were combined with positions from over 140 earlier catalogues to derive proper motions. Observations began in 1998 February at Cerro Tololo Inter-American Observatory (Chile), surveying from the south celestial pole to $\delta \sim +30°$ (dependent on R.A.). When southern surveying was complete, the telescope was moved to the USNO Flagstaff Station (Arizona), where the remainder of the northern hemisphere was surveyed. The surveying phase was completed in 2004 May.

The UCAC-1 catalogue (Zacharias *et al.*, 2000) was based on survey data through 1999 November 8 and contains 27 425 433 objects from the south celestial pole to an R.A.-dependent upper limit of $-21° < \delta < -6°$. The UCAC-1 has a positional accuracy of ± 0″.02 at $R = 10$ to ± 0″.07 at $R = 16$, proper-motion uncertainty better than ± 0″.015 yr^{-1} and photometric uncertainty of ± 0.3 mag in a band about halfway between *V* and *R*.

The UCAC-2 catalogue (Zacharias *et al.*, 2004a) was based on survey data through 2002 December 7 and contains 48 330 571 objects from the south celestial pole to an R.A.-dependent upper limit of $+40° < \delta < +52°$. The UCAC-2 reduction procedures were improvements over those used for UCAC-1. UCAC-2 has similar positional and photometric accuracy to the UCAC-1, with proper-motion uncertainty of ± 0.007″ yr^{-1}.

The UCAC-3 catalogue (Zacharias *et al.*, 2009) was the long-awaited all-sky version and was released at the 2009 IAU General Assembly in Rio. It contains 100 776 420 objects in the survey magnitude range 8–16, with positional errors under 0″.02 for objects brighter than mag. 14 and

proper motions given for 95% of the entries. Initial reactions to the new catalogue among the minor-planet astrometric community were mixed, following the discoveries that roughly one million stars that were in UCAC-2 were missing from UCAC-3, and that there were a significant number of erroneous proper motions. A further iteration of the catalogue, the UCAC-4, which will include measures from more old plate material in order to improve the proper motions, was announced prior to the release of the UCAC-3.

3.7.8: CMC-14

The Carlsberg Meridian Catalogue (Evans *et al.*, 2002) contains entries for 95 858 475 objects with $-30° < \delta < +50°$ and Sloan r' magnitudes in the range 9 to 17. The catalogue was constructed from observations obtained with the Carlsberg Meridian Telescope, a CCD-equipped 0.178-m f/15 refractor operated in drift-scan mode and located on La Palma. The astrometric and photometric accuracies range from $\pm 0''.047$ and ± 0.025 mag. at $r' = 13$, to $\pm 0''.108$ and ± 0.170 mag. at $r' = 16$. The entry for each star in CMC-14 includes the H, J and K magnitude extracted from the 2MASS catalogue.

3.7.9: NOMAD

The USNO Merged Astrometric Dataset (NOMAD) (Zacharias *et al.*, 2004b) is a merged catalogue, built by selecting stars from a number of compiled catalogues (including Tycho-2, UCAC-2 and USNO-B1.0). It contains 1 117 612 732 objects, each entry inheriting the properties and uncertainties from the original source catalogue. For the purposes of this thesis, observations reduced with respect to the NOMAD catalogue will be treated as if the USNO-B1.0 catalogue was used, since this latter catalogue supplied 88.8% of the astrometric positions, 60.4% of the B magnitudes and 89.4% of the R magnitudes.

3.8: Taxonomic Classifications

I collected minor-planet taxonomic classifications, in both the Tholen (1984) and Bus and Binzel (2002) schemes, from a hierarchy of sources in the published literature. The hierarchy is listed in descending order in Table 3.3. Where a specific object has classifications in both schemes, I prefer use of the Bus

and Binzel classification when processing the observations of that object.

Table 3.3: Hierarchy for taxonomic classifications

Order	Reference	Scheme(s)	Number
1	Tholen (1984)	Tholen	974
2	Bus and Binzel (2002)	Bus-Binzel	1444
3	Lazzaro *et al.* (2004)	Bus-Binzel	820
4	Karlsson *et al.* (2009)	Tholen, Bus-Binzel	27
5	Fornasier *et al.* (2004, 2007)	Tholen	76
6	Dahlgren and Lagerkvist (1995)	Tholen	4
7	Masi *et al.* (2008)	Pseudo-Tholen	39 752

The Masi *et al.* (2008) classifications are based on assigning taxonomic classes by using colours derived from the five Sloan-band photometric measurements of objects in the SDSS Moving Object Catalogue (Ivezić *et al.*, 2002), hereafter MOC, and comparing them with the colours of objects classified by Bus and Binzel (2002). The classifications were rather coarse and limited to just types C, S and V. A total of 42 626 classifications were reported. After removing multiple classifications for the same objects (rejecting the object completely if the multiple classifications differed) and rejecting those that had no type reported, I was left with 39 752 objects. As a result of the limited number of types included in the Masi results, I label them as pseudo-Tholen.

Warner *et al.* (2009) pointed out that the Masi classifications can help distinguish between S- and E-type Hungarias. The Hungarias are a mix of family members and orbital group members. The Hungarias are the objects in non-Mars-crossing orbits that are constrained by the 4:1 mean-motion resonance with Jupiter and the ν_5, ν_6 and ν_{16} secular resonances (see Appendices 3.5 [p. 220]and 3.6 [p. 221]). Within this group is a collisional family (Williams, 1979). The family members are type E. The orbital group members are mostly type S, with a few non-family E types. In the Masi classification, a type E would be classified as type C, therefore any Hungarias classified as type C by Masi are probably type E. I adopted this reclassification in my processing of the Masi classifications.

3.8.1: Taxonomic Classifications from NEOWISE Albedos

Recent results from the Wide-Field Infrared Survey Explorer (NEOWISE) space mission include albedo determinations for 131 927 minor planets (Masiero *et al.*, 2011, Grav *et al.*, 2011, Mainzer *et*

al., 2011, Grav *et al.*, 2012). These albedo data can be used to generate coarse taxonomic classifications (Warner *et al.*, 2009), specifically C (albedo range 0.037–0.077), S (0.130–0.276) and E (0.411–0.547). For Jupiter Trojans, class C can be distinguished from class D (0.038–0.060). The albedo data files from the four referenced papers were downloaded from the *Astrophysical Journal* website. The four files were combined into one. This 141 709-line file was then processed, converting the given visual albedo data for each object into a taxonomic classification and updating the designations for those objects newly numbered or identified with other unnumbered objects since the NEOWISE team prepared the data files. For 9782 objects, there were two entries in this combined file. Objects with albedos outside the ranges specified above were ignored, while identical classifications for the same object were combined. An object was also ignored if it had two entries showing different classifications. This left unique taxonomic classifications for 68 404 numbered minor planets. I treat the NEOWISE-albedo taxonomic classifications as "pseudo-Bus-Binzel". For 943 objects that already had a Bus-Binzel classification I removed the NEOWISE determination. The remaining 67 461 classifications were adopted for use in this thesis.

The objects that fell outside the above-listed albedo ranges were divided more coarsely into taxonomic classes S and C. If the albedo was between 0.1 and 0.3, then the object was assumed to be class S; if 0.1 or less, class C. There were 23 958 entries in the output file, which reduced to 23 172 entries after identical classifications for the same object were combined. There were 264 objects with two classifications that differed. The removal of those objects left 22 644 objects. Of these, 2046 already had Bus-Binzel classifications and were removed from the file to be inserted. The remaining 20 598 entries were adopted for thesis use.

3.8.2: Adopted Taxonomic Classifications

Where there is no published taxonomic classification for a particular minor planet, I adopted a classification based on family or orbital group membership. The classifications described for family and orbital group members (Table 3.4) and for various orbital types (Table 3.5) are based broadly on those defined by Warner *et al.* (2009). The orbital parameters used for the family and group classifications are: a, semimajor axis (in astronomical units); e, eccentricity; and i, inclination (in degrees). The abbreviations used in Table 3.5 are Near Earth Asteroid (NEA), Main Belt (MBA), Scattered Disk Object (SDO) and Trans-Neptunian Object (TNO). Additional orbital elements used

in Table 3.5 are: q, perihelion distance (in astronomical units); and Q, aphelion distance (in astronomical units).

Table 3.4: Adopted taxonomic classes for family and group members

Family/ Orbital Group	Orbital Parameters	Class
Hungaria	$1.78 < a < 2.0, e < 0.18, 16 < i < 34$	E
Flora	$2.15 < a < 2.35, 0.03 < e < 0.23, 1.5 < i < 8$	S
Vestoid	$2.26 < a < 2.48, 0.03 < e < 0.16, 5 < i < 8.3$	S
Phocaea	$2.25 < a < 2.5, e \geq 0.1, 18 < i < 32$	S
Erigone	$2.32 < a < 2.40, 0.15 < e < 0.22, 4 < i < 6$	C
Nysa	$2.4 < a < 2.5, 0.12 < e < 0.21, 1.3 < i < 4.3$	S
Eunomia	$2.53 < a < 2.72, 0.08 < e < 0.22, 11 < i < 16$	S
Koronis	$2.83 < a < 2.91, e < 0.11, i \leq 3.5$	S
Eos	$2.99 < a < 3.03, 0.01 < e < 0.13, 8 < i < 12$	S
Themis	$3.08 < a < 3.24, 0.09 < e < 0.25, i \leq 3$	C

Table 3.5: Adopted taxonomic classes for various orbital types

Orbital Type	Orbital Parameters	Class
NEA	$q < 1.3$	S
Mars Crosser	$1.3 \leq q < 1.668, Q < 5.0$	S
Jupiter Trojan	$4.95 \leq a < 5.4, e < 0.25$	D
Centaur/SDO	Planet crossing with $a > 5.2$	C
TNO	$a > 30$	C
Other	Anything not covered above	C

For objects that do not fit into any of the above classifications, the adopted taxonomic classifications will be assumed to be S for $a < 2.7$ AU, otherwise C.

3.9: Colours

In a similar fashion to the taxonomic classification, I collected published minor-planet colours from a hierarchy of sources. The hierarchy is listed in descending order in Table 3.6 [p. 64], which indicates, for each reference, the number of objects and the range of colours present. While there are a number of large collections of *U–B* and *B–V* colours in the literature, there do not appear to be similar collections of *V–R* and *R–I* (or *V–I*) colours. Collection of most of the *V–R* and *R–I* colours for this thesis has involved extracting colours for one or a handful of objects from numerous published papers.

The penultimate entry in Table 3.6 combines a large number of literature references into one table entry. Most of the references combined into this entry contained colours for only one or two objects. To list all of these references separately in the table would have resulted in a table that stretched across many pages.

Determination of colours involving Sloan bands cannot be made until after the photometric catalogues have been built. Discussion of such colours will be deferred until Section 6.8 [p. 140].

Table 3.6: Hierarchy for colours

Order	Reference	Number of objects	Colours
1	Tedesco (1975)	1021	*U–B, B-V*
2	TRIAD	28	*U–B, B–V*
3	Karlsson *et al.* (2009)	27	*U–B, B–V, V–R, R–I*
4	Fornasier *et al.* (2004, 2007)	76	*B–V, V–R, R–I*
5	Piironen *et al.* (1998)	33	*U-B, B-V, V-R, R-I*
6	Hansen (1976)	60	*V–R, R–I*
7	Lagerkvist *et al.* (1998)	16	*B–V*
8	Warner (2007)	60	*V–R*
9	Dandy *et al.* (2003)	60	*B–V, V–R, V–I*
10	Sheppard (2010)	33	*B–V, V–R, R–I*
11	See Appendix 4	many	*U–B, B–V, V–R, R–I*
12	This work	104 415	*U–B, B–V, V–R, R–I*

I determined the bulk of the colours listed in Table 3.6 from the photometric observations included in the MOC. The catalogue contains 471 569 observations of moving objects, 220 101 of which have been identified with known objects. For each identified object, I converted the SDSS-band magnitudes to *UBVRI* using the transformation equations of Jester *et al.* (2005) and derived the *U–B*, *B–V*, *V–R* and *R–I* colours. Since I am interested in using these colours only for objects with normal colours, I rejected individual colour measurements if they were outside the normal range for that colour. Although this approach rejected the rare object with extreme colours, it also rejected the far more common case of objects with erroneous extreme colours. To determine what constitutes a "normal" range for each colour, I examined the measured colours extracted from the literature and counted how many objects appeared in each 0.01-magnitude bin and displayed the data graphically (see Figure 3.6).

Many objects appear more than once in the MOC. In such cases, the individual colours from each observation were averaged, removing obvious outliers via an iterative process that rejected individual measurements that were more than 0.1 mag. away from the previous iteration's mean. The 220 102 identified observations were reduced to 218 272 observations with at least one colour in the allowable range. The number of individual objects represented was 104 420, of which four were rejected because the individual colour measurements were too discordant and one was rejected because the designation used in the MOC has been deleted by the Minor Planet Center.

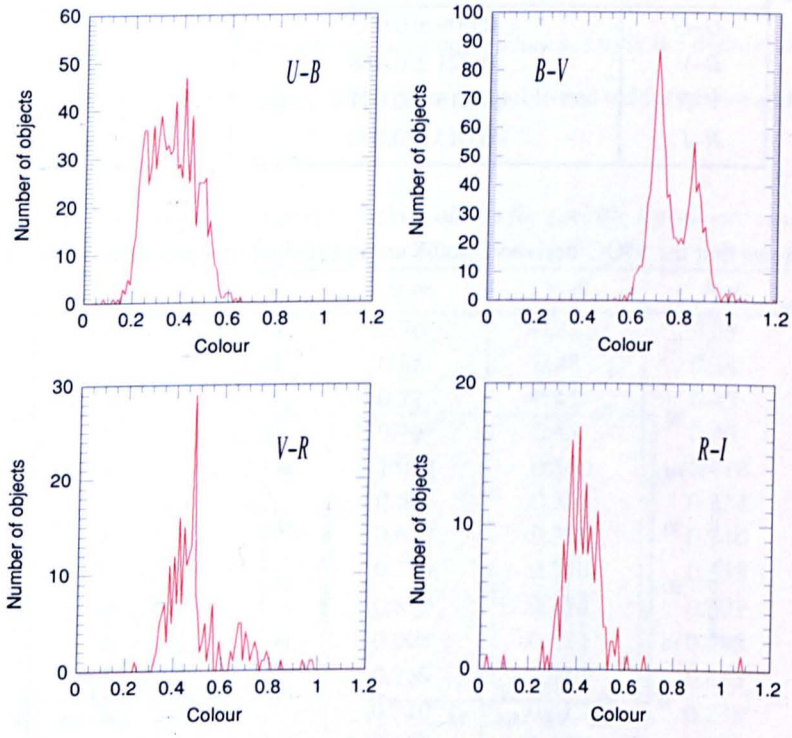

Figure 3.6: Colour ranges from MOC observations

Table 3.7 shows the allowable range of colours I used to trim the MOC-derived colours, as determined by visual examination of Figure 3.6.

Table 3.7: Allowable ranges for SDSS MOC colours

U–B	*B–V*	*V–R*	*R–I*
0.15–0.62	0.60–1.00	0.33–0.80	0.25–0.55

There are 1159 objects with at least one colour extracted from the literature and 196 of these are present and have at least one colour determination in the MOC. I needed to confirm that the MOC-derived colours have at least some basis in reality, so I examined the differences, in the sense MOC minus literature value, for each of the four colours. The means and standard deviations of the differences, along with the number of matching objects, for each colour are given in Table 3.8.

Table 3.8: Colour differences (MOC minus literature)

Band	Mean and s.d. of differences	Number of objects
U–B	0.009 ± 0.053	152
B–V	0.021 ± 0.068	190
V–R	–0.015 ± 0.071	32
R–I	–0.013 ± 0.074	31

Table 3.8 shows that the MOC-derived colours are in satisfactory agreement with colours extracted from the literature.

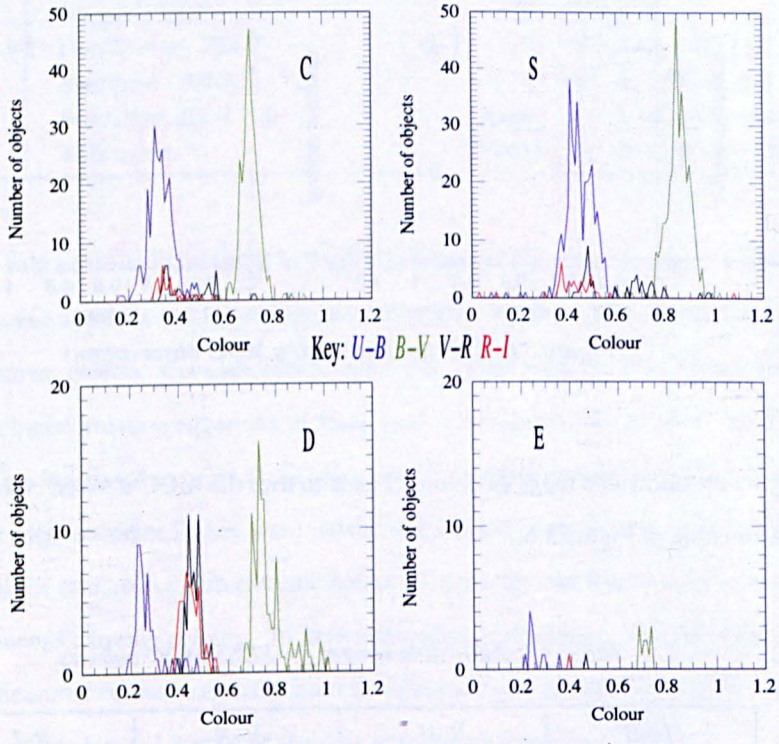

Figure 3.7: Colour range for various taxonomic types

3.9.1: Default Colours

In the absence of colour-index information for specific objects, I adopted default colours for objects for each of the main taxonomic classes. These default colours are derived from considering the range in each colour from the data collected from the literature. The MOC-derived colours are not included in this analysis. The colour ranges for each of the main taxonomic types are shown in Figure 3.7.

Table 3.9 lists the adopted colours for the main taxonomic types (C, S, D and E) as determined from examination of Figure 3.7. For other Tholen taxonomic classes, I took the default values from Dandy *et al.* (2003), deriving the values of *R–I* from the published values of *V–I* and *V–R*.

Table 3.9: Adopted Johnson-Cousins colours for specific taxonomic classes

Type	*U–B*	*B–V*	*V–R*	*R–I*
C	0.30	0.70	0.35	0.35
S	0.40	0.85	0.48	0.38
D	0.25	0.72	0.45	0.45
E	0.22	0.70	0.45	0.40
A		1.018	0.560	0.418
B		0.666	0.361	0.334
F		0.633	0.366	0.346
G		0.739	0.370	0.358
Q		0.817	0.424	0.301
R		0.905	0.479	0.288
T		0.769	0.447	0.463
V		0.810	0.413	0.238
X		0.697	0.410	0.408

In the absence of information on the taxonomic class for a specific object, Table 3.10 lists the default corrections used to reduce non-*V*-band observation to *V*. The values for the Sloan bands are derived from Equation 3.2 [p. 68], using default values for *B–V*, *R–I* and *U–B* derived from Table 3.10.

Table 3.10: Default colour corrections

Band	*V*–band correction
U	–1.30
B	–0.80
g	–0.38

V	0.00
r	+0.26
R	+0.40
C	+0.40
W	+0.40
i	+0.43
z	+0.51
I	+0.80
J	+1.20

It should be noted that colour indices are slightly dependent on phase angle, as first noted by Gehrels (1970). Gehrels observed an increase (or reddening) of the colour indices with increasing phase angle for the moon and several minor planets, and quoted an average value of +0.002 mag/° for the change in *B–V*. Using Gehrels' value, this effect amounts to a change in *B–V* of only 0.05 mag at $\beta = 25°$ and so will be ignored for this study. This is a reasonable decision as the colour-index behaviour with phase is not known for more than a handful of objects. Consideration of the effect of variable colour indices can be included in future studies.

3.9.2: Deriving *V*–Sloan Corrections

I derived relations relating the *B–V* and *R–I* colours and SDSS-band magnitudes to *V* from Jester *et al.* (2005):

$$\left.\begin{aligned} V-g &= -0.60\,(B-V) + 0.12 \\ V-r &= +0.42\,(B-V) - 0.11 \\ V-i &= +0.91\,(R-I) + 0.42\,(B-V) - 0.31 \\ V-z &= +1.72\,(R-I) + 0.42\,(B-V) - 0.52 \end{aligned}\right\} \qquad (3.2)$$

For objects with a taxonomic classification, but without measured *B–V* and/or *R–I* colours, the Sloan to Johnson-Cousins conversions are taken from Table 3.11, which is derived from Equation 3.2 assuming the adopted default *B–V* and *R–I* colours for various taxonomic types given in Table 3.9 [p. 67].

Table 3.11: Adopted Johnson-Cousins–Sloan colours for specific taxonomic classes

Type	*V–g*	*V–r*	*V–i*	*V–z*
C	–0.30	+0.18	+0.30	+0.38
S	–0.39	+0.25	+0.39	+0.49
D	–0.31	+0.19	+0.40	+0.56
E	–0.30	+0.18	+0.35	+0.46
A	–0.49	+0.32	+0.50	+0.63
B	–0.28	+0.17	+0.27	+0.33
F	–0.26	+0.16	+0.27	+0.34
G	–0.32	+0.20	+0.33	+0.41
Q	–0.37	+0.23	+0.31	+0.34
R	–0.42	+0.27	+0.33	+0.36
T	–0.34	+0.21	+0.43	+0.60
V	–0.37	+0.23	+0.25	+0.23
X	–0.30	+0.18	+0.35	+0.47

3.9.3: Effect of Incorrect Taxonomic Classification on Colours

It is obvious that an incorrect taxonomic classification by the methods outlined in section 3.8 will have implications for the derived colours. An incorrect taxonomic classification will skew the conversion of all the magnitudes that require correction from a non-*V* band to *V*. The usual situation will be that this will affect only a fraction of the observations of most objects.

The error in a derived Johnson-Cousins colour is simply the difference in the colour correction for the (unknown) correct taxonomic class and the incorrect assumed class. For the Sloan colours, the errors in the colours due to an incorrect taxonomic classification are given by Equation 3.3:

$$\left.\begin{aligned} d(V-g) &= -0.60\, d(B-V) \\ d(V-r) &= 0.42\, d(B-V) \\ d(V-i) &= 0.91\, d(R-I) + 0.42\, d(B-V) \\ d(V-z) &= 1.72\, d(R-I) + 0.42\, d(B-V) \end{aligned}\right\} \qquad (3.3)$$

where *d(<colour>)* is the difference between the (unknown) correct taxonomic class and the incorrect assumed class.

Although the errors in the assumed colours can be found by examination of Table 3.9 and 3.11, it is instructive to list the errors in a separate table (see Table 3.12). The entries in the table are for the various combinations of the three main taxonomic classes.

Table 3.12: Errors in assumed colours for C, S and D types

Taxonomic Class		Error in assumed colour (correct minus assumed)						
Correct	Assumed	*B–V*	*V–R*	*R–I*	*V–g*	*V–r*	*V–i*	*V–g*
C	S	–0.15	–0.13	–0.03	+0.09	–0.07	–0.09	–0.09
C	D	–0.02	–0.10	–0.10	+0.01	–0.01	–0.10	–0.18
S	C	+0.15	+0.13	+0.03	–0.09	+0.07	+0.09	+0.09
S	D	+0.13	+0.03	–0.07	–0.08	+0.06	–0.01	–0.07
D	C	+0.02	+0.10	+0.10	–0.01	+0.01	+0.10	+0.18
D	S	–0.13	–0.03	+0.07	+0.08	–0.06	+0.01	+0.07

The absolute values of the majority of the entries in Table 3.12 are 0.1 mag. or less. As noted earlier (for most objects) not all the observations will be affected by any errors caused by incorrect taxonomic classification, so the resulting error in H will be < 0.1 mag.

3.10: Default Slope Parameters

When a slope parameter, G, has not been determined for a particular object, past practice at the Minor Planet Center has been to assume $G = 0.15$ (see note in Tedesco *et al.*, 1990). It is worth noting that in the original definition of the *HG* system the default value of G was 0.25 (Marsden, 1985), although it was remarked that, if further sophistication was desired, one could adopt $G = 0.15$, if the object was a member of the Nysa family or had $a > 2.7$ AU, or $G = 0.40$, if the object belonged to the Hungaria family. The Minor Planet Center adopted the single value $G = 0.25$ as the default for orbits computed after 1985 December, changing to the single value $G = 0.15$ in 1990 December. It is interesting to note that orbits computed at the Institute of Theoretical Astronomy, Leningrad, and published in both the *Minor Planet Circulars* and the *Ephemerides of Minor Planets*, used the sophisticated version of default G values from 1986 onwards.

Table 3.13 lists the adopted slope parameters for various taxonomic classes. I take the values from Warner *et al.* (2009), with one difference: type E is a separate entry.

Table 3.13: Adopted slope parameters

Taxonomic class	Adopted G
C, G, B, F, P, T, D	0.12
M	0.20
S, Q	0.24
V, R	0.43
E	0.48

For objects without a taxonomic classification, I assume $G = 0.24$ if $a < 2.7$ AU and $G = 0.12$ otherwise.

3.11: Storage of the Physical Parameters

For ease of handling, the taxonomic classifications and colours are stored in a single file, called `PHYSICAL.IDX`. This is a direct-access keyed-access indexed file, allowing a program to access any entry in the file very quickly by specifying a relevant index key value. Keyed-access files are an extension to the Fortran language (F77/F90/F95) standard that is present in the OpenVMS compiler. Keyed-access file support is also present in other languages under OpenVMS, as the handling of these special files is handled by a part of the OpenVMS operating system (OS) known as RMS (Record Management System). The inclusion of keyed-access file support as part of the OS means that users can use their preferred programming language to manipulate their data and do not have to resort to using a database, such as MySQL. A keyed-access file can be indexed using multiple keys, but here I use just one primary key, the packed designation of the minor planet.

For each object in `PHYSICAL.IDX`, the following information is stored: number or provisional designation; taxonomic classification in the Tholen scheme; taxonomic classification in the Bus and Binzel scheme; *U–B*; *B–V*; *V–R*; *R–I*; and codes indicating the source for each of the classifications and colours. A Fortran 95 program, called `PHYSICAL_IDX`, was written to manipulate the `PHYSICAL.IDX` file. The program allows the initialisation of the file, the insertion of new data, the removal of existing data and extraction of the entire data set as a text file. New entries for existing entries can either overwrite the existing entries, be merged with the existing entries or be ignored, depending on whether or not the program is called with the `REPLACE` or `MERGE` flags. New library subroutines were written to allow any program to open `PHYSICAL.IDX` for reading and to extract one or more physical parameters for a specific object.

4: Catalogue Preparation

4.1: Introduction

An obvious requirement for a project that involves correcting (astro)photometric measures is a reliable photometric catalogue that goes as deep and that covers as much sky as possible in as many standard magnitude bands as is practical. This chapter details the steps that were undertaken to produce four special photometric catalogues for use in this thesis: the SDPC (Sloan-Derived Photometric Catalogue) and the CDPC (CMC-14-Derived Photometric Catalogue), containing the multi-band photometry extracted from the SDSS (see Section 5.2.6 [p. 100]) and the CMC-14 (see Section 3.7.8 [p. 60]) data; and the ASTCAT-S and ASTCAT-C, which are versions of, respectively, the SDPC and the CDPC with photometric data from the astrometric reference catalogues added to each entry.

4.2: Initial Catalogue Planning

An initial aim was to obtain a catalogue of reliable photometric magnitudes (to ± 0.1 mag. or better) in several magnitude bands (*B*, *V*, *R* and *I*) that went as faint as $R = 20$ over as much of the celestial sphere as possible. Although there are numerous astrometric catalogues that cover the entire sky (e.g., USNO-Ax.0 and USNO-B1.0, see Sections 3.7.5 [p. 58] and 3.7.6 [p. 58]) and go deeper than $R = 20$, the photometry in these catalogues is known to be of rather poor quality as it was derived from photographic plates obtained with a number of different emulsions and filters. The UCAC catalogues are derived from CCD images, but the photometry is good to only ± 0.3 mag in a band somewhere between *V* and *R*. In the absence of a suitable existing catalogue, I had to derive my own catalogue(s).

Each of the two photometric catalogues that had to be produced needed to have a corresponding supplementary catalogue which contained, for each object in the photometric catalogue, the magnitudes for that object as listed in each of the astrometric catalogues that have been most used in the past few decades. The list of astrometric catalogues to be included was chosen by looking at which catalogues had been most used in recent years. The catalogues chosen were (in alphabetical order): GSC-1; GSC-2; GSC-ACT; UCAC-1; UCAC-2; USNO-(S)A1.0; USNO-(S)A2.0; and USNO-B1.0. Table 4.1 [p. 74] shows the count of observations of numbered minor planets reduced with respect to each of these

catalogues that are present in the files of the Minor Planet Center as of 2011 June 18. The total number[1] of observations of numbered minor planets was 70921566. Although these statistics pre-date the closing date for the usage of astrophotometric observations in this thesis, the counts are representative of the counts in the data files that were used.

Table 4.1: Astrometric catalogue usage

Catalogue	Number of observations
GSC-1	603 590
GSC-2	176
GSC-ACT	380 156
UCAC-1	187 580
UCAC-2	18 810 763
USNO-(S)A1.0	2 403 406
USNO-(S)A2.0	35 930 520
USNO-B1.0	8 156 726

In Table 4.1, the counts for the GSC-1 catalogue usage include 273 608 observations where the catalogue was reported as "GSC" without a version number. Most of these observations were probably made with respect to one of the GSC-1.x versions and will be treated as such. The count of GSC-2 usage looks low, but may be correct due to the difficulty of working with this catalogue as it was not generally available for complete download.

4.3: The loneos.phot List of Reliable Photometry

The loneos.phot list is a collection of stars with reliable photometry, compiled by Brian Skiff of Lowell Observatory. Brian Skiff has been a research assistant at the Lowell Observatory since 1976. He is an experienced photometric observer who has (co-)published a large number of photometric sequences for variable star (e.g., Skiff, 2000a, 2000b, 2000c, 2000d, 2000e, 2000f), minor-planet lightcurves (e.g., Warner *et al.*, 2011) and identifications of variable stars (e.g., Skiff and Williams,1997). The stars included in loneos.phot, in the range $7 < V < 21$, cover the whole sky and most entries have one or more colours listed to allow determination of B, R and I magnitudes. Skiff created the list by combining photometric measurements of a number of photometric standard stars from various Selected Areas with photometric measurements of a much larger number of stars extracted from numerous literature sources. The file is freely available at `ftp://ftp.lowell.edu/pub/bas/starcats/loneos.phot`. This

1 Strictly speaking, the total number of observation *lines*, since some observations (principally those obtained from earth orbit) are stored on two lines.

thesis uses a version dated 2003 July 15 that contains 33 921 objects. A references file is also available[2] listing the papers from which the photometric measurements were extracted.

4.4: 2MASS

The first published catalogue to be considered as the basis for one of the needed photometric catalogues was the all-sky 2MASS (Skrutskie *et al.*, 2006). A procedure for converting 2MASS *JHK* magnitudes into *BVRI* colours was demonstrated by Warner (2007). An examination of this procedure (see Appendix 7.3 [p. 230]) shows that the 2MASS catalogue alone is not a suitable source for the photometric catalogues required by this thesis.

4.5: The Sloan Digital Sky Survey and the SDPC

Another large-coverage survey, though not all-sky, with good photometry is the Sloan Digital Sky Survey (SDSS). The SDSS is a collaboration of 25 institutions, which from 2000–2008 obtained deep, multi-colour images of about a quarter of the sky using a dedicated 2.5-m reflector at Apache Point Observatory, NM, and a 120-million pixel CCD. The five SDSS bands, with central wavelengths and limiting magnitudes, were: *u*, 355.1 nm, 22.0; *g*, 468.6 nm, 22.2; *r*, 616.5 nm, 22.2; *i*, 748.1 nm, 21.3; and *z*, 893.1 nm, 20.5. Magnitudes were determined with an absolute accuracy of ~ 0.01 mag. The saturation limit for the five bands ranged from 14.1 (for *g* and *r*) to 12.1 (for *u*). The surveying was performed in two distinct phases: SDSS I (2000–2005), which imaged ~ 8000 sq. deg and obtained spectra of galaxies and quasars; and SDSS II (2005–2008), which completed the SDSS I imaging, surveyed an additional 3500 sq. deg. to probe the structure of the Milky Way and repeatedly imaged 300 sq. deg to discover supernovae and other variable objects. A third phase, SDSS III (2008–2014), is currently underway and it intends to continue mapping the distribution of galaxies and the structure of the Milky Way, and undertake radial-velocity monitoring of 11 000 stars in order to detect giant planets. The seventh data release (DR7) from this survey (Abazajian *et al.*, 2009) contains 357 million objects covering 11 163 sq. deg. (about 25% of the sky; a GIF showing the sky coverage is available at `http://www.sdss.org/dr7/dr7photo_big.gif`) with accurate photometric measurements in the five survey bands.

[2] `ftp://ftp.lowell.edu/pub/bas/starcats/loneos.ref`

From the viewpoint of this thesis, in addition to being an invaluable source of accurate photometric data on stars, the SDSS is also a valuable source of accurate photometry (and positions) of minor planets.

Several sets of transformation equations converting the SDSS u, g, r, i magnitudes to standard U, B, V, R_c and I_c bands are available in the literature. The expressions of Jester *et al.* (2005) were adopted for use in this study. Two sets of transformation equations, derived from examination of SDSS magnitudes of Landolt standard stars, were given. Equations 4.1 are for stars with colours $R_c–I_c < 1.15$ and $U–B < 0$:

$$\left.\begin{aligned} U–B &= 0.77\ (u–g) - 0.88 \\ B–V &= 0.90\ (g–r) + 0.21 \\ V–R_c &= 0.96\ (r–i) + 0.21 \\ R_c–I_c &= 1.02\ (r–i) + 0.21 \\ B &= g + 0.33\ (g–r) + 0.20 \\ V &= g - 0.58\ (g–r) - 0.01 \end{aligned}\right\} \qquad (4.1)$$

Equations 4.2 are for other stars with $R_c–I_c < 1.15$:

$$\left.\begin{aligned} U–B &= 0.78\ (u–g) - 0.88 \\ B–V &= 0.98\ (g–r) + 0.22 \\ V–R_c &= 1.09\ (r–i) + 0.22 \\ R_c–I_c &= 1.00\ (r–i) + 0.21 \\ B &= g + 0.39\ (g–r) + 0.21 \\ V &= g - 0.59\ (g–r) - 0.01 \end{aligned}\right\} \qquad (4.2)$$

Practical implementation of these transformations involves determining $U–B$ and $R_c–I_c$ using Equations 4.1, rejecting the star from further processing if $R_c–I_c > 1.15$ or switching to Equation 4.2 if $U–B > 0$.

4.5.1: Assessing the SDPC

I needed to demonstrate that magnitudes derived from SDSS photometric data are in agreement with accurate photometric observations from other sources. SDSS sources begin to be saturated at about $V = 14.5$, so finding good faint photometric data from other sources can be problematic. I used the loneos.phot listing to find a suitable test case.

I decided to make a comparison with some stars from Selected Area 57 (SA57, see Appendix 3.9 [p. 224]), which is located near the galactic north pole (galactic latitude ~ +85°). The SDSS data archive uses SQL databases. Appropriate SQL query statements were written to allow me to extract objects from the SDSS database. Objects were extracted from the SDSS archive in a 60′ radius around $\alpha = 13^h09^m$, $\delta = +29°20'$ (J2000.0) and converted into a small test photometric catalogue using the Jester *et al.* (2005) expressions. The *V* magnitudes for the SA57 stars were taken from the loneos.phot file, supplemented by values for two of the stars taken from Majewski *et al.* (1994). The comparison between the SDSS magnitudes (V_{SDSS}) and the loneos.phot magnitudes (V_{SA}) is shown in Table 4.2.

Table 4.2: Comparison of SA57 star measures with SDSS measures

Star ID	Position (J2000.0)	V_{SA}	V_{SDSS}
SA57-8684	13 09 17.09 +29 20 52.2	20.685 ± 0.013	20.599 ± 0.043
SA57-8408	13 09 18.57 +29 20 29.2	20.354 ± 0.024	20.338 ± 0.035
SA57-B35	13 08 11.92 +29 25 12.6	19.08	18.793 ± 0.016
SA57-B51	13 09 00.46 +29 26 15.7	18.50	18.596 ± 0.023
SA57-B45	13 08 47.96 +29 23 56.2	17.52	17.426 ± 0.013
SA57-P35	13 08 26.49 +29 20 34.6	14.96	14.961 ± 0.011

The agreement between V_{SA} and V_{SDSS} is generally within 0.1 mag. The one exception is SA57-B35 (hereafter B35), which shows a discrepancy of almost 0.3 mag. The entry in loneos.phot is derived (Skiff, 2012) from an unpublished measurement by W. A. Baum. Skiff also pointed out that the "star" B35 is actually the $z = 3$ quasar J130812.1+292513 = 1305+296C. Quasars are known to exhibit (usually) small variations in brightness, so the apparent discrepancy in the V_{SA} and V_{SDSS} measurements for B35 is probably of no concern. Confirmation of this view comes from Hewitt and Burbidge (1993), who list $V = 19.17$, taken from Chiu (1980), in their catalogue of quasars, and note that it is known to vary.

This small analysis of SA57 made me confident that it was worthwhile proceeding with construction of a photometric catalogue from the SDSS photometric data. I call this photometric catalogue the Sloan-Derived Photometric Catalogue, or SDPC. A full comparison of SDPC magnitudes with the reliable photometry present in the loneos.phot catalogue is presented in Section 4.5.3 [p. 79].

4.5.2: Building the SDPC

The CfA maintains a local copy of most of the data files from each SDSS Data Release. The SDSS project distinguishes between primary photometric objects and secondary photometric objects that are linked to primary objects. Primary objects are typically isolated detections, disconnected from any other detection, such as stars. Complex structures, such as galaxies, nebulae or very dense star fields, contain two or more distinct detections that are (or appear to be) connected. In each complex structure, one detection is selected as the primary detection (or parent), while the other detections are secondary detections (or children). The data file that is of most use to this thesis is the PhotoPrimary file from SDSS Data Release 7. This data file contains the SDSS detections that are determined to be "primary" detections. The decision was made to use the local copy for the extraction of my photometric catalogue, rather than attempting to get the same data from the SDSS site. Using the local copy meant that the catalogue could be generated in one step. If I had used the SDSS site, I would have had to write many hundreds of SQL queries.

A Fortran 95 program (called CONVERTSDSSMAG) was written to scan the local copy of the SDSS database, convert the SDSS data into the SDPC format, remove those objects that did not meet the selection criteria and write out those entries that did. Objects were rejected if the uncertainty in the derived B, V or R magnitude was more than 0.1 mag, or more than 0.2 mag in I. The SDSS photometric information has a 64-bit flag value (stored as two 32-bit flags, labelled flags and flags2) for each object that indicates various problems with the observations or the reductions. Examples of flagged situations are "object is saturated", "object may be false detection" and "couldn't find peak". A full list of the flag values examined is given in Appendix 7.4 [p. 233]. CONVERTSDSSMAG also produced the index entries necessary to allow rapid searching of the SDPC and ASTCAT-S.

I made a first attempt to extract the necessary data from the SDSS data set. It appeared to work successfully. However, it turned out that the weeding of objects based on the SDSS photometric flags was not as rigorous as I had planned. In particular, objects were accepted that were false detections embedded in the diffraction spikes of bright objects! A minor modification was made to CONVERTSDSSMAG to check more of the SDSS flag values and the SDPC was regenerated. Even using the local copy of the DR7 photometric data, it takes about 40 hours to run this program.

The procedure that built the SDPC also created the ASTCAT-S (see Section 4.7 [p. 87]), although at this stage the latter catalogue had no magnitudes from the astrometric catalogues.

4.5.3: Verifying the SDPC

With the SDPC prepared, it was necessary to verify that the values in the catalogue were in agreement with published values in the literature. In particular, it was important to ascertain that there were no systematic errorss over the magnitude range covered by the SDPC.

I again used Skiff's loneos.phot listing. This file contains entries for over 33 000 objects with reliable V magnitudes and $B–V$ colours, distributed over the whole sky. There are 2212 loneos.phot objects present in the SDPC: many of the loneos.phot objects present in the regions covered by SDPC are too bright for inclusion in the latter catalogue. For each matched object, the V magnitudes were extracted from both catalogues. A plot was prepared (see Figure 4.1 [p. 80]) relating, for each matched object, the SDPC V magnitude against the loneos.phot V magnitude. A visual inspection shows that the vast majority of the plotted points lie on or very close to the expected straight line and that there are no systematic trends at either the bright or faint limits. The mean and standard deviation of the differences between the two catalogues, in the sense SDPC minus loneos.phot and considering all 2213 matched objects, are 0.00 ± 0.26 mag. Iteratively removing objects with differences exceeding three times the standard deviation from the previous iteration led, after five iterations and utilizing 1974 matched objects, to values for the mean and standard deviation of the differences of -0.01 ± 0.04 mag. Transformations, derived from 1974 matched objects, between loneos.phot and SDPC V magnitudes can be achieved using:

$$V_{loneos.phot} = +0.013 + 1.000\, V_{SDPC} \qquad (4.3)$$

with a goodness of fit, R^2, equal to 1.000. See Appendix 7.2 [p. 229] for details on the goodness of fit.

For 74 objects the difference between the SDPC and loneos.phot magnitudes exceeded 0.25 mag. In 23 of these cases the difference exceeded one magnitude. I decided to investigate these outliers before declaring the SDPC to be valid photometrically.

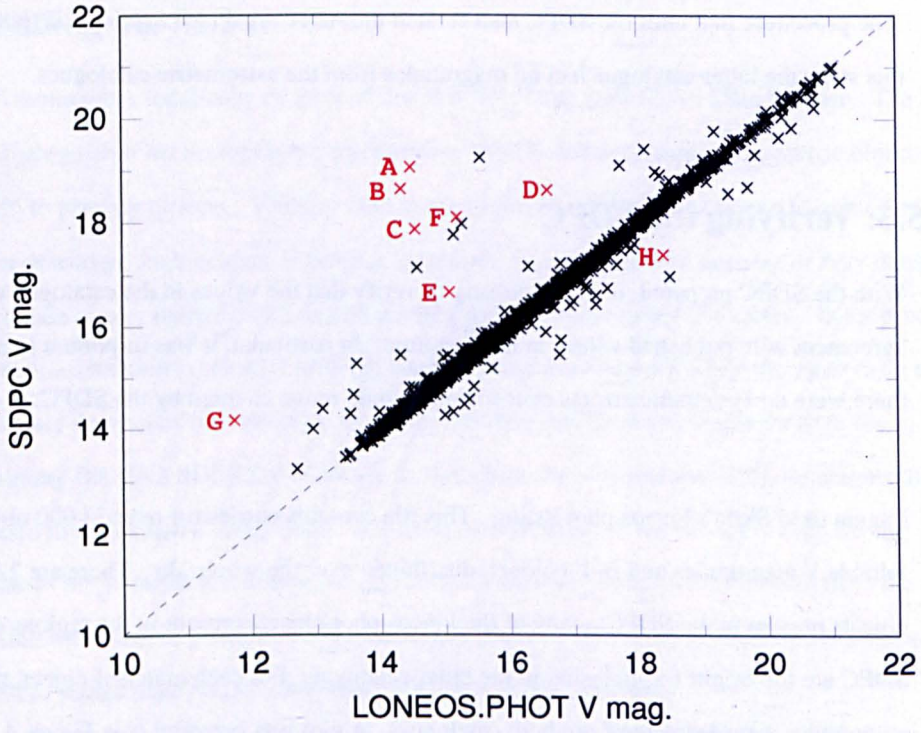

Figure 4.1: Comparison of SDPC vs. loneos.phot

The loneos.phot file has an associated references file (loneos.ref), listing the references used by Skiff in the compilation of the list. Unfortunately, the two files are not cross-referenced[3] and in many cases determining which reference was used for an entry in loneos.phot is problematic. More than twenty published papers listed by Skiff were examined to try and determine why discrepancies were occurring.

Quite a number of the problem cases have been solved, as follows (the letter designations refer to the points so marked in red in Figure 4.1):

- A: SDPC measure is of a companion, primary is not in SDPC.
- B: Comparison star "UZ Boo 3" misidentified in loneos.phot. See finder charts in Misselt (1996) and Downes and Shara (1993). Correct candidate not in SDPC.
- C: Comparison star "NGC 4414 9" misidentified in loneos.phot. See finder chart in Pratchett and Wood (1976). Correct candidate is not in SDPC.
- D: Comparison star "NN Set 15" misidentified in loneos.phot. See finder chart in Henden and Honeycutt (1995). Correct candidate has $V = 16.62$ and $B–V = +0.73$ in SDPC vs. $V = 16.61$ and $B–V = +0.74$ in loneos.phot.

3 Recent versions of the loneos.dat file have the reference included, but the inclusion is not yet complete.

- E: Comparison star "GP Com 9" misidentified in loneos.phot due to erroneous position for GP Com in Henden and Honeycutt (1997). Correct candidate is not in SDPC.
- F: Comparison star "NGC 5548 Curry 2" marked incorrectly on finder chart in Curry *et al.* (1998). SDPC object with $V = 15.34$ (vs. loneos.phot $V = 15.29$) seems to be the correct candidate.
- G: Identification seems secure. Presumably SDPC entry is a non-flagged saturated object.
- H: Identification seems secure based on finder chart in Suntzeff *et al.* (1988). Magnitude discrepancy almost exactly 1 mag., other comparison stars from this reference match their SDPC counterparts to within a few hundredths of a magnitude. This is probably just a typo: an attempt to confirm this with the paper's lead author did not produce a response.

Many of the other discrepant objects are other examples of the cases listed above. In the as-yet-unresolved cases, it was not possible to locate the reference in which a finder chart was published. The findings on the discrepant cases have been reported to Skiff, who has incorporated the necessary changes into his list.

It appears, however, that the SDPC contains reliable photometry. I moved on to the task of matching the SDPC photometry to the magnitudes contained in the astrometric catalogues.

4.6: Carlsberg Meridian Catalogue 14 and the CDPC

A study by Dymock and Miles (2009), using the CMC-14 catalogue r' magnitudes and 2MASS J–K colours to derive V magnitudes, showed more promise. Using 100 stars from Landolt (1992), lying more than 10° from the galactic equator and with J–K values restricted to the range 0.3 to 0.7, they derived the following expression:

$$V = 0.6278\,(J-K) + 0.9947r' \tag{4.4}$$

with a claimed accuracy of ± 0.043 mag for stars brighter than $V = 14$. I decided that a full analysis of the transformation of the CMC-14 magnitudes was necessary, if only to confirm the general correctness of Equation 4.4.

A program, called `MatchLoneosCMC14`, was written that matched the ~34 000 loneos.phot stars to the ~95.9 million stars in CMC-14. The loneos.phot stars were rejected from the matching step if they did not have a B–V value. Some of the loneos.phot stars also have values of V–R and V–I. When matches were found, entries were written to an output file. Each entry in the output file contained the r', J, H and K magnitudes from the CMC-14, as well as the V, B, R and I magnitudes from loneos.phot. If there were no values for V–R or V–I, the corresponding values of R and I were set to zero. The total number of matches between the two catalogues was 16 049.

Another program, called `DeriveLoneosCMC14`, was written that analysed the output file from `MatchLoneosCMC14` and derived expressions relating each of the loneos.phot B, V, R and I magnitudes to the CMC-14 r' magnitude. The solution for each expression was derived iteratively, at each iteration rejecting stars with residuals more than three times the standard deviation of the previous iteration. It was important to see whether I needed to reject stars within a certain distance of the galactic equator and what ranges of J–K colours allowed good transformations. It was also worth investigating if alternate expressions could be derived for stars with extreme colours. To allow these questions to be investigated, `DeriveLoneosCMC14` is able to restrict the analysis to stars lying within certain ranges of galactic latitude and/or with certain ranges of J–K colours.

For ease of comparison with the expression of Dymock and Miles, I will also restrict my analysis to stars more than 10° from the galactic equator with $0.3 < J\text{–}K < 0.7$. Transformation Equations 4.5 were derived:

$$\left.\begin{aligned} V &= 0.5955\,(J\text{–}K) + 0.9960\,r' \\ B &= 2.0964\,(J\text{–}K) + 1.0011\,r' \\ R &= -0.1562\,(J\text{–}K) + 0.9894\,r' \\ I &= -0.7894\,(J\text{–}K) + 0.9811\,r' \end{aligned}\right\} \qquad (4.5)$$

Consideration was also given to transformation equations utilizing two colours. Equations 4.6 were derived using the J–K and H–K colours:

$$\left.\begin{aligned} V &= 0.6346\,(J\text{–}K) - 0.1944\,(H\text{–}K) + 0.9958\,r' \\ B &= 2.2291\,(J\text{–}K) - 0.6314\,(H\text{–}K) + 1.0002\,r' \\ R &= -0.1481\,(J\text{–}K) - 0.0551\,(H\text{–}K) + 0.9895\,r' \\ I &= -0.8239\,(J\text{–}K) + 0.1988\,(H\text{-}K) + 0.9812\,r' \end{aligned}\right\} \qquad (4.6)$$

The fit of both sets of transformations is given in Table 4.3. For each set of transformations, the columns give the number of stars used in the fit and the number of stars available for fitting, and the mean and standard deviation of the fit.

Table 4.3: Comparison of one- and two-colour transformation equations

Band	One-Colour Transformations		Two-Colour Transformations	
	Stars Used/Avail.	Fit Mean and s.d.	Stars Used/Avail.	Fit Mean and s.d.
V	8502/9044	0.000 ± 0.060	8495/9044	0.000 ± 0.059
B	8709/9044	–0.002 ± 0.118	8753/9044	–0.002 ± 0.118
R	1649/1748	0.000 ± 0.053	1654/1748	0.000 ± 0.054
I	1417/1514	0.002 ± 0.070	1419/1514	0.002 ± 0.070

Equations 4.6 do not give a better fit than Equations 4.5, so I adopted the one-colour transformation Equations 4.5 to convert CMC14 r' magnitudes. Figure 4.2 [p. 83] shows the magnitude distribution of the residuals from the one-colour transformation Equations 4.5. As is to be expected, the scatter is less at brighter magnitudes and the best fit is found for the transformations to R.

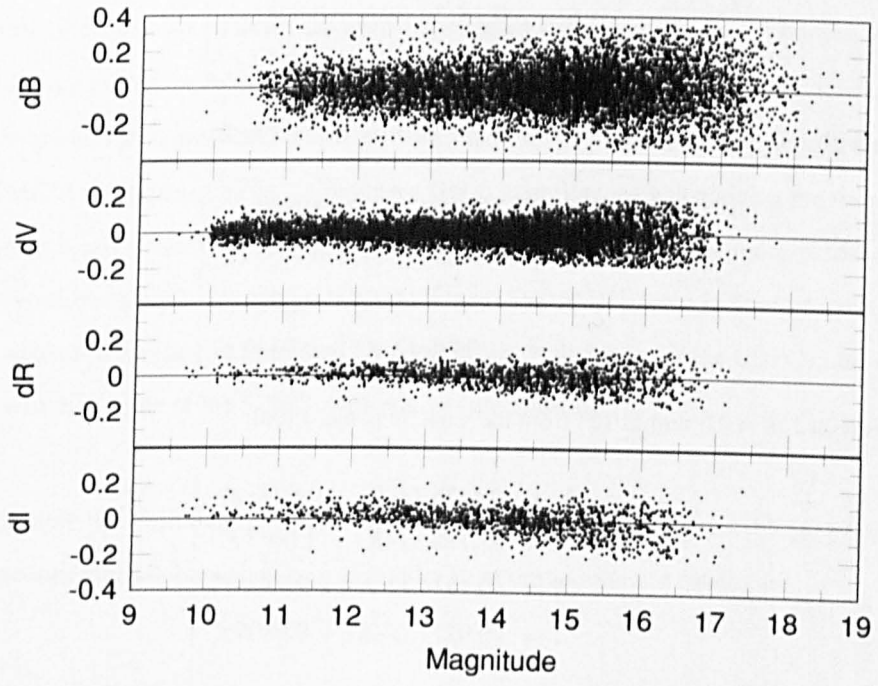

Figure 4.2: Magnitude distribution of residuals from one-colour transformation equations

I also used `DeriveLoneosCMC14` to derive expressions for objects with different ranges of J–K colours and at different galactic latitudes.

For stars with $0.3 < J–K < 0.7$ within 10° of the galactic plane, I find:

$$\left.\begin{aligned} V &= 0.6182\,(J–K) + 0.9973\,r' \\ B &= 2.1702\,(J–K) + 1.0066\,r' \\ R &= -0.1585\,(J–K) + 0.9861\,r' \\ I &= -0.8826\,(J–K) + 0.9743\,r' \end{aligned}\right\} \quad (4.7)$$

For stars with $J–K \geq 0.7$ more than 10° from the galactic plane, I find:

$$\left.\begin{aligned} V &= 0.5040\,(J–K) + 1.0044\,r' \\ B &= 2.0042\,(J–K) + 1.0107\,r' \\ R &= -0.2452\,(J–K) + 0.9938\,r' \\ I &= -1.0825\,(J–K) + 0.9945\,r' \end{aligned}\right\} \quad (4.8)$$

For stars with $J–K \geq 0.7$ within 10° from the galactic plane, I find:

$$\left.\begin{aligned} V &= 0.7057\,(J–K) + 0.9912\,r' \\ B &= 2.2823\,(J–K) + 0.9994\,r' \\ R &= -0.3325\,(J–K) + 0.9947\,r' \\ I &= -1.2003\,(J–K) + 0.9912\,r' \end{aligned}\right\} \quad (4.9)$$

For stars with $J–K \leq 0.3$ more than 10° from the galactic plane, I find:

$$\left.\begin{aligned} V &= 0.7395\,(J–K) + 0.9930\,r' \\ B &= 2.3825\,(J–K) + 0.9975\,r' \\ R &= -0.1315\,(J–K) + 0.9885\,r' \\ I &= -1.0496\,(J–K) + 0.9846\,r' \end{aligned}\right\} \quad (4.10)$$

For stars with $J–K \leq 0.3$ within 10° from the galactic plane, I find:

$$\left.\begin{aligned} V &= 0.6576\,(J–K) + 0.9948\,r' \\ B &= 2.1899\,(J–K) + 1.0045\,r' \\ R &= -0.1934\,(J–K) + 0.9875\,r' \\ I &= -0.9177\,(J–K) + 0.9805\,r' \end{aligned}\right\} \quad (4.11)$$

The fit of Equations 4.7 through 4.11 is given in Table 4.4. The columns give the number of stars used in the fit and the number of stars available for fitting, and the mean and standard deviation of the fit.

Table 4.4: Fit of CMC14-transformation equations

Band	$0.3 < J–K < 0.7$	$J–K \geq 0.7$		$J–K \leq 0.3$	
	$\|b\| < 10°$ Mean and s.d. Used/Avail.	$\|b\| \geq 10°$ Mean and s.d. Used/Avail.	$\|b\| < 10°$ Mean and s.d. Used/Avail.	$\|b\| \geq 10°$ Mean and s.d. Used/Avail.	$\|b\| < 10°$ Mean and s.d. Used/Avail.
V	0.001 ± 0.083 1660/1734	0.002 ± 0.093 1283/1381	0.000 ± 0.075 786/845	0.001 ± 0.050 1956/2087	0.000 ± 0.054 967/1006
B	0.001 ± 0.157 1668/1734	0.000 ± 0.164 1295/1381	0.000 ± 0.153 789/845	0.000 ± 0.102 1966/2087	0.001 ± 0.117 979/1006
R	0.000 ± 0.084 447/447	0.000 ± 0.059 296/331	–0.003 ± 0.073 262/273	0.002 ± 0.053 291/291	0.001 ± 0.045 146/149
I	–0.001 ± 0.155 378/402	–0.002 ± 0.121 285/315	–0.007 ± 0.141 226/244	0.000 ± 0.087 253/253	0.002 ± 0.116 118/118

With all the necessary transformation equations derived, I built a photometric catalogue based on the CMC-14. This catalogue is called the CMC14-Derived Photometric Catalogue or CDPC.

4.6.1: Building the CDPC

The CMC-14 catalogue was downloaded from `http://www.ast.cam.ac.uk/~dwe/SRF/cmc14.html`. It is distributed as seventeen gzip-compressed files, each file containing stars in a 5°-wide strip of declination. These files were downloaded and decompressed. A Fortran 95 program, called `ConvertCMC14`, was written to convert each CMC14 file into the CDPC format, utilizing the correct transformation equation for each star based on its *J–K* colour and galactic latitude. For each CMC14 file `ConvertCMC14` produced five output files, each containing the stars in a 1° declination band. In addition, a single additional output file contained the index entries (for all five 1° bands) allowing rapid searching of the CDPC and ASTCAT-C: these individual index files were simply appended together to form the CDPC index file. The format of the CDPC index entries is identical to the format of the SDPC index entries (see Table A5 [p. 237]).

The procedure that built the CDPC also created the ASTCAT-C (see Section 4.7 [p. 87]), although at this stage the latter catalogue had no magnitudes from the astrometric catalogues.

4.6.2: Verifying the CDPC

With the CDPC prepared, it was necessary to verify that the values in the catalogue were in agreement with published values in the literature. As with the SDPC, it was important to ascertain that there were no systematic effects over the magnitude range covered by the CDPC by comparing the CDPC to loneos.phot. There are 6863 loneos.phot stars that are present in the CDPC. For each matched object, the *V* magnitudes were extracted from both catalogues and a plot (see Figure 4.3) was prepared showing how the magnitudes from the two catalogues agreed.

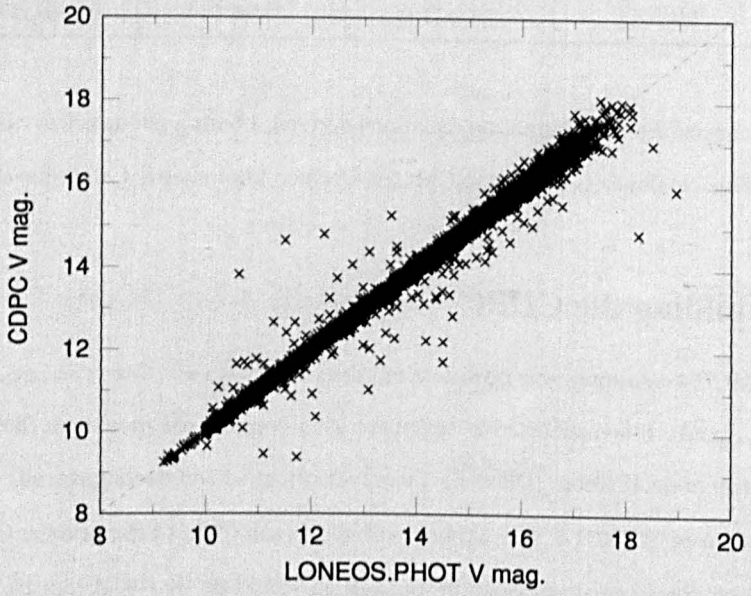

Figure 4.3: Comparison of CDPC vs. loneos.phot

As with Figure 4.1 [p. 80], the majority of the plotted points line on or very close to the expected straight line and, although the scatter increases as the objects get fainter, there are no systematic trends at either the bright or faint limit. The points that lie off the expected line are occurrences of the problems found with certain SDPC entries in Section 4.5.3 [p. 79]. The mean and standard deviation of the differences between the two catalogues, in the sense CDPC minus loneos.phot and considering all 6863 matched objects, are –0.01 ± 0.17 mag. Iteratively removing objects with differences exceeding three times the standard deviation from the previous iteration led, after five iterations and utilizing 6423 objects, to values for the mean and standard deviation of the differences of 0.00 ± 0.06 mag. Transformations, derived from 6423 matched objects, between loneos.phot and CDPC *V* magnitudes can be achieved using:

$$V_{loneos.phot} = -0.009 + 1.001\, V_{CDPC} \quad (4.12)$$

with a goodness of fit, R^2, equal to 1.000.

4.7: Building the ASTCAT-S and ASTCAT-C

ASTCAT-S is the name given to the catalogue that combines the entries from the SDPC with the corresponding entries from various astrometric catalogues. ASTCAT-C is the name given to the catalogue that combines the entries from the CDPC with the corresponding entries from various astrometric catalogues. ASTCAT is the generic name that refers to either catalogue.

Not all of the SDPC entries will have magnitudes in the astrometric catalogues, as the SDPC goes a couple of magnitudes deeper than the other catalogues.

Using the list of catalogues to be included in the ASTCAT, listed in Section 4.2 [p. 73], I determined how to query these catalogues in an efficient manner. Although many data centres have copies of all the catalogues mentioned above, it would be very time- and bandwidth-consuming to query the catalogues remotely. Fortunately, there was a local solution at CfA: Jessica Mink of the Optical & Infrared division makes available a program called `scat` [4], which is installed on the Computation Facility (CF) machines and which can extract stars in a user-defined region from a large number of locally-stored catalogues, including all the ones in which I have an interest. The USNO-A2.0 effectively replaced the USNO-A1.0 catalogue and Mink had removed the latter catalogue from the local disks; at my request, she restored it. The method used to populate the ASTCAT files is described in Appendix 7.9 [p. 240].

The arrangement of objects in the ASTCAT files is the same as the SDPC/CDPC files, so the Fortran 95 library routines written previously to extract data from the SDPC/CDPC can be used (with a trivial extension) to extract data from the corresponding ASTCAT.

The format of each entry in the ASTCAT is shown in Table 4.5. The variable types are: Integer (4 bytes); DP (double-precision real, 8 bytes); and SP (single-precision real, 4 bytes).

4 See `http://tdc-www.harvard.edu/software/wcstools/wcsprogsc.html` for details.

Table 4.5: Format of an ASTCAT entry

Offset		Format	Use
ASTCAT-S	ASTCAT-C		
0	0	Integer	Object number within declination band
4	4	DP	Right Ascension (J2000.0)/deg.
12	12	DP	Declination (J2000.0)/deg.
20	—	SP	*U* magnitude
24	20	SP	*B* magnitude
28	24	SP	*V* magnitude
32	28	SP	*R* magnitude
36	32	SP	*I* magnitude
40	36	SP	USNO A-1.0 *B* magnitude
44	40	SP	USNO A-1.0 *R* magnitude
48	44	SP	USNO A-2.0 *B* magnitude
52	48	SP	USNO A-2.0 *R* magnitude
56	52	SP	GSC-1 *B*, *V* or *R* magnitude
60	56	SP	UCAC-1 *C* magnitude
64	60	SP	UCAC-2 *C* magnitude
68	64	SP	UCAC-3 *C* magnitude
72	68	SP	GSC-2 *F* magnitude
76	72	SP	GSC-2 *J* magnitude
80	76	SP	GSC-2 *V* magnitude
84	80	SP	GSC-2 *N* magnitude
88	84	SP	USNO-B1.0 *B1* magnitude
92	88	SP	USNO-B1.0 *R1* magnitude
96	92	SP	USNO-B1.0 *B2* magnitude
100	96	SP	USNO-B1.0 *R2* magnitude
104	100	SP	USNO-B1.0 *N* magnitude
108	104	SP	CSS *V* magnitude
112	108	SP	Spare
116	112	SP	Spare
120	116	Char*4	Notes 1
124	120	Char*4	Notes 2

Notes 2 is simply copied from Notes in the SDPC/CDPC. Notes 1 contains notes specific to the ASTCAT version.

4.8: Number of Entries in ASTCAT-* Files

Table 4.6 lists the number of entries for each catalogue and magnitude band in the ASTCAT-S and ASTCAT-C catalogues. The seemingly-low counts for several entries in the table (e.g., the ASTCAT-S UCAC-1, GSC-1 and CSS counts) can be explained by the limited number or non-existence of faint

entries in each catalogue and/or the limited overlap of the sky coverage with the ASTCAT-*. In particular, the UCAC-1 has an upper declination limit of –6° and the ASTCAT-S has a lower limit of –13°, with the faint limit of the UCAC-1 only about two magnitudes fainter than the bright limit of the ASTCAT-S.

Table 4.6: Breakdown of entries in the ASTCAT- files*

ASTCAT-S	ASTCAT-C	
57 135 244	67 137 127	Total number of entries
35 677 365	—	*U* magnitude
57 135 244	67 137 127	*B* magnitude
57 135 244	67 137 127	*V* magnitude
57 135 244	67 137 127	*R* magnitude
57 135 244	67 137 127	*I* magnitude
33 848 682	59 535 293	USNO A-1.0 *B* magnitude
33 838 353	59 547 867	USNO A-1.0 *R* magnitude
34 026 125	60 409 019	USNO A-2.0 *B* magnitude
34 026 130	60 445 865	USNO A-2.0 *R* magnitude
964 266	9 537 417	GSC-1 *B*, *V* or *R* magnitude
49 926	4 711 977	UCAC-1 *C* magnitude
2 649 838	25 227 206	UCAC-2 *C* magnitude
0	0	UCAC-3 *C* magnitude
51 726 474	63 549 724	GSC-2 *F* magnitude
50 685 920	55 784 469	GSC-2 *J* magnitude
24 857 398	45 148 408	GSC-2 *V* magnitude
37 581 273	62 256 648	GSC-2 *N* magnitude
38 246 007	61 643 382	USNO-B1.0 *B1* magnitude
44 294 020	62 502 144	USNO-B1.0 *R1* magnitude
48 737 556	62 896 469	USNO-B1.0 *B2* magnitude
49 384 568	62 435 899	USNO-B1.0 *R2* magnitude
42 016 798	62 974 055	USNO-B1.0 *N* magnitude
334 846	2 128 854	CSS *V* magnitude

4.9: Comparison of SDPC and CDPC

I have demonstrated previously that the mean agreement of both the SDPC and CDPC with the reliable photometry in the loneos.phot catalogue is good to within 0.01 mag. over the magnitude ranges 14–21 and 9–18, respectively. I now demonstrate that the SDPC and CDPC magnitudes are consistent with each other. Rather than attempt a full comparison between the 57 million SDPC and 67 million CDPC entries, I decided to do a more limited comparison. I chose four random fields in parts of the sky covered by both the CDPC and SDPC. I extracted stars from both catalogues in regions 1° by 1° around

the chosen field centres. Table 4.7 lists the field centres, along with the number of stars found in both catalogues and the number of stars common to both catalogues.

Table 4.7: Details of the field used for SDPC/CDPC comparison

Center	Number of stars in		
	SDPC	CDPC	common
$08^h, -10°$	8760	3386	1255
$12^h, +18°$	2272	389	239
$14^h, +10°$	3430	462	234
$16^h, +00°$	6999	1175	846

I wrote a Fortran 95 program to do the matching of objects from the two catalogues. This program also wrote the *B*, *V*, *R* and *I* magnitudes (for the 2574 stars in common) from both catalogues into four separate output files (one for each of the bands), as well as the mean and standard deviation of the differences between the two catalogues for each band. The means and standard deviations are listed in Table 4.8. The data in the output files were used to generate Figure 4.4, showing for each band the magnitude-dependent agreement between the CDPC and SDPC.

Table 4.8: SDPC–CDPC magnitude difference means and standard deviations

Band	SDPC–CDPC magnitude difference	
	Mean	SD
B	+0.006	0.317
V	–0.002	0.178
R	+0.004	0.153
I	–0.004	0.190

About 30 of the stars plotted on each diagram are outliers. These may be cases where the SDPC and CDPC entries, which were assumed by the matching procedure to be the same object, are actually different objects. Or they could be variable stars.

The small number of outlier cases does not impact the conclusion that the agreement between the CDPC and SDPC is satisfactory.

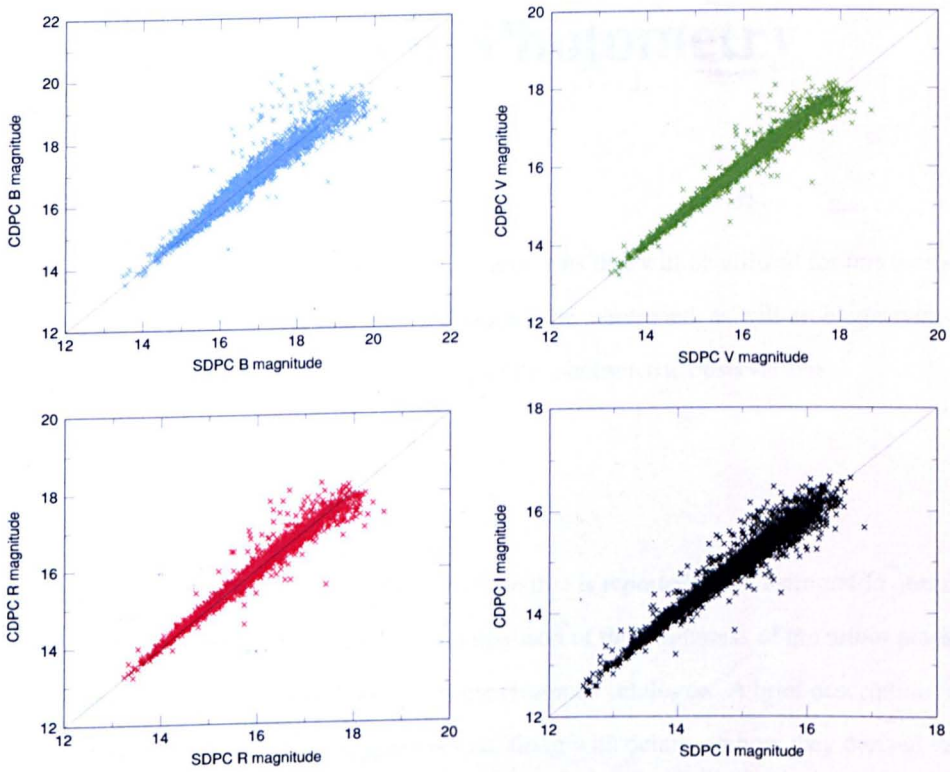

Figure 4.4: Comparison between SDPC and CDPC B, V, R and I magnitudes

4.10: Summary

The necessary photometric catalogues that will be used to correct the astrophotometric observations have been prepared and verified.

5: Sources of Photometry

5.1: Introduction

This chapter discusses the sources of photometric observations that will be utilized for this thesis. Problems with accessing certain potential data sources will be mentioned, as will problems with the published literature that prevent rereduction of many of the photometric observations.

5.2: Astrophotometry

An astrophotometric observation is a magnitude estimate that is reported on an astrometric observation. Such magnitude estimates are derived mainly by comparison of the brightness of the minor planet with the magnitudes of the comparison stars taken from the reference catalogue. A brief description of each of the major professional CCD surveys is given below, along with details on how they derived their astrophotometric magnitudes. The LINEAR and Catalina Sky Survey (CSS) descriptions include details on the internal procedures used by those surveys to adjust comparison catalogue magnitudes before use in determining survey magnitudes. My reprocessing of the LINEAR and CSS magnitudes will need to apply these same procedures to the magnitudes extracted from the astrometric reference catalogues before attempting to remove the systematic catalogue error.

A magnitude is coded in six columns of the MPC's 80-column astrometric observation record. The numeric value of the magnitude occupies columns 66–70, with the decimal point in column 68. The magnitude band is indicated in column 71. The most common bands are visual (*V*), red (*R*) and photographic (*B*). If column 71 is blank, the band is assumed to be photographic if the observation was obtained using photographic plates or films, and assumed (unless otherwise indicated) to be *R* if made using a CCD.

This thesis will concentrate on the astrophotometry produced by the seven big professional surveys (not all of which are active currently) described below. The justification for this is simple: the twelve MPC observatory codes representing the seven big professional surveys are responsible for ~89% of the published observations made in a given year (Williams, 2012a). The counts of observations and

percentages for recent years are given in Table 5.1. The 2010 percentage is anomalously low due to the more than 1.5 million observations made that year by the NEOWISE space mission (see Section 3.8.1 [p. 61]).

Table 5.1 : Observation contribution by the seven big professional surveys 2008–2012

Year	Total observations made in year	Big Survey Observations (BSO)	BSO Percentage
2012	3 461 002	3 233 401	93.4
2011	7 067 354	8 017 351	88.2
2010	6 598 376	11 517 464	57.2
2009	5 945 975	7 080 801	84.0
2008	7 417 060	8 064 144	91.9

5.2.1: LINEAR

The Lincoln Near-Earth Asteroid Program (LINEAR) (Stokes *et al.*, 2000), MPC observatory code 704, has operated two 1.0-m f/2.15 reflectors at the Lincoln Laboratory Experimental Test Site located near Socorro, NM, since 1996. Management of the program and data reduction is performed at the Lincoln Laboratory, Lexington, MA. Derived from technology developed for the U.S. Air Force's Ground-based Electro-Optic Deep Space Surveillance (GEODSS) system, the LINEAR CCDs are large-format, high quantum efficiency, frame transfer, fast readout and low-noise devices. The limiting magnitude is $V \sim 19.5$. Objects brighter than $V \sim 14$ usually have bad magnitudes, as the images are saturated in the LINEAR frames. The astrometry of such objects is also often bad. It is not uncommon for a low-numbered minor planet to have a measured magnitude of fainter than 19, even if the astrometry is good. To eliminate these erroneous magnitudes, normal Minor Planet Center policy on processing LINEAR observations is to delete automatically all magnitude estimates from minor-planet observations of objects with numbers less than 2000. It is known that some observations which should have had the magnitudes removed still have them. Any such observations will be ignored during the processing of LINEAR observations for this thesis.

According to Stuart (2008), LINEAR derives CCD visual magnitudes for the comparison stars from their *B* and *R* magnitudes in the USNO-A2.0 catalogue using the following logic:

- If $B–R < 0$ or $B–R > 2.6$ then reject the star.
- Otherwise, use Table 5.2 below to determine the value of ΔB used to adjust the catalogued B magnitude to V_{CCD}, an approximation to V:

$$V_{CCD} = B + \Delta B \tag{5.1}$$

The USNO-A2.0 catalogue records magnitudes to a precision of 0.1 magnitudes, so the values of $B–R$ can take only the discrete values listed in Table 5.2.

Table 5.2: Values of ΔB used in the reduction of LINEAR magnitudes

$B–R$	ΔB	$B–R$	ΔB	$B–R$	ΔB	$B–R$	ΔB
0.0	+0.26	0.7	–0.28	1.4	–0.84	2.1	–1.44
0.1	+0.19	0.8	–0.36	1.5	–0.92	2.2	–1.52
0.2	+0.11	0.9	–0.44	1.6	–1.00	2.3	–1.60
0.3	+0.03	1.0	–0.52	1.7	–1.09	2.4	–1.69
0.4	–0.05	1.1	–0.60	1.8	–1.18	2.5	–1.77
0.5	–0.12	1.2	–0.68	1.9	–1.27	2.6	–1.86
0.6	–0.20	1.3	–0.76	2.0	–1.35		

Prompted by an enquiry from me, Stuart (2009) reported that the computer code that LINEAR uses for magnitude determinations has an error: if $B–R = 2.6$, the correction for $B–R = 2.5$ is applied. This error is deliberately replicated in my reduction procedure for correcting the LINEAR magnitudes used in this thesis, to ensure that I process the LINEAR observations in the same way they were processed by the survey.

Figure 5.1 [p. 96] compares the V magnitudes from the SDPC with the pseudo-V magnitudes obtained using Equation 5.1 for 2000 stars in the $\delta = +42°$ band. There are 217 752 stars in the SDPC +42° band that are in the USNO-A2.0 catalogue. Utilizing all 217 752 stars, the mean and standard deviation of the difference SDPC minus LINEAR are +0.38 ± 0.45 mag. Iteratively removing objects with differences exceeding three times the standard deviation from the previous iteration led, after fourteen iterations and utilizing 194 123 objects, to values for the mean and standard deviation of the differences of +0.28 ± 0.27 mag.

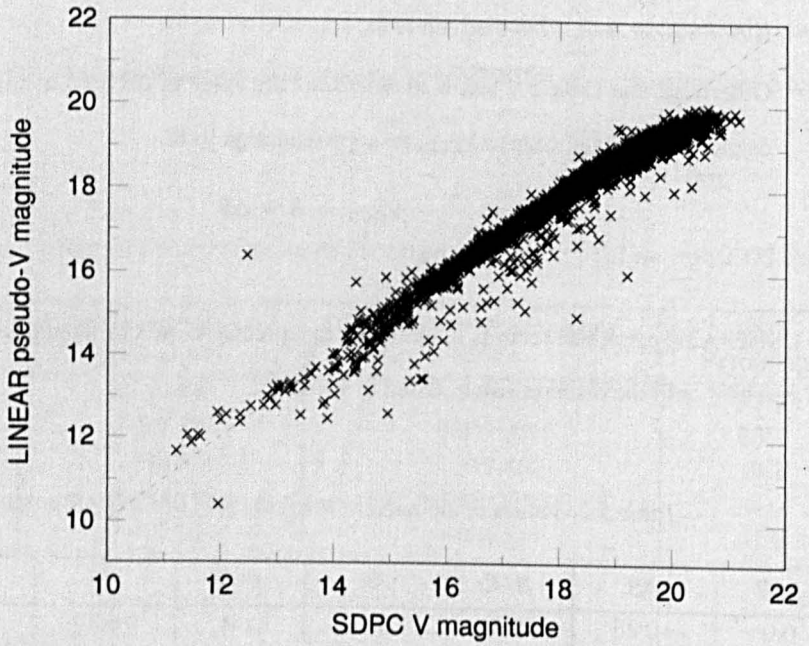

Figure 5.1: Comparison of LINEAR pseudo-V and SDPC V magnitudes

Noting that the scatter in Figure 5.1 is smaller at *V* brighter than 18 than at *V* fainter than 18, it seemed reasonable to consider just those objects with a SDPC *V* magnitude brighter than 18. This gave, utilizing 75 575 objects, a mean and standard deviation of the differences of $+0.21 \pm 0.47$ mag. Iteratively removing objects with differences exceeding three times the standard deviation from the previous iteration led, after nine iterations and utilizing 69 189 objects, to values for the mean and standard deviation of the differences of $+0.11 \pm 0.25$ mag.

Although observations (particularly those of objects brighter than $V \sim 18$) reduced in this fashion should be marked as *V*, historical LINEAR policy has been to not indicate any magnitude band. This has caused their astrophotometry to be treated as photographic by the Minor Planet Center when it incorporated the LINEAR observations into new absolute magnitude determinations.

In mid-2009, LINEAR implemented a new observation processing pipeline (Stuart, 2009). In addition to moving from USNO-A2.0 to USNO-B1.0 for their astrometric reductions, LINEAR is now using a custom photometric catalogue derived from five years of images taken with the LINEAR telescopes. This custom catalogue is not yet available publicly. However, the details of the new reduction procedure have been made available (Stuart, 2012). The USNO-B1.0 catalogue

magnitudes were converted into the CCD passband by use of the expression:

$$C = R_U + 0.021 + (0.1617 - 0.0378(B–R)) * (B–R) \quad (5.2)$$

where R_U is the catalogue R magnitude, $B–R$ is the catalogue $B–R$ colour and C is the CCD-passband magnitude.

5.2.2: Catalina Sky Survey

The Catalina Sky Survey is a consortium of three individual surveys: the Catalina Sky Survey (CSS, code 703); the Siding Spring Survey[1] (SSS, code E12); and the Mt. Lemmon Survey (MLS, code G96). The CSS uses a 0.68-m Schmidt equipped with a 4K × 4K CCD, located on a ridge some 300 meters below the Mt. Lemmon summit. It covers about 800 sq. deg. per night to a limiting magnitude of $V \sim 21$. The SSS uses the 0.5-m Uppsala Schmidt, located near Coonabarabran, NSW, and has a limiting magnitude $V \sim 20.5$. The MLS uses the Steward Observatory's 1.5-m reflector located on Mt. Lemmon, AZ, equipped with a 4K × 4K CCD that covers a ~ 1°-wide field to a limiting magnitude of $V \sim 22$. In addition, follow-up observations are obtained with the Siding Spring 1.0-m reflector. Project management is based at the Lunar and Planetary Laboratory, Tucson, AZ.

I ascertained that although the Catalina Sky Survey (CSS) uses the UCAC-2 for its astrometric reductions, its astrophotometry is based on an internally-generated V-band catalogue derived from 2MASS data (Beshore, 2007). The CSS kindly made their catalogue available and also supplied details on their photometric processing. Initially. there was some confusion over exactly what procedure CSS was using, but I determined (Beshore, 2008) that for their survey processing they are deriving the visual magnitude from the simple expression:

$$V = K + 1.46 \quad (5.3)$$

where K is the 2MASS K-band magnitude given in their catalogue. This correction was applied to all objects in the CSS catalogue (CSSC).

1 Catalina Sky Survey support for the Siding Spring Survey ended in 2012. At time of writing, no long-term replacement funding source has been found.

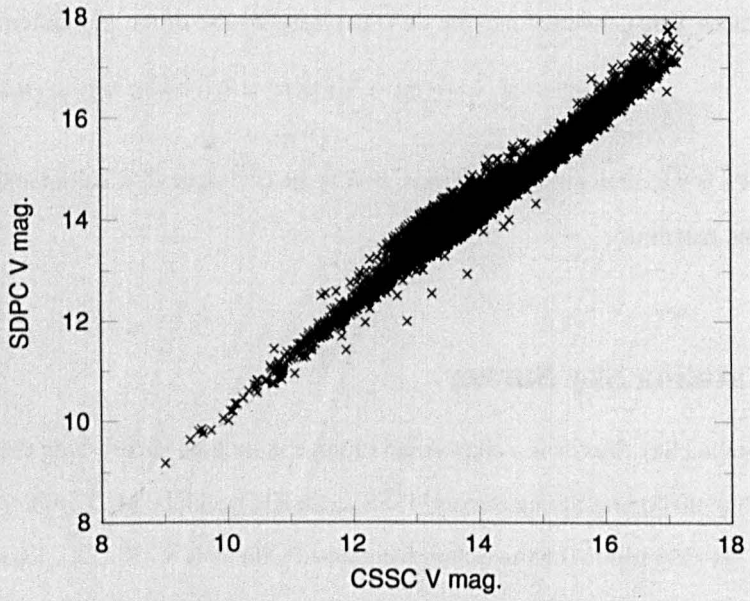

Figure 5.2: Comparison of SDPC vs. CSSC

A visual inspection of Figure 5.2 shows a much noisier fit than Figure 5.1 [p. 96]. This is not surprising considering the simplistic manner in which the 2MASS infrared magnitudes were transformed to V. The mean and standard deviation of the differences between the two catalogues, in the sense SDPC minus CSSC and considering all 315 883 matched objects, are $+0.24 \pm 0.21$ mag. Iteratively removing objects with differences exceeding three times the standard deviation from the previous iteration led, after fourteen iterations and utilizing 210 443 matched objects, to values for the mean and standard deviation of the differences of $+0.12 \pm 0.09$ mag. Transformations, derived from 210 443 matched objects, between CSSC and SDPC V magnitudes can be achieved using:

$$V_{CSSC} = -0.606 + 1.025\, V_{SDPC} \tag{5.4}$$

with a goodness of fit, R^2, equal to 0.985.

5.2.3: Spacewatch

The Spacewatch project is managed at the Lunar and Planetary Laboratory, Tucson, AZ, and operates two telescopes on Kitt Peak, AZ. The Steward Observatory's 0.9-m Newtonian reflector (code 691) began searching for NEOs in 1984 using drift scanning, which was supplemented in 2001 by a 1.8-m reflector (code 291) operated in stare mode.

The Spacewatch project does not tie its astrophotometry to the astrometric reference catalogues they use (Scotti and Larsen, 2009). Rather, they calibrate their photometric observations on a nightly basis via comparison with observations of objects in Selected Areas. This means that it will not be possible to apply catalogue corrections to the data from Spacewatch.

5.2.4: LONEOS

The Lowell Observatory Near-Earth Object Search (LONEOS) operated from 1998 to 2008, utilizing a CCD-equipped 0.59-m Schmidt at the Anderson Mesa Station of the Lowell Observatory, AZ. Monthly sky coverage was ~6000 sq. deg. with a limiting magnitude ~18.5. In 2000, the CCD was upgraded to a 4096^2-pixel device with twice the quantum efficiency of the previous CCD, allowing a reduction in exposure times from 45s to 12s, with a consequent increase in monthly sky coverage to ~20 000 sq. deg. Limiting magnitude was $V \sim 19.5$.

5.2.5: NEAT

The Near-Earth Asteroid Tracking (NEAT) program (Helin *et al.*, 1997, Pravdo *et al.*, 1999) operated a number of CCD-equipped telescopes between late 1995 and 2007: a 1.0-m reflector at Haleakala, HI (MPC observatory code 566) and the 1.2-m Oschin Schmidt at Mt. Palomar, CA (code 644). In addition, observations were also obtained with the U.S. Air Force Maui Optical Site's 1.2-m reflector (code 608), also located at Haleakala. The project management was located at the Jet Propulsion Laboratory in Pasadena, CA. Sky coverage at codes 566 and 608 was about 4500 sq. deg. per month. Limiting magnitude was about $R \sim 19$.

A complication with the NEAT observations is that the availability of (compressed) images via the SkyMorph service[2], which allows anyone to search for known or new minor planets and report the observations to the Minor Planet Center. When the SkyMorph service began, the MPC made a conscious decision to not distinguish between NEAT observations submitted by different individuals. At a number of other observatory codes, program codes are used to distinguish between observations submitted by different individuals/teams, but the expected large number of different users of the NEAT data suggested that using program codes for NEAT data would be unnecessarily

2 http://skyview.gsfc.nasa.gov/skymorph/skymorph.html

complex. Experience has shown that this was the correct move from the viewpoint of efficiency in processing incoming observations. Unfortunately for this thesis, the NEAT observations are not as homogeneous as the other major surveys and I have no way to reliably distinguish between observations reduced (using a variety of procedures) and reported by different individuals.

5.2.6: Sloan Digital Sky Survey

The minor-planet observations produced by the Sloan Digital Sky Survey (SDSS) were an incidental by-product of the survey, the primary purpose of which was the investigation of large-scale structures in the universe. The observations were obtained at the Apache Point Observatory, NM, using a 2.5-m reflector equipped with a 120-megapixel camera (comprising thirty 2048^2-pixel CCDs), operated in drift-scan mode. The thirty CCDs are arranged in five rows of six chips, with each row having a different SDSS filter (Section 3.4.4 [p. 53]). As objects drift across the field of view, observations are obtained in all five filters. The astrometric and photometric data originally submitted to the Minor Planet Center were not in the usual format and considerable work was necessary to make the data useable. The submitted data included magnitudes in each of the five SDSS bands, as well as SDSS-derived B and V magnitudes. It was these derived magnitudes that were included on the published observations.

5.2.7: Pan-STARRS

The Panoramic Survey Telescope and Rapid Response System (Pan-STARRS) is currently a single 1.8-m reflector, known as PS1, located at Haleakala, HI, and equipped with a 1.4-gigapixel camera, containing sixty 4800^2-pixel CCDs with $0''.6$ pixels and a 3°-wide field of view. The eventual aim is to build four identical telescopes that will form the fully-functional system, which will produce a catalogue of all objects down to 24^{th} magnitude over the sky visible from Hawaii.

I believed initially that the colour corrections from the Pan-STARRS band to V would be essentially identical to those for the SDSS observations. Unfortunately, when the first Pan-STARRS observations were reported, I very quickly determined that the colour corrections were not at all similar to the SDSS corrections. Pan-STARRS uses a number of different filters (Chambers, 2006), specifically g, r, i, z, y and w. The first four filters are centred at similar wavelengths to the SDSS

g', r', i' and z' bands (see Section 3.4.4 [p. 53]), but are broader. The y filter is centred at 1020 nm and the wide w filter covers the combined wavelength range of the g, r and i filters. The transmission of all six filters is shown in Figure 5.3 (the data being taken from the Pan-STARRS website[3])

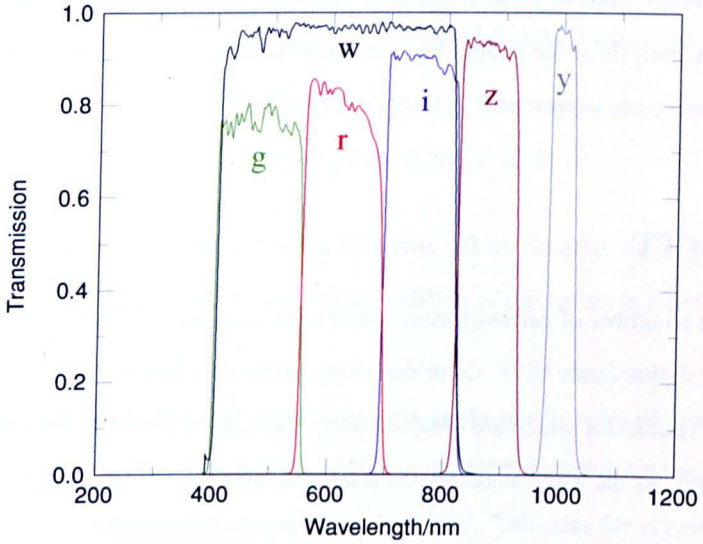

Figure 5.3: Pan-STARRS filter band transmission curves

There was discussion within the Pan-STARRS project about the colour corrections that should be used. I became involved in the discussion in November 2010, when I provided Pan-STARRS with the values of the colour corrections we use for SDSS magnitudes and, somewhat later, the colour corrections we were using for Pan-STARRS magnitudes. I had derived this latter set of values by comparing the reported Pan-STARRS magnitudes to the predicted magnitudes. While I can say that both sets of colour corrections were in good agreement with values reported by other groups with the project, I cannot be more specific about the agreement as the results have not yet been published. What I can do is list the Pan-STARRS colour corrections that I submitted to the discussion and that were in use by the Minor Planet Center at that time (see Table 5.3).

Table 5.3: MPC values for Pan-STARRS filter corrections (up to early 2012)

Colour	Correction
$V-g$	–0.70
$V-r$	–0.19
$V-i$	–0.01
$V-z$	0.00

3 `http://pan-starrs.ifa.hawaii.edu/~morgan/PS1%20Filters`

V–y	0.00
V–w	–0.46

Unfortunately, the colour-correction issue for Pan-STARRS is not yet fully resolved. At the time of writing, observations of Landolt standard fields have been obtained in each of the Pan-STARRS filters, but analysis of the images has not yet been made. Further discussion of the Pan-STARRS colour corrections is presented in Section 6.8 [p. 140].

5.2.8: FASTT

There are a number of current/former astrometric programs at the U.S. Naval Observatory's Flagstaff station (code 689). Of primary interest for this thesis is the FASTT program (Stone, 2000), the observations for which are obtained using the 0.20-m Flagstaff Astrometric Scanning Transit Telescope. As the name suggests, the telescope is a transit instrument.

The magnitudes reported from this program are not quite Johnson *V* magnitudes, but they can be adjusted to the standard system by applying the additive correction:

$$\Delta V = 0.363\,[(B\text{–}V) - 0.8] \qquad (5.5)$$

to the published *V* magnitude (Stone, 2000). An accuracy of ± 0.04 mag. (for *V* brighter than 12) to ± 0.11 mag. (at $V = 18$) was claimed. Prior MPC experience with the FASTT photometry has indicated that it is of substantially better quality than standard astrophotometry. Getting access to the FASTT observational data has been problematic in recent years. The last batch of FASTT observations from the program was received from principal investigator Ron Stone at the MPC on 2004 October 27. Since Ron Stone's death the following year, no further data submissions have been made to the MPC by the FASTT program, in spite of a number of enquiries made over the years[4]. The FASTT program does make observations of the minor planets that are predicted to occult stars in the next few months available on their website and at irregular intervals I go and collect these observations and process them for publication in the *Minor Planet Circulars*.

4 On 2012 August 5 (local date), an e-mail submission of observations from the new FASTT PI was received. It is hoped that regular submissions of this very useful data will resume in the near future.

5.3: Recalibrated LINEAR Photometry

A recalibration of the LINEAR photometry was undertaken by Sesar *et al.* (2011). All of LINEAR's available archived images, covering the time period 2002–2008, were run through SExtractor (Bertin and Arnouts, 1996) to obtain instrumental magnitudes, which were then calibrated using SDSS photometry. Sesar *et al.* derived an expression relating the originally-reported LINEAR magnitude, labelled as L ("LINEAR" band magnitude), to the V magnitude:

$$V = L + 0.65\ [(B-V) - 0.78] + 0.18 \qquad (5.6)$$

Application of Equation 5.6 shows a scatter of about 0.45 mag. which Sesar *et al.* attribute to random calibration errors. This scatter value is nicely consistent with one of the values in Section 5.2.1 [p. 94].

The authors supplied me with a 157 515-line data file containing the newly-reduced data. Each data line contained a magnitude and position (as originally reported to the MPC by LINEAR) and a newly-reduced magnitude and position reduced with respect to the SDSS. This data file is extremely useful as it allows me to compare my catalogue-corrected values to independently-derived values improved by use of the SDSS data using the original images. Unfortunately, this data file does not contain observations in the MPC format and they omitted to supply the identification for each observation.

In order to make the data useful I would have to attach an identification with a known object to each observation. This would entail converting the observations into the MPC format, adding a temporary self-assigned designation to each observation. Each converted observation would be written to one of eleven output files, each output file containing observations made within ± 100 days of a 200-day standard epoch (i.e., a Julian Date where the integer part of the date is exactly divisible by 200). The range of 200-day-standard epochs covered in the output files would be from JD 2452600.5 (2002 Nov. 22.0) to JD 2454600.5 (2008 May 14.0). Each of these output files would be used as input to the standard MPC checking routines, which attempt to identify unidentified objects with known objects. The resulting identifications would then be added to the MPC-format observations, allowing me to compare the newly-reduced data to the catalogue- and observer-corrected original data.

I decided not to take the route outlined in the previous paragraph for reasons of efficiency. Rather, I applied Equation 5.6 directly to all the uncorrected LINEAR photometry and compared the resulting

corrected magnitudes to my catalogue- and observer-corrected magnitudes. The results of this comparison are detailed in Section 9.9 [p. 179].

5.4: "Real" Photometry

"Real" photometry, obtained by standard photometric procedures, can be either individual observations, taken at some random point during a minor planet's rotation, or single mean observations, derived from lightcurve observations. Many of the photometric observations used in this thesis have been taken from the *Fifth Update of the Asteroid Photometric Catalogue* (Lagerkvist *et al.*, 2000), hereafter APC. In addition to examining the printed volume, I also obtained a CD-ROM from Lagerkvist containing the raw data files for each reference. The APC was superseded by the Standard Asteroid Photometric Catalogue (Piironen *et al.*, 2001).

A large number of published papers were examined to see whether it was possible to correct the original data with updated comparison star magnitudes. Unfortunately, this has turned out to not be possible in the majority of cases. Many authors fail to make any mention of which stars were used as comparisons, or, when the comparison is identified, omit mention of what magnitude they used in their reduction. When the photometry is derived from lightcurve studies, many authors will present plots of the light variation, with the zero point either being the mean or an extremum of the curve, but will fail to indicate either the absolute or relative offset of the zero point of the plot. Composite lightcurves are particularly troublesome as nightly adjustments are applied to get the curves from different nights to overlap, but values of these adjustments are frequently omitted. In an ideal world, observers would report the individual photometric measurements without applying any corrections. In practice, observers often report times of observation that have the light-travel time removed or measurements that have been reduced to 1 AU and/or have the phase correction removed. All of these corrections require knowledge of the position of both the observer and the minor planet, information that is derived from the orbit. But one does not know, in most cases, which orbit the observer used to apply their corrections or how they computed those corrections. The possibility of gross errors in the application of observing corrections by the observer is ever present. The quality of the orbits for many of the numbered objects, even as late as the early 1980s, was rather poor, with ephemeris errors of more than 1′ being not uncommon.

When extracting photometric observations from the literature, I use only observed magnitudes or

magnitudes reduced to unit distance. Observations that have been converted to absolute magnitudes are ignored. By converting to an absolute magnitude the observer has removed the phase effect. For modern studies, this involves a derived or assumed G; for older studies, a derived or assumed phase coefficient p has been used. In either case, the value of the assumed quantity may or may not be stated explicitly in the paper.

In addition to utilizing published data where it is possible to correct the comparison star magnitudes, I also undertook a literature search for other photometry. A large number of papers were located that presented mean or maximum magnitudes from lightcurve investigations, either listed conveniently in tabular form or buried in the body of the article. Many of these papers also included colour index measurements. The lists of papers from which colour or photometry data were extracted are detailed in Appendices 4 [p. 224]and 5 [p. 225], respectively. An examination of selected photometric papers from the minor-planet literature, showing a variety of issues related to the extraction of photometric observations from the literature, is undertaken in Appendix 7.11 [p. 242].

5.4.1: Indication of Manipulated Magnitudes

Observers who make adjustments to unit distance or remove the phase effect should indicate that the observed magnitudes have been manipulated. It should be noted again that many authors use α for the phase angle.

If visual-band observations are reduced to unit distance by removing the 5 log ($r\Delta$) term, the magnitudes are indicated as $V(\beta)$. If the phase effects are also removed, the magnitudes are indicated as $V(0)$: this is also a single measurement of the absolute magnitude (rough, in that the effects of rotation are not removed). Of course, if the observations are made in some other band, the V is replaced as appropriate.

If the magnitudes are mean magnitudes, averaged over one rotation of the minor planet, they are indicated as $\bar{V}$, $\bar{V}(\beta)$ or $\bar{V}(0)$, as appropriate. $\bar{V}(\beta)$ is equivalent to $H(\beta)$, the absolute magnitude of the object at the stated phase angle.

The above notation is due to Bowell and Lumme (1979), who dropped the "1" from the earlier notations, referred to as the Gehrels and Tedesco form. In the earlier system, $V(1,\beta)$ is equivalent to $V(\beta)$. Both $V(0)$ and $V(1,0)$ are extrapolated from observations made at non-zero phase angles.

Some authors report the maximum brightness of a lightcurve, rather than the mean. Such observations are indicated as V_o, $V_o(1,\beta)$ or $V_o(1,0)$, as appropriate. In order to be useful for determination of absolute magnitudes, such observations have to be accompanied by a value for the amplitude of variation. For the purposes of this research, the maximum brightness is converted to a mean magnitude by adding half the lightcurve amplitude. Harris *et al.* (1984a) note that the time-averaged mean brightness is generally slightly brighter than the mid-extrema brightness because lightcurve minima are normally sharper than the maxima. This difference is typically only a few hundredths of a magnitude: for the two objects investigated by Harris *et al.*, the differences were 0.01 mag. for (82) Alkmene and 0.015 mag. for (444) Gyptis.

5.4.2: Converting to the MPC Observation Format

While the data in the APC for each object is stored in a consistent format, this format is not optimal for automated processing. The data from one reference is stored in a multi-line format in one file, which may contain data on one or more objects each on one or more nights. The multi-line format consists of header and trailer lines, along with keyword/value pairs.

A sample file (Barucci and Dipaoloantonio, 1983) is shown below. The bulk of the individual photometric observations have been removed for space reasons. The observations are of (22) Kalliope made on 1981 Nov. 30 with the 0.50-m reflector at Teramo Observatory. The *V* photometry is relative, but the comparison star is not identified, and the times of observation have not been corrected for light-travel time.

```
format atlas 4.
********************************************************************************
begin generic
UPDATE.....: 0
OBJECT.....: 22 Kalliope
REFERENCE..: Barucci and Dipaoloantonio (1983)
OBSERVING SITE: Teramo
TELESCOPE..: 0.50-m reflector
COLUMNS....: #V
```

```
RELATIVE PHOT.: T
LT CORRECTED..: F
OBSERVING TIME: 2444938.5      (1981 Nov 30)
ZERO TIME.....: 2444938.5       1981 Nov 30.0
ZERO MAG......: 00.00
end
*******************************************************************************
include generic
GEOMETRY......:
        system: J2000.0 ecliptic
         epoch: 2444938.5  (1981 Nov 30.0)
         Earth:   0.370154   0.914089   0.000021   -0.016227  0.006394  0.000000
        object:   0.973371   2.426915   0.016440   -0.010020  0.004146  0.002649
ASPECT DATA...:  2.6149  1.6287   0.20   68.30   0.60  2444938.50000  J2000.0
INFORMATION...: ASPECT ERROR !!!
DATA:
  18.920   0.096
...
*******************************************************************************
END OF FILE
```

A Fortran 95 program, FORMATAPCREFS, was written to convert this multi-line format into a one-line MPC format. The program finds the mean of the magnitudes listed in the DATA: section by locating maxima and minima. (Treating the individual magnitude values as discrete points on a continuous function, the search is for turning points.) If the program does not find either a maximum or a minimum, no mean can be determined and the APC file cannot be reduced to a MPC observation. If more than one maximum/minimum pair is found in the DATA: section, FORMATAPCREFS outputs a MPC observation for each pair. FORMATAPCREFS was made to be flexible, in that it could process one file or many at a time. The input is a list of one or more APC files, each formatted as shown earlier. The output is a file containing MPC photometric-format observations. The sample file produces the following single-line output:

```
00022         L1981 11 30.85929                                R...R  0.17V AA117037
```

where "00022" is the packed number of the minor planet, "L" indicates that this is a photometric record (this is an extension to the documented MPC observation format), "1981 11 30.85929" is the UT date and time of observation, "R...R" is five flag values, "0.17" is the mean magnitude, "V" is the magnitude band, "AA117" is the reference and "037" is the observatory code for Teramo. The meaning of the flag values stored in columns 60–64 is shown in Table 5.4 [p. 108].

Table 5.4: Meaning of flag values on MPC photometric records

Column	Value	Meaning
60	?	Unknown if absolute or relative photometry
	A	Absolute photometry
	R	Relative photometry
61	.	Not reduced to 1 AU
	R	Reduced to 1 AU
62	.	Not corrected for light-travel time
	L	Corrected for light-travel time
63	.	No additional notes (assumed to be mean value)
	0	Given comparison star magnitude is mean value of more than one comparison star
	1	Observation is a single measure, not a mean value
	2	Observation is of primary maximum
	3	Observation is of primary minimum
	4	Observation is of secondary maximum
	5	Observation is of secondary minimum
64	A	Derived magnitude is absolute
	R	Derived magnitude is relative
65		Uncertainty (in units of 0.01 mag) in Base-62 format, omitted if greater than 0.61 mag.

If the information on which star was used as the comparison is available, the J2000.0 α and δ (both in decimal degrees), the magnitude used for the comparison star and the magnitude offset of the minor planet are stored between the date of observation and the flags.

In the description of column 63, it is important to note that the primary maximum is not necessarily M1 and the primary minimum is not necessarily m1, where M1 and m1 are defined by a paper's authors. Similarly, the secondary maximum is not necessarily M2 and the secondary maximum is not necessarily m2, as defined by a paper's authors. The term "primary" indicates the brighter maximum and fainter minimum and the term "secondary" indicates the fainter maximum and brighter minimum. Base-62 format allows 62 different values to be stored in a single printable ASCII character, using the digits 0 through 9, the twenty-six capital letters and the twenty-six lowercase letters.

In the sample observation shown previously, the resulting MPC-format observation is of no use in determining the absolute magnitude parameters of (22) Kalliope since the observation remains relative. An obvious question therefore arises: Can the comparison star that was used be identified?

I sent a query to the lead author of the 1983 paper asking if there was any unpublished information regarding which comparison star was used: the response was "As it was relative photometry, the used stars were those in the field...I cannot give more information" (Barucci, 2009). Using the MPC's Minor Planet and Comet Ephemeris Service[5], an on-line service that I worte, the J2000.0 position of (22) at the mid-point of the observations was found to be $\alpha = 04^h24^m40.7^s$, $\delta = +22°18'05''$, with a predicted magnitude of $V = 9.7$. Since the relative magnitude was found to be +0.17, I needed to find a comparison star with $V \sim 9.5$. A check of the UCAC-2 catalogue showed two candidates of about the right magnitude within 20′ (this search radius was entirely arbitrary) of the position of (22); these are summarized in Table 5.5, with the column Dist. indicating the distance in seconds of arc from the candidate to the minor planet.

Table 5.5: Candidates for Barucci and Dipaoloantonio (1983) comparison star

Candidate	J2000.0 Position	Dist./″	*V*
HD 284385 = UCAC-2 225.015351	04 23 28.17 +22 07 02.4	1198	9.77
HD 284386 = UCAC-2 225.015399	04 23 52.73 +22 04 39.0	1033	10.0

HD 284385 is the better fit, leading to a rereduced mean magnitude of $V = 9.94$ for the 1981 observation of (22) Kalliope. Unfortunately, I cannot justify using this identification since I have no information on whether the assumption I made about the size of the search area is valid. However, I can use the identification to demonstrate the format of a MPC photometric observation when the comparison star is identified:

```
00022         L1981 11 30.85929 065.8674+22.1173 9.77V 0.17R...A  9.94V AA117037
```

It is important to note that I am not criticizing the data storage format of the APC with this reformatting of the photometric observation data. The standardized storage of data in a sub-field when homogeneous formats have been a rarity is to be applauded.

5 http://www.minorplanetcenter.net/iau/MPEph/MPEph.html

5.4.3: Extraction of Photometric Observations

In the absence of sufficient information to rereduce a set of photometric observations, I simply extract the mean magnitudes from the published literature. A large number of published papers were examined to find photometric observations. Although some of the data are available in computer-readable files, the overhead of converting such files into a format useable for this thesis meant that for most data sets it was simply quicker to enter the observations manually from a printout of the paper. Conversion of available machine-readable data files (provided either by the authors or extracted from the PDF versions of the papers) was performed only when there were more than 50 or so observations in the file. The list of references from which photometric observations were extracted is given in Appendix 5 [p. 225].

Many authors fail to relate the mean magnitude to a specific date and time, giving only the date. In such cases, I have adopted a single decimal of a day of observation. This is usually .0, unless the observation was made at a site known for its astrometric observations, where an appropriate decimal for local midnight at that site was adopted. Other authors quote a single mean magnitude derived from more than one night of observation, but fail to indicate a date to which that magnitude applies.

A number of authors gave maximum magnitudes rather than mean magnitudes: if lightcurves were published in the paper or if the amplitudes are given in tabular form, I determined the mean magnitudes by adding half the amplitude (taken either from a table or from a plot) to the maximum magnitude.

5.4.4: Good Observing Practices: Some Recommendations

Harris and Lupishko (1989) made a number of recommendations regarding good practices when reporting photometric observations in the literature, noting that observers cannot be sure what use will be made of their raw observational data in the future. They recommend that quantities such as the identification of the minor planet, the comparison stars and the standard stars, the magnitudes and colours of the comparison and standard stars, be published in a form that preserves full accuracy. This would either be a table that would be included in the published paper or, if too large for publication, made available through a data center or by request. Information that can be

reconstructed, such as aspect data, need not be published in great details, a summary of sky position and phase-angle covered would be sufficient. Figures should not be used to convey information that is better presented in tabular form, but if not so provided, the figures should be clear enough to allow individual data points to be extracted.

I would make the further recommendation that if an observer goes to the effort of putting their observations onto a standard system, then a table listing the mean magnitude (along with the maximum magnitude, if desired) on each night should be included in any published paper. For objects with periods longer than a single night's run, the mean magnitudes would have to be derived from knowledge of the shape of light curve and knowledge of where each night's observations lay on the curve. For objects with very short periods (a few hours or shorter), there could be several mean magnitudes reported per night, if an observing run was long enough.

5.5: Amateur Lightcurve Observations

Here I use the term "amateur" in its positive meaning: one who undertakes a project for enjoyment or enlightenment. Many amateurs who undertook astrometric observations in the early days of CCD observing became discouraged once the major professional surveys starting sweeping up most new objects that were within the reach of amateur equipment. These amateur observers switched to photometric projects, principally the determination of rotation periods from observations of light curves. A substantial number of the 5000-plus minor-planet rotation-period determinations are derived solely or mostly from amateur observations. Unfortunately, a majority of the amateur lightcurves obtained in the past have used relative photometry, which is not tied to a standard system. Relative photometry is adequate when all one is interested in is determining a rotation period, but is of no use for deriving mean magnitudes to use in *HG* determinations. The availability of an all-sky deep-photometric catalogue (such as the APASS catalogue, see Section 10.3.5 [p. 197]) will allow all photometric observers to produce standard-system magnitudes easily.

5.5.1: ALCDEF and the MPC Archive of Lightcurve Observations

The Asteroid Lightcurve Database (Warner *et al.*, 2009), known as the LCDB, is intended as a central repository for lightcurve data on minor planets, storing information such as rotation period,

amplitude, albedo and absolute magnitude on each object in the database. In addition to making information available via file download, there is also an on-line interface[6] allowing user-defined queries to be made. However, the information present in the LCDB is not sufficient for certain projects, such as shape modelling or spin-axis determination, which require access to the raw photometric observations. Unfortunately, in the view of Warner *et al.* (2009), a universal format for the distribution and archiving of raw minor-planet photometric observations did not exist. The existing APC and SAPC formats (see Section 5.4.2 [p. 106]) did not meet their requirements. Stephens *et al.* (2010) addressed this issue by proposing the Asteroid Lightcurve Data Exchange Format (ALCDEF), a FITS-like format that is easy to write and easy to read. In addition to defining the format, the authors suggested that there should be a central archive for ALCDEF data. At a 2009 meeting in Baltimore (Maryland), Tim Spahr suggested to Brian Warner that the archive be hosted by the Minor Planet Center. I was agreeable to the suggestion and the MPC interface to the ALCDEF data was brought on-line at the start of 2011. The MPC ALCDEF interface allows observers to upload new data files and to extract raw photometric data on specific objects. Users can request files containing the individual magnitude measurements made by a single observer during a single observing program of a single object. A single observing program may contain observations from only one, or many, nights. Observations may be unfiltered or made through standard filters (see Section 3.4 [p. 50]), as documented as the header of each ALCDEF file. Free use of the data contained in the ALCDEF database provided appropriate acknowledgement is made to the observers who obtained the data.

5.6: Visual Observations

A skillful visual observer of variable stars is capable of making magnitude estimates that are good to ± 0.1 mag. These magnitudes estimates are in the visual system of the human eye, rather than the Johnson *V* band. Visual determinations of minor-planet magnitudes can be made using techniques familiar to observers of variable stars. Since most variable stars do not move significantly with respect to other stars on time-scales of a few decades, it is possible to prepare standard finder charts listing visual magnitudes for comparison stars that typically have solar-type colours. (One notable exception is Barnard's Star = V2500 Ophiuchi, a BY-Draconis-type variable[7], which has an annual proper motion of

6 `http://www.minorplanet.info/lightcurvedatabase.html`

7 BY-Draconis-type variables are late-type (usually K or M) main-sequence stars that exhibit variability due to the rotation of the star, combined with star spots (analogous to sun spots) and chromospheric activity. Some of these stars, including V2500 Ophiuchi, have shown flare activity (Paulson *et al.*, 2006).

10.36″. This nearby variable star moves one Moon-width across the sky every 180 or so years.) A typical observing technique is to use two comparison stars in the field of view, one brighter and one fainter than the variable. The brightness interval between the brighter and fainter comparison is then (mentally) divided into a small number of steps. An estimate is then made of how many steps the brightness of the variable is from either of the comparisons. If comparison A has $V = 12.3$ and comparison B has $V = 12.9$, and the brightness difference is divided into three parts, and the variable is determined to be one step fainter than A, then one step = 0.2 mag. and the variable is $V = 12.5$. Of course, if the variable is determined to be exactly equal to a comparison star, no further work is necessary. It requires an experienced observer to make magnitude determinations good to ± 0.1 mag. Finder charts for variable stars are prepared and distributed by a number of groups, including the American Association of Variable Star Observers and the British Astronomical Association. Similar observing techniques can be used for determining minor-planet magnitudes visually, but since minor planets move over the course of a single night, pre-prepared comparison-star finder charts are not practical. Comparisons must be made to whatever stars are present in the field of view.

Light is detected by the human eye using two different kinds of photoreceptors (cellular structures coated with light-sensitive pigments). The first kind of photoreceptor is the cones, which perform colour detection. There are three types of cones, differing in the pigment and the number and placement within the eye, which detect different wavelength ranges of light. These wavelength ranges overlap and our colour perception is based on how much each kind of cone is stimulated. Cones do not work in low-light conditions and humans thus have poor colour perception at night. The second kind of photoreceptor is the rods, which are extremely sensitive to light (responding to a single photon, as opposed to the ~ 100 photons required to activate a cone) but which have only one kind of light-sensitive pigment and thus play (little or) no role in colour vision. It is the rods that are responsible for human night version. In daylight, the eye is sensitive to light with wavelengths in the approximate range 380 to 700 nm. At night, this range is roughly 400 to 620 nm. The human eye is not a standardized detector. There is variation between individuals, even between those individuals deemed to have "normal" vision. Figure 5.4 [p. 114] shows the wavelength-dependent response of the rods in the human eye. The data are taken from `http://www.cvrl.org/database/data/lum/scvle_1.csv`. According to these data, rods are most sensitive to light at 507 nm—this value is somewhat different than the oft-quoted value (see, e.g., the Wikipedia entry on scotopic [low-light-level] vision) of 498 nm. Either value can be compared with the 540-nm peak for the Johnson *V* band. However, the general shape of the response curve should

not be dependent on which of the two values is "correct". Since this response curve is different to that of the Johnson *V* band, a visual magnitude can not be considered as a true Johnson *V* magnitude, only as an approximation.

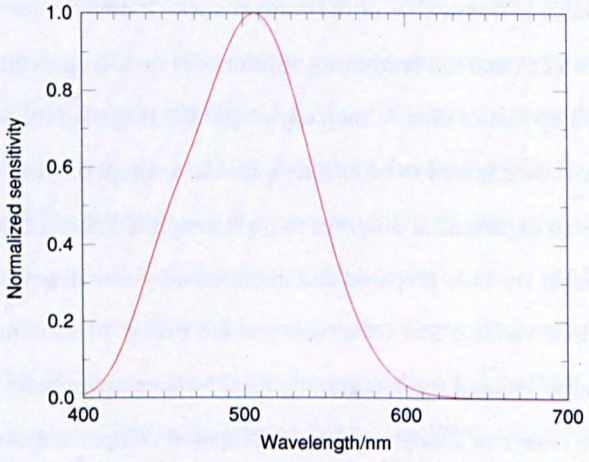

Figure 5.4: Response of human eye

The visual magnitudes used for this thesis are taken from the data file distributed by the Magnitude Alert Project (MAP), which was set up by amateur astronomers (Garrett, 1997) to identify objects with poorly-determined absolute magnitudes and obtain observations of those objects. The observations included in the MAP data files were obtained via a mixture of methods—visual, photographic and CCD. I downloaded the last complete distribution[8] of the main MAP data files, as well as the update[9] with the latest observations. For this thesis, I extracted only the visual magnitude estimates, those marked as being of magnitude type "AMv". This turned out to be a non-trivial task. Decompression of the zip file of the complete distribution produced an Excel file. Upon loading this file into Open Office, I discovered that the spreadsheet was arranged in a way that precluded easy extraction of the data. Rather than each observation line containing the designation of the observed object along with the observation (date and time of observations, observed magnitude and name of observer), there was a line with the designation, with the observational data listed on subsequent lines! In addition, the file of latest observations was not supplied as an Excel spreadsheet, but as an HTML page. Fortunately, the format of the HTML page and the comma-separated-value data extracted from the spreadsheet were broadly similar, so after some manual editing of both files, I was able to write a single program to read both sets of data and convert them into the MPC format. A total of 1678 visual observations, made by eight

8 `http://www.astrosurf.com/map/MAP_DATABASE_measures.zip`
9 `http://www.astrosurf.com/map/NEW_MAP_MEASURES.htm`

different observers, were extracted. In lieu of assigned observatory codes, I generated "pseudo observatory codes" from the first three letters of the observer surnames. The uncertainty of each visual estimate was set to 0.15 mag., this being half of the mean amplitude for objects with known lightcurves (see Section 2.2 [p. 13]).

5.7: Complications With Recent Amateur Astrophotometry

One of the most widely used astrometric-reduction computer programs used within the amateur observing community (as well as by many within the professional community) is Astrometrica (Meyer and Raab, 1995). In addition to producing quality astrometry, it also computes magnitudes. Recent versions of this program have attempted to improve the quality of the magnitudes that are produced. Version 4.5.0.372 (issued on 2008 July 26) introduced the ability to determine high-precision *V* and *R* magnitudes when using the CMC-14 catalogue, using a method described by Dymock and Miles (2009) that is virtually identical to the method I used to generate the CDPC and ASTCAT-C. Version 4.6.5.389 (issued 2010 November 1) extended this enhanced photometric capability to the UCAC-3 catalogue. Observations that have magnitudes produced with such enhanced versions of Astrometrica should not have catalogue corrections applied when the observations are processed for this thesis. Unfortunately, there is no indication on the observational record that these versions of Astrometrica have been used. In an attempt to determine which observatory codes used this enhanced photometric capability, I posted a request on the Astrometrica Yahoo Groups page asking observers to report the date on which they started using the relevant versions of Astrometrica. A number of observers responded; the details of the observatory codes affected and the dates when they started using the Astrometrica versions are stored in a file called `ASTROMETRICA.TXT`, which is included on the thesis website.

5.8: Observing From New Mexico

Although I have never considered myself much of an observer, having always been more interested in astronomical computing, I did feel that it was important for me to provide some of my own observational data for this project. Lacking both a personal telescope and a decent observing site, and realizing that getting time on a CfA telescope was next to impossible, I decided to purchase time on various telescopes operated by the Global Rent-a-Scope (GRAS) service (now known as iTelescopes.net[10]). GRAS operated numerous telescopes at three sites in the U.S., Spain and Australia: Mayhill, NM; Nerpio;

10 `http://www.itelescope.net`

initially at Moorook, SA, then at Officer, VA (the Australian instruments are being relocated to Siding Spring Observatory, NSW). All the telescopes were controlled remotely by a web-based interface and had the ability to run scripted observing at specific times. Most of my observations were obtained from the Mayhill site with a now-decommissioned 0.25-m f/3 reflector or the 0.50-m reflector, both of which were equipped with *UBVRI* photometric filters. Observations were obtained through either the *V* or the *R* filter and were reduced with versions of Astrometrica that had enhanced photometric-reduction capability (see Section 5.7 [p. 115]). Two different types of observation were attempted: multi-hour multiple-night photometry of a small number of targets for lightcurve determination; and short-arc multiple-night photometry of known low-lightcurve-amplitude targets for phase-angle coverage. Analysis of the lightcurve data is not yet complete and any results that are forthcoming will be reported to *The Minor Planet Bulletin*, the premier journal for lightcurves. The lightcurve observations were hampered by equipment failures and weather issues. The observation of low-lightcurve-amplitude objects produced more immediate results. Since these objects had low-amplitude rotational variations (under 0.1 mag.), a single observation at any time would be within 0.05 mag. of the mean magnitude that would derived from a long series of observations that covered at least one rotation The total number of observations published so far is 34 (Guido *et al.*, 2011)[11].

11 *Minor Planet Circular* references were not being inserted into the Astrophysical Data System (ADS) during the period when I did the bulk of my observing, so only one of my observing runs is indexed. In addition, the way that ADS references are constructed for sites with multiple program codes (such as Mayhill) is somewhat misleading. The individual program codes do not get their own bibcodes, as all observers at the same site are lumped into the same ADS entry. This is why the reference to my observations is Guido *et al.*, 2011 and not Williams and Marsden, 2011. Since I am the author of the internal procedure that prepares the *MPC* references for ADS, I have only myself to blame for this...

6: Reduction Procedures

6.1: Introduction

I discuss how the various types of observations are prepared for processing, including selection of observations, reformatting to include information needed for the processing and the reduction to unit distance. I describe the operation of a number of Fortran programs and command files/scripts used in this work: PCHECK and GETRAWDATA, which prepare the astrometric observations for processing; CATCORR, which applies the catalogue-specific corrections; and WORKOUTH, which applies the observer-specific corrections and works out the new *HG* values.

6.2: Reduction Steps

The reduction steps necessary to convert a set of observed magnitudes (possibly in bands other than *V*) for one or more minor planets, into a set of *HG* magnitude parameters are shown, in pseudo-code, below:

INPUT: A series of files containing photometry or astrophotometry
PREPARE `colsandtax.txt` FILE
FOR EACH FILE:

- •CONVERT FILE TO STANDARD FORMAT USING **PCHECK** AND **GETRAWDATA**
- •CALCULATE CATALOGUE CORRECTIONS USING **CATCORR**
  - GENERATE **.FITFILE**

FOR EACH OBJECT IN FILE:

- •ASSUME DEFAULT UNCERTAINTIES FOR ALL OBSERVATIONS
- •ITERATE:
  - CALCULATE NEW HG VALUES USING **WORKOUTH**
  - DETERMINE NEW VALUES FOR UNCERTAINTIES OF EACH OBSERVATION
  - DETERMINE NEW VALUES FOR OBSERVER-SPECIFIC CORRECTIONS
  - CHANGE REJECTION/ACCEPTANCE OF OBSERVATIONS
- •UNTIL CONVERGENCE

It is important to note that the magnitudes after processing by CATCORR are still in the local photometric system defined by an observer's telescope and CCD setup. Placing the corrected magnitudes onto a standard photometric system requires the use of observer-specific corrections.

6.3: Pre-Processing Observations

In order to simplify the processing of the observations, I need to convert the various input formats into a standard format that is better suited for the processing of magnitudes, as well as adding various important or useful information that is not present in the input formats.

6.3.1: PCHECK & Reduction to Unit Distance

PCHECK (Perturbed residual CHECKer) is the standard command-line tool I wrote for use at the MPC for checking the residuals of newly-submitted observations. PCHECK scans a file of observations, examines the designation on each observation record, locates the latest published orbit for that designation, integrates the orbit to the date of observation, predicts where the object should have been as seen from the observation site at that time and produces the observed minus calculated (O–C) residuals in right ascension and declination. It then outputs the observation, with the O–C residual, the solar elongation, the phase angle and the predicted *V* magnitude added. Additional data that it is useful to have precomputed when processing a (astro)photometric observation are the correction to unit geocentric and heliocentric distances (the 5 log ($r\Delta$) term in Equation 2.1 [p. 13]) and the coordinates of the PAB. All these quantities can be supplied by PCHECK.

Before undertaking the thesis research, I added a couple of command-line flags to PCHECK, in the expectation that they would be of use in this thesis. These flags were /MAGSONLY (`--magsonly`, in the Linux version), which ignores any observation without a magnitude estimate, and /DMAG (`--dmag`), which adds the value 5 log ($r\Delta$) to the output for each observation. The first new flag meant that the programs for correcting the astrophotometry would not need to weed out observations without magnitude estimates, while the second flag provided a precomputed value allowing reduction to unit distance utilizing perturbed values for the geocentric and heliocentric distances. In order to assist with the processing of the photometric observations, two other command-line flags were added later: /ABSONLY (`--absonly`), to consider only absolute photometric magnitude estimates (i.e., column 64 of the observation record contains 'A', see Table 5.4 [p. 108]), thus rejecting relative observations; and /PAB (`--pab`), to output the Phase Angle Bisector.

6.3.2: GETRAWDATA

GETRAWDATA is the program used to convert output files generated by PCHECK into Standard Format files. It is not normally run as a stand-alone process. Rather, it is part of a command file (script) that takes a *.DAT file, runs PCHECK to create a *.RES file, then runs GETRAWDATA to convert the *.RES file into a Standard Format *.OBS file.

6.3.3: The Standard Format

The Standard Format is the basic storage form used for the processing of the observations. It is generated by GETRAWDATA using the output files from PCHECK as input. The Standard Format is described in Table 6.1.

Table 6.1: The Standard Format as generated by GETRAWDATA

Columns	Format	Use
1–7	I7	Minor planet number
9–22	F14.6	JD of observation (UTC)
23	A1	Mode of observation: 'C' = CCD; 'P' = photographic; 'T' = transit circle; 'M' = micrometer; 'A' = (probably) photographic; 'L' = photometric; '*' = visual
25–27	A3	Observatory code
28	A1	Program code, used to distinguish between multiple observing programs at the same site. Blank if no code.
29–32	Z4	Reference catalogue code
33–37	F5.3	Observed magnitude
38	A1	Observed magnitude band
39	A1	Observed magnitude uncertainty (Base-62 format)
40–48	F9.4	5 log ($r\Delta$)
49–54	F6.2	Phase angle (in decimal degrees)
55-64	A10	Reference to publication of the observation
66–72	F7.3	Observed Right Ascension (in decimal degrees)
73-79	F7.3	Observed Declination (in decimal degrees)
81–86	F6.2	PAB Right Ascension (in decimal degrees)
87–92	F6.2	PAB Declination (in decimal degrees)

If the reported magnitude has already been corrected to unit distance, then columns 40–48 will contain zero.

6.3.4: Converting MPC Astrometric Observations

In its internal operation, the Minor Planet Center stores the observations of the numbered minor planets in over 300 separate files, each file containing the observations belonging to a variable range of consecutively-numbered objects. Each filename has the form `Nxxxxx.DAT`, where `xxxxx` indicates the number of the first object included in that file. This arrangement is in contrast to that used for the numbered minor-planet observations made available to outside users, which is distributed as a single 5.5 GB file. For the low-numbered minor planets, a file can contain as few as ten numbered objects, but most of the files contain the observations of one thousand consecutively-numbered objects. This storage arrangement has great advantages for the updating of these files during the preparation of each batch of monthly *Minor Planet Circulars*; the principal reason being that the insertion, correction or removal of a single observation does not require a rewrite of the entire multi-GB file. A similar internal storage arrangement applies to the observations of unnumbered minor planets, as well as numbered and unnumbered comets and natural satellites.

The publication cutoff for including observations in the first iteration of this study was the batch of *Minor Planet Circulars* dated 2009 October 4. At that time there were 221 945 numbered minor planets. For observations made by Pan-STARRS, which had reported only 9500 minor-planet observations from its commissioning test phase by the 2009 Oct. 4 cutoff date, the cutoff date was 2011 May 23.

The conversion of the MPC astrometric observations was done in five passes. The first pass, which was performed in October 2009, examined each `N*.DAT` file and ran `GETRAWDATA` to produce a corresponding `N*.OBS` file. The second pass, performed in September 2010, examined each `N*.DAT` file, extracted observations made by SDSS (code 645) or Pan-STARRS (code F51) and ran `GETRAWDATA` to produce a corresponding `R*.OBS` file. At the same time, the SDSS observations that were present in the `N*.OBS` files were removed. A third pass in May 2011 extracted Pan-STARRS observations published since the second pass and observations from the USNO Flagstaff Station. A fourth pass in June 2011 extracted newly-published observations from the USNO Flagstaff Station. The fifth pass is described in Section 7.2 [p. 151].

6.3.5: Converting Photometric Observations

Since the MPC astrometric database does not yet contain photometric observations (as described in Section 5.4 [p. 104]), the photometric observations collected from the literature are stored in a single file. This file is broken up periodically into `P*.DAT` files, the filenames of which mirror the `N*.DAT` filenames (e.g., the files `N00101.DAT` and `P00101.DAT` contain observations of the same range of numbered objects). Each `P*.DAT` file is run through `PCHECK` and `GETRAWDATA` to produce a Standard Format `P*.OBS` file.

6.3.6: Converting Visual Magnitude Observations

The visual magnitude estimates collected from the Magnitude Alert Project are stored in a single file. This file is broken up periodically into `V*.DAT` files, the filenames of which mirror the `N*.DAT` filenames (e.g., the files `N00001.DAT` and `V00001.DAT` contain observations of the same range of numbered objects). Each `V*.DAT` file is run through `PCHECK` and `GETRAWDATA` to produce a Standard Format `V*.OBS` file.

6.3.7: Converting Lightcurve Observations

Since most lightcurve observers do not report mean magnitudes in their publications, it is necessary to process the individual photometric observations (if available) to determine the lightcurve.

The lightcurve of a minor planet can be represented as (e.g., Harris *et al.*, 1989a):

$$V(\beta, t) = \overline{V}(\beta) + \sum_{l=1}^{n}\left[A_l \sin\left(\frac{2\pi l}{P}(t - t_0)\right) + B_l \cos\left(\frac{2\pi l}{P}(t - t_0)\right)\right] \qquad (6.1)$$

where $\overline{V}(\beta)$ is the mean reduced magnitude at phase angle β, n is the order of the fit, t is the time of observation, t_0 is a time of mean magnitude near the middle of the span of observations, P is the rotation period of the minor planet (in the same timescale as t and t_0), and A_l and B_l are the Fourier coefficients of the fit. When fitting photometric observations to determine the mean magnitude, the rotation period is assumed known and the $V(\beta,t)$ are reduced to unit distance.

To assist the determination of colour indices from non-simultaneous observations in two colour bands, it is useful to differentiate Equation 6.1 with respect to time to get Equation 6.2, an expression for the rate of change of magnitude.

$$\dot{V}(\beta, t) = \sum_{l=1}^{n}\left[A_l\frac{2\pi l}{P}\cos\left(\frac{2\pi l}{P}(t - t_0)\right) - B_l\frac{2\pi l}{P}\sin\left(\frac{2\pi l}{P}(t - t_0)\right)\right] \qquad (6.2)$$

where $\dot{V}(\beta, t)$ is the rate of change of magnitude in magnitudes per unit time (where the unit time is in the same scale as P).

6.3.8: CATCORR

CATCORR is the program that determines whether it is possible to determine a catalogue correction for an observation and, if possible, determines what the catalogue correction should be for that observation. CATCORR scans a file of observations, formatted according to the Standard Format specification (see Table 6.1 [p. 119]), looking for observations reduced using one of the reference catalogues listed in Table 3.2 [p. 55]. When the program finds such an observation, it extracts the observed position of the minor planet and sees whether that position lies within the sky coverage of the SDPC. If it doesn't, CATCORR checks whether the CDPC covers the observed position. If neither the SDPC nor CDPC catalogue covers the observed position, the observed magnitude cannot be corrected for systematic catalogue error since I do not have any reliable comparison star magnitudes for that region of sky.

If CATCORR is run with the qualifier /NOCORRECTIONS, then no catalogue corrections are derived. No catalogue corrections are applied to the P*.OBS or R*.OBS files, so all such files are processed with the /NOCORRECTIONS flag. (Note that the corrections to the FASTT observations, described in Section 5.2.8 [p. 102], are not treated as catalogue corrections. The FASTT correction is still applied when the /NOCORRECTIONS flag is specified.)

An obvious optimization technique, to cut down the number of I/O requests when extracting entries from the large photometric catalogues, is to initiate a new read from the catalogue only when the new observed position is more than some defined distance from the previous observed position. For the purposes of this study, this distance is 15′. For observations that utilize the same comparison

stars, but that are made using different filters, another optimization technique is to determine a new transformation equation only when the filter changes. It is, of course, necessary to determine new transformation equations whenever a new read of a photometric catalogue occurs. For efficiency, CATCORR buffers the last ten transformation equations computed, so that interleaved observations from different sites using different reference catalogues do not require the same transforms to be recomputed repeatedly. As a further efficiency, the observed coordinates of the minor planet are snapped to a 15′-resolution grid before extracting stars from the photometric catalogues or finding the transforms. It is important to note that the right-ascension grid spacing is 15′ in *coordinate* space, not in *sky* space—i.e., there is no allowance for the cos δ term: the α grid points are 0°, 0°.25, 0°.5, ..., 359°.5 and 359°.75, regardless of the declination. Clearly, this approach means that near either celestial pole the spacing between adjacent α-grid points tends to zero. In practice, this does not cause any problems as very few observations of minor planets are made at declinations within 30° of either celestial pole.

6.3.8.1: Correcting a Bad Design Decision

As originally conceived, the extended Standard Format was supposed to include a colour correction, taxonomic classification and slope parameter, information that would be needed by WORKOUTH, on every observation. A lot of this additional information originally added by CATCORR would be the same for all observations of the same object; the only difference being the colour correction relevant to each observation. This was determined to be an unwise design decision, as it meant that modification of any physical parameter for an object would require CATCORR to be rerun on the entire file containing that object. Or, worse still, a modification to, or error in, the implementation of any of the data tables used by CATCORR would require the entire data set to be reprocessed! This latter situation is what prompted the design change, following an e-mail exchange with Brian Warner about his *HG* determination for the Hungaria-type object (5427) Jensmartin. Warner (2012a) obtained $H = 14.41$ for an assumed $G = 0.43$, compared to the MPC values of 13.5 and 0.15, respectively. I remarked that my new determination, based on this thesis work, was $H = 14.01 \pm 0.05$ for an assumed $G = 0.24$, but that I was concerned that my assumed G value was incorrect. An examination of the CATCORR source code showed that Table 3.4 [p. 63] had not been implemented correctly: Hungarias were being assumed to be S type, rather than E type. The program was corrected and the file

containing the observations of (5427) was reprocessed: the new values were found to be $H = 14.26 \pm 0.05$ for an assumed $G = 0.48$ (excluding the observer-specific corrections, which weren't ready at the time). Since this CATCORR error affected every Hungaria, it meant that it was necessary to rerun the program on all the observations. I made the decision to separate out certain information stored in the extended Standard Format into a file `colsandtax.dat`, that could be read by WORKOUTH, so that if a similar problem arose in the future, it would not be necessary to do a complete CATCORR run.

6.3.9: CATCORR Extensions to the Standard Format

The Standard Format is extended by CATCORR, which adds (if possible) the corrected magnitude in the observed band to each observation. CATCORR also adds an identifier to an entry in an associated Fit File (`.FITFILE`), which contains the details of the transformation equations used in the correction of the observed magnitude. Each file that is processed by CATCORR generates a corresponding Fit File. The additional information added by CATCORR is detailed in Table 6.2.

Table 6.2: Additions to the Standard Format added by CATCORR

Columns	Format	Use
94	A1	Source for catalogue correction: 'S' = SDPC; 'C' = CDPC; 'A' = high-quality Astrometrica observation; 'T' = TNO observation treated as "corrected"
96–101	F6.3	Corrected magnitude in observed band
103–114	A12	Fit File identifier, blank if column 94 = 'T'
116	A1	'?' = poor fit for transformation equation, blank otherwise

The format of a Fit File is detailed in Table 6.3. The current implementation of CATCORR uses a linear fit to determine the transformation equations between the SDPC/CDPC and an astrometric reference catalogue. The format of a Fit File is expandable, to accommodate higher-order fits for the transformation equations, if future work shows this to be necessary.

If the goodness of fit for a derived transformation equation is less than 0.9, it is marked as a potential poor fit by setting column 130 of the extended Standard Format to '?' (see Table 6.2 and Section 7.3.1 [p. 156]).

Table 6.3: Format of a Fit File

Columns	Format	Use
1–12	A12	Fit File identifier (as given in columns 118–129 of the Standard Format)
14–19	F6.2	Right ascension/°
21–26	F6.2	Declination/°
28	I1	Observed magnitude band code
30–31	I2	Astrometric catalogue band code
33–38	I6	Number of comparison stars available for fit
40–45	I6	Number of comparison stars used in fit
47–51	F5.3	Goodness of fit
53–56	F4.2	R.m.s. of the fit (in mag.) for used comparison stars
58	I1	Order of fit (1 = linear fit, 2 = quadratic fit, etc.)
60–66	F7.3	Constant term in fit
68–74	F7.3	Linear term in fit
76–82	F7.3	Quadratic term in fit
...	...	...

6.3.10: The `colsandtax.dat` File

The `colsandtax.dat` file (the name is derived from "colours and taxonomy") contains the measured or assumed values for the colour indices, the taxonomic class and the slope parameter for every numbered minor planet. The file is derived from a file of physical parameters of minor planets (both numbered and unnumbered) that I built and maintain within the internal MPC operation, augmented by data derived from various tables described in chapter 3. The data for each object is stored on a separate line and the format of each line is described in Table 6.4. There are two sets of colours for the Sloan filters: one is for the Pan-STARRS observations; the other is for everyone else.

Table 6.4: Format of `colsandtax.dat` file

Columns	Format	Use
1– 7	I7	Designation
9	A1	Taxonomic classification
10	A1	Source for taxonomic classification: 'B' = Bus-Binzel; 'T' = Tholen; 'P' = Pseudo-Tholen; 'F' = family membership; 'O' = orbit classification; 'D' = default
12– 14	A3	Colours-based taxonomic class (best three fits)
16– 20	F5.2	Adopted *G*
21	A1	Source for adopted *G*: 'T' = taxonomic classification; 'O' = orbit classification

23– 29	F6.3,A1	*U–B* colour and source. Source of colour: 'M' = measured; 'S' = derived from SDSS measures; 'P' = derived from Pan-STARRS measures; 'T' = assumed based on measured taxonomic class; 'D' = otherwise assumed
31– 37	F6.3,A1	*B–V* colour and source
39– 45	F6.3,A1	$V–R_c$ colour and source
47– 53	F6.3,A1	$R_c–I_c$ colour and source
55– 61	F6.3,A1	Pan-STARRS *V–u′* colour and source (as for *U–B* colour, lower-case letters denote values derived from Equation 3.2 [p. 68] using data from the associated capital-letter source)
63– 69	F6.3,A1	Pan-STARRS *V–g′* colour and source
71– 77	F6.3,A1	Pan-STARRS *V–r′* colour and source
79– 85	F6.3,A1	Pan-STARRS *V–i′* colour and source
87– 93	F6.3,A1	Pan-STARRS *V–z′* colour and source
95–101	F6.3,A1	Pan-STARRS *V–w′* colour and source
103–109	F6.3,A1	Pan-STARRS *V–y′* colour and source
111–117	F6.3,A1	*V–u′* colour and source (as for Pan-STARRS *V–u′* colour)
119–125	F6.3,A1	*V–g′* colour and source
127–133	F6.3,A1	*V–r′* colour and source
135–141	F6.3,A1	*V–i′* colour and source
143–149	F6.3,A1	*V–z′* colour and source
151–157	F6.3,A1	*V–w′* colour and source
159–165	F6.3,A1	*V–y′* colour and source

6.3.11: Transformation Equations

The current version of WORKOUTH derives linear transformation equations relating astrometric-catalogue magnitudes in a specified band (m_{cat}) to the photometric magnitudes in the same band (m_{phot}):

$$m_{phot} = a m_{cat} + b_0 \tag{6.3}$$

If the agreement between the two catalogue were perfect, $a = 1$ and $b_0 = 0$. Even a small deviation of the fitted slope parameter, a, from the ideal value of 1 leads to a large value for the intercept, b_0. This can make it hard to spot erroneous fits. For this reason, I decided to offset the catalogue magnitudes during the fitting process to a value somewhere within the range covered by the catalogues. This offset would not affect the slope of the fit, but would reduce the value of the intercept. The value chosen for the offset was 17.0. The transformation equations thus become:

$$m_{phot} - 17.0 = a(m_{cat} - 17.0) + b \tag{6.4}$$

The fitting process proceeds in the following manner. Using the data extracted from either the

ASTCAT-S or ASTCAT-C, the fitting procedure determines which columns of data need to be read from each data line. This is determined from the magnitude band of the observation that is being corrected and from the astrometric catalogue used for the reduction of that observation. Not all the stars extracted from the relevant ASTCAT file will have magnitudes in the required band. A preliminary fit for a and b is performed for each star that does have a magnitude. The residuals from the fit are determined for each star and a residual mean and standard deviation is determined. The fit is then repeated rejecting any star that had a residual of more than three standard deviations from the previous iteration. This process is repeated until either the number of rejected stars does not change from the previous iteration or the number of iterations equals five.

6.3.12: WORKOUTH

WORKOUTH is the program that combines the observations files (i.e., the N*.OBS, P*.OBS and V*.OBS files) corresponding to a single range of objects and computes new values for the absolute magnitude, H, and slope parameter, G. WORKOUTH computes four sets of HG parameters for each object: unconstrained fits to both H and G; unconstrained fit to H assuming a value for G based on taxonomic classification or dynamical classification; and unconstrained fits to H assuming two default values for G. The four possible HG solutions are labelled as follows:

- HG_U, where solutions are made for both H and G;
- HG_A, where a solution is made for H on the basis of a measured or assumed G;
- HG_S, where a solution is made for H assuming $G = 0.24$, the default value for S-class objects.
- HG_C, where a solution is made for H assuming $G = 0.12$, the default value for C-class objects.

If the measured or assumed G is the same as one of the default G values, then the HG_A solution will be identical to either the HG_S or the HG_C solution. The computation of one or more of these solutions may fail. The most common failure is expected to be that for the HG_U solution.

WORKOUTH writes three output files: a *.H file containing all four sets of computed HG parameters, one solution per line; a *.HG file containing the adopted HG solution (see Section 6.5 [p. 132]); and a *.H_DEFG file containing the HG_A solution. Each entry in the .H file contains

only the r.m.s. of the included-observation residuals for that particular solution (e.g., if it is a HG_A solution, then columns 161–165 and 173–183 will be blank), while the corresponding entry in the .HG file contains the r.m.s. residuals for all four solutions. The format of these three output files is described in Table 6.5.

Table 6.5: Format of output from WORKOUTH

Columns	Format	Use
1– 7	I7	Minor planet number
9– 14	I6	Total number of magnitude estimates available
16– 31	I6,X,I4,X,I4	Number of astrophotometric/photometric/visual observations available
33– 43	F5.1,X,F5.1	Range of phase angles for available observations
45– 48	I4	Number of observations available at $\beta < 7°$
50– 53	I4	Number of observations available at $\beta < 2°$
55– 68	F7.4,X,F6.4	H and uncertainty
70– 83	F7.4,X,F6.4	G and uncertainty If G is assumed or a default value, then the uncertainty is omitted
85– 90	I6	Total number of magnitude estimates used in solution
92–107	I6,X,I4,X,I4	Number of astrophotometic/photometric/visual observations used for solution
109–119	F5.1,X,F5.1	Range of phase angles for observations included in solution
121–124	I4	Number of observations included in solution at $\beta < 7°$
126–129	I4	Number of observations included in solution at $\beta < 2$
131–136	F6.4	Bias-corrected mean squared residual for included observations
138	A	Type of solution: = "U", unconstrained fit for both H and G = "A", unconstrained fit for H using an assumed G = "S", unconstrained fit for H using $G = 0.24$ = "C", unconstrained fit for H using $G = 0.12$
140	A	= "*", if solution is the adopted solution, blank otherwise
142–147	I6	Total number of corrected astrophotometric, photometric and visual observations available
149–153	F5.1	Percentage of available corrected observations included in solution
155–159	F5.1	Percentage of available observations included in solution
161-165	F5.2	r.m.s. of included-observation magnitude residuals for HG_U solution
167–171	F5.2	r.m.s. of included-observation magnitude residuals for HG_A solution
173–177	F5.2	r.m.s. of included-observation magnitude residuals for HG_S solution
179–183	F5.2	r.m.s. of included-observation magnitude residuals for HG_C solution
185–193	F9.1	Julian Date of the middle of the arc that was considered in this solution, given only if /BYOPP was specified

If there is insufficient information for any solution, the string "Solution failed: insufficient information" is output in columns 55–96, and columns 97–137 and 139 onwards are blanked out. If an individual solution fails, the string "Solution failed!" is output in columns 55–70 and columns 71–137 and 139 onwards are blanked out.

WORKOUTH also writes out a new version of the N*.OBS file, incorporating any observations from P*.OBS and V*.OBS files, and adding additional information to the Standard Format. The command file (script, when run under Linux) that runs WORKOUTH can operate either on an individual N*.OBS, (R*.OBS,) V*.OBS or P*.OBS file, or on any combination of those files. This flexibility allows me to perform runs using just the real photometry, or the reliable photometry, to assist in the determination of the observer-specific corrections.

The additional information added on to every observation by WORKOUTH is detailed in Table 6.6. The magnitude residuals in columns 158–180 are observed minus computed residuals.

Table 6.6: Additions to the Standard Format added by WORKOUTH

Columns	Format	Use
118–123	F6.3	Colour correction to *V*
124	A1	Colour source
126–131	F6.3	Observer-specific correction
133–138	F6.3	Catalogue- and observer-corrected *V* magnitude
140–144	variable	*V* magnitude (rounded to original precision)
146–151	F6.3	Uncertainty in *V*
153–156	4A1	For each of the four solutions: = 'A', if observation included in solution = 'R', if observation rejected from solution = 'I', if observation ignored = 'X', if no solution
158–162	F5.2	Residual from HG_U solution (see Section 6.5 [p. 132])
164–168	F5.2	Residual from HG_A solution (see Section 6.5)
170–174	F5.2	Residual from $G = 0.24$ HG_S solution (see Section 6.5)
176–180	F5.2	Residual from $G = 0.12$ HG_C solution (see Section 6.5)

Various command-line options (shown first as the VMS version, with the Linux version given parenthetically) can be specified to alter the way WORKOUT processes the data:

- /MINNUM=<value> (--minnum=<value>), sets the minimum number of observations required to attempt a solution (default = 10);
- /MINPHOTNUM=<value> (--minphotnum=<value>), sets the minimum number of photometric observations required to accept a solution (default = 5);
- /MINPHASERANGE=<range> (--minphaserange=<range>), sets the minimum phase range required to attempt a solution (default = 15°);

- `/OBSCODE=<obscode>` (`--obscode=<obscode>`), considers only observations made at the specified observatory code; and
- `/BYOPP` (`--byopp`), computes *HG* values on an opposition-by-opposition basis.

Some other `WORKOUTH` options, related to solution selection, are described in Section 6.5 [p. 132].

6.4: Computing *H* and *G*

With reduced magnitudes available, new H and G values for the numbered minor planets are derived. The method for the computation of H and G and associated errors outlined below is that described by Bowell *et al.* (1989), again noting that I use β for the phase angle, rather than α. Appendix 7.10 [p. 241] describes the errors I detected in two of the equations published in that reference.

Given n reduced magnitudes $V_i(\beta_i)$ with associated errors ε_i, the following quantities are computed:

$$\left.\begin{aligned} I_i &= 10^{-0.4V_i(\beta_i)} \\ h_{jk} &= \sum_{i=1}^{n} \frac{\Phi_j(\beta_i)\,\Phi_k(\beta_i)}{\varepsilon_i^2 I_i^2} \quad j,\, k = 1,2 \\ g_j &= \sum_{i=1}^{n} \frac{\Phi_j(\beta_i)}{\varepsilon_i^2 I_i} \\ D &= h_{11}h_{22} - h_{12}^2 \end{aligned}\right\} \tag{6.5}$$

In equation 6.5, I_i is the intensity corresponding to the reduced magnitudes $V_i(\beta_i)$, while h, g and D are intermediate values in the least-squares determination of H and G. The functions Φ_1 and Φ_2 are given by Equations 2.3 [p. 15]. Two auxiliary quantities, a_1 and a_2, are determined from Equations 6.6:

$$\left.\begin{aligned} a_1 &= (h_{22}g_1 - h_{12}g_2)/D \\ a_2 &= (h_{11}g_2 - h_{12}g_1)/D \end{aligned}\right\} \tag{6.6}$$

Values for H and G then follow from Equations 6.7:

$$\left.\begin{aligned} H &= -2.5\log(a_1 + a_2) \\ G &= \frac{a_2}{a_1 + a_2} \end{aligned}\right\} \tag{6.7}$$

To determine the uncertainties, ΔH and ΔG, in the H and G determinations, compute magnitude residuals r_i from Equation 6.8:

$$r_i = V_i(\beta_i) - H + 2.5\log[(1 - G)\Phi_1(\beta_i) + G\,\Phi_2(\beta_i)] \tag{6.8}$$

then:

$$\left.\begin{aligned}
\beta_0 &= \sum_{i=1}^{n}(\beta_i/\varepsilon_i^2) \Big/ \sum_{i=1}^{n}(1/\varepsilon_i^2) \\
\sigma^2_{H(\beta_0)} &= 1 \Big/ \sum_{i=1}^{n}(1/\varepsilon_i^2) \\
\sigma^2_{\beta} &= 1 \Big/ \left[\sum_{i=1}^{n}(\beta_i^2/\varepsilon_i^2) - \beta_0^2 \sum_{i=1}^{n}(1/\varepsilon_i^2)\right] \\
s^2 &= \frac{1}{n-2}\sum_{i=1}^{n}(r_i/\varepsilon_i)^2 \\
\Delta H(\beta_0) &= \pm s\,\sigma_{H(\beta_0)} \\
\Delta\beta &= \pm s\,\sigma_{\beta} \\
\Delta G &= \pm\Delta\beta/(0.0673 - 0.1132G + 0.0615G^2) \\
\Delta H(\beta) &= \pm\sqrt{(\Delta H(\beta_0))^2 + \Delta\beta^2(\beta - \beta_0)^2}
\end{aligned}\right\} \tag{6.9}$$

where β_0 is the weighted mean phase angle of the observations, $\Delta H(\beta_0)$ is the uncertainty in the reduced magnitude at β_0 and s^2 is the bias-corrected mean squared residual (or χ^2 per degree of freedom).

For an assumed value of G, the computation of H follows from Equation 6.10:

$$H = \frac{\sum_{i=1}^{n}\dfrac{V_i(\beta_i) - \Delta m(\beta_i)}{\varepsilon_i^2}}{\sum_{i=1}^{n}(1/\varepsilon_i^2)} \tag{6.10}$$

The uncertainty analysis then proceeds as for the unconstrained case, except that $\Delta\beta$ is determined from the expression for ΔG.

Bowell *et al.* suggest that caution is necessary when combining magnitude estimates from more than one opposition, due to possible aspect changes. This is sensible advice and I can try to avoid problems caused by aspect changes by determining H and G values on a per-opposition basis for each object, if it appears that only a small fraction of the available observations are included in a solution.

6.5: Selecting an *HG* Solution

WORKOUTH will produce either zero, one, two, three or four *HG* solutions for each object, not all of which will be distinct solutions. Which solution should be adopted? The worst-case scenario, zero solutions, will arise when the available astrophotometry is limited in either quantity or phase coverage, the lightcurve amplitude is large and/or there is *H* variability. Most objects will produce three distinct solutions, since the measured/assumed *G* will often be equal to one of the default *G* values.

The decision tree for selecting a *HG* solution, and the method that is programmed into WORKOUTH, is as follows:

- if there is a HG_A solution, adopt it.
- if there is a HG_U solution:
  - adopt it if $G_{min} \leq G_U \leq G_{max}$, if there are included observations at both $\beta \leq 2°$ and $2° < \beta < 7°$; if the phase coverage is at least G_{pr}; if the uncertainty in G_U is less than G_{unc}; and if the percentage of observations included is no more than 5% less than that of the HG_A solution.
- if there is a HG_S or HG_C solution:
  - adopt whichever of the two solutions includes more observations, if both of the other solutions are not adopted; or, the solution with the greater included-observation percentage, if it is at least 5% greater than the HG_A or HG_U solution.

The "5% greater/less" rule in the above decision tree is an attempt to prevent the selection of an adopted solution with an unreasonable *G* parameter that just happens to include more observations that the solution with a reasonable *G* parameter. The determination of the 5% value is purely empirical and was selected on the basis of examining the solution selection of early WORKOUTH runs.

The behaviour of WORKOUTH in selecting the solution that is to be adopted can be modified by various command line flags. The default value of G_{min}, the minimum acceptable value for *G*, is 0. The default value of G_{max}, the maximum acceptable value for *G*, is 0.5. These default values may be overridden by specifying either `/GMIN=<value>` or `/GMAX=<value>` (`--gmin=<value>` or `--gmax=<value>` on the Linux version). The default value for G_{unc}, the maximum allowable

uncertainty in G, is 0.1: this value may be overridden by specifying `/GUNC=<value>` (`--gunc=<value>`). G_{pr} is the minimum value of the phase coverage for a solution to be accepted. The default value is 15° and can be overridden with the `/GPR=<value>` flag (`--gpr=<value>`). The empirical 5% value can be modified using the `/EMPIRICAL=<value>` flag (`--empirical=<value>`).

6.6: Observer-Specific Corrections

The observer-specific corrections are the adjustments that must be made to the catalogue-corrected values to convert from the local photometric system to a standard system. A rigorous conversion requires observations made through standard filters and nightly observation of standard fields to obtain transforms between the local and standard photometric systems. The techniques for obtaining minor-planet magnitudes referred to standard photometric systems are covered in great detail by Henden and Kaitchuck (1982) and by Warner (2005). I cannot use the rigorous methods described in the afore-mentioned references, as the required information simply isn't available. What I can do is compare the catalogue-corrected magnitudes to some set of reliable magnitudes to derive observer-specific corrections that correct, in some fashion, to a standard system. The simplest way to achieve this is to derive *HG* parameters from the reliable magnitudes, then compare the catalogue-corrected magnitudes to predictions based on those parameters. The derivation of the reliable *HG* parameters is described below, while the comparison to the catalogue-corrected magnitudes and the determination of the observer-specific corrections is described in Section 7.3 [p. 152].

6.6.1: Using the `R*.OBS` and `P*.OBS` Files

The `R*.OBS` files contain observations from observatory codes 645 (SDSS), F51 (Pan-STARRS-1) and 689 (U.S. Naval Observatory's Flagstaff Station). The 645 and F51 observations were obtained through standard filters and are referred to standard photometric systems. The only U.S. Naval Observatory's Flagstaff Station observations that were included in the `R*.OBS` files are those made with the 0.2-m FASTT instrument, which are made in a system close to Johnson *V*, but which can be corrected to the standard system (see Section 5.2.8 [p. 102]).

The P*.OBS files contain photometric observations extracted from the literature, taken through standard filters and referred to standard photometric systems.

In order to get good *HG* fits, it is necessary to have observations at a wide range of phase angles, covering a range of 15° or more, with observations at $\beta < 7°$ and, ideally, observations at β near 0°. The large phase-range coverage is necessary to characterize the linear part of the phase curve, while observations near to $\beta = 0°$ are necessary to characterize the opposition surge.

6.6.2: Deriving *HG* from SDSS Observations

The criteria used to select SDSS observations were: at least 10 observations (i.e., at least five nights of observation); phase angle coverage of at least 20°; and a minimum phase angle < 2°. Twenty-one objects matched these criteria: (4994) Kisala; (8056) Tieck; (20230) Blanchard; (25529) 1999 XL_{127}; (35701) 1999 FF_7; (55197) 2001 RN_{17}; (69510) 1997 EN_5; (71939) 2000 WZ_{74}; (72153) 2000 YE_{97}; (75960) 2000 CS_{96}; (106422) 2000 VC_{42}; (115093), 2003 SQ_{16}; (116505), 2004 BN_{25}; (143661), 2003 SM_{73}; (167861), 2005 EV_{19}; (170281) 2003 QY_{105}; (170352), 2003 ST_{176}; (170373) 2003 SX_{245}; (172459), 2003 RO_5; (209085), 2003 SS_{26}; and (209133) 2003 SY_{236}. The observations of each of these objects were extracted from the R*.OBS files, appended together and then run through WORKOUTH. The results are given in Table 6.7, along with the *H* values (H_{MPC}) in use at the Minor Planet Center as of 2011 July 13 (all of the objects have the default value of *G* of 0.15). In addition, the WORKOUTH output files are included on the thesis website. In a number of cases, the solved-for *G* values were outside the range 0 to 0.5; in such cases, *G* was set to the default value for the known or assumed taxonomic class. In addition, when the uncertainty in the solved-for *G* was more than 0.1, *G* was set to the default value for the known or assumed taxonomic class.

Table 6.7: HG determinations from SDSS observations

Object	*H*	*G*	H_{MPC}	Problems?
(4994)	13.94 ± 0.08	0.24	13.8	Only 4 of 10 obs used
(8056)	14.25 ± 0.07	0.24	13.7	
(20230)	15.95 ± 0.12	0.24	15.5	
(25529)	13.93 ± 0.09	0.24	13.7	
(35701)	16.34 ± 0.02	0.27 ± 0.03	15.9	
(55197)	14.89 ± 0.06	0.12	14.6	

(69510)	15.90 ± 0.04	0.24	15.7	
(71939)	16.40 ± 0.05	0.24	16.1	
(72153)	16.29 ± 0.02	0.24	16.3	
(75960)	15.41 ± 0.04	0.24	15.1	
(106422)	17.05 ± 0.02	0.24	16.7	
(115093)	16.96 ± 0.06	0.12	16.9	
(116505)	17.03 ± 0.11	0.24	16.5	Only 4 of 10 obs used
(143661)	18.08 ± 0.05	0.24	17.8	
(167861)	17.12 ± 0.07	0.24	16.8	
(170281)	17.29 ± 0.02	0.24	17.2	
(170352)	17.07 ± 0.06	0.24	17.1	
(170373)	17.46 ± 0.05	0.24	17.4	
(172459)	16.85 ± 0.02	0.24	16.8	
(209085)	17.24 ± 0.02	0.28 ± 0.03	17.0	
(209133)	17.40 ± 0.04	0.24	17.3	

In most cases, the uncertainty in *H* is under 0.1 magnitude. The determinations for two of the objects are poor: only four of ten observations of both (4994) and (116505) were included in the solution. It is possible that these poor fits are a consequence of large lightcurve amplitudes. It is not possible to confirm this suspicion at the present time as the lightcurves of these objects have not yet been studied.

6.6.3: Deriving *HG* from Pan-STARRS-1 Observations

`WORKOUTH` was run on all the `R*.OBS` files with flags `/OBSCODE=F51/MINNUM=10`, so that only the Pan-STARRS observations were utilized and that ten observations were required to attempt a solution. The resulting `.H` and `.HG` files were appended together and these concatenated files are included on the thesis website. *HG* solutions were obtained for 2391 objects, a sample of which is shown in Table 6.8 [p. 136]. Included in the table is the fraction of available Pan-STARRS observations that were included in each solution, along with the current (as of 2011 July 15) MPC *HG* value.

The uncertainties in the *H* determinations in Table 6.8 are larger than those for the SDSS observations and, as shown in the next subsection, the FASTT observations. This may be a consequence of the poorly-characterised Pan-STARRS colour corrections.

Table 6.8: HG determinations from Pan-STARRS observations

Object	H	G	Fraction Included	H_{MPC}
(730)	13.96 ± 0.21	0.24	0.833	14.0
(1916)	14.77 ± 0.07	0.24	0.917	14.93
(1962)	12.27 ± 0.22	0.24	0.800	11.9
(2028)	14.98 ± 0.13	0.24	1.000	14.5
...				
(218929)	16.15 ± 0.22	0.24	1.000	16.5
(221917)	12.53 ± 0.15	0.24	1.000	12.5

6.6.4: Deriving *HG* from USNO FASTT Observations

The USNO FASTT observations are made with a transit-circle instrument, so only one observation of each object is obtained each night. For some low-numbered minor planets there are more than 300 observations available, made over multiple oppositions and covering almost the entire possible range of phase angles. Other objects have been observed on only one or a handful of nights. A total of 3265 different minor planets have been observed to date, but only 2690 had sufficient coverage to allow the determination of *HG* parameters.

Table 6.9 lists a small sample of the *HG* determinations from the FASTT observations. The complete WORKOUTH output file, including those objects for which there was insufficient information to determine a solution or the solution failed, is included on the thesis website.

Table 6.9: Samples of HG determinations from FASTT observations

Object	H	G	Fraction Included	H_{MPC}	G_{MPC}
(1)	3.40 ± 0.01	0.12	0.807	3.34	0.12
(2)	4.15 ± 0.01	0.12	0.737	4.13	0.11
(3)	5.31 ± 0.01	0.24	0.736	5.33	0.32
(4)	3.22 ± 0.01	0.37 ± 0.02	0.797	3.20	0.32
...					
(42284)	13.16 ± 0.07	0.24	0.684	12.7	0.15
(46992)	12.66 ± 0.08	0.24	0.857	12.2	0.15
(55538)	12.40 ± 0.08	0.24	0.833	12.3	0.15

There is no overlap between the objects observed by SDSS and by FASTT, so a comparison between the SDSS-only and FASTT-only determinations is not possible.

An examination of the file of FASTT-only *HG* values showed that there were a large number of determinations where less than half of the available observations were included. Two obvious explanations for low inclusion values are large lightcurve amplitudes and variable *H* values (due to changing viewing angles for non-spherical objects). To see which of these explanations was correct, Figure 6.1 was prepared. It shows the fraction of included observations plotted against the maximum lightcurve amplitude (taken from Harris *et al.*, 2007). It was decided to plot against the maximum amplitude, rather than the minimum or mean, since the FASTT observations can cover many oppositions and it is likely in such circumstances that an amplitude maximum (or near maximum) will occur in the period covered by the observations.

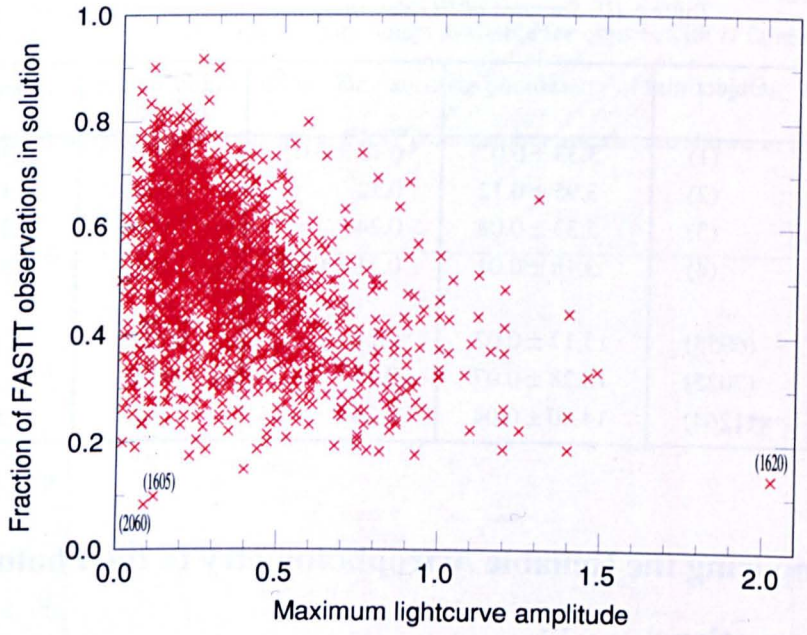

Figure 6.1: Included fraction of FASTT observations vs. maximum lightcurve amplitude

If the fraction of included FASTT observations for a specific object was related *only* to the maximum lightcurve amplitude for that object, then all the data points plotted in Figure 6.1 should lie in a narrow band stretching from upper left to lower right. The appearance of Figure 6.1 clearly does not match this ideal view as there are numerous objects with small lightcurve amplitudes that

have very low inclusion fractions. The two most egregious examples are labelled in Figure 6.1: (2060) Chiron and (1605) Milankovitch. The elongated large-lightcurve-amplitude near-Earth asteroid (1620) Geographos is also marked. The cases of (2060) Chiron and (1605) Milankovitch are discussed in Section 9.10 [p. 180].

6.6.5: Deriving *HG* from Photometric Observations

All of the `P*.OBS` files, comprising 4278 observations of 747 objects, were appended together and run through `WORKOUTH` in a single pass with `/MINNUM=5`. Solutions were found for 169 objects; there were insufficient photometric observations available for the remaining 578 objects. The complete output files from the `WORKOUTH` run are included on the thesis website. Table 6.10 contains a sample of the results.

Table 6.10: Samples of HG determinations from photometric observations

Object	H	G	Fraction Included	H_{MPC}	G_{MPC}
(1)	3.33 ± 0.01	0.12 ± 0.02	1.000	3.34	0.12
(2)	3.95 ± 0.12	0.12	0.913	4.13	0.11
(3)	5.33 ± 0.08	0.24	1.000	5.33	0.32
(4)	3.18 ± 0.01	0.31 ± 0.04	1.000	3.20	0.32
...					
(6053)	15.17 ± 0.02	0.24	0.211	15.1	0.15
(7025)	18.28 ± 0.07	0.24	1.000	18.3	0.15
(11264)	14.40 ± 0.04	0.24	1.000	14.0	0.15

6.7: Comparing the Reliable Astrophotometry to the Photometric Observations

The final comparisons that should be made are between the *HG* values determined from the different sets of reliable astrophotometry, as well as comparisons of determinations from the reliable astrophotometry to the values determined from photometric observations.

Only three objects have been observed by more than one of the reliable astrophotometry sites. All three objects were observed by both Pan-STARRS and FASTT, and Table 6.11 summarizes the determinations.

Table 6.11: Comparison of reliable-photometry HG determinations

Object	Pan-STARRS		FASTT		Pan-STARRS–FASTT
	H	*G*	*H*	*G*	ΔH
(730)	13.69 ± 0.21	0.24	13.95 ± 0.03	0.27 ± 0.07	–0.26
(1916)	14.77 ± 0.07	0.24	15.00 ± 0.04	0.24	–0.23
(1962)	11.94 ± 0.22	0.24	12.00 ± 0.03	0.24	–0.06

Although this is a very limited sample, the rather poor agreement between the two sets of values is a concern. However, it is probable that the current poorly-constrained Pan-STARRS colour corrections are a major contributor to the discrepancies.

To demonstrate the agreement between the photometric and reliable astrophotometry *HG* determinations, I decided to use the FASTT determinations for two reasons: it is by far the most voluminous of the reliable photometric data sets; and the formal uncertainties are small. There are 154 objects in common between the two data sets. There are only six data points available for objects with *H* fainter than 12. This is a consequence of the difficulties of obtaining accurate photometry of faint objects. The differences in the *H* determinations, in the sense FASTT minus photometric, are shown in Figure 6.2.

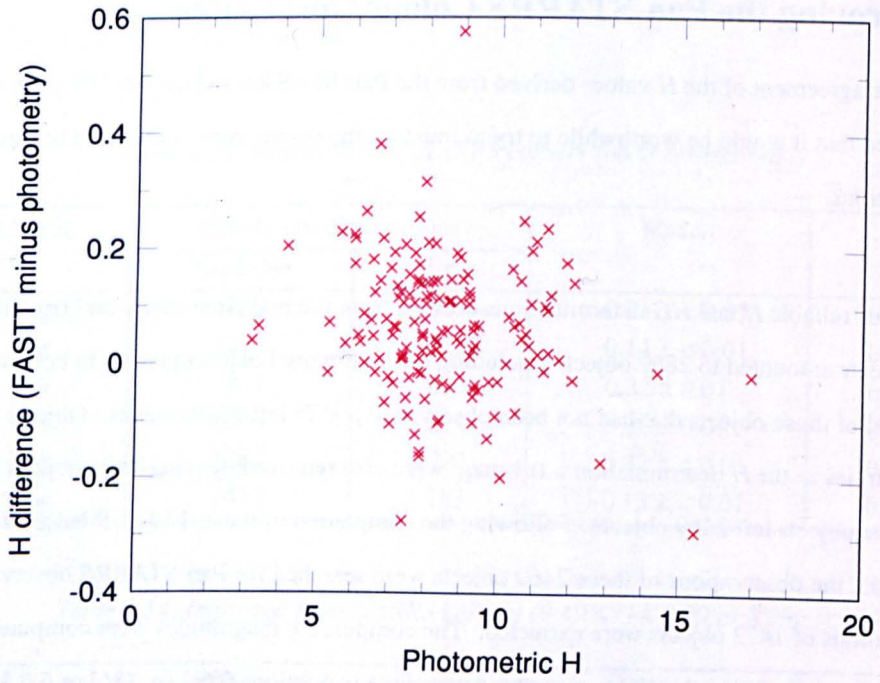

Figure 6.2: Comparison of photometric and FASTT H values

The mean (and its uncertainty) and standard deviation of all 154 *H* differences are 0.06 ± 0.01 and 0.12, respectively. The bulk of the determinations (145 of the 154) are for objects with photometric *H* values in the range 5 to 12. Within that *H* range, there is no apparent dependence of the difference on the *H* value. I determined means and standard deviations for *H*-magnitude-bin subsets of the 154 *H* differences. The results are displayed in Table 6.12. All but one of the individual *H*-magnitude-bin subset mean-difference values are within 1.4 standard deviations of 0.06, showing that there is no obvious dependence of the difference on *H*.

Table 6.12: H-dependent comparison of photometric and FASTT H values

H range	Mean and uncertainty	Standard deviation	Number of data points
5–6	0.11 ± 0.04	0.10	5
6–7	0.10 ± 0.03	0.11	19
7–8	0.05 ± 0.02	0.12	41
8–9	0.08 ± 0.02	0.12	35
9–10	0.01 ± 0.02	0.08	20
10–11	0.06 ± 0.03	0.11	15
11–12	0.09 ± 0.03	0.08	10

6.8: Improving the Pan-STARRS Colour Corrections

The poor agreement of the *H* values derived from the Pan-STARRS and the FASTT photometry suggested that it would be worthwhile to try to improve the colour corrections used for the Pan-STARRS observations.

The set of reliable *H* and *HG* determinations derived from the real photometry and from the FASTT photometry amounted to 2859 objects (including over a hundred objects present in both sets of data). Removal of those objects that had not been observed at $\beta < 7°$ left 2729 objects. Objects with uncertainties in the *H* determination > 0.1 mag. were also removed, leaving 2591 objects. Removing duplicate objects left 2469 objects. Following the completion of the 2012 Jan. 9 batch of *Minor Planet Circulars*, the observations of these 2469 objects were searched for Pan-STARRS observations: 9007 observations of 1472 objects were extracted. The computed *V* magnitudes were computed for all 9007 observations, assuming the *HG* parameters determined in Sections 6.6.4 [p. 136] or 6.6.5 [p. 138], and compared to the observed Pan-STARRS magnitude. Observations where the predicted *V* magnitude was

brighter than 14.5 were eliminated, to try to avoid problems associated with (potentially) saturated images. The differences between the observed and computed magnitudes of the 8223 observations that remained were determined. The differences were written to different output files, depending on which Pan-STARRS magnitude band was reported on the observation record. The end result was six files, each containing magnitude differences between the computed *V* and one of the Pan-STARRS bands. Each file was then processed to determine the mean colour differences. An initial determination of the mean and standard deviation of the differences used all the available observations. Final determinations of the difference mean and standard deviation were obtained by iteration, each iteration rejecting differences that differed from the last-determined mean by more than twice the last-determined standard deviation. Convergence typically took only a few iterations, the final iteration typically rejecting 10–20% of the available data set. Four sets of corrections were computed from each of the six files of differences. The first set used all available differences, without any consideration of the slope parameter. The other three sets used only differences for objects with slope parameters, *G*, in specific ranges.

Table 6.13 contains the improved Pan-STARRS colours, computed without consideration of the slope parameter, *G*. Tables 6.14, 6.15 and 6.16 [p. 141] contain the colours computed for various *G* ranges—specifically, 0.19–0.29, 0.07–0.17 and > 0.35, respectively. The first two ranges correspond to the taxonomic classes S and C, respectively, while the third range includes taxonomic classes V and E (see Table 3.13 [p. 71] for further information).

Table 6.13: Improved Pan-STARRS colours (no G restriction)

Colour	Number of observations		Mean	σ
	Available	Used		
V–g	1249	961	$-0.35 \pm < 0.01$	0.14
V–r	1371	1129	$0.14 \pm < 0.01$	0.14
V–i	841	613	0.32 ± 0.01	0.12
V–z	1003	871	0.26 ± 0.01	0.19
V–y	1287	1020	$0.32 \pm < 0.01$	0.15
V–w	2472	183	$-0.13 \pm < 0.01$	0.15

Table 6.14: Improved Pan-STARRS colours ($0.19 \leq G \leq 0.29$ or S class)

Colour	Number of observations		Mean	σ
	Available	Used		
V–g	631	487	-0.38 ± 0.01	0.14

V–r	738	600	0.13 ± 0.01	0.14
V–i	460	311	0.35 ± 0.01	0.10
V–z	514	440	0.26 ± 0.01	0.19
V–y	688	539	0.34 ± 0.01	0.16
V–w	1404	1040	–0.11 ± < 0.01	0.16

Table 6.15: Improved Pan-STARRS colours (0.07 ≤ G ≤ 0.17 or C class)

Colour	Number of observations		Mean	σ
	Available	Used		
V–g	489	352	–0.30 ± 0.01	0.12
V–r	489	406	0.15 ± 0.01	0.15
V–i	307	220	0.26 ± 0.01	0.12
V–z	362	317	0.24 ± 0.01	0.18
V–y	455	382	0.28 ± 0.01	0.15
V–w	763	570	–0.15 ± 0.01	0.14

Table 6.16: Improved Pan-STARRS colours (G ≥ 0.35 or V/E class)

Colour	Number of observations		Mean	σ
	Available	Used		
V–g	44	39	–0.45 ± 0.03	0.17
V–r	51	39	0.12 ± 0.02	0.11
V–i	19	14	0.45 ± 0.03	0.11
V–z	51	50	0.21 ± 0.04	0.25
V–y	60	52	0.21 ± 0.02	0.17
V–w	73	69	0.02 ± 0.03	0.28

To see whether the differences between the class-specific colours are significant, I use a Student's *t*-test. The null hypothesis is that there is no significant difference between the colours found for one *G* range (or taxonomic class) and the colours found for another *G* range (or taxonomic class). The alternate hypothesis is that the colours for the various *G* ranges (or taxonomic classes) are significantly different. Checks were made for each colour combination at the 99.95%, 99.5%, 99%, 95%, 90% and 80% confidence levels, in the order listed. The results are shown in Table 6.17. Once an alternate-hypothesis confidence level was found that rejected the null hypothesis for a particular colour comparison, no further checks were made and that confidence-level value is listed in the table. In the table, t_c is the *t*-statistic two-tailed critical value, E is the one-tailed uncertainty in the mean value ($E = t_c \sigma / \sqrt{n}$, where σ is the standard deviation of the colour mean and n is number of observations used in the

solution) and Mean shows the range in the colour for the second-mentioned taxonomic class at the stated confidence level. The t_c values are not taken from tables, but are calculated directly from my own implementation of the t-distribution Cumulative Distribution Function.

Table 6.17: Student's t-test results on significance of colour differences

Comp-arison	Colour	Conf. level/%	Alternate hypothesis			Null hypothesis	
			t_c	E	Mean	Mean	Rejected?
G vs. S	*V–g*	99.95	3.3184	0.021	[–0.32, –0.28]	–0.38	Y
	V–r	95	1.6486	0.012	[0.14, 0.16]	0.13	Y
	V–i	99.95	3.3353	0.027	[0.23, 0.29]	0.35	Y
	V–z	90	1.2842	0.013	[0.23, 0.25]	0.26	Y
	V–y	99.95	3.3162	0.025	[0.25, 0.31]	0.34	Y
	V–w	99.95	3.3076	0.019	[–0.17, –0.13]	–0.11	Y
G vs. V/E	*V–g*	95	1.6849	0.046	[–0.50, –0.40]	–0.38	Y
	V–r	80	0.8509	0.015	[0.11, 0.13]	0.13	N
	V–i	99.5	3.0123	0.092	[0.36, 0.54]	0.35	Y
	V–z	80	0.8489	0.030	[0.18, 0.24]	0.26	Y
	V–y	99.95	3.4878	0.082	[0.13, 0.29]	0.34	Y
	V–w	99.95	3.4374	0.116	[–0.10, 0.14]	–0.11	Y
S vs. V/E	*V–g*	99.95	3.5580	0.097	[–0.55, –0.35]	–0.30	Y
	V–r	90	1.3036	0.023	[0.10, 0.14]	0.15	Y
	V–i	99.5	3.0123	0.092	[0.36, 0.54]	0.35	Y
	V–z	80	0.8489	0.030	[0.18, 0.24]	0.18	N
	V–y	99	2.4002	0.057	[0.15, 0.27]	0.28	Y
	V–w	99.95	3.4374	0.116	[–0.10, 0.14]	–0.11	Y

With only three exceptions, the colour differences between the different taxonomic classes are found to be significant at the 90% (or greater level). There is a caveat: the sample size for the V/E class colours is small. But I am justified in implementing taxonomic-specific Pan-STARRS colours in my reduction procedures.

6.9: Verifying the CATCORR Corrections

Before running CATCORR on all the N* and R* files, I must demonstrate that the corrections that the program is making are consistent with what has been documented earlier. This involves a manual examination of the intermediate data values and final catalogue corrections for example observations. One test case will be examined for each of the observatory codes that have specific reduction details listed in Section 5.2 [p. 93], along with two test cases as being representative of all the other observatory

codes that do not have specific reduction details. A full manual examination of each test case is clearly impractical. It would simply take far too long to extract entries from the SDPC/CDPC manually, adjust (if necessary) the extracted astrometric magnitudes, determine the transformations between the astrometric and photometric catalogues, and derive the catalogue corrections. Rather, I will demonstrate, via use of the `/DEBUG` (`--debug`) flag on the `CATCORR` program to display intermediate values of interest on the screen during program execution, that the values determined during the processing of single observations are valid and consistent with the methods described herein.

6.9.1: Correcting USNO Flagstaff Observations

As noted in Section 5.2.8 [p. 102], there is a simple colour-dependent correction, implemented via Equation 5.5 [p. 102], that is to be applied to the USNO Flagstaff FASTT *V* magnitudes to convert them to Johnson *V*. For this demonstration, I will correct the following observation of (12218) Fleischer:

```
12218        2C2004 03 28.38460614 11 08.371-04 58 35.69          17.29Vgl5489689
```

which was published on *MPS* 115489. I do not have a measurement of the *B–V* colour or the taxonomic class for this object. On the assumption of it being an S type, based on an assumed membership of the Flora family (see Table 3.4 [p. 63]), the *B–V* colour (from Table 3.9 [p. 67]) is 0.85. Applying Equation 5.5 [p. 102], the correction that is to be added to the observed magnitude is then 0.363 (0.85–0.8) = 0.018, in agreement with the value computed by `CATCORR`. The corrected magnitude is thus 17.29 + 0.018, which, when rounded appropriately, is 17.31. This also agrees with the `CATCORR` value and requires no additional correction, since it is already a *V* magnitude.

6.9.2: Correcting LINEAR Observations

The methods in Section 5.2.1 [p. 94] were applied to the following LINEAR observation of (152001) 2004 JH_{18}:

```
F2001        C2003 01 01.28409 05 01 05.77 +13 27 37.7          19.5 ch0199704
```

which was published on *MPS* 70199. The pseudo-*V* magnitude as published is 19.5 and the position of the minor planet is in the part of the sky covered by the SDPC. The comparison catalogue used by LINEAR is the USNO-A2.0. The number of comparison stars extracted from the SDPC in a 12′×12′ region centred around the 15′-resolution grid position (α = 75°.25, δ = +13°.5) was 1506, of which 923 have entries in the USNO-A2.0 catalogue. The first of these comparison stars has *B* =

19.8 and R = 19.0, thus B–R = +0.8: Table 5.2 [p. 95] shows that for B–R = +0.8, ΔB = –0.36. Equation 5.1 [p. 95] then leads to a pseudo-V for this star of 19.8 – 0.36 = 19.44. CATCORR agrees with this value and, using 862 of the 923 comparison stars, derives the following transformation between the pseudo-V LINEAR magnitudes (V_{CCD}) and the SDPC V magnitudes:

$$V - 17.0 = -0.004 + 1.097(V_{CCD} - 17.0) \qquad (6.11)$$

with a goodness of fit, r^2, = 0.979 and a r.m.s. residual of 0.18 magnitudes for a single data point. The individual data points are shown in Figure 6.3 and the best-fit line is shown as a dotted red line, along with a dotted blue line showing the ideal fit between the two systems.

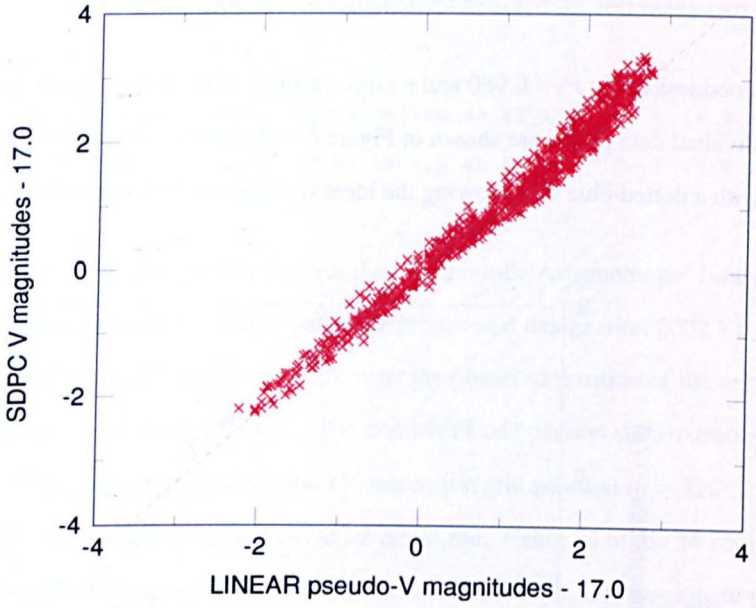

Figure 6.3: Comparison star fit for sample LINEAR observation

Using Equation 6.11, the catalogue-corrected magnitude for the sample LINEAR observation is:

$$V - 17.0 = -0.004 + 1.097(19.5 - 17.0) \qquad (6.12)$$

thus V = 19.739, which is to be rounded to V = 19.7. CATCORR agrees with both values. There is no need to apply any colour corrections to this value and processing of this observation is complete.

6.9.3: Correcting CSS Observations

To verify the handling of CSS observations as documented in Section 5.2.2 [p. 97], I chose another observation of (152001) 2004 JH_{18}:

```
F2001          C2007 02 10.26912 09 40 31.54 +02 09 55.1           18.9 Vrt9471703
```

which was published on *MPS* 199471. The observed position is within the region covered by the SDPC. The number of comparison stars extracted from the SDPC in a 30′×30′ region centred on the 15′-resolution grid position (α = 145°.25, δ = +2°.25) around the observed position was 3171, of which 23 have entries in the CSS catalogue. Using 17 of the 23 comparison stars, the following transformation expression relating CSS V magnitudes (V_{CSS}) to SDPC V magnitudes was derived:

$$V = 0.157 + 1.019\,(V_{CSS} - 17.0) \qquad (6.13)$$

with a goodness of fit, r^2, = 0.980 and a r.m.s. residual of 0.11 magnitudes for a single data point. The individual data points are shown in Figure 6.4 and the best-fit line is shown as a dotted red line, along with a dotted blue line showing the ideal fit between the two systems.

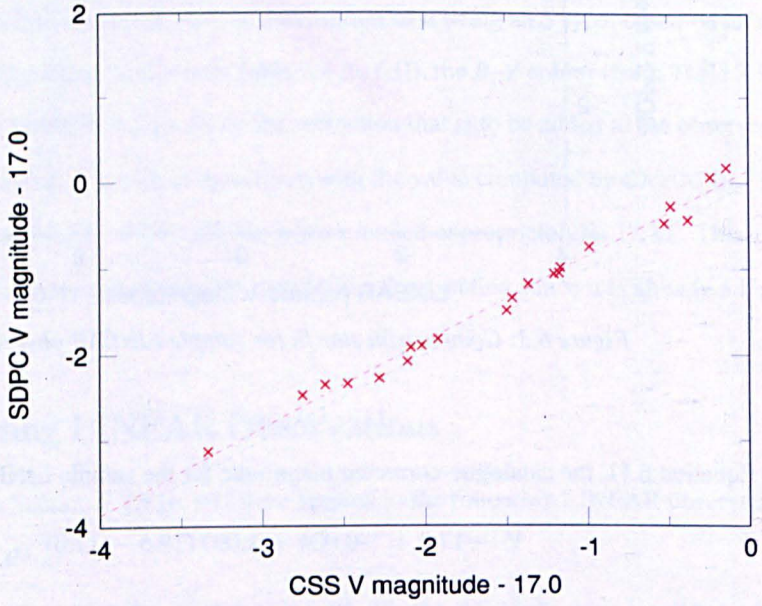

Figure 6.4: Comparison star fit for sample CSS observation

Using Equation 6.13, the catalogue-corrected magnitude for the sample CSS observation is:

$$V - 17.0 = 0.157 + 1.019(18.9 - 17.0) \tag{6.14}$$

thus $V = 19.093$, which is to be rounded to $V = 19.1$. CATCORR agrees with the rounded value, but gets $V = 19.094$, since it retains more decimal places in the fit coefficients—this difference is of no consequence. There is no need to apply any colour corrections to this value and processing of this observation is complete.

6.9.4: Correcting Observations of Other Observers

To verify the handling of other observers' observations, I selected the following two observations, made at amateur sites:

```
C0004K02Y24B  C2005 09 24.94609 23 52 54.98 +00 44 43.5          18.7 Rro2630185
K0174J99J12V  C2008 11 27.11795 07 43 01.69 +19 45 56.6          19.9  c~01eSA77
```

The first is an observation of (120004) made at the Observatoire Astronomique Jurassien, Vicques (Switzerland), published on *MPS* 142630 under the provisional designation 2002 YB_{24}. The *R* magnitude as published is 18.7 and the SDPC covers the observed position of the minor planet. The comparison catalogue used is the UCAC-2. The number of comparison stars extracted from the SDPC in a 15′×15′ region centred around the 15′-resolution grid position ($\alpha = 358°.25$, $\delta = +0°.75$) was 799, of which 54 have entries in the UCAC-2 catalogue. Using 53 of the 54 comparison stars, CATCORR derives the following transformation between the observed R magnitude (R_{CCD}) and the SDPC *R* magnitudes:

$$R - 17.0 = -0.555 + 0.857(R_{CCD} - 17.0) \tag{6.15}$$

with a goodness of fit, r^2, = 0.969 and a r.m.s. residual of 0.10 magnitudes for a single data point. The individual data points are shown in Figure 6.5 [p. 148] and the best-fit line is shown as a dotted red line, along with a dotted blue line showing the ideal fit between the two systems.

Using Equation 6.15, the catalogue-corrected magnitude for this sample observation is:

$$R - 17.0 = -0.555 + 0.857\,(18.7 - 17.0) \tag{6.16}$$

thus $R = 17.902$. To correct to V, I use the measurement of the V–R colour derived from the SDSS measurements (see Section 3.9 [p. 63]): V–$R = 0.41$. Applying this to the corrected value of R, leads to $V = 17.902 + 0.41 = 18.312$, which is to be rounded to $V = 18.3$. CATCORR agrees with the rounded value.

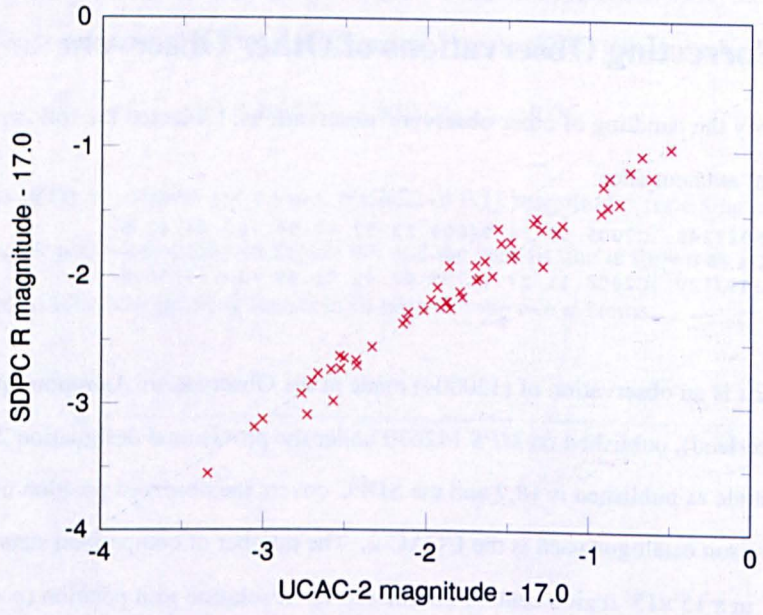

Figure 6.5: Comparison star fit for sample code 185 observation

The second is an observation of (200174) made at the Observatoire Chante-Perdrix, Dauban (France), published on *MPS* 266352 under the provisional designation 1999 JV_{12}. The observed position is within the region covered by the SDPC. The comparison star catalogue used is the USNO-A2.0. The magnitude band is blank, which is to be interpreted as R since this is a CCD observation (see Section 3.3). The number of comparison stars extracted from the SDPC in a 12′× 12′ region centred on the 15′-resolution grid position ($\alpha = 115°.75$, $\delta = +19°.75$) around the observed position was 1227, of which 712 have entries in the USNO-A2.0 catalogue. Using 666 of the 712 comparison stars, the following transformation expression relating USNO-A2.0 R magnitudes (R_U) to SDPC R magnitudes was derived:

$$R - 17.0 = 0.056 + 0.916\,(R_U - 17.0) \tag{6.17}$$

with a goodness of fit, r^2, = 0.977 and a r.m.s. residual of 0.19 magnitudes for a single data point. The individual data points are shown in Figure 6.6 and the best-fit line is shown as a dotted red line, along with a dotted blue line showing the ideal fit between the two systems.

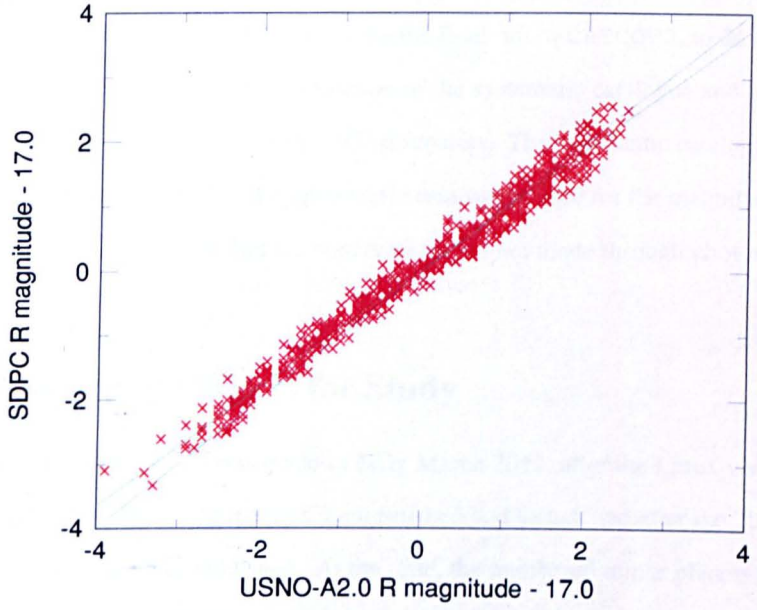

Figure 6.6: Comparison star fit for sample code A77 observation

Using Equation 6.17, the catalogue-corrected magnitude for this sample observation is:

$$R - 17.0 = 0.056 + 0.916\,(19.9 - 17.0) \tag{6.18}$$

thus R = 19.712. To correct to V, I use the measurement of the V–R colour derived from the SDSS measurements (see Section 3.9 [p. 63]): V–R = 0.36. Applying this to the corrected value of R, leads to V = 19.712 + 0.36 = 20.072, which is to be rounded to V = 20.1. CATCORR agrees with the rounded value.

6.10: Summary

I have documented the reduction procedures that are used to correct the astrophotometry and to process the photometry and visual observations. I have demonstrated that the computer programs that will do the corrections and processing behave in a manner consistent with what is documented here. The number of astrophotometric observations without specified magnitude bands that were assumed to be R band was 4 608 558.

7: Correcting the Observations

7.1: Introduction

This chapter describes the procedures undertaken to do the final run of CATCORR, to derive observer-specific corrections, to perform the *en masse* correction of the systematic catalogue and observer errors in the observations, and the determination of the *HG* parameters. The systematic catalogue errors arise from the imperfect magnitudes present in the astrometric catalogues used for the magnitude reductions, while the observer errors arise from the fact the observations are not made through photometric filters.

7.2: The Final Selection of Objects for Study

The final selection of objects for study was made in early March 2012, after the Linux versions of the various programs needed for processing the data were finished and tested, and after the 2012 March 8 batch of *Minor Planet Circulars* was published. At the time, the numbered minor planets totalled 322 611. This was an increase of 100 666, or 45%, in the number of objects available in the first iteration (see Section 6.3.4 [p. 120]). Using some 80 cores on the MPC's Linux cluster, it proved possible to pre-process all 322 611 objects in under two hours: the PCHECK step took about 90 minutes and the GETRAWDATA step took about 12 minutes.

7.2.1: The Final CATCORR Run

An initial attempt was made to run CATCORR across 80 cores on the MPC Linux cluster. Each job would have to process four or five .OBS files. Prior tests had suggested that the entire run would take under six hours if all 80 cores could be utilized appropriately. One hour after submitting the 80 jobs, a check on the progress of each job was made. The results were disappointing: only five or six objects in each of the first files (each containing, mostly, 1000 objects) had been processed. This suggested that the actual runtime would be about a week! Examination of the processes using the Linux `top` command showed that each job was using only 3 to 7% of the CPU core. The running jobs were stopped. A single job was submitted and observed using `top`. This process was using more than 90% of the CPU core. This suggested that the slowness when submitting 80 jobs was due to extreme IO loading. Although the IO requirements of an individual CATCORR job are quite

modest, the requirements of 80 simultaneous jobs are too much for the disk system to deal with. The decision was made to run only one CATCORR job on each machine. Each job used more than 60% of the CPU core and the entire CATCORR run took 80 hours.

7.3: Determining the Observer-Specific Corrections

To determine the observer-specific corrections, I decided to use the FASTT-only *HG* determinations of those objects which had numbers above (300), thus eliminating the very brightest objects that the major surveys are unlikely to have observed, and had at least 60% of the available FASTT observations included in the solutions. The FASTT data (see Section 5.2.8 [p. 102]) was chosen as it was the largest available set of single-source reliable magnitudes. The 171 924 observations of these 428 objects were extracted from the uncorrected N*.OBS files and merged together in one file, called OBSCORR.OBS. This merged file was then run through CATCORR, producing a new file, OBSCORR_CATCORR.OBS. The 54 339 observations of the same 428 objects were extracted from the catalogue-corrected R*.OBS files and appended onto OBSCORR_CATCORR.OBS. This file, now containing 226 263 observations, was then sorted, first by the designation, then by the date of observation. It was then run through DETERMINEOBSCORRS, a program which determined, for each observatory code (and each observing program at that observatory code), the mean and standard deviation of the difference between the observed *V* astrophotometric magnitude (either catalogue-corrected or uncorrected) and the *V* magnitude predicted from the FASTT photometry. If the number of observations available for an observatory code was less than twenty, the standard deviation was set to 0.70, to avoid spurious small uncertainties caused by limited data sets. In addition to determining the mean and standard deviation of all observations associated with a particular observatory code, similar statistics were also computed for one-magnitude (based on predicted magnitude) binned data from that code. Statistics were generated for each magnitude bin from (listing the bright limit of each bin) $V = 10$ to 20, with additional bins for $V < 10$ and $V > 21$.

The output from DETERMINEOBSCORRS is written to two files. The first output file, called OBS_CORR.TXT, contains one or two lines for each observatory code or each observatory program code. Each line contains either the observer-specific corrections for uncorrected (astro)photometry or catalogue-corrected (astro)photometry. A short extract of the output file is included in Table 7.1, along with a column guide to assist in reading the line, which is truncated after column 86. The complete

output file is included on the thesis website. The format of the output file is described in Table 7.2.

Table 7.1 : Extract of the raw output from the DETERMINEOBSCORRS program

```
          1         2         3         4         5         6         7         8
12345678901234567890123456789012345678901234567890123456789012345678901234567890123456
001  U          1 -1.93
006  U         90 -1.59  0.37        14 -1.49  0.44        23 -1.75  0.41        35 -1.53
007  U          1 -0.58
008  U       1003 -1.73  0.54        71 -1.77  0.78       187 -1.84  0.51       296 -1.80
010  U          3 -0.44  0.27
0101 C          1  1.95
0101 U         21  1.75  0.47
```

In the small extract shown above, it can be seen that correction for code 008 (Algiers), based on all 1003 observations, has a mean of –1.73 mag. and standard deviation of 0.54 mag. The mean value determined here is in good agreement with –1.40, the value found by Gehrels (1957) and listed in Table 2.4 [p. 31].

Table 7.2 : Format of the raw output file from DETERMINEOBSCORRS

Column	Format	Use
1– 3	A3	Observatory code
4	A1	Program code
6	A1	'C' = corrections are for catalogue-corrected observations 'U' = corrections are for uncorrected observations
12–17	I6	Total number of observations available
19–23	F5.2	Mean offset
26–29	F4.2	Standard deviation of offset
Offset+0	I6	Number of observations in this magnitude range
Offset+7	F5.2	Mean offset
Offset+14	F4.2	Standard deviation of offset

The corrections for observations predicted to be brighter than $V = 10$ begin at offset 37 on each line. Those for observations predicted to be $n \leq V < n+1$ begin at offset $(n–9)*21+37$. The corrections for $V \geq 21$ begin at offset 289. The complete raw data file is included on the thesis website. In the small extract shown in Table 7.1, it can be seen the correction for code 008 (Algiers) for objects brighter than $V = 10$ is -1.77 ± 0.78, that for objects with $10 \leq V < 11$ it is -1.84 ± 0.51 and for objects with $11 \leq V < 12$ it is -1.80 ± 0.51. There is no clear dependence of the mean value on V, so for code 008 it is reasonable to take a single value as the observer-specific correction.

The format of the second output file, called OBS_CORRS.TXT, is described in Table 7.3. As with the first output file, this file contains one or two lines per observatory code or per observing program. Each line contains either the observer-specific corrections for uncorrected (astro)photometry or catalogue-corrected (astro)photometry. A short extract of the output file is included in Table 7.4, along with a column guide to assist in reading the line.

Table 7.3 : Format of observer-corrections files used by WORKOUTH

Column	Format	Use
1–3	A3	Observatory code
4	A1	Program code
6	A1	'C' = corrections are for catalogue-corrected observations 'U' = corrections are for uncorrected observations
8–15	I8	Earliest date to which these corrections apply (YYYYMMDD form)
17–24	I8	Latest date to which these corrections apply (YYYYMMDD form)
26–30	F5.2	Standard deviation of a single observation
32–36	F5.2	Constant offset or constant term of linear fit
39–43	F5.2	Slope of linear fit
45–50	F6.2	Brightest *V* magnitude to which these corrections apply
52–56	F6.2	Faintest *V* magnitude to which these corrections apply
58	A1	Magnitude band to which these corrections apply. If blank, corrections apply to all bands.
60	A1	Taxonomic class to which these corrections apply. If blank, corrections apply to all classes.

For every entry the earliest and latest dates were set to 00000000 and 99999999, respectively, the bright and faint magnitude limits were set to –9.99 and 99.99, respectively, and the slope of the linear fit was set to zero. This output file was then copied to OBS_CORRECTIONS.TXT and examined in conjunction with the OBS_CORR.TXT file. I looked for sites where the magnitude-binned data suggested that a linear representation of a magnitude-dependent observer-specific correction might be appropriate. When potential cases were found, I reran DETERMINEOBSCORRS with the /OBSCODE option, which restricted the program to examining observations from just the specified observatory code, the /BMAG and /FMAG options, which ignored magnitude estimates outside the specific range, and the /BEFORE and /SINCE options, which restrict the temporal range of observations. When used with any of these options, DETERMINEOBSCORRS assumes that a linear magnitude-dependent expression is to be derived for the observer-specific correction and determines that expression from the unbinned magnitudes that match the observatory code and magnitude constraints. An example of the use of these options is /OBSCODE=704/BMAG=16.0/FMAG=18.5 to determine the linear expression for code 704

(LINEAR) observations between magnitudes 16.0 and 18.5. None of the determined magnitude-dependent expressions were found to be significant: e.g., the LINEAR expression had a goodness of fit, R^2, equal to 0.261. The `/OBSCODE` option was also used with those observatory codes who had reported usage of the new versions of Astrometrica (see Section 5.7 [p. 115]). In addition, for very productive observatory codes, the `/CLASS=<taxonomic class>` option was used to generate corrections for specific taxonomic classes. For this study, the `/CLASS` option was used on the active, large professional surveys, as well as one amateur survey (code J75, the Spanish OAM Observatory, La Sagra, survey).

The resulting file, containing corrections for 940 observatory codes (or observatory code/program code combinations) and called `OBS_CORRECTIONS.TXT`, is included on the thesis website. An extract from the file, showing how multiple entries for a single observatory code are stored, is included as Table 7.4 (a column guide is included to assist comparison with Table 7.3).

Table 7.4: Sample entries from `OBS_CORRECTIONS.TXT`

```
          1         2         3         4         5         6
12345678901234567890123456789012345678901234567890123456789012345678901
240   C 00000000 99999999  0.28 -0.10   0.00  -9.99 99.99
704   C 19980101 99999999  0.39  0.30   0.00  -9.99 99.99    C
704   C 19980101 99999999  0.39  0.25   0.00  -9.99 99.99    S
704   C 19980101 99999999  0.39  0.27   0.00  -9.99 99.99
J93   C 00000000 99999999  0.70  0.03   0.00  -9.99 99.99
J98   C 00000000 99999999  0.70 -0.10   0.00  -9.99 99.99
      C 00000000 99999999  1.00  0.00   0.00  -9.99 99.99
```

The entries in `OBS_CORRECTIONS.TXT` are arranged so that special cases for a specific observatory code are listed first, followed by the general case for the same code. By indexing the array into which this data file is read, `WORKOUTH` can find the observer-specific correction needed for a specific observation very quickly. The final entry in the file (and the last entry in Table 7.4) is used if no other entries in the file match. When the relevant observer-specific correction is determined for a particular observation, the value is subtracted from the catalogue-corrected magnitude.

7.3.1: Poor Transformation Equation Fits

When examining the OBSCORR.FITFILE generated during the preparation of OBSCORR_CATCORR.OBS, I noticed that a small number of fits had goodness of fit values less than 0.9. No such cases had shown up in previous small-scale test runs. Examination of the .FITFILE files generated during early runs of WORKOUTH (see Section 7.4 [p. 158]) showed that 139 635 of the 14 675 098 transformation equations generated had goodness of fit values less than 0.9. It would be impractical to check all the problem transformations, but the examination of a small number of cases serves to identify the reasons for the poor fits. I therefore selected two problem cases, with very bad goodness of fit values, for examination and the details of both transformations are listed in Table 7.5.

Table 7.5: Two sample problem transformation equations

Fit File ID	R.A. /°	Decl. /°	Magnitude band Observed/Catalogue	Goodness of fit	Number of obs Available/Used
152241_00008	29.75	–02.25	*R* / USNO-B1.0 *R*	0.305	73/13
152322_00016	30.50	+02.25	*R* / USNO-B1.0 *R*	0.120	90/22

The generation of both these transformation equations had used *R* magnitudes taken from the CDPC and *R* magnitudes from the USNO-B1.0. I extracted from the Standard Format observation files the observations that had been "corrected" using each of these transformation equations and ran them through CATCORR with the /DEBUG flag, to write out, amongst other useful debugging information, the magnitudes extracted from both afore-mentioned catalogues that had been used to derive the transformation equations. I displayed the agreement between the magnitudes from the two catalogues graphically (see Figures 7.1 and 7.2). The plots look nothing like the straight-line distributions shown in Figures 3.1 [p. 48] and, e.g., 6.4 [p. 146]. It is known that the photometric calibration of a number of the Schmidt plates used in USNO-A/B catalogues are simply wrong. Since I'm working in R.A./Decl. and not directly in terms of the Schmidt fields used to build the USNO-A/B catalogues, I do not have available the number of affected USNO-A/B fields. An order of magnitude estimate would be ~ 1%, based on the fraction of suspect transformation equations, which equates to ~ 70 fields for the USNO-B1.0 (see Section 3.7.6 [p. 58]). The two cases investigated here are probably examples of erroneous photometric calibration in the astrometric catalogue.

The strange distribution of points in Figures 7.1 and 7.2 may simply be the result of an incorrect sign on one term in a photometric-fit equation used in the preparation of the USNO catalogue.

When a transformation equation has a goodness of fit less than 0.9, any observations that make use of it are flagged with a "?" (see Table 6.2). Observations so flagged are not considered in the calculation of new *HG* values by `WORKOUTH`.

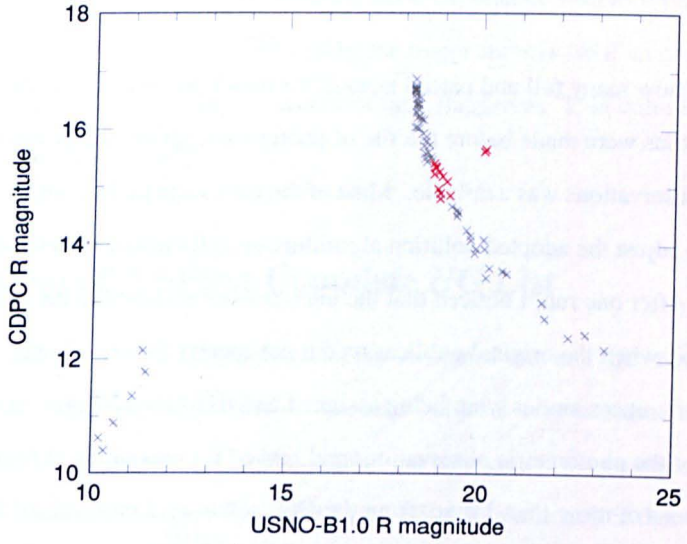

Figure 7.1: Poor agreement between CDPC and USNO-B1.0 R magnitudes, FITFILE ID 152241_00008, red indicates data included in fit, grey data excluded

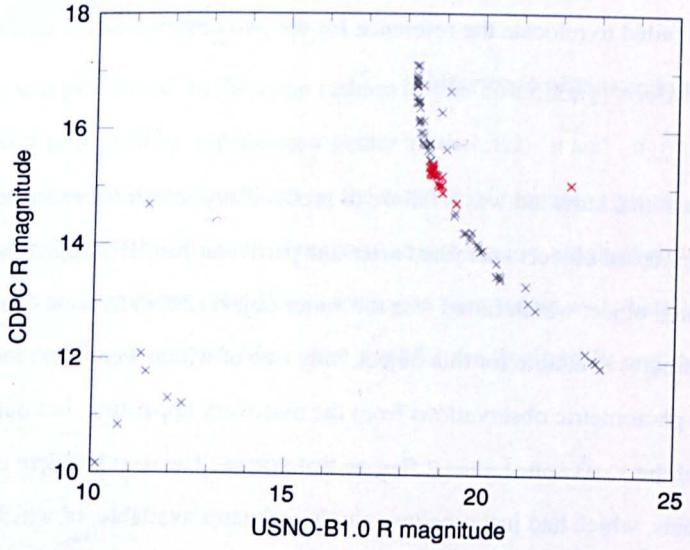

Figure 7.2: Poor agreement between CDPC and USNO-B1.0 R magnitudes, FITFILE ID 152322_00016, red indicates data included in fit, grey data excluded

7.4: The First *n* Iterations of WORKOUTH

The first complete WORKOUTH run attempted to use 80 cores on the MPC's Linux cluster. As with the attempt to utilize all cores for the CATCORR run, this resulted in very poor IO performance. The WORKOUTH run was aborted, then restarted running one job on each of the eight available machines. Even with this restricted number of processes, the wall-clock runtime for a complete WORKOUTH run is under 30 minutes, if the systems are not otherwise in use. When the systems are heavily loaded, the wall-clock runtime can be 120 minutes.

I did not count how many full and partial WORKOUTH runs I performed over the course of some two weeks. Some runs were made before the file of photometric observations was finished, others before the file of visual observations was available. Most of the runs were performed to tweak the formatting of the output files, to adjust the adopted-solution algorithm, or to fix minor issues with the processing of the observations. After one run, I noticed that the uncertainties assigned to the photometric observations were not correct when the original publication did not specify the uncertainty. I determined that the astrophotometric uncertainties were being assigned and fixed the program. After another run, I extracted the residuals of the photometric observations and looked for anomalies. I found about 60 observations that had residuals of more than 1 mag. from the HG_A solution. I reexamined the original references for each problem observation and fixed a number of incorrectly-entered dates of observation and magnitude bands. While fixing one incorrect magnitude band I noticed that the reference for two photometric observations was incorrect, as they had inherited the reference of the observations entered immediately before them. I failed to relocate the reference for the two observations in question, so I removed them from the file of photometric observations.

Another problem that surfaced was a failure to produce any solutions for a small number of objects. Of the 322 611 numbered objects examined after one particular run, 151 objects had no *HG* solution. The lowest-numbered object which failed was the Amor object (2608) Seneca. There were just fifteen magnitude estimates available for this object, only two of which were correctable. A literature search produced two photometric observations from the discovery apparition, but output of a *HG* solution required use of the `--minphotnum=2` flag on WORKOUTH. The next problem case was the Apollo object (4581) Asclepius, which had just nine magnitude estimates available, of which only three (made at phase angles in the range 52° to 77°) were correctable. Use of the `--minnum=3` flag allowed a *HG* solution to

be found, albeit it with a large *H* uncertainty (*H* = 20.27 ± 1.13). I noticed an apparent pattern in the type of object that failed to produce a *HG* solution, so I extracted the orbits of all the problem objects from internal MPC orbit files. The problem objects comprised 138 distant objects (Centaurs, Trans-Neptunian Objects and Scattered Disc Objects), 12 Near-Earth Objects (three Atens, five Apollos and four Amors) and one probable extinct comet. The *HG* solutions for the distant objects failed because they cannot meet the default 15° phase coverage requirement for a solution to be accepted. This problem was fixed by a tweak to `WORKOUTH` which disables the phase-coverage requirement for objects with perihelion distances above 6 AU. In addition, since the MPC experience with astrophotometry of TNOs is that it is better than the astrophotometry produced by the major surveys, so if an object is a TNO, any uncorrected reported magnitudes are treated as corrected (and flagged as 'T' in column 94 of the Standard Format, see Table 6.2 [p. 124]).

7.4.1: Examination of the First Complete *HG* List

The multiple `*.HG` files produced by `WORKOUTH` were combined into one file: `TOT.HG`. This file was sorted in various ways and various sets of "problem" objects were extracted. "Problem" objects included those that produced no *HG* solution, that had large *H* uncertainties or that had low included-observation percentages (see Section 9.2 [p. 167]). Examination of these problem cases identified a number of minor issues with `WORKOUTH`, which were corrected as necessary.

7.5: The Final `WORKOUTH` Run

A final `WORKOUTH` run was performed, in the same fashion as that described previously. Files `TOT.HG`, `TOT.H` and `TOT.H_DEFG` were built by appending together all the `.HG`, `.H` and `.H_DEFG` files. The decision of which run was the final run was based on the number of remaining problem cases. When the number of such problems dropped by an order of magnitude into the low single digits, the decision was made to accept the results as they stood. The afore-mentioned files, along with the associated Standard Format observation files and the `.FITFILE` files, were used for the final results and the subsequent analysis.

8: Results

8.1: Introduction

In this chapter, I present summaries of the results obtained in this thesis and describe how the results are distributed. I also present a few examples of phase curves.

8.2: *HG* Determinations for the Numbered Minor Planets

By applying catalogue and observer corrections to the bulk of the astrophotometry present on the astrometric observations records, I have determined new H and G parameters for the vast majority of the numbered (as of 2012 March 8) minor planets.

8.2.1: Complete *HG* Data Tables

It is impractical to present the complete *HG* data tables in this printed document (or even in the PDF version). A "back of the envelope" calculation suggests that it would require about 10 000 pages to present all the results. The complete data tables are available on the thesis website (see Appendix 6 [p. 226]) and data on individual objects, or groups of objects, are accessible via a web-based MySQL database (see Section 8.4 [p. 165]).

8.2.2: Extract of *HG* Data Tables

The format of the *HG* data tables is documented in Table 6.5 [p. 128]. Table 8.1 [p. 162] contains an extract of the complete data tables. It shows some of the information that is available in the complete data file for a handful of objects. The objects listed in the table are the first four discovered, along with a selection of objects of personal relevance to me or to this thesis. The column "Num. obs." gives the number of available catalogue- and observer-corrected observations, while the column "% Incl." gives the percentage of those observations included in the fit.

Table 8.1: Extract of HG data tables

Object	MPC		Thesis		β range	Num. obs.	% Incl.
	H	G	H	G			
(1)	3.34	0.12	3.32 ± 0.01	0.04 ± 0.01	1.3–22.7	358	74.3
(2)	4.13	0.11	4.16 ± 0.01	0.12	1.2–27.1	570	64.4
(3)	5.33	0.32	5.32 ± 0.01	0.24	2.3–29.8	491	72.7
(4)	3.20	0.32	3.30 ± 0.01	0.43	1.7–26.9	249	73.9
(719)	15.4	0.15	15.65 ± 0.06	0.24	1.8–47.4	209	90.9
(878)	14.6	0.15	14.82 ± 0.03	0.01 ± 0.03	1.0–32.8	352	91.2
(1877)	10.9	0.15	11.04 ± 0.04	0.12	0.2–17.5	331	92.7
(2072)	12.61	0.15	13.11 ± 0.03	0.48	0.8–29.2	770	90.8
(2298)	12.7	0.15	13.25 ± 0.03	0.24	0.3–30.4	874	89.9
(2975)	13.0	0.15	13.45 ± 0.03	0.24	0.6–29.8	893	90.1
(3202)	10.8	0.15	11.18 ± 0.03	0.12	0.2–16.6	727	91.2
(4421)	12.2	0.15	12.65 ± 0.04	0.24	2.8–27.4	682	93.4
(6354)	12.2	0.15	12.49 ± 0.04	0.12	0.6–28.5	460	90.4
(9831)	15.0	0.15	15.50 ± 0.03	0.24	0.8–31.2	464	95.5
(10257)	12.8	0.15	13.43 ± 0.03	0.07 ± 0.06	0.1–18.4	613	96.9
(12984)	13.8	0.15	14.52 ± 0.03	0.03 ± 0.05	1.6–27.4	627	93.0
(15834)	13.2	0.15	13.74 ± 0.08	0.24	1.4–25.2	253	97.2

8.2.3: Sample Phase Curves

To show the general quality of the catalogue- and observer-corrected astrophotometry, I present four sample phase curves, plotting the reduced V magnitudes (i.e., with the 5 log($r\Delta$) term removed) against the phase angle. These phase curves demonstrate that the corrections described in chapters 6 [p. 117] and 7 [p. 151] only removed the systematic errors in the observational data, but did not (and could not!) fix the random errors. Data points in each figure are coloured red if they were included in the adopted solution, and black if rejected. The adopted *HG* fit is indicated by the green line. The error bars, which are typically in the range 0.3 to 0.5 mag. for the astrophotometric observations, have been suppressed in these diagrams, simply to prevent them looking too "cluttered".

The first sample phase curve (Figure 8.1) is for the eponymous object, (3202) Graff, which is a Hilda minor planet. The adopted *HG* solution has $H = 11.18 \pm 0.03$ and an assumed $G = 0.12$, derived from 663 of 727 corrected observations covering $0°.2 < \beta < 16°.6$.

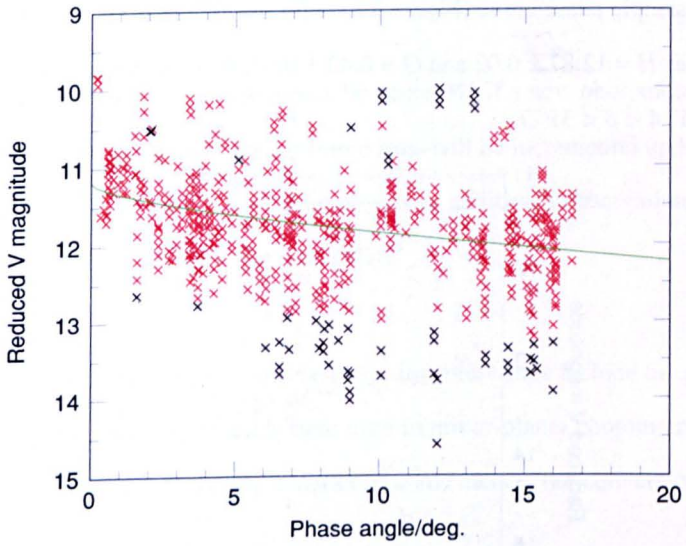

Figure 8.1: Phase curve for (3202) Graff

The second sample phase curve (Figure 8.2) is for (75326) 1999 XZ_{50}, a routine MBA. The adopted *HG* solution has $H = 17.24 \pm 0.04$ and $G = 0.25 \pm 0.07$, derived from 219 of 229 corrected observations covering $1°.4 < \beta < 30°.0$.

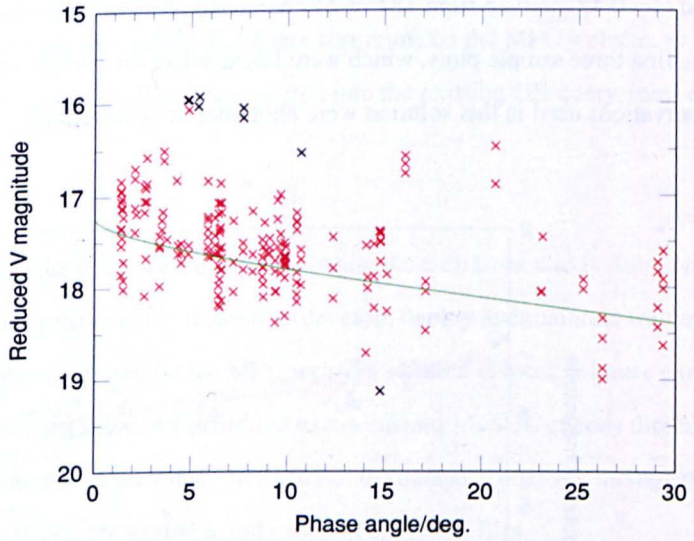

Figure 8.2: Phase curve for (75326) 1999 XZ_{50}

The third sample phase curve (Figure 8.3) is for the Hungaria (1025) Riema. The adopted *HG* solution has $H = 12.87 \pm 0.02$ and $G = 0.42 \pm 0.03$, derived from 379 of 428 corrected observations covering $1°.4 < \beta < 31°.7$.

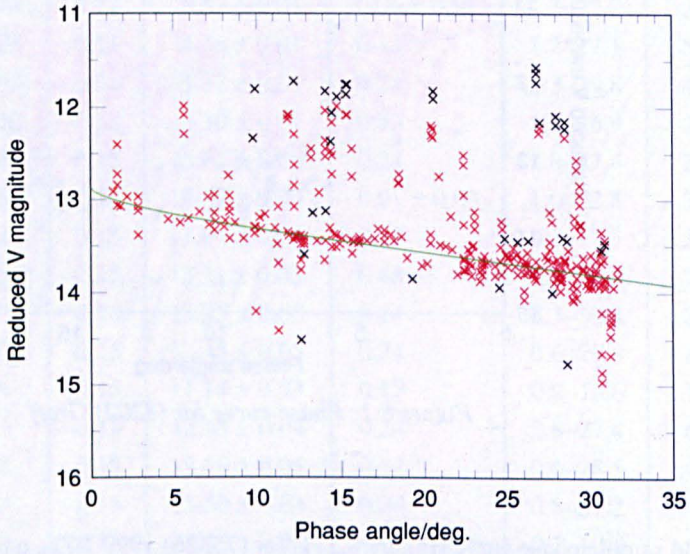

Figure 8.3: Phase curve for (1025) Riema

The final sample phase curve (Figure 8.4) is for (4) Vesta. The adopted *HG* solution has $H = 3.30 \pm 0.01$ and $G = 0.43$, derived from 184 of 249 corrected observations covering $1°.7 < \beta < 26°.9$. Unlike the first three sample plots, which were based solely on astrophotometric observations, 41% of the observations used in this solution were photometric observations.

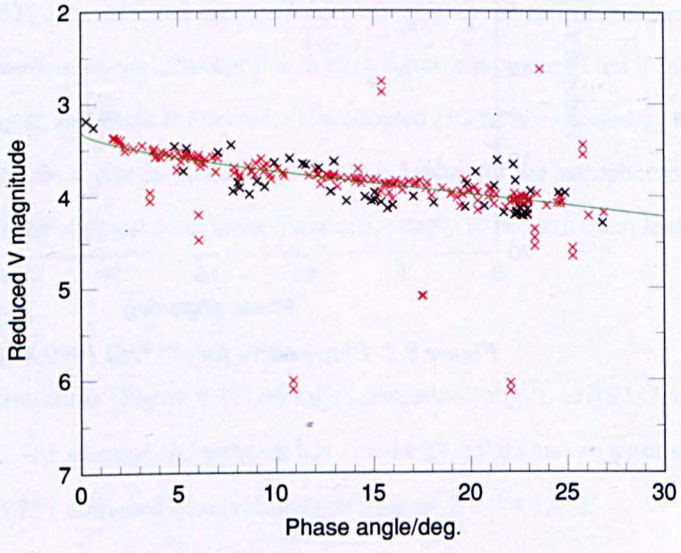

Figure 8.4: Phase curve for (4) Vesta

8.3: Future Runs

A complete reprocessing of the observations will only be necessary if a new photometric catalogue is prepared for use by CATCORR. The usual case for future runs will be incremental updates, correcting only those observations (whether of newly-numbered objects or additional observations for previously numbered objects) published since the last complete update.

Modifications to the described procedure that will be made for future runs include the use of ecliptic coordinates for the PAB, as that is the standard system used in minor-planet photometry. The use of equatorial coordinates in this thesis was merely a matter of convenience, but conversion from equatorial to ecliptic coordinates is trivial.

8.4: Web-Based MySQL Database

The complete *HG* data files, associated raw observation files, and taxonomic/colour and FitFile data files are large. For many potential users of the data, access to information about one particular object, or group of objects, may be useful without the need to download the complete data sets. To fulfil this access requirement, I decided to set up a web-based query form, that would allow users to query many of the data files associated with this thesis. The query form runs on the MPC website, as I anticipate that many data items from this work will be incorporated into the existing DB query-form output on our website.

The database back-end is the open-source MySQL, while the web front-end is Ruby on Rails. Ruby on Rails is a framework designed to make it easier to develop, deploy and maintain web applications. Both MySQL and Ruby on Rails are used on the MPC website, so there is local in-house experience in their use. For security reasons, users are not permitted to run custom MySQL queries directly. Access is permitted only via the interfaces provided. In addition, the database does not include the ASTCAT-C and ASTCAT-S catalogues, which are available only as gzip'ed ASCII files.

Table 8.2 lists the MySQL tables that are accessible via the web interface, the column headed "Reference" indicates where information on what information is contained in each table may be found.

Table 8.2: MySQL tables accessible via the web interface

MySQL table name	Contents	Reference
`old_hgs`	Current MPC *HG* values	Table 8.3
`hgs`	New *HG* values, including all four solutions for each object	Table 6.5 [p. 128]
`obsphots`	Data on every observation that contains (astro)photometry	Tables 6.1 [p. 119], 6.2 [p. 124] and 6.6 [p. 129]
`colours_and_taxonomies`	Colour and taxonomic data	Table 6.4 [p. 125]
`albedos`	New albedo and diameter determinations for NEOWISE-observed minor planets	Table 9.12 [p. 193]
`fitfiles`	The transformation equations used for the catalogue corrections	Table 6.3 [p. 125]

The `old_hgs` table contains the *H* and *G* values extracted from the MPC file of orbits of numbered minor planets. The format of the corresponding data file on the thesis website is shown in Table 8.3.

Table 8.3: Format of the old_hgs data file

Columns	Format	Use
1– 5	A5	Minor planet number in packed form (see Appendix 1.4.2 [p. 214]
8–12	F5.2	Slope parameter, *G*
14–18	F5.2	Absolute magnitude, *H*

All the MySQL tables, with the exception of the `fitfiles` table, contain additional information that is not included in the flat data files included on the website. This additional information consists of three data items: a coarse orbit classification (a single character indicating whether the object is an NEO, Jupiter Trojan or distant object); a finer orbit classification (an integer indicating the orbit type) and a flag value that is set if the object is a Potentially-Hazardous Asteroid (see Appendix 3.8 [p. 223]). This information was added to allow easy extraction of information on all the objects of a particular orbit type. The integer orbit classification uses the same scheme as that in the MPC's public orbit file, MPCORB, and the valid values are documented on the MPC's website[1].

1 `http://www.minorplanetcenter.net/iau/info/MPOrbitFormat.html`

9: Analysis

9.1: Introduction

In this chapter, I present analysis of my *HG* results, comparing my new determinations to other values in the literature and examining problem cases. I also present a new determination of the albedos of the objects observed by NEOWISE.

9.2: Remaining "Problem" Objects

Quite a number of the *HG* determinations can be classified as "problem" cases, for a variety of reasons.

9.2.1: Objects With No *HG* Solution

Four unusual objects produced no *HG* solution: (5335) Damocles, an object on a 40-year-period comet-like orbit; (6130) Hutton, an object with an orbital eccentricity, e, of 0.54 and a perihelion distance, q, of 1.36 AU; (9767) Midsomer Norton, an object with $e = 0.57$ and $q = 1.46$ AU; and (15836) 1995 DA_2, a trans-Neptunian object (TNO) in the 4:3 mean-motion resonance with Neptune.

(5335) Damocles has been observed at only two oppositions (1991 and 1992) and was never observed above a declination of –62°. In addition, only four of the available astrometric observations have magnitude estimates: the discovery observation, made photographically at Siding Spring (Australia), with the magnitude rounded to the integer (actually, such photographic measures were rounded to the nearest 0.5 mag.); and three photographic observations from the Mt. John Observatory (New Zealand). None of these observations is correctable currently.

Although observed at five oppositions from 1984 to 2010, the observational coverage of (6130) Hutton is rather spotty. There are four photographic magnitude estimates made at Siding Spring between 1984 and 1989, and a single CCD magnitude from Spacewatch in 2002. None of these observations is correctable currently.

Also observed at five oppositions, this time from 1980 to 2010, (9767) is also poorly observed (astro)photometrically. Only seven observations include magnitude estimates, and two of them are given only to an integer value. The remaining five observations were made on only two different nights, and the transformation fit on one of the nights was bad. This left a single useable night and essentially zero phase-angle coverage.

(15836) was discovered in 1995, observed at five subsequent oppositions and last seen in 2002. Only four magnitudes, all on different nights, are available for this object. The transformation fits for the two observations made at the discovery apparition were bad, leaving just two useable observations.

Further observations of all four objects are desirable, but none of them will be easy targets in the near future. Observers will have to wait until 2029 before (5335), which has recently passed through its aphelion, next gets as bright as $V = 22$. (6130) doesn't get brighter than $V = 22$ until early 2014, while (9767) remains below $V = 22$ until the middle of 2016. (15836) never gets as bright as $V = 22$, but is observable at each opposition, albeit at $V = 23.7$. The limit of $V = 22$ was selected as it is obtainable by large amateur-owned or amateur-operated telescopes.

9.2.2: Objects With Large *H* Uncertainties

Of the 322 607 *H* solutions, the formal uncertainties in the absolute magnitude is less than 0.1 mag. for 288 143 of the objects. A further 32 812 solutions have uncertainties in the range 0.1–0.2 mag. There are 146 objects where the *H* uncertainty was ≥ 0.5 mag. The distribution of *H* uncertainties is shown in Figure 9.1, noting that the Y axis plots the base-10 logarithm of the bin counts, in order to encompass the large range in the bin counts.

Of the 146 objects with *H* uncertainties ≥ 0.5 mag., 70 were TNOs and 46 were NEOs. Counting the number of objects that matched specific criteria that could account for the large *H* uncertainty produced the following: 55 objects had less than ten observations included in the solution; 107 objects had a phase-angle coverage of $< 15°$; and 41 objects had no observations at phase angles $< 20°$. Many objects matched more than one of these criteria, as shown in Figure 9.2. Two objects, both NEOs, matched all three criteria: (152561) 1991 RB and (289227) 2004 XY_{60}.

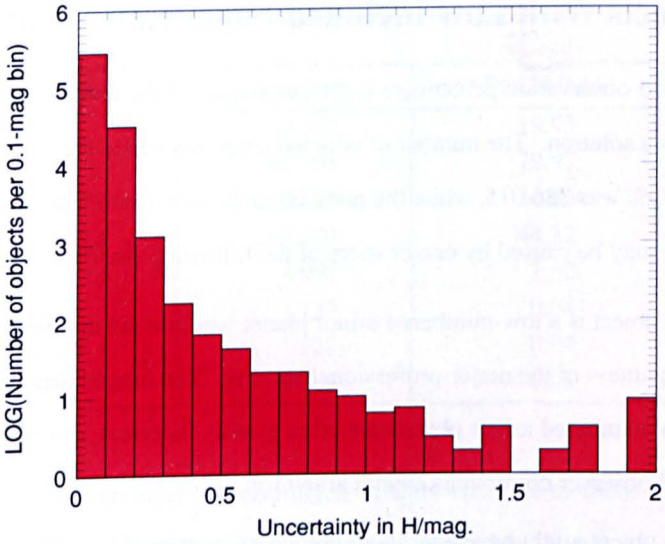

Figure 9.1: Base-10 logarithmic H uncertainty distribution

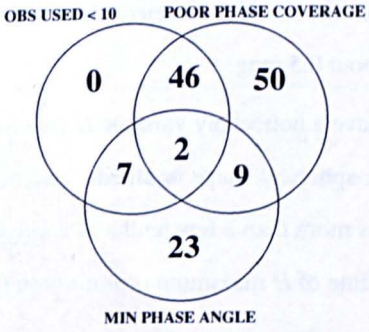

Figure 9.2: Venn diagram showing counts of uncertain-H objects matching various combinations of criteria

For many of the objects not seen at phase angles below 20°, the individual magnitude-estimate residuals are a few-tenths of a magnitude, so the uncertainty in these *H* determinations is simply a result of the uncertainty introduced in the extrapolation of the phase curve back to 0°. Nine objects did not match any of the criteria: (53429) 1999 TF_5, an Apollo object; (65674) 1988 SM, (65717) 1993 BX_3, (205388) 2001 DV_8 and (306595) 2000 GG_{147}, all Amor objects; (243881) 2000 YP_{33} and (315175) 2007 HW_{14}, both Hungarias; (17493) Wildcat, an object with $e = 0.44$, $q = 1.53$ AU; and (258102) 2001 QO_{170}, a routine MBA. It is not possible to do anything further with these objects at this time. Further observations of these objects, especially at phase angles not covered in the current data set, are to be encouraged.

9.2.3: Objects With Low Included-Observation Percentages

The included-observation percentage is the percentage of the corrected observations that are included in a solution. The number of adopted solutions where the included-observation percentage was over 90% was 286 015, while the number under 80% was 2969. A low included-observation percentage may be caused by one or more of the following reasons:

1 An object is a low-numbered minor planet which is always brighter than the saturation brightness of the major professional surveys. The magnitudes from those surveys for low-numbered minor planets are often grossly incorrect, something that the catalogue and observer corrections cannot allow for.

2 An object might have a large-amplitude lightcurve. Since the professional surveys randomly sample the lightcurves, some of their observations will be obtained near lightcurve minima, others near lightcurve maxima. Such observations may be far enough away from the mean to be rejected from the solution, if the lightcurve amplitude is greater than about 0.5 mag.

3 An object may have a noticeably variable H (see Section 9.10 [p. 180]), due either to a significantly non-spherical shape or albedo variations across the surface. If the variability in H is more than a few tenths of a magnitude, perfectly good observations obtained near a time of H maximum or minimum may get rejected from a solution.

9.3: Slope Determinations

No HG_U solution was found for 154 026 objects. The remaining 168 581 objects have HG_U solutions, but those solutions were preferred over one of the other solutions in only 64 348 cases. Of the unadopted HG_U solutions, 30 661 were rejected because there were no observations used at $\beta \leq 2°$ or $2° < \beta < 7°$, 68 451 were rejected because the uncertainty in G was greater than 0.1, and the remainder were rejected either because the phase-angle coverage was insufficient or the percentage of included observations was more than 5% less than the included percentage for the HG_A solution. The breakdown of the number of each type of adopted solution is shown in Table 9.1.

Table 9.1 : Breakdown of type of adopted HG solution

Solution type	Number	Percentage
HG_U	64 348	19.95
HG_A	257 998	79.97
HG_A, $G = 0.12$	110 118	34.13
HG_A, $G = 0.24$	142 978	44.32
HG_A, $G = 0.48$	4 902	1.52
HG_S	127	0.04
HG_C	134	0.04
None	4	< 0.01

The small number of HG_S/HG_C solutions is reassuring, as it shows that the methods I used to assign the adopted G values are broadly correct, at least within the framework of this thesis.

The distribution of the G values for the 64 348 adopted HG_U solutions is shown in Figure 9.3.

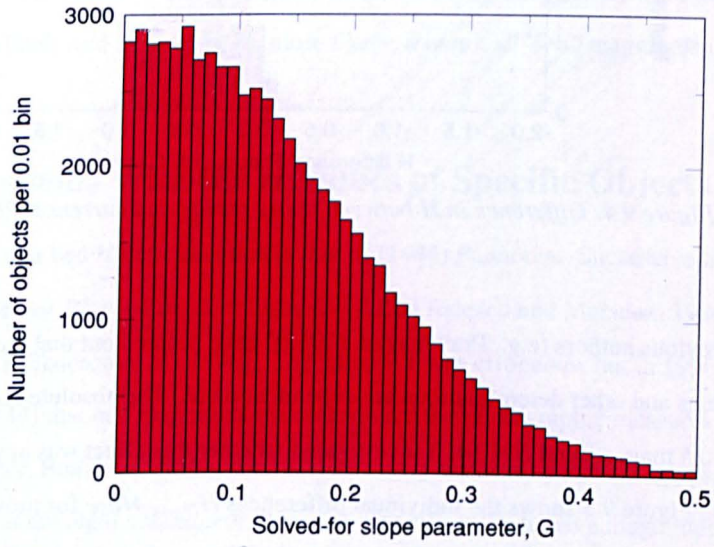

Figure 9.3: Distribution of solved-for G solutions

The distribution shown in Figure 9.3 suggests that the solved-for G values are meaningful physically, at least for $G > 0.05$, as there are far more objects with $G < 0.2$ than there are with $G > 0.4$, which is the distribution we would expect. The large number of entries with G close to zero is probably an artifact of the *HG* fitting process, as the method described in Section 6.4 [p. 130] seems to produce G values near zero when the observations are noisy.

9.4: Comparison to Previous MPC *H* Values

The newly-determined H values (H_{Thesis}) were compared to the existing MPC H values (H_{MPC}). The distribution of the differences H_{Thesis}–H_{MPC} is shown in Figure 9.4, the distribution mean and standard deviation being +0.36 and 0.21, respectively. The fact that the mean value is positive shows that the current MPC H values are, in general, too bright, confirming the findings of other authors (e.g., Pravec *et al.*, 2012).

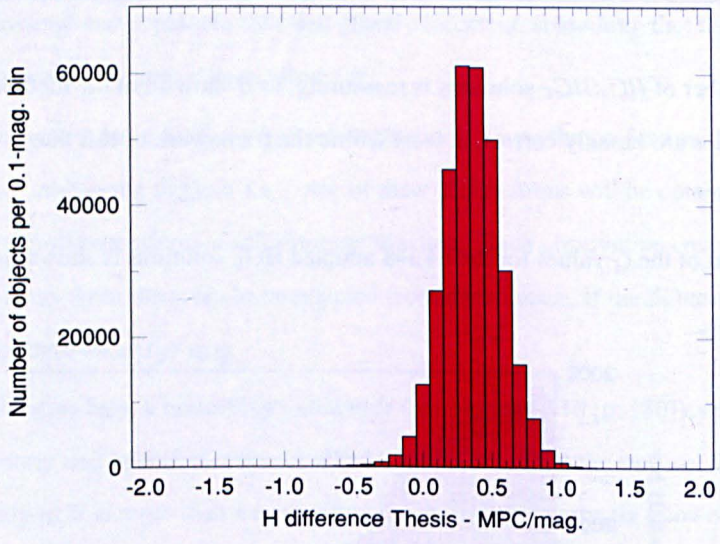

Figure 9.4: Difference in H between thesis results and current MPC values

A number of previous authors (e.g., Pravec *et al.* (2012)) have pointed out that the differences between the MPC H values and other determinations are dependent on H. The absolute size of this difference peaks at about 0.5 mag. around $H \approx 14$. I investigated whether this effect was apparent in my new determinations. Figure 9.5 shows the individual differences H_{Thesis}–H_{MPC} for most of the minor planets studied in this thesis. The handful of big TNOs with $H < 0$ are excluded, other TNOs are shown as blue crosses, while red crosses are used for non-TNOs.

The black line in Figure 9.5 is the mean difference within each 0.1-magnitude-wide bin in the range $8 < H < 20$. The greatest mean differences (+0.49 mag.) are found in the H range 14.2 to 14.5, which are consistent with the values +0.50 and 14 found by Pravec *et al.* (2012) (see Section 2.6.2 [p. 32]).

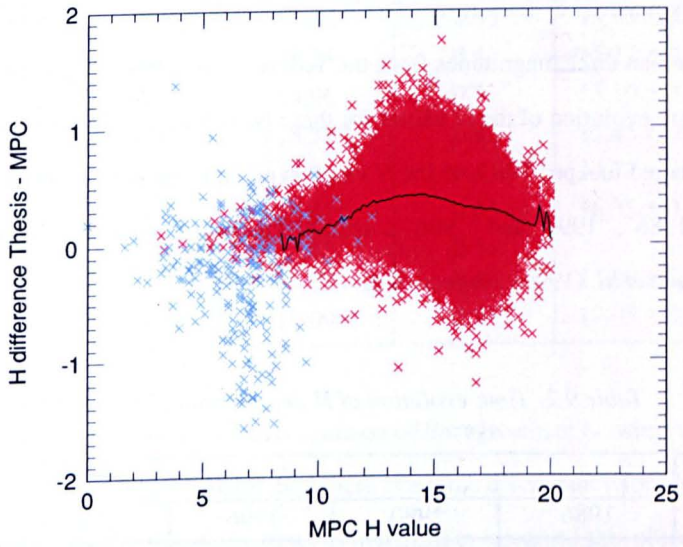

Figure 9.5: Absolute-magnitude dependence on H differences

There are a large number of TNOs in the range $5 < H < 10$ with new H determinations more than 0.5 mag. from the previous values. This suggests either that all the astrophotometric observations of TNOs are not as good as I believed them to be or, more likely, that not all TNO magnitudes are of equal quality.

9.5: Known Problems With the *H* Values of Specific Objects

The "classic" case of a bad H determination is that of (1444) Pannonia. Successive lists of *HG* parameters in the *Minor Planet Circulars* listed $H = 11.0$ (Tedesco and Marsden, 1986), 10.6 (Tedesco *et al.*, 1990) and 9.1 (Tedesco *et al.*, 1996). The value 9.1 was erroneous, but in 1996 the only available observations of (1444) that had magnitude estimates were the photographic measures obtained at the Konkoly Observatory, Budapest, during the 1938 discovery and 1941 recovery oppositions. None of the observations made at the eight subsequent observed oppositions included a magnitude. The 1938/41 magnitude estimates should have had a correction of +1.5 or +2 magnitudes applied before computing H, but for some reason, this correction was not applied. It is possible that there was no entry for Konkoly Observatory in the magnitude-weighting file in use in 1996. The first modern magnitude estimates were reported during the 1997 opposition, but the H value was not corrected (to $H = 11.1$) until September 2008. The current MPC H value for (1444) is 11.3, while the value determined in this thesis is $H = 11.77 \pm 0.03$, for $G = 0.38 \pm 0.09$.

In the explanatory material to Tedesco *et al.* (1996), mention is made of two objects whose *H* value had changed by more than three magnitudes from the Tedesco *et al.* (1990) list: (2143) Jimarnold and (3578) Carestia. The time-evolution of the *H* values for these two objects is shown in Table 9.2, noting that (3578) was numbered in April 1987, so the *H* value in parentheses is from when it was numbered. The table headings "1986", "1990" and "1996" correspond to Tedesco and Marsden (1986), Tedesco *et al.* (1990) and Tedesco *et al.* (1996), respectively.

Table 9.2: Time-evolution of H determinations for problem cases

Object	*H* determination				
	1986	1990	1996	Current	Thesis
(2143)	14.1	11.2	14.3	13.5	13.95 ± 0.03
(3578)	(10.5)	8.1	11.6	10.1	10.36 ± 0.04

The erroneous *H* for (3578) in Tedesco *et al.* (1990) caused this object to be highlighted by Marsden (1996) as an anomalous recent discovery of an intrinsically bright main-belt minor planet.

9.6: Comparisons With Other Recent *H* Determinations

Warner (2012a, b) reported a number of *HG* determinations from lightcurve observations made at his private observatory. He noted that the MPC *HG* values used by the NEOWISE team led to unrealistic albedos. The comparison between Warner's *HG* values and the new values presented here are shown in Table 9.3. Note that Warner supplied two *H* values, based on different *G* values, for two of the objects.

Table 9.3: Comparison of new HG values to Warner (2012a, 2012b) HG values

Object	Current MPC		Warner (2012a, b) value		Thesis	
	H	*G*	*H*	*G*	*H*	*G*
(3260)	12.6	0.15	12.80	0.15	13.02 ± 0.02	0.24
(4898)	13.9	0.15	14.72	0.41	14.64 ± 0.05	0.48
(5427)	13.5	0.15	14.41	0.43	14.19 ± 0.05	0.48
(6087)	14.8	0.15	15.61	0.43	15.53 ± 0.05	0.34 ± 0.06
(6646)	14.3	0.15	14.9	0.15		
			15.2	0.43	15.04 ± 0.06	0.48
(7829)	14.0	0.15	13.94	0.15		
			14.26	0.43	14.76 ± 0.08	0.48
(11058)	14.3	0.15	15.13	0.43	15.14 ± 0.07	0.25 ± 0.07

(16426)	13.9	0.15	14.62	0.43	14.65 ± 0.05	0.48
(16585)	14.4	0.15	15.24	0.43	15.17 ± 0.06	0.48
(16589)	14.3	0.15	14.96	0.43	15.10 ± 0.05	0.48
(26383)	14.7	0.15	15.58	0.43	15.45 ± 0.06	0.33 ± 0.07
(45898)	14.0	0.15	14.90	0.43	14.72 ± 0.06	0.48
(49678)	15.8	0.15	16.61	0.43	16.35 ± 0.06	0.48
(138666)	15.0	0.15	15.72	0.15		
			15.97	0.43	15.88 ± 0.08	0.48
(141018)	18.9	0.15	19.09	0.15	19.05 ± 0.03	0.12 ± 0.02

Due to the use of different *G* values, a direct comparison of the agreement between the two sets of *H* values is not possible. It is obvious, though, that there is a large discrepancy for (7829) Jaroff, of about 0.5 mag. One possible reason for this discrepancy is that Warner observed this object only over phase angles from 10°.0 to 13°.7, whereas my value is based on observations over a phase-angle range of 8°.1 to 33°.3.

A recent paper by Chiorny *et al.* (2011) initially looked like a useful source of new *H* determinations for a number of small minor planets. However, all the objects had phase-angle coverage that was rather limited. None of the eleven objects studied had observations over more than a 10° range of phase angle, and one object was observed on one night only. For this reason, I decided not to compare their *H* determinations with my new determinations.

Pravec *et al.* (2012) determined *HG* parameters for 583 main-belt minor planets and Near-Earth Objects. The authors kindly supplied their table of results in advance of publication and I compared their *H* values (H_{Pravec}) to mine (H_{Thesis}). The distribution of the differences H_{Pravec}–H_{Thesis}, in 0.1-magnitude bins, for the 560 objects in common between the two studies is shown in Figure 9.6 [p. 176]. The mean of the differences is –0.07 mag. and the standard deviation is 0.18 mag. For 31 of the objects, the difference was more than three standard deviations away from the mean. According to the on-line version of the Asteroid Lightcurve Database (Warner *et al.*, 2009), fifteen of these objects have lightcurves amplitudes exceeding 0.5 mag. An initial thought was that the astrophotometric observations were being obtained preferentially near the times of lightcurve maximum. This would make the Pravec *et al. H* determinations fainter than mine. Ten of the fifteen large-amplitude objects do have H_{Pravec}–$H_{Thesis} > 0$. But this explanation would require these objects to be faint, such that their mean (lightcurve-averaged) magnitude would be fainter than the limiting magnitude of the majority of the major professional surveys

for most of the time. This simply isn't true, so some other explanation is necessary. At present, I do not have another explanation and resolution of this problem may require the publication of the mean magnitudes used in the Pravec *et al.* study.

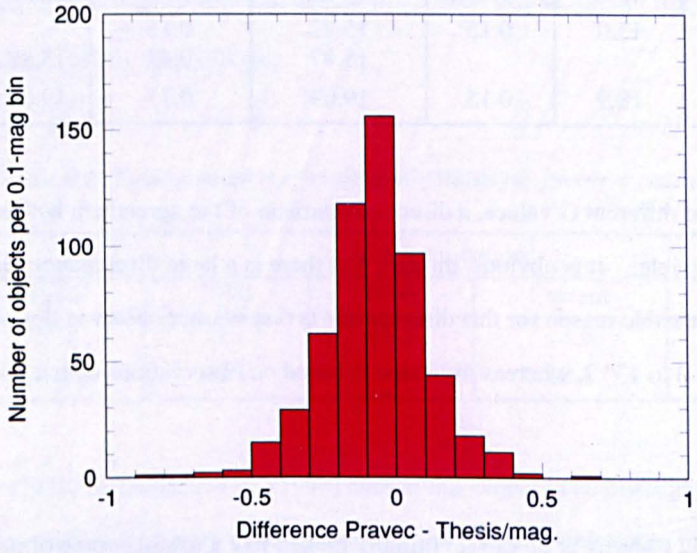

Figure 9.6: Difference in H determinations between Pravec et al. (2012) and this thesis

9.7: Comparisons With the Magnitude Alert Project

Comparison of the results obtained in this thesis with the results obtained by the Magnitude Alert Project (Garrett, 1997) is not easy. Quite apart from the difficulties encountered in getting the MAP data into a useable format (see Section 5.6 [p. 112]), there is the issue that the MAP *H* values are derived by combining CCD measurements with visual measurements. Since the compilers of MAP have not applied any catalogue- or observer-corrections to the CCD measures, which were made using a number of astrometric reference catalogues, the resulting *H* values cannot be compared to the values obtained in this thesis. It would be instructive to compare the *H* values where there were only visual measurements. A manual inspection of the Excel file of MAP measures located twenty objects where most or all of the available observations were made visually. These objects are listed in Table 9.4, along with the MAP-derived *H* magnitude (H_{MAP}), the difference between that value and the MPC *H* magnitude (H_{MPC}, as of early 2010), the current MPC *H* value, the thesis-derived *H* value (H_{thesis}) and the difference (rounded to 0.1 mag.) between the thesis and MAP values (H_{thesis}–H_{MAP}).

Table 9.4: Comparison of MAP and thesis H values

Object	MAP		MPC	Thesis	
	H	H_{MPC}–H_{MAP}	H	H	H_{thesis}–H_{MAP}
(902)	12.0	+0.3	12.0	12.32 ± 0.02	+0.3
(919)	11.8	–0.5	11.3	11.45 ± 0.02	–0.4
(920)	11.0	+0.2	11.19	11.29 ± 0.02	+0.3
(933)	12.1	–0.3	12.5	12.49 ± 0.02	+0.4
(942)	10.9	–0.6	10.9	11.02 ± 0.02	+0.1
(959)	10.7	–0.5	10.7	11.17 ± 0.02	+0.5
(989)	11.8	0.0	11.8	12.11 ± 0.02	+0.3
(1018)	10.7	–0.1	10.62	11.31 ± 0.02	+0.6
(1022)	10.4	+0.1	10.2	10.42 ± 0.02	0.0
(1067)	10.7	+0.3	10.99	11.08 ± 0.01	+0.4
(1077)	11.9	+0.4	12.2	12.53 ± 0.01	+0.6
(1097)	12.5	–0.8	11.9	12.20 ± 0.02	–0.3
(1130)	11.9	+0.2	12.0	12.26 ± 0.02	+0.3
(1131)	12.7	+0.3	12.9	13.15 ± 0.02	+0.4
(1148)	10.6	–0.4	10.15	10.26 ± 0.02	–0.3
(1155)	11.8	–0.3	11.9	12.14 ± 0.02	+0.3
(1166)	9.9	+0.5	10.3	10.56 ± 0.02	+0.7
(6042)	13.3	–0.6	12.8	13.13 ± 0.03	–0.2
(9219)	11.8	0.0	11.9	12.14 ± 0.03	+0.3
(93768)	14.2	–0.3	14.1	14.48 ± 0.04	+0.3

The mean value of the H_{MPC}–H_{MAP} differences is –0.1 mag., while the mean value of the H_{thesis}–H_{MAP} is +0.2 mag. I note that many of the MAP objects were added to the program when the H_{MPC}–H_{MAP} differences were much larger.

9.8: Comparison with SuperWASP Determinations

Parley (2008) undertook a photometric survey of minor planets using observations obtained serendipitously by the SuperWASP project, a search for extra-solar planetary transits. SuperWASP uses 2048×2048-pixel CCD cameras attached to 200-mm f/1.8 telephoto lenses. Arrays of individual cameras are attached to single mounts located on La Palma in the Canary Islands and at the South African Astronomical Observatory in Sutherland. The field size is 61 sq. deg., which results in an image scale of 13″.7 per pixel. The limiting magnitude is about 15. Using data obtained in 2004 and 2006, Parley identified 378 673 useable observations of 1466 minor planets. He derived 570 lightcurves for 277 different minor planets. Of these, 17 were for objects with no previous published lightcurve and 30 were

period improvements. In addition, absolute magnitudes for more than 130 objects and slope parameters for 123 objects were reported. Unfortunately, the magnitudes obtained by SuperWASP are in a local system, as the reduction of the raw images was complicated by inter-field and intra-field calibration issues. Although the SuperWASP photometry pipeline tied each field's photometry to the V_T Tycho-2 magnitudes (see Section 3.7.2 [p. 57]), the calibration issues caused problems in the night-to-night linking of magnitudes. Parley was partly successful in applying nightly offsets to bring magnitudes from different nights into better agreement, but the resulting H magnitudes cannot be compared directly to the results from this thesis. However, an examination of Parley's G values would be useful.

Parley's thesis Table C3 contains, amongst other data, 259 sets of HG parameters for 254 different numbered minor planets. Seventeen of the solutions were made using the catalogued G value. The data lines from Table C3 were extracted into a text file from a PDF version of Parley's thesis. This file was then sorted on various columns so that objects with H uncertainties > 0.3 mag., G values outside the range 0–0.5 or G uncertainties > 0.1 could be removed easily. This process reduced the data to 123 sets of HG parameters for 120 different objects.

Figure 9.7 shows Parley's raw G distribution (before my earlier-described culling of suspect data). The distribution does not look realistic, as compared to Figure 9.3 [p. 171], based on the large number of objects with slope parameters above 0.5 and below –0.1. Figure 9.8 shows the comparison of G values determined by Parley (2008) to the values in this thesis. The plotted points are coloured according to whether or not either of the G values are assumed values: black indicates that both G values were solved for (28 cases); red indicates that the thesis G value was assumed (78 cases); and green indicates that both G values were assumed (17 cases). There were no instances where the thesis value was solved for and the Parley value was assumed. The dashed line indicates where the thesis and Parley values would be in agreement.

The vertical stripes of points in Figure 9.8 correspond to default $G = 0.12$ and $G = 0.24$ thesis solutions. The gray-shaded area indicates that there is some broad agreement between the two sets of G values, in that both sets tend to agree on whether a particular G value is small or large. But there does not appear to be good agreement between the individual G values determined in this thesis and the values determined by Parley. The reason for this lack of agreement between the slope parameters for specific objects is not obvious to me. It may not be surprising, given that the results have come from two

completely different reduction techniques applied to two different sets of low-quality data.

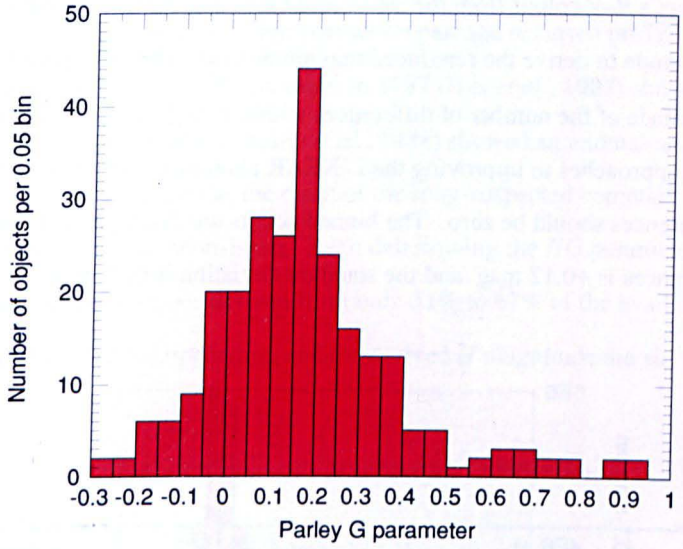

Figure 9.7: G distribution from Parley (2008)

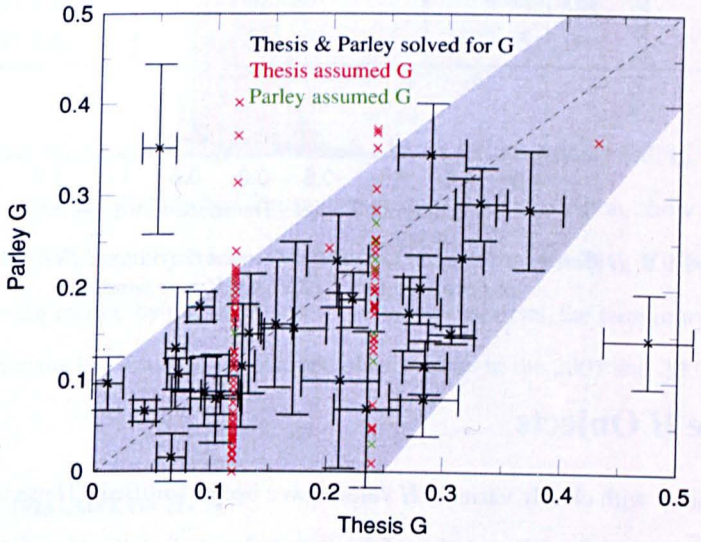

Figure 9.8: Comparison of Parley (2008) G values to thesis G values

9.9: Corrected Astrophotometry and LINEAR Rereduction Comparison

As noted in Section 5.3 [p. 103], it is possible to compare the LINEAR rereduced photometry to the catalogue- and observer-corrected originally-submitted photometry derived in this thesis by use of Equation 5.6 [p. 103]. A program was written (`linearredux.f90`) that scanned the

`obscorr/N*.OBS` files, looking for corrected LINEAR observations. When matching observations were found, the program extracted the original magnitude and the corrected magnitude (V_C). It then extracted the object's *B–V* colour from the `colsandtax.dat` file and applied Equation 5.6 [p. 103] to the original magnitude to derive the rereduced magnitude (V_R). The difference $Vc–V_R$ was then formed and counts were made of the number of differences within ± 0.05 mag. of 0.1-magnitude-wide bins. If the two different approaches to improving the LINEAR photometry produce identical results, the mean value of the differences should be zero. The binned counts are displayed in Figure 9.9. The mean of the 28 878 880 differences is +0.12 mag. and the standard deviation is 0.23 mag.

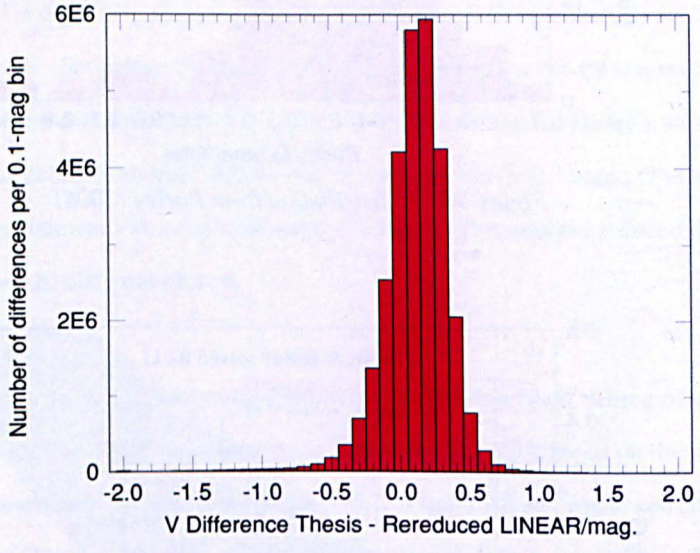

Figure 9.9: Differences between thesis-determined corrected LINEAR V magnitudes and the rereduced LINEAR V magnitudes

9.10: Variable *H* Objects

A couple of objects with clearly variable *H* values have been identified. These variations are distinct from the variations caused by the rotation of the minor planet. Rotational variations, as observed by lightcurve observers, are caused by short-term changes (on timescales of hours or days) in aspect (that is, in the amount of the minor planet's surface that is visible to the observer). Variable *H* values are caused by long-term changes (on timescales of months or years) in aspect due to the changing relative position of the minor planet and Earth in their respective orbits.

9.10.1: (2060) Chiron

(2060) Chiron (also known under its dual-status designation 95P/Chiron) is a comet which shows cometary activity near perihelion. The last perihelion passage occurred on 1996 Feb. 14 at a heliocentric distance of 8.45 AU. Observations in 1987 (Bus *et al.*, 1987) showed nothing unusual, but observations the following year (Tholen *et al.*, 1988) showed an anomalous brightening of 0.7 magnitudes, which was interpreted as the onset of the long-suspected cometary activity. The FASTT observations of this object are inconsistent. Even determining the *HG* parameters on an opposition-by-opposition basis leads to values derived from only 31% to 67% of the available observations: the Phase Angle Bisector (PAB) at opposition and the derived *H* magnitude are shown in Table 9.5.

Table 9.5: Variable H values for (2060) Chiron

Opposition	PAB ($R.A._{J2000.0}$)	*H*	Fraction included
1998 May	225.64	6.65±0.05	0.63
1999 May	240.73	6.85±0.04	0.57
2001 June	265.85	5.98±0.05	0.33
2003 July	285.17	5.75±0.04	0.31

The FASTT observations in 1998 and 1999 show Chiron's *H* magnitude fading, whereas observations in 2001 and 2003, when Chiron was further from perihelion, show *H* brightening. This behaviour was also observed by Romon-Martin *et al.* (2003) and Bauer *et al.* (2001), and has been interpreted as being caused by post-perihelion explosive outbursts, the temporary nature of which would account for the low fraction of included observations in the 2001 and 2003 solutions.

9.10.2: (1605) Milankovitch

The case of (1605) Milankovitch is interesting. It seems to be a clear example of a routine main-belt minor planet with a detectable variable *H*. The maximum lightcurve amplitude is 0.12 (Harris *et al.*, 2007), based on observations by Cooney (2005). The *HG* parameters were determined on an opposition-by-opposition basis: the *H* magnitude (for an assumed $G = 0.12$) and the associated PAB at opposition are shown in Table 9.6 [p. 182].

Table 9.6: Variable H values for (1605) Milankovitch

Opposition	PAB (R.A.$_{J2000.0}$)	*H*
1999	224.74	10.1268 ± 0.0377
2000	298.40	10.7153 ± 0.0457
2001	16.90	10.1060 ± 0.0201
2003	116.91	10.6859 ± 0.0346
2004	207.05	10.0542 ± 0.0703
2006	357.21	10.2456 ± 0.0325
2007	93.46	10.5623 ± 0.0419

Even at a casual glance, the PAB/*H* values in Table 9.6 appear to be periodic with an amplitude of about 0.8 mag. This was confirmed by generating Figure 9.10, which shows the values from Table 9.6, along with the best-fit double-sine curve, which was determined to be:

$$H = 10.369 + 0.361 \sin(2(PAB - 77.3)) \quad (9.1)$$

which represents the *H* values in Table 9.6 within 0.02 ± 0.04 mag.

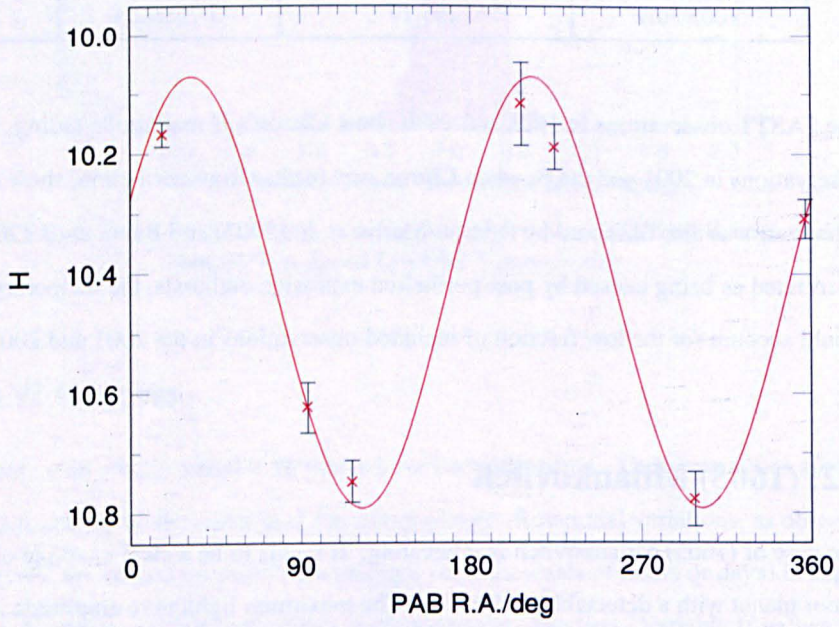

Figure 9.10: Variable H of (1605) Milankovitch

Cooney (2005) reported lightcurve observations on four nights, 2004 Apr. 16/17/19/27, and derived a lightcurve amplitude of 0.12 mag. when the PAB R.A. was 207°. This would imply that

H = 10.01, very near its maximum brightness. Behrend (2011) reports (seemingly) unpublished observations showing a lightcurve amplitude of 0.14 mag. obtained by Antonini from observations on 2006 Oct. 14 and Nov. 16, when the PAB R.A. was 357° and 0°, respectively, leading to H = 10.25 and 10.21, respectively.

Under the standard assumption of a uniform triaxial ellipsoid shape ($a \times b \times c$, with $a \geq b \geq c$), the projected surface area (Gehrels, 1970) would be a maximum of πab, when we see the polar regions face-on. When the equatorial region was face-on, the projected surface area would vary from a maximum of πac to a minimum of πbc. The magnitude difference between those two extremes would be:

$$\Delta m = 2.5 \log (\pi ab / \pi bc) = 2.5 \log (a / c) \qquad (9.2)$$

Setting Δm to 0.722 (the amplitude of the H curve) leads to a/c = 1.9. This is to be interpreted as a lower limit, as it is unknown whether the pole is ever visible face-on. It seems probable that $b \approx c$, given that there are no substantial differences between the individual opposition HG fits. I cannot say anything definite about the pole orientation. The fact that the mean magnitude changes with the viewpoint indicates that the pole direction is not perpendicular to the line of sight, as there would be no change in mean magnitude with changing viewpoint. Neither does the pole direction lie exactly in the line of sight, as there would no lightcurve when the pole was pointed at the observer. Two independent studies have shown 0.1-magnitude-level lightcurves near times of H maxima, which suggests that the pole direction might lie near to the line of sight. Lightcurves obtained near time of H minima would be necessary to confirm this supposition.

9.10.3: Other Objects

The variable nature of the H value for (1605) Milankovitch seems secure. An examination of other low-lightcurve-amplitude objects with low inclusion fractions did not show any other such clear examples. Closer examination of these objects is a job for the future. High-amplitude objects should also be examined, but such cases will be less clear cut than the low-amplitude objects as more observations will be rejected from the solutions simply because of the large lightcurve amplitudes.

9.11: Differential *H* Distributions

Although the thesis set of *HG* determinations does not encompass the entire set of minor planets with reliable orbital elements (objects numbered after the 2012 March 8 batch of *Minor Planet Circulars* and multi-opposition unnumbered objects are missing from the data presented here), the set is large enough that it is essentially complete for objects that can get as bright as $V = 19.2$. This is demonstrated in Figure 9.11, which shows the distribution of the discovery V magnitude (as given by the observer, corrected as necessary from non-V bands) for minor planets discovered in 1991, 2001 and 2011. In 1991, there were 5459 provisional designations assigned, of which 1075 (~20%) had no discovery magnitude reported. The V range 15.2–18.9 encompassed 90% of the 1991 discoveries, with a broad peak at $V \sim 17$. In 2001, there were 75 007 provisional designations assigned, of which 495 (0.7%) lacked magnitudes, with 90% of the discovery magnitudes in the range 17.3–20.7 and a peak at $V \sim 18.5$. In 2011, there were 52 409 provisional designations assigned, of which 1172 (2.2%) lacked magnitudes, with 90% of the discovery magnitudes in the range 19.2–21.6 and a peak at $V \sim 20.7$. The strange peaks in the 2001 distribution are a consequence of many observers rounding their magnitude estimates to the nearest half magnitude.

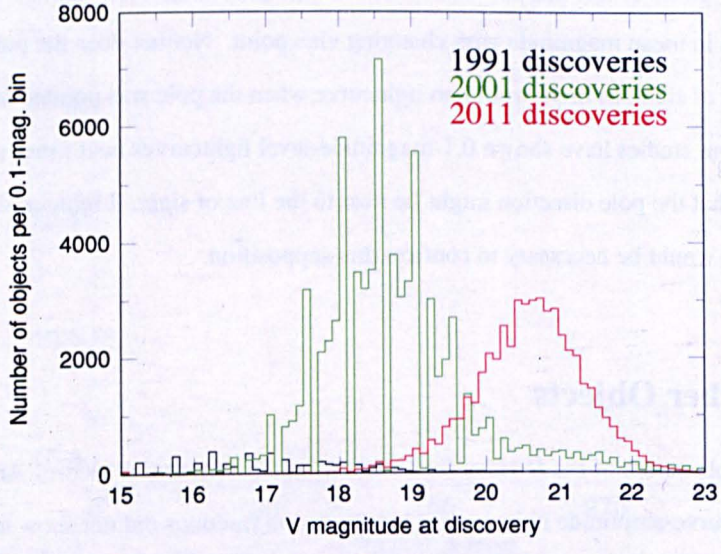

Figure 9.11: Discovery-magnitude distribution of minor planets assigned provisional designations in 1991, 2001 and 2011

A completeness magnitude of $V = 19.2$ corresponds to the absolute-magnitude completeness estimates listed in Table 9.7. The visual albedos, p_V, listed are taken from Warner *et al.* (2009). The quoted corresponding diameters, D, are estimates derived from Equation 9.3 (Bowell *et al.*, 1989):

$$2 \log (D) = 6.241 - 0.4 H - \log (p_v) \quad (9.3)$$

Table 9.7: Absolute-magnitude completeness estimates and corresponding diameters

Group/Region	Semimajor axis/AU	H completeness	Diameter/km
Hungaria	1.9	18.0	0.6 for $p_v = 0.3$
Inner edge of Main Belt	2.2	17.1	1.1 for $p_v = 0.2$
Middle of Main Belt	2.8	15.7	3.0 for $p_v = 0.1$
Outer edge of Main Belt	3.28	14.8	5.9 for $p_v = 0.06$
Hilda	3.9	13.9	8.9 for $p_v = 0.06$
Jupiter Trojan	5.2	12.5	17.0 for $p_v = 0.06$

I have no need to perform any debiasing of my *HG* solutions as my data set is essentially complete to the stated level of $V = 19.2$. This is a luxury that has not been available to many earlier studies. Differential H-distribution plots were prepared using my new H values. In addition to preparing one plot that incorporates all objects, additional plots were prepared for various orbit classes, as well as various zones in the Main Belt (MB). The orbit classes and zones considered were: Near-Earth Objects (NEOs, objects with perihelia, q, < 1.3 AU), Hungarias; Inner Main Belt (Inner MB) objects, Middle Main Belt (Middle MB) objects; Outer Main Belt (Outer MB); Hildas; and Jupiter Trojans. See Section 2.8 and Table 3.4 for definitions of the non-MB orbit classes. The subdivision of the MB objects into the three zones was made with respect to major Kirkwood gaps (see Section 2.8). The MB zones were defined as follows, noting that all classes required the perihelion distance to be beyond the orbit of Mars: Inner MB objects have semimajor axes, a, between the inner edge of the MB and the 3:1 mean-motion resonance (MMR, see Appendix 3.5) with Jupiter ($2.15 < a < 2.5$ AU); Middle MB objects have semimajor axes between the 3:1 and 5:2 MMRs with Jupiter ($2.5 \leq a < 2.82$ AU); and Outer MB objects have semimajor axes between the 5:2 and 2:1 MMRs with Jupiter ($2.82 \leq a < 3.28$ AU). The H distribution of objects in each class or zone is shown in Figure 9.12.

The green lines in six of the plots show the H distribution slopes fitted to the linear parts of the distributions. Since the y axis is logarithmic, the slope, a, is the exponent in a power law of the form $N \propto 10^{a}$, where N is the number of objects in an H-magnitude bin. For the Inner MB distribution, it was necessary to perform separate fits to the linear regions for the bright and the faint objects (the orange line showing the fit at the bright end, the blue line showing the faint-end fit).

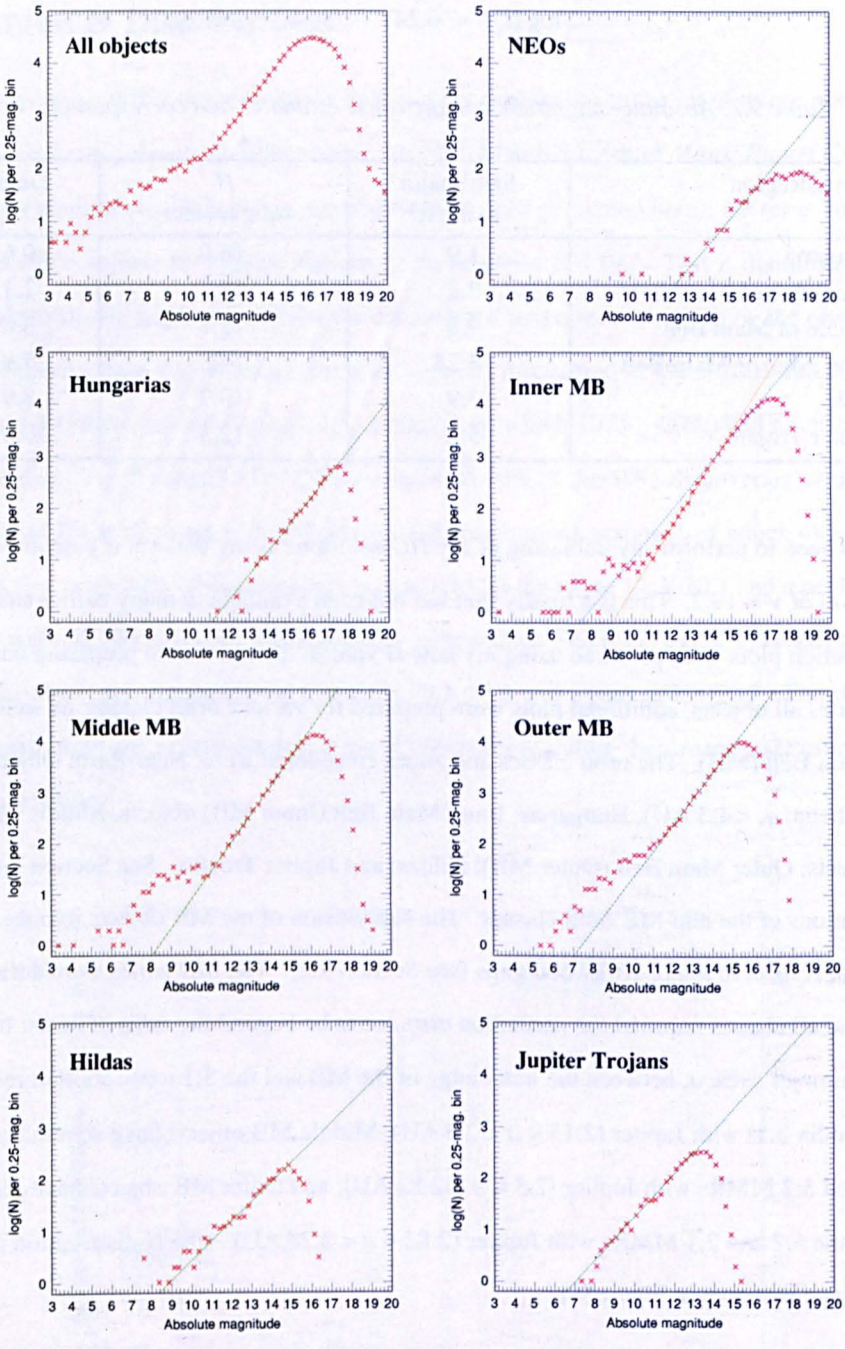

Figure 9.12: Differential absolute magnitude distributions for various classes of object

Table 9.8 lists the *H* distribution slopes determined for the various object classes shown in Figure 9.12, along with the *H* range that was used for the fit, the estimated *H* completeness level and the number of objects in the class. The estimated completeness values are taken from visual inspection of the plots in Figure 9.12 and are the *H* values at which the observed distribution falls off from the green (or blue) line. If comparison is made to the *H*-completeness estimates derived from Figure 9.11, it must be remembered

that those values are only for the stated heliocentric distances, while the values in Table 9.8 are for all objects within a range of semimajor axes. No fit has been computed for the "All objects" distribution as this contains a mixture of objects: NEOs; MBAs; Jupiter Trojans; and TNOs.

Table 9.8: Derived slopes and estimated completeness levels for classes shown in differential absolute-magnitude distributions

Object class/ zone	Distribution slope	H range for fit	Estimated H completeness	Number of objects
NEOs	0.453 ± 0.030	12.50–16.50	16	1252
Hungarias	0.479 ± 0.013	14.25–17.50	17.5	4087
Inner MB	0.609 ± 0.013	11.00–14.00		
	0.468 ± 0.008	14.00–16.50	17.0	111504
Middle MB	0.557 ± 0.006	10.50–15.50	15.8	111853
Outer MB	0.514 ± 0.007	11.25–15.25	15.3	86633
Hildas	0.379 ± 0.017	11.25–15.00	15.0	1344
Jupiter Trojans	0.432 ± 0.012	8.00–13.00	12.5	2945

The plots of all three of the MB zones show that there are excesses of large objects, over what one would expect from a naive extrapolation of the H distribution slopes. In each zone, the excess occurs in objects brighter than about $H = 11.0$, which corresponds to a diameter of 19 km at the inner edge of the MB and 34 km at the outer edge, for average visual albedo values (Warner *et al.*, 2009). There may be small excesses for Hildas and Jupiter Trojans if I perform fits to the H ranges 12.5–15.0 and 11.0–13.0. A review article by Davis *et al.* (2002) discusses possible reasons for the existence of these excesses.

Matching SDSS Moving Object Catalogue 4 detections of minor planets to the ASTORB catalogue, Parker *et al.* (2008) determined H distribution slope values for the Main Belt. They matched 220 000 SDSS observations to 104 000 objects, and used the SDSS observations to correct the ASTORB H magnitudes. With an average of only 2.1 observations per object, this study would not be able to average out the lightcurve effects for individual objects. Their H-distribution slope determinations were divided up into Main-Belt zones in the same manner as mine, but the number of objects in each of their zones was only about one third of the number in my zones. They found it necessary to make different fits to the "bright" and "faint" objects in each MB zone.

By applying his new debiasing method to the Palomar-Leiden Survey (PLS) of minor planets (van Houten *et al.*, 1970), Spahr (1998) also derived H-distribution slopes for three regions in the MB, based

solely on the PLS observations. Spahr's regions differ from mine (and Parker *et al.*'s) in that they cover the semimajor axis regions 2.0–2.6 AU, 2.6–3.0 AU and 3.0–3.5 AU, so that his results could be easily compared to the earlier work by Durda and Dermott (1997) and Durda *et al.* (1998). The limiting magnitude of the PLS was $V \sim 20$, but the total number of objects observed in the PLS was under 2500, as the survey only covered a 18° × 12° region. Spahr's debiased estimates of the number of objects in 0.5-magnitude bins in each zone is shown in his Figures 28–30. His estimates for the number of objects in the inner region in the bin centred at $H = 16.25$ is 20 000 ± 1500 (my estimate from his Figure 28, as Spahr does not list the values of the points he plotted). This is to be compared to my counts of 7615 and 9260 for the two bins centred at $H = 16.125$ and 16.375, giving a total of 17 875 objects. Given that Spahr's inner zone extends out to 2.6 AU, his PLS-debiased estimates appear to be essentially correct, to within (much better than) a factor of two. This supposition was confirmed by modification of my program that binned the H values to conform to Spahr's zones. The counts of object in the $H = 16.125$ and 16.375 bins increased to 11 439 and 13 119, respectively, giving a total of 24 558 objects. Spahr's debiased value for the number of inner MB objects with $16.0 < H < 16.5$ is therefore within ~20% of my count of known objects. So why are Spahr's distribution slopes different from mine? Apart from the difference in the zone coverages, there is also the issue that Spahr underestimated the objects at the bright end of the distributions in each zone, as the low number of such PLS-detected objects did not debias well. The large uncertainties in the debiased numbers of bright objects meant that Spahr restricted his determination of the H-distribution slopes to the H range 13.25 to 16.25/15.75/15.25 (for the inner, middle and outer zones, respectively). While the faint limits for the slope fittings in each zone are consistent with my limits, my bright limits are typically two magnitudes brighter.

I note that my slope values are close to the means of Parker's bright and faint slope values (see Table 9.9). Further, my Inner MB faint object slope matches their Inner faint object slope.

Table 9.9: Comparison of my H distribution slope values to Parker et al. (2008) and Spahr (1998) slope values

Zone	Parker *et al.* (2008) slope			Spahr (1998) slope	Thesis slope
	Bright	Faint	Mean		
Inner MB	0.76	0.46	0.61	0.453	0.609 & 0.468
Middle MB	0.73	0.42	0.58	0.482	0.556
Outer MB	0.56	0.40	0.48	0.489	0.514

Standard procedure when examining distributions in the Main Belt is to convert an H-distribution slope, α, into a mass index (also known as a mass-frequency slope), q, via the procedure devised by Dohnanyi (1969), who assumed that the internal strength of all objects is the same, regardless of size. As stated by Durda and Dermott (1997), the conversion is achieved, assuming that all objects have the same albdeo, using Equation 9.4:

$$q = 1 + \frac{5}{3}\alpha \tag{9.4}$$

Dohnanyi predicted $q = 1.83$ for a collisionally-evolved population in equilibrium. For the entire Main Belt, Durda and Dermott obtained $q = 1.78 \pm 0.02$, while Spahr obtained $q = 1.76 \pm 0.08$. My q values are listed in Table 9.10.

Table 9.10: Mass indices determined from my H-distribution slopes

Object class/ zone	Distribution slope	Mass index
NEOs	0.453 ± 0.030	1.756 ± 0.051
Hungarias	0.479 ± 0.013	1.798 ± 0.022
Inner MB	0.609 ± 0.013	2.016 ± 0.021
	0.468 ± 0.008	1.781 ± 0.014
Middle MB	0.557 ± 0.006	1.928 ± 0.011
Outer MB	0.514 ± 0.007	1.857 ± 0.011
Hildas	0.379 ± 0.017	1.631 ± 0.028
Jupiter Trojans	0.432 ± 0.012	1.720 ± 0.020

Three of the values in Table 9.10 are greater than Dohnanyi's value of 1.83 for a collisionally-evolved population in equilibrium. The study of collisional processes in the Main Belt (and elsewhere in the solar system) is beyond the scope of this thesis and is a complex topic that is worthy of another thesis.

9.12: Improving the NEOWISE Albedo Determinations

The NEOWISE albedos presented in Masiero *et al.* (2011), Grav *et al.* (2011), Mainzer *et al.* (2011) and Grav *et al.* (2012) are based on late-2010 or early-2011 *HG* determinations from the Minor Planet Center orbit files. As such, the (at the time) imperfectly-known *HG* values led to anomalous albedos for a large number of objects. This was a known problem with the NEOWISE albedo data set and has been commented on by a number of authors (e.g., Masiero *et al.*, 2011, and Warner, 2012a). The *HG* values

presented here are an improvement over what was available to the NEOWISE project, so a redetermination of the NEOWISE albedos is worthwhile.

Figure 9.13 shows the distribution of albedos, in bins 0.01 wide, determined by the NEOWISE team for the numbered minor planets. The number of data lines was 104 762, of which 1225 contained no albedo data. For 8479 minor planets, two albedos were reported. In such cases, both values are included in the figure. The count of objects with albedos greater than 0.55, which is approximately the upper bound of the albedo range for E-type minor planets (Warner *et al.* 2009), is 1894. The number of objects with albedos greater than 0.9 is 61, of which 24 are perfect reflectors (albedo = 1). The 1894 anomalous albedos represent 1.8% of the entire data set.

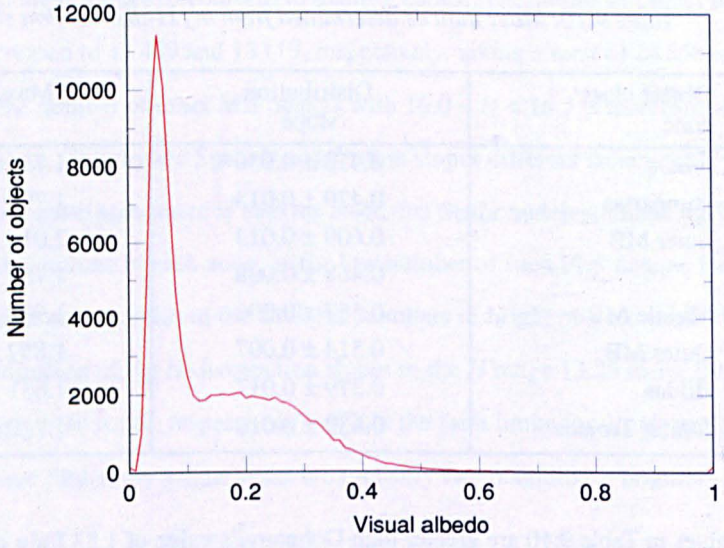

Figure 9.13: Distribution of NEOWISE-determined albedos

The new *HG* determinations summarized in Section 8.2 [p. 161] were combined with the NEOWISE data to derive new albedos and diameters using the approximate method of Harris and Harris (1997). While the authors describe their method of using new *HG* values to determine new albedos and diameters as "approximate", it does give results essentially identical to full rigorous rereductions. Their method is outlined below in Equations 9.5 to 9.8:

$$q = 0.290 + 0.684G \tag{9.5}$$

$$p_v' = \left[q' + \left(\frac{1}{p_v} - q \right) 10^{(H' - H)/2.5} \right]^{-1} \tag{9.6}$$

$$D' = \frac{1329}{\sqrt{p_v'}} 10^{-H'/5} \tag{9.7}$$

$$\sigma_p' \approx p_v' \sqrt{0.85\,\sigma_H'^2 + 4\left(\frac{\sigma_D'}{D}\right)^2} \tag{9.8}$$

where: q is the phase integral (Bowell *et al.*, 1989); H is the absolute magnitude; σ_H is the uncertainty in H; G is the slope parameter; p_v is the visual albedo; D is the diameter (in km); σ_p is the albedo uncertainty; σ_D is the uncertainty in the diameter; and primed quantities refer to the new values.

A small program, `NEWALBEDO.FOR`, was written to read in the NEOWISE data files and the new *HG* data set, implement Equations 9.5 through 9.8, and output a file of new albedos and diameters. An excerpt of the new values generated by `NEWALBEDO` is shown in Table 9.11 [p. 192]. The full table is included on the thesis website and the format of that data file is shown in Table 9.12 [p. 193]. The albedo distribution from the new determinations is shown in Figure 9.14, along with the NEOWISE distribution for comparison. The number of objects with albedos above 0.55 is now 37, under 0.04% of the entire data set.

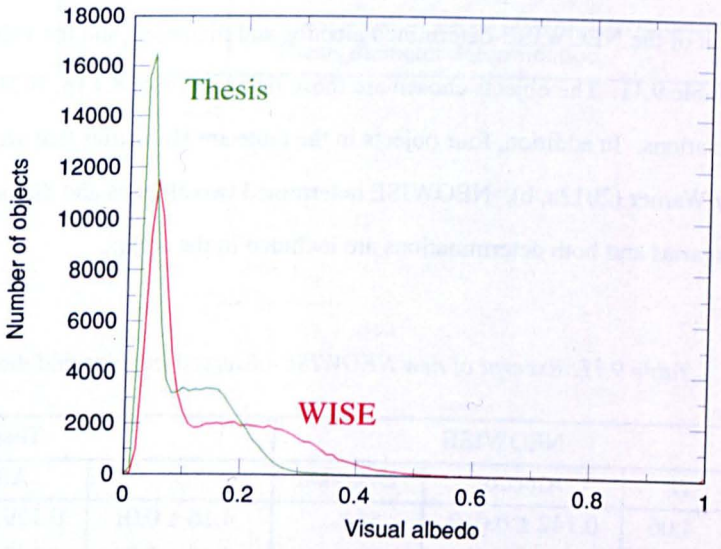

Figure 9.14: Distribution of thesis-determined albedos (with NEOWISE determinations for comparison)

The peak in the thesis albedo distribution around $p_v = 0.05$ is sharper and taller, and centred about 0.01 (1%) closer to zero, than that in the NEOWISE distribution. The broad plateau between $0.1 < p_v < 0.3$ visible in the NEOWISE distribution is not obvious in the thesis distribution, where a secondary peak may be visible around $p_v = 0.16$. The tail of the NEOWISE distribution is visible to $p_v > 0.5$, but only to

$p_v \sim 0.32$ in the thesis distribution. A close-up view of the tails of both distributions is shown in Figure 9.15. The large number of anomalously-high albedos in the NEOWISE determinations is obvious.

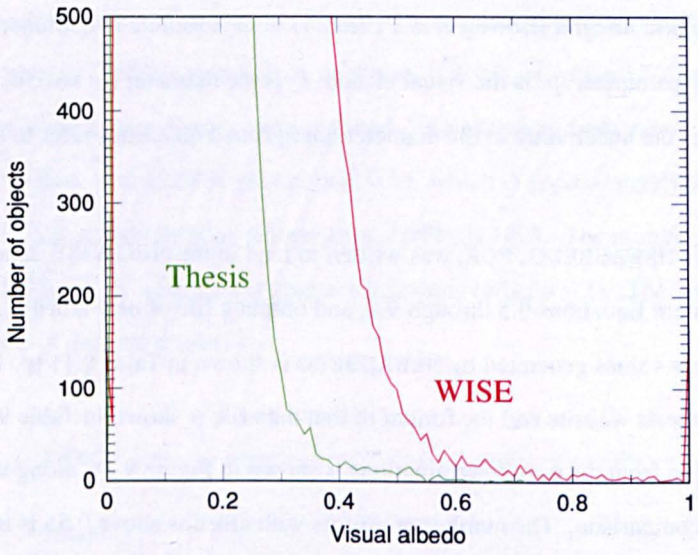

Figure 9.15: Detail view of thesis vs. NEOWISE high-albedo objects

A small selection of the NEOWISE-determined albedos and diameters and the values found in this work is included in Table 9.11. The objects chosen are those listed in Table 8.1 [p. 162], that have NEOWISE albedo determinations. In addition, four objects in the table are Hungarias that are included in recent publications by Warner (2012a, b). NEOWISE determined two albedos and diameters for (2) Pallas and two of the Hungarias and both determinations are included in the table.

Table 9.11: Excerpt of new NEOWISE-observed albedos and diameters

Object	NEOWISE			Thesis		
	H	Albedo	Diam/km	*H*	Albedo	Diam/km
(2)	4.06	0.142 ± 0.019	544	4.16 ± 0.01	0.129 ± 0.020	543
(2)	4.06	0.142 ± 0.046	544	4.16 ± 0.01	0.130 ± 0.029	543
(878)	14.6	0.399 ± 0.218	2.53	14.82 ± 0.03	0.347 ± 0.105	2.45
(2298)	12.9	0.317 ± 0.029	6.21	13.25 ± 0.03	0.235 ± 0.013	6.15
(2975)	12.7	0.404 ± 0.044	6.03	13.45 ± 0.03	0.217 ± 0.008	5.82
(4898)	13.9	0.994 ± 0.125	2.18	14.64 ± 0.05	0.545 ± 0.108	2.12
(4898)	13.9	0.548 ± 0.246	2.98	14.64 ± 0.05	0.289 ± 0.046	2.91
(5427)	13.4	0.630 ± 0.025	3.50	14.19 ± 0.05	0.324 ± 0.026	3.39
(5427)	13.4	0.777 ± 0.141	3.16	14.19 ± 0.05	0.405 ± 0.024	3.04
(12984)	13.7	0.249 ± 0.135	4.85	14.52 ± 0.03	0.124 ± 0.056	4.69

(15834)	13.1	0.161 ± 0.024	7.96	13.74 ± 0.08	0.091 ± 0.009	7.87
(26383)	14.2	1.000 ± 0.172	1.78	15.45 ± 0.06	0.409 ± 0.122	1.69
(45898)	14.0	0.645 ± 0.244	2.62	14.72 ± 0.06	0.350 ± 0.143	2.56

The format of the albedos and diameters data file available on the thesis website is documented in Table 9.12.

Table 9.12: Format of albedos and diameters data file

Columns	Format	Use
1– 5	A5	Minor planet number in packed form (see Appendix 1.4.2)
8–12	F5.2	*H* used by NEOWISE
14–18	F5.2	*G* used by NEOWISE
21–25	F5.3	Albedo determined by NEOWISE
28–32	F5.3	Uncertainty in NEOWISE albedo determination
35–40	F6.2	Diameter determined by NEOWISE
43–48	F6.2	Uncertainty in NEOWISE diameter determination
51–55	F5.2	Thesis value of *H*
58–61	F4.2	Uncertainty in thesis *H* determination
63–67	F5.2	Thesis value of *G*
70–74	F5.3	Thesis albedo determination
77–81	F5.3	Uncertainty in thesis albedo determination
84–89	F6.2	Thesis diameter determination

10: Conclusions

10.1: Introduction

In this chapter I summarize the work undertaken in this thesis and suggest avenues for future related work on this topic.

10.2: Results Summary

The results can be summarized as follows:

- I have derived approximate *U–B*, *B–V*, *V–R* and *R–I* colours for 104 415 minor planets.
- I have determined expressions for relating the Pan-STARRS bands to *V*.
- I have applied catalogue-specific and observer-specific corrections to 70 299 951 astrophotometric observations.
- I have made new *H* determinations for 322 607 numbered minor planets.
- I have made new *G* determinations for 64 348 numbered minor planets.
- For 258 259 numbered minor planets where *G* was not solved for in the adopted solution, I have adopted better *G* values than the old default value of 0.15.
- I have redetermined 104 760 albedos for 96 281 numbered minor planets, using my new *HG* determinations in combination with published NEOWISE data.
- I have modified the internal procedures of the Minor Planet Center to use the methods outlined in this thesis for all future determinations of magnitude parameters. This has been done in a modular fashion, allowing any part of the procedure to be easily updated if new data sources are found or if new processing methods are developed.
- The first observations of mean magnitudes derived from lightcurves that have been placed on standard systems have been published in the *Minor Planet Circulars* (Baker *et al.*, 2012). It is hoped that more lightcurve observers will see the *Circulars* as a route for publishing such observations in the future.

In addition, a number of issues with external data sources or software used in the preparation of this thesis have been identified. Fixes for each of these problems have been implemented, thus proving to be of use to the general astronomical community.

- I have identified the comparison stars and provided accurate J2000.0 coordinates and modern magnitude determinations for eight photometric papers. I anticipate that this information will be useful for the expansion of the ALCDEF to historical data.
- I have identified a number of issues with the `scat` software, principally its failing to extract objects from a source catalogue when the search radius is small, but finding objects (within the original search area) when the search radius is large.
- I have found a number of publications in ADS that should have full scans available, but that are inaccessible: the PDF is either not available or is corrupt.
- I have fixed the erroneous dates of publication stored in ADS for 34 445 papers published in volumes 1–256 of the *Astronomisches Nachrichten*. In 7560 cases, the fixing of the date of publication required a change in the ADS bibcode.
- I have added ADS references for a number of *Minor Planet Circulars* published between 1947 and 1990, to ensure that all *MPC* references included in this thesis have ADS entries. This is part of a longer-term project to include the entire *MPC* run in ADS.
- I have identified a problem with spurious duplicates in the photometry database of the SDSS DR7.

10.3: Future Work

A number of obvious avenues for future work present themselves.

10.3.1: Extension to Newly-Numbered and Multi-Opposition Objects

A first priority is to extend this work to cover the minor planets that were numbered after the 2012 March 8 batch of *Minor Planet Circulars*. A secondary priority is to extend it to the multi-opposition unnumbered minor planets. The opportunity will also be taken to tighten up the *HG* solution selection algorithm, which in the current iteration of the WORKOUTH code ignores the s^2 and magnitude residual r.m.s. values when choosing which solution to adopt.

10.3.2: More Real Photometry!

I do not pretend that my extraction of minor-planet photometric observations from the astronomical literature is complete. It seems that every paper I found that contained photometric observations referenced several other papers that also contained photometry. It was not always clear from the title of a paper that it would contain any useful data. A continuation of my extraction of data from the old literature, as well as keeping an eye on the new literature, would be a sensible move.

10.3.3: More Colour Data and Taxonomic Classifications

Likewise, it is highly probable that I have missed numerous papers containing colour data and/or taxonomic classifications. It will be worthwhile to do further literature searches to collect these data to improve the colour corrections that are made in future runs.

10.3.4: More Mean Lightcurve Photometry

Lightcurves that are referred to standard systems are a rich potential source of good-quality photometry. To date, this source has not produced a great number of useful observations. This will change in the future, but more encouragement of observers will be necessary. Complaints about the quality of the absolute magnitude values have been quite common for many years. Some of the most vociferous complaints have come from members of the photometric community. Yet those same observers seem reluctant to publish mean magnitudes, instead just reporting H determinations from their own observations. I note with pleasure that there a number of papers giving mean lightcurve magnitudes in the 2012 July–September issue of *The Minor Planet Bulletin*.

10.3.5: Making Use of the AAVSO Photometric All-Sky Survey

The American Association of Variable Star Observers (AAVSO) announced (Henden, 2009) the AAVSO Photometric All-Sky Survey (APASS), an ambitious four-year project to derive accurate five-colour photometry for all objects in the magnitude range 10 to 17. The five colour bands chosen are Johnson B and V, and Sloan g', r' and i'. Observations of the northern sky from the Dark Ridge Observatory using a pair of 0.20-m f/3.6 astrographic refractors in New Mexico began in October 2009. When the northern surveying was completed, the telescopes were moved to Chile to

complete the survey. A preliminary data release (DR0) of B and V magnitudes of ~ 450 000 stars covering ~800 sq. deg. was made in February 2010. In June 2012, the AAVSO announced data release 6 (DR6), the first version with two-visit "all-sky" (~95%) coverage. The final release of data, incorporating at least four visits per object, is expected in 2014.

The availability of the full-sky APASS will allow future observations to include high-quality astrophotometry, as well as allowing rereduction of earlier astrophotometry across the whole sky. Some work will be necessary to convert the g', r' and i' band magnitudes into R_c and I_c magnitudes, but I do not anticipate this to be a major issue. The new version of the ASTCAT that will be prepared from the APASS data will be known as the ASTCAT-A. I have already obtained the complete APASS DR6 data set from the AAVSO. I will perform tests in the coming months to see if DR6 is good enough to serve as the basis for the ASTCAT-A or whether it will be necessary to await the final 2014 release. If I do find DR6 is found to be adequate for my needs, replacement of the APASS DR6 data by any later updates will be trivial.

10.3.6: Incorporating Photometric Data From Pan-STARRS

In addition to observing minor planet and comets, the Pan-STARRS 1 telescope is building a stellar catalogue of the sky visible from Hawaii. Use of Pan-STARRS stellar data will enable me to extend the ASTCAT-A, at least in the stellar regions covered by Pan-STARRS, from a limiting magnitude of ~17 to fainter than 20.

10.3.7: Use of Minor Planet Models for Variable H Values

For irregularly-shaped minor planets, the use of a fixed H value may be problematic. The number of minor planets with known shapes, modelled via lightcurve inversion using the methods of Kaasalainen and Torppa (2001) and Kaasalainen *et al.* (2001), is increasing rapidly. Ideally, it would be useful to use the shape determinations of minor planets to adjust their H magnitudes depending on the orientation of the pole.

10.3.8: Three-Parameter Magnitude Systems

The three-parameter magnitude system proposed by Muinonen *et al.* (2010) was published too late for consideration in this thesis. An obvious next avenue of investigation is to apply the system to the rereduced astrophotometry derived in this work. If the fits for a wide selection of different types of object are better than the current *HG* system, it may be desirable to adopt the HG_1G_2 system as a new standard. Unfortunately, that is not a decision that can be made by me or even by the Minor Planet Center, as it is the International Astronomical Union, through its Division III and Commission 20, that dictates the standards (principally reference systems, time-scales and magnitude systems) that the Minor Planet Center use.

10.4: Applications of Improved Absolute Magnitude Parameters

The database of absolute magnitudes and slope parameters derived during the course of this research will have a number of uses in the astronomical community. Brief discussions of a number of these uses are given below.

10.4.1: Improved Predictions for Observers

The current *HG* values in use in the Minor Planet Center datasets have been shown to be imperfect, affected by large systematic errors in the astrophotometric observations used to derive those parameters. I freely admit that my primary reason for undertaking this thesis research was selfish: to improve the absolute magnitude data distributed by the Minor Planet Center in its files of orbital elements, thus allowing us to help astrometric and photometric observers to better plan their observing runs by providing more accurate predicted magnitudes at those times. The predicted magnitude is a major consideration when deciding whether to attempt the recovery of an object or whether to select an object for lightcurve or spectroscopic studies, particularly for those faint objects that are near an observer's limiting magnitude.

Improved *H* values equate to better predictions through simple application of Equation 2.1 [p. 13]. A simple extraction of examples of objects with large differences between the MPC and thesis values of *H* is complicated, since the MPC *H* values present in the MySQL `old_hgs` table (see Table 8.3 [p. 166]) were the values in use as of 2012 June 8. Since that date 274 393 of the 360 190

numbered minor planets have had their orbits recomputed at least once, with new H values generated (using the existing MPC procedure) when each new orbit is published. Using the 2012 June 8 values, there are 198 examples where the MPC H value requires correction by more than one magnitude (see Figure 9.4 [p. 172]). An example is the Hungaria (31849) 2000 EZ_{21} which has $H_{MPC} = 15.6$; $H_{thesis} = 16.62 \pm 0.05$.

This ability to make better determinations of when to make observations is particularly important for investigations of Near-Earth Objects, which are often observed at phase angles greater than 50°. For example, the phase angle for 2012 DA_{14} five days before its 2013 Feb. 15 encounter with Earth (miss distance from the geocentre = 0.00027 AU) peaked at 117°. The use of the current default $G = 0.15$ will lead to large errors in the predicted V magnitude for an object at large phase angles if its slope parameter is significantly different from the default assumed value. Figure 10.1 shows the effect of the phase function Φ for various values of G over the phase angle range 0°–150°, and is an extension in phase-angle space of Figure 2.1 [p. 14].

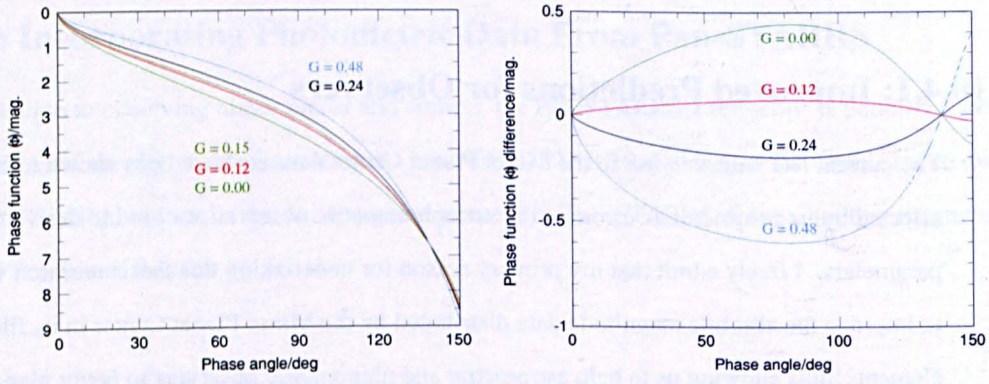

Figure 10.1: Effect of the phase function, Φ, for various values of the slope parameter, G, extended to $\beta = 150°$, and the difference (correct minus assumed) in the phase function when an incorrect G value is assumed

It can be seen from Figure 10.1 that the error in the value of the phase function caused by the assumption of $G = 0.15$ for an object with a substantially different slope parameter can be more than 0.5 mag. in the phase-angle range 50°–120°. Even around $\beta = 30°$, which is a typical maximum value for a MBA, the error can be 0.4 mag. Better selection of assumed slope parameters, or adoption of derived slope parameters, will assist observers in determining whether or not to observe faint objects.

10.4.2: Improved Albedos and Diameters

When combined with infrared observations, the improved *HG* values lead to improved values for albedos and diameters. Derivation of these physical parameters depends on the thermal model used (see brief discussion in Appendix 8 [p. 249]). Independent constraints on diameters for specific objects can come from visitations from spacecraft or from multi-station observations of stellar occultations. It may be possible to use such independent constraints, along with improved *HG* values, to fine tune the thermal models currently in use, or develop even more sophisticated models.

The space weathering of planetary surfaces by impacts and solar wind interaction can alter the albedo of certain taxonomic classes (Clark *et al.*, 2002): the albedo of S types can be lowered by ~50%; Q types, lowered by ~30%; C types show little or no change in albedo. Having good albedos for a wide range of objects allows broad investigation of the effects of space weathering.

The Yarkovsky effect (Bottke *et al.*, 2002) is a non-gravitational force caused by the delayed infrared re-emission of solar radiation. The delay before re-emission is a consequence of the thermal inertia of the body, and causes the recoil force to not be aligned in the sun-radial direction. The non-radial component of the force affects the semimajor axis of an object's orbit, increasing it ($da/dt > 0$) if the object's rotation is direct and decreasing it ($da/dt < 0$) if the rotation is retrograde. This Yarkovsky force is tiny, but acting over millions of years, it is capable of delivering meteoroids from the Main Belt to Earth and allowing km-sized minor planets to escape from the Main Belt via semimajor axis drift into mean-motion or secular resonances (see Appendix 3.5 [p. 220] and 3.6 [p. 221]). The Yarkovsky force also disperses members of minor planet families in a size-dependent fashion. Two of the parameters involved in determination of the Yarkovsky force on a specific object are the object's albedo and diameter. The albedo is used in the determination of the surface temperature across an object's surface, which is a boundary condition for the object's internal temperature, and which determines the thermal-emission distribution. Clear detection of the Yarkovsky effect in the motion of individual minor planets has been demonstrated in only a few cases to date—e.g., (6489) Golevka by Chesley *et al.*, 2003)—and all such detections to date have required the inclusion of radar observations. Since the size of the Yarkovsky effect is inversely related to the size of the object, mapping of the effect for families is accomplished using simple *H* versus semimajor axis plots. Nugent *et al.* (2012) have used NEOWISE measurements of visual

albedo and diameter to make predictions of which objects should should show the greatest Yarkovsky effect. Objects such as 2010 JG_{87} and 2006 HY_1 are predicted to have Yarkovsky-induced $|da/dt|$ rates almost two magnitudes greater than that found for (6489) Golevka. A number of the objects identified by Nugent *et al.* are poorly observed (at only one opposition) or do not have radar observations.

The YORP (Yarkovsky-O'Keefe-Radzievskii-Paddack) effect (Rubincam, 2000) is related to the Yarkovsky effect and induces torques that alter the rotation rate and the spin orientation of objects. The YORP effect can significantly alter rotation periods and obliquities, and has been invoked as an explanation for the observed populations of small, rapidly-rotating monolithic minor planets (with rotation periods under ~ 2.2 hours) and slow rotators (with rotation periods up to many hundreds of hours). The first detection of a YORP-induced rotational-period change was by Lowry *et al.* (2007), who observed a fractional change of -1.7×10^{-6} year^{-1} in the 730-second rotation period of (54509) YORP and demonstrated that only a small fraction of this change was due to the period changes caused by the object's annual close encounters with Earth. Lowry *et al.* predict that the YORP effect will cause the rotation rate of (54509) YORP to double in 550 000 years. A uniform (in albedo and surface temperature) triaxial ellipsoid will experience no YORP effect. If YORP effects are present, the evolution of the semimajor axis drift will be affected as the Yarkovsky effect is also dependent on the obliquity. The YORP effect explains the spin states of members of the Koronis family (Slivan *et al.*, 2003). The Koronis family was formed by the disruption of a large parent body about 2 billion years ago. The spin states of the resulting fragments would be expected to be random, but observations, confirming theoretical considerations, show that the spin states of the larger family members fall into two distinct groups.

The density of an object can give clues as to the internal composition. Density depends on the mass and the volume (via the diameter). Reliable masses are currently available for very few objects. The earliest mass determinations were made by observing the perturbation a large object caused in the motion of a small object (e.g., Williams, 1992). Other techniques include measurement of unmodelled perturbations in the orbit of Mars (Standish and Hellings, 1989), perturbations of passing or orbiting spacecraft (e.g., Yeomans *et al.*, 2000), and observations of natural satellites (e.g., Fang *et al.*, 2012). The measured densities for minor planets (Hilton, 2002) range from 1.3 g cm^{-3} to 3.5 g cm^{-3}, with typical uncertainties of 10%–40%. These values are lower than the

densities of the rocky (albeit compressed) terrestrial planets: Mercury, 5.4 g cm^{-3}; Venus, 5.2 g cm^{-3}; Earth, 5.5 g cm^{-3}; and Mars, 3.9 g cm^{-3}. The minor planet densities are also lower than the densities found from meteorites (Britt and Consolmagno, 2004): ordinary chondrites, 3.0–3.6 g cm^{-3}; enstatite chondrites, 3.4–3.7 g cm^{-3}; carbonaceous chondrites, 1.9–3.5 g cm^{-3}; achondrites, 2.8–3.4 g cm^{-3}; stony-irons, 4.2–4.9 g cm^{-3}; and irons, 7–8 g cm^{-3}. This suggests that there might be ices or voids inside many objects. Voids (macroporosity) would be the result of an object being a rubble pile, rather than a single contiguous body. Meteorites also show evidence for microporosity. The forthcoming observations from the GAIA satellite mission should determine masses for ~ 100 minor planets (Dell'Oro and Cellino, 2008), and the discovery of further minor-planet satellites will produce more mass determination. These new sources of masses lead to new determinations of densities, allowing estimation of the macroporosity of the bodies concerned.

Physical characterization of potential/intended space-mission targets is an important stage in the planning of those missions. Extensive ground-based observing programs were initiated prior to the 1991 encounter of Galileo with (951) Gaspra (Veverka *et al.*, 1994), the 1997 encounter of NEAR Shoemaker with (253) Mathilde (Veverka *et al.*, 1999) and the 2010 encounter of Rosetta with (21) Lutetia (Schulz *et al.*, 2012), as well as for the targets of the orbiting spacecraft: NEAR Shoemaker at (433) Eros (Miller *et al.*, 1995) and Hayabusa at (25143) Itokawa (Ishiguro *et al.*, 2004). A good size estimate is required for planning when to start taking images for science purposes, to ensure that the image resolution is sufficient for the intended research. A rotation period and rotation axis determination allows an estimate of how much of the surface will be visible during the encounter. A shape model, determined from inversion of lightcurves (Kaasalainen and Torppa, 2001; Kaasalainen *et al.*, 2001), allows the determination of the volume of the body. Measurement of the deflection of a spacecraft during an encounter allows the mass to be determined.

10.4.3: Improved Size-Frequency Distributions

What is the current size-frequency (SFD) of the Main Belt? Of Near-Earth Objects? Of other populations of minor planets? A good knowledge of the diameters of the observed population leads to an observed SFD, which can be debiased to derive the true population SFD. Considering just the Near-Earth Objects, an improved population SFD will allow better estimates to be made of the current SFD of impacts with Earth and Moon. On Earth, comparison of the estimated impact rate

based on the SFD with the observed impact rate is possible across a broad size range from sub-mm-sized dust grains (a typical size for the average naked-eye meteor) to objects with diameters ~ 50 metres (e.g. the Tunguska impactor of 1908). On Jupiter, such small impacts are not visible from Earth and observed impacts are restricted to objects larger than about 100 metres: e.g., the numerous fragments of D/1993 F2 (Shoemaker-Levy) that hit the planet in 1994 (Marsden, 1993); and the unknown object, perhaps several hundred metres in diameter, that hit in 2009 (Orton *et al.*, 2009). Current estimates of impact rates can be compared to historical rates via measurement of the crater SFD on the target bodies. Within the Main Belt, improved SFDs will help constrain the frequency of collisions between minor planets, and quantify the relative importance of collisional- and YORP-related modification of rotation rates and axes, and allow investigation of the effect of the size-dependent Yarkovsky effect on the distribution of members of minor-planet families.

In the absence of albedo data for more than a few percent of the numbered population of minor planets, the absolute magnitude has to serve as a proxy for the diameter for the majority of objects. While unwise for specific objects, this approach is valid when considering large populations. As demonstrated in Section 9.11 [p. 184], the observed population of MBAs is essentially complete to the absolute magnitude limits and sizes (assumed, based on average albedos) listed in Table 9.7 [p. 185]. The improved H values presented here comprise the largest set of systematically-corrected absolute magnitudes available.

I have removed a bias in the NEOWISE-determined albedos and diameter estimates using my improved *HG* values. These new values can also be used to correct the albedo and diameter determinations for the objects observed in other infra-red surveys, such as IRAS (Tedesco *et al.*, 1992, 2002), which observed 2470 minor planets between 1983 and 1984, and Akari (Usui *et al.*, 2011), which observed 5120 minor planets between 2006 and 2007. Additional infrared data is provided by the Spitzer catalogue of 35 000 minor-planet observations (Trilling *et al.*, 2007) and the Warm Spitzer ExploreNEOs program (Trilling *et al.*, 2010). ExploreNEOs observed some 600 Near-Earth Objects (NEOs) with the intention of probing differences in the physical properties (sizes, size distribution and albedos) and evolution of km- and sub-km-sized NEOs. A number of erroneous albedos are present in Trilling *et al.* (2010): e.g., (4953) 1990 MU is assigned the unrealistic albedo $p_v = 0.79$, based on $H = 14.1$; using the thesis $H = 15.19$ leads to the more reasonable $p_v = 0.35$. Thomas *et al.* (2011) note that mean albedos determined by ExploreNEOs for

various taxonomic groups amongst the NEO population are higher than the corresponding means in the Main Belt, but note that this conclusion may be dependent to some extent on the poorly-known *HG* values.

10.4.4: Use of Phase Parameters

The opposition effect is the result of the coherent backscattering mechanism (Muinonen, 1994), whereby incident light is multiply scattered by regolith particles that are separated by distances that are small (one to hundreds) integer multiples of the wavelength of the incident light. These multiply-scattered rays interfere with each other constructively when travelling through the reflecting medium in identical, but opposite, paths. At small phase angles this results in a brightening of the reflected light.

Recent work by Muinonen *et al.* (2010) on a three-parameter (HG_1G_2) magnitude system is intriguing in that the authors claim that the G_{12} parameter, used in place of G_1 and G_2 parameters when the available photometry is noisy (such as the astrophotometry used here) or limited, is correlated rather closely to the taxonomic classification, as G_{12} (like the *HG*-system *G* parameter) is dependent on albedo, composition, porosity, roughness and grain size distribution. This view is strengthened by Oszkiewicz *et al.* (2011, 2012), who investigated the HG_1G_2 system using almost 47 million *V*-band magnitude estimates (taken directly from or derived from the MPC observational database) that were calibrated using the magnitudes on the SDSS observations of minor planets. This is a less sophisticated correction method for the systematic errors present in the astrophotometry than that used in my investigation. The authors present tables and plots of the relationship between the G_1/G_2 parameters and the mean albedos determined for a number of minor-planet families (the plot is reproduced here in a modified form as Figure 10.2 [p. 206]).

Examination of the HG_1G_2 system using the corrected magnitudes presented in this work should be a priority, given that the IAU is considering replacing the two-parameter *HG* system with the three-parameter HG_1G_2 system. Do the claims for the G_{12} correlation survive (or even strengthened) when my values for the corrected magnitudes are used?

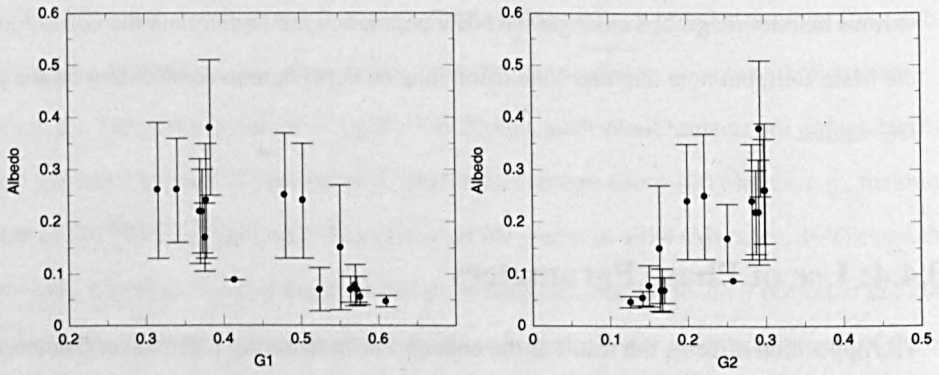

Figure 10.2: Relationship of Oszkiewicz et al. (2011) G_1 and G_2 parameters with the mean albedo of various minor-planet families

10.4.5: Identification of Unusual Photometric Behaviour

Changes in the photometric behaviour of minor planets, due either to long-term or cyclic processes such as outgassing from icy bodies or short-term processes such as impacts, may have been masked by the former poor knowledge of *HG* values. It remains to be seen whether the scatter left in the catalogue-corrected astrophotometry will permit the identification of high-amplitude lightcurve objects. Examination of time-ordered magnitude residuals for individual objects will allow the determination of whether the residuals are due to large light-curve amplitudes (no time-dependence on the mean of the magnitude residuals) or due to aspect effects, such as those seen in (1605) Milankovitch (see Section 9.10.2 [p. 181]). In the latter case, the mean of the magnitude residuals over time will vary from zero, in a manner similar to that shown in Figure 9.10 [p. 182].

The discovery (Larson *et al.*, 2010) of a long-lived dust cloud around the main-belt minor planet (596) Scheila, interpreted as being caused by the impact of an unknown minor planet less than 100 metres in diameter (Bodewits *et al.*, 2011), implies that smaller impacts occur on a much more frequent basis. These smaller impacts may not produce visible clouds, but may cause enhancement of the brightness of the impacted body. Detection of such events will be difficult, but the improved *HG* values will help.

The onset of cometary activity in outer Main Belt icy bodies or Centaurs/Scattered-Disk Objects is characterized by an anomalous brightening of an object (e.g., Tholen *et al.*, 1988). Improved *HG* values, in conjunction with improved knowledge of the rotational lightcurves, will make it easier to detect such onset events. Those outer Main Belt bodies that show cometary features are known as

the Main Belt Comets (MBCs). To date seven (or possibly) eight MBCs are known: (7968) Elst-Pizarro = 133P/Elst-Pizarro (Elst, 1996); 238P/Read (Read *et al.*, 2005); (118401) LINEAR = 176P/LINEAR (Hsieh *et al.*, 2006); 259P/Garradd (Garradd *et al.*, 2008); P/2010 R2 (La Sagra) (Nomen *et al.*, 2010); (300163) 2006 VW139 (Hsieh *et al.*, 2011); P/2012 F5 (Gibbs) (Gibbs *et al.*, 2012); and P/2012 T1 (PANSTARRS) (Wainscoat *et al.*, 2012). The identification of P/2012 F5 as a MBC is uncertain, as Stevenson *et al.* (2012) interpret the dust tail as being the result of an impact event. MBCs appear to be in stable, low-eccentricity orbits in the outer Main Belt. The locations in *a-e* space of the eight MBCs in relation to the Main Belt and short-period comets are shown in Figure 10.3.

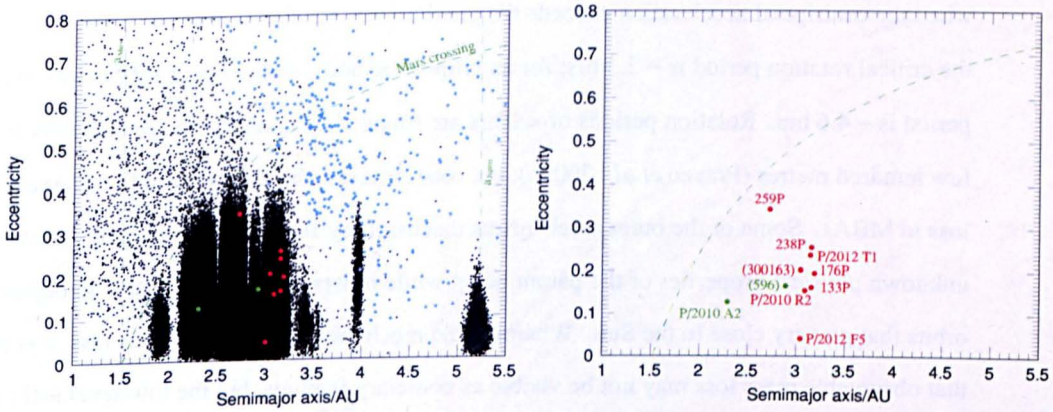

Figure 10.3: The location of the Main-Belt Comets (MBCs), generated from Minor Planet Center orbit files. Individual MBCs are shown as red dots and are identified on the right-hand diagram. Disrupted minor planets are shown as green dots and are also identified on the right-hand diagram.

One possible mechanism for the cometary activity in MBCs is impacts with other bodies that break through the surface of a MBC, revealing ices in the interior, which then sublimate, ejecting gas and dust from the surface. Prialnik and Rosenberg (2009) showed that crystalline ices could survive in the interior of 133P, at surface depths below ~ 50 metres, for the age of the solar system, and that modelling of post-impact effects on exposed ices results in activity similar to that observed. Cometary activity may be sporadic, as in the case of 133P, which was active at discovery in 1996, but asteroidal in the prediscovery images. Or it may be continuous (although some of the MBCs do not yet have long observational histories of cometary activity to prove this belief). The ability to see cometary activity may be size dependent, as the escape velocity may be too high to allow ejected dust particles to escape. The time-scale over which a single impact causes cometary activity and the level of that cometary activity are unclear at present, as they are dependent on quantities that are

unknown, time-variable and/or poorly known: How much ice is present? How are the ices distributed within the body? What is the rate of loss of volatiles? What types of ices are present?

Mechanisms other than impact-induced sublimation are discussed by Jewitt (2012). It is unlikely that primordial surface ices could survive for the age of solar system for the MBCs in their present locations. There is the possibility that 259P/Read, located near to the 8:3 MMR resonance with Jupiter (see Appendix 3.5 [p. 220]) and affected also by the ν_6 secular resonance (see Appendix 3.6 [p. 221]), has migrated from elsewhere in the solar system within the last 20–30 million years. Of the other mechanisms discussed by Jewitt, the most plausible is rotational instability. Rotational instability is the ejection of dust particles due to the rapid rotation of the parent body and this occurs when the centripetal acceleration exceeds the gravitational acceleration of the body. For a sphere, the critical rotation period is ~ 2.3 hrs; for an ellipsoidal body with $a/b = 2$, the critical rotation period is ~ 4.6 hrs. Rotation periods of < 2 hrs are found only in objects with diameters less than a few hundred metres (Pravec *et al.*, 2002b), but rotational instability may lead to observable mass loss in MBAs. Some of the other mechanisms discussed by Jewitt are conjectural, dependent on unknown physical properties of the parent body, while others are only applicable to objects with orbits that go very close to the Sun. Whatever the mechanism that causes mass loss, it is the case that observable mass loss may not be visible as cometary features, but the low-level activity will enhance the observed magnitude. Improved H values may make detection of such events possible and allow some constraint of the underlying mechanisms.

10.5: Concluding Remarks

In a project of this kind, there is always a nagging suspicion that the results are spurious, as they may be derived from observations that have been corrected by some process that has no basis in reality. Confirmation of such results from independent sources is necessary in order for them to carry any weight. I believe that I have such confirmation, for the following reasons:

- I have shown that the existing MPC H determinations are generally too bright;
- I have shown that the differences between my new H determinations and the current MPC determinations are greatest around H ~ 14 and that the size of that maximum correction is +0.5 mag., agreeing with previous published studies; and

- I have demonstrated that, for one of the major professional surveys (LINEAR), the catalogue- and observer-specific corrected observations that I generated are consistent with new values determined via a completely independent rereduction.

Fortunately, for this particular project, this is ample confirmation that the corrections being applied are realistic and make me confident that the final results are both correct and a significant improvement over what was available previously.

Appendices

The appendices contain various items related to the thesis. A discussion of the designation systems used for minor planets is followed by a review of relevant historical journals, a brief discussion of useful astronomical terms connected to orbital mechanics, a listing of the references for the colours combined into the penultimate entry of Table 3.6 [p. 64], a listing of the references for the photometric observations mentioned in Section 5.4 [p. 104], and details on accessing complete data sets or information on specific objects or groups of objects through the thesis website. Also included are a number of sections that were moved from the main body of the text on the recommendation of the viva committee.

1: Minor Planet Designation Systems

The designation systems used for minor planets, both provisional and permanent, are described in this section. The bulk of the text is taken from various documentation webpages that I have written in the past for the Minor Planet Center's website.

1.1: Provisional Designations

The Minor Planet Center (MPC) assigns new provisional designations when it is in possession of at least two nights of observations of an object that cannot be identified immediately with some already designated object. New designations are also assigned when it is necessary to redesignate some already-published observations because the identification has been shown to be incorrect. One of the observations of the new object is defined as the discovery observation: this will normally be indicated by the observers; if omitted by the observers the MPC assumes that the chronologically earliest observation is the discovery observation.

The provisional designations are based on a scheme proposed by Bower (1924). The standard designation consists of the following parts, all of which are related to the date of discovery of the object: a four-digit number indicating the year; a space; a letter to show the half-month; another letter to show the order within the half-month; and an optional number to indicate the number of times the second letter has been repeated in that half-month period.

The half-month of discovery is indicated using the following scheme ('I' is omitted and 'Z' is unused), shown in Table A1.

Table A1: Provisional designations: Half-month letters

Letter	Period	Letter	Period
A	Jan. 1–15	N	July 1–15
B	Jan. 16–31	O	July 16–31
C	Feb. 1–15	P	Aug. 1–15
D	Feb. 16–29	Q	Aug. 16–31
E	Mar. 1–15	R	Sept. 1–15
F	Mar. 16–31	S	Sept. 16–30
G	Apr. 1–15	T	Oct. 1–15
H	Apr. 16-30	U	Oct. 16–31
J	May 1–15	V	Nov. 1–15
K	May 16–31	W	Nov. 16–30
L	June 1–15	X	Dec. 1–15
M	June 16–30	Y	Dec. 16–31

The order within the half-month is indicated as in Table A2 using letters (omitting 'I').

Table A2: Provisional designations: Half-month order letters

Letter	Order	Letter	Order	Letter	Order	Letter	Order
A	1	H	8	P	15	W	22
B	2	J	9	Q	16	X	23
C	3	K	10	R	17	Y	24
D	4	L	11	S	18	Z	25
E	5	M	12	T	19		
F	6	N	13	U	20		
G	7	O	14	V	21		

If there are more than 25 discoveries in any one half-month period, the second letter is recycled and a numeral '1' is added to the end of the designation. If more than 50 discoveries, the second-letter is again recycled, with a numeral '2' appended after the second letter. Discoveries 76–100 have numeral '3' added, numbers 101–125 numeral '4', etc. Where possible, these additional numbers should be indicated using subscript characters. As an example, the order of assignment of designations in the second half of June 2010 is as follows: 2010 MA, 2010 MB, ..., 2010 MY, 2010 MZ, 2010 MA_1, ..., 2010 MZ_1, 2010 MA_2, ..., 2010 MZ_9, 2010 MA_{10}, etc.

This designation scheme has been extended to newly-designated pre-1925 discoveries—such designations are indicated by the replacement of the initial digit of the year by the letter 'A'. Thus, A904 OA is the first object designated that was discovered in the second half of July 1904.

1.2: Survey Designations

Four special minor-planet surveys, undertaken between 1960 and 1977 by the van Houtens and Gehrels, have designations that consist of a four-digit number (identifying the order within the survey), a space and a survey identifier. The survey identifiers are as follows: Palomar-Leiden (1960), P-L; First Trojan Survey (1971), T-1; Second Trojan Survey (1973), T-2; and Third Trojan Survey (1977), T-3. Example designations are 2040 P-L, 3138 T-1, 1010 T-2 and 4101 T-3.

1.3: Permanent Designations

When a minor planet has been well observed at four or more oppositions, it is eligible to be numbered by the Minor Planet Center. Once numbered, a name may be proposed by the discoverer. For NEAs, numbering can occur after three (or, exceptionally, two) well-observed oppositions.

1.4: Packed Designations

The Minor Planet Center uses a packed form of the provisional and permanent designations on its observation and orbit records. The packed form has great advantages for the easy sorting of observations and orbits, as well as being more concise than the full form.

1.4.1: Packed Provisional Designations

Packed provisional designations are stored in seven characters. The non-survey designations are handled differently from the survey designations.

Non-Survey Designations

The first two digits of the year are packed into a single character in column 1: designations beginning A8 use 'I'; beginning A9 or 19 use 'J'; and beginning 20 use 'K'. Columns 2 and 3 contain the last two digits of the year. Column 4 contains the half-month letter and column 7

contains the second letter. The cycle count is coded in columns 5 and 6, using a letter in column 5 when the cycle count is larger than 99—upper-case characters are used for cycle counts 100 to 350 and lower-case characters for counts 360 to 610.

Examples: 2000 AA = K00A00A; 1995 XL_1 = J95X01L; 1995 FB_{13} = J95F13B; 2008 SJ_{103} = K08SA3J; 2008 TZ_{359} = K08TZ9Z; 2008 TA_{360} = K08Ta0A.

Survey Designations

Columns 1 to 3 contain a code indicating the survey and columns 4-7 contain the number of the object within the survey. The codes used are PLS for the 1960 Palomar-Leiden survey, T1S for the 1971 First Trojan Survey, T2S for the 1973 Second Trojan Survey and T3S for the 1977 Third Trojan Survey.

Examples: 2040 P-L = PLS2040; 3138 T-1 = T1S3138; 1010 T-2 = T2S1010; 4101 T-3 = T3S4101.

1.4.2: Packed Permanent Designations

For objects with numbers under 100000, the packed form is simply the five-digit zero-padded representation of the number. E.g., (1) = 00001, (3202) = 03202 and (43929) = 43929.

For objects with numbers above 99999, the packed form is a five-character string where the first character is `CHAR(55+NUM/10000)` and characters two through five are the four-digit zero-padded representation of `MOD(NUM,10000)`, where `NUM` is the number, `CHAR` is a standard Fortran intrinsic character function to convert the specified ASCII code into the corresponding character. E.g., (100000) = A0000, (123456) = C3456 and (217933) = L7933.

1.5: Old-Style Provisional Designations

In the first half of the 19th century, minor planets were referred to simply by name. The assignment of ordinal numbers, ostensibly in order of discovery, was introduced in the early 1850s. Initially, new numbers were assigned by the editors of the *Astronomisches Nachrichten* (*AN*) immediately upon receipt of the announcement of a new discovery from an observer.

In 1892 a system of provisional designations was introduced by the *AN* (Krueger, 1892). A definitive number was subsequently given to those objects for which reasonable orbital elements had been computed. The provisional designation scheme consisted initially of a year and a single letter: e.g., 1892 A, 1892 B, etc., omitting the letter 'I'. In 1893, the 25 available letters proved to be insufficient and a series of double-letter designations was introduced: e.g. 1893 AA, 1893 AB, etc., omitting the letter 'I'. The sequence of double letters was not restarted anew each year, so, e.g., 1894 AQ followed 1893 AP. In 1916, the letters reached ZZ and, rather than starting a series of triple-letter designations, the double-letter series was restarted with 1916 AA. In old publications, it is common to see 'J' as the omitted letter instead of 'I'—the sequence going 1892 H, 1892 I, 1892 K, etc. Modern usage would consider 1892 I to be the same as 1892 J.

In the double-letter scheme it was not generally possible to insert new discoveries into the sequence once designations had been assigned in a subsequent year. The scheme used to get round this problem was rather clumsy and used a designation consisting of the year and a lower-case letter in a manner similar to the old provisional-designation scheme for comets. For example, 1915 a (note that there is a space between the year and the letter in order to distinguish this designation from the old-style comet designation 1915a). In 1914 designations of the form "year plus Greek letter" were used in addition.

In addition, there were numerous other schemes used by individual observatories. A description of a number of historical-designation schemes that I wrote for the MPC website is available on-line[1].

2: Historical Journals

There are a number of journals that are important to this thesis that may not be familiar to many readers. These journals are described briefly below.

2.1: Astronomische Nachrichten

Founded in 1821 by H. Schumacher, the *Astronomische Nachrichten* (*AN*) was the first truly international astronomical journal, in the modern sense of the term. Astronomers would report their observations or theoretical musings via letter to Schumacher, who would publish the letters in the

1 http://www.minorplanetcenter.net/iau/info/TempDesDoc.html

AN in the language in which they were written. Most articles are in German, but there are many written in English, French, Italian and Spanish. The first issue appeared in 1823 and the journal is still in existence, being the oldest astronomical journal still being published. Schumacher edited the journal at Altona Observatory (then in Denmark, later in Prussia, today in Germany) until his death in 1850. Such was the prestige of the *AN* that B. A. Gould used it in 1850 as the model for the format and publication frequency of the *Astronomical Journal* (Gingerich, 1999). The *AN* is a rich source of early astrometric observations of minor planets and comets; most of the observations are not yet in machine-readable format for use by orbit computers. For the past twenty years, I have run the Astrometric Literature Extraction, a part-time project which aims to extract all the astrometric observations from the old literature and insert the observations into the observation archive of the Minor Planet Center. Where possible, micrometric measures are rereduced using modern positions for the comparison stars. Although tens of thousands of observations have been extracted and inserted into the archive, many tens of thousands of observations remain to be collected.

With regard to the *AN*, it is worth noting that ADS had incorrect dates of publication for the first 256 volumes of this publication. In most cases the date of publication (which in ADS is recorded as MM/YYYY) was given as 00/YYYY (i.e., no month given). The year of publication was the date of publication of the last issue in the volume. A handful of volumes had an apparently proper MM/YYYY date of publication, but the date was the same for all the issues in the volume. In these cases, the MM was the month of publication of the first issue, while the YYYY was the year of publication of the last issue! Since the *AN* is one of the primary sources for historical background for this thesis, I thought it important to correct these erroneous dates of publications. As a consequence of pre-thesis work on extracting astrometric positions of minor planets and comets from the *AN*, I had available a list of month and year dates of publication for 70 volumes of the *AN*. I approached ADS, offered them these data and proposed extracting the dates of publication for the remaining volumes. The proposal was accepted and some time was spent completing the extraction of publication dates for the other 186 volumes. ADS then supplied lists of bibliographic entries (including the bibcode) on a volume-by-volume basis. Each volume's entries had the date of publication added, then they were returned to ADS for ingestion into their system. Accurate dates of publication for 34 445 bibliographic entries were added. The ADS bibcodes include the year of publication: as a result of this work, 7560 out of 34 445 bibcodes required modification. As of mid-August 2009, the ADS returns the proper MM/YYYY dates of publication for the first 256 volumes

of the *AN*. It was not possible to correct the publication dates for the subsequent volumes, which were published during World War II, as these issues seem to be lacking publication dates. It would be difficult to make educated guesses of publication dates, especially as issue frequency became more sporadic as the War progressed, so this effort was not undertaken.

2.2: Berliner Astronomisches Jahrbuch

The *Berliner Astronomisches Jahrbuch* (*BAJ*) was the annual German astronomical ephemeris almanac, containing ephemerides and orbital elements for solar system objects and positional data on fundamental stars. Publication began in 1774 with the 1776 edition and continued until the edition for 1959, after which the *BAJ*'s functions were taken over by the *Astronomical Ephemeris* and *Apparent Places of Fundamental Stars* as part of the IAU's efforts to rationalize the publication of annual ephemeris data.

2.3: Kleine Planeten

The *Kleine Planeten* (*KP*) was an annual supplement to the *BAJ* that contained ephemerides and orbital elements for the minor planets. First appearing in the 1912 *BAJ* volume (published in 1910), the *KP* first appeared as a stand-alone volume for 1917 (published 1916). Publication continued until the 1945 edition (published 1944), although an edition for 1946 was prepared and subsequently published by the Nautical Almanac Office of the U.S. Naval Observatory.

2.4: Minor Planet Circulars

The *Minor Planet Circulars* (*MPC*s) began publication in 1947 and were the direct successor to the *Rechen-Institut Circulars* that had been published by the Astronomisches Rechen-Institut, located in Dahlem, a suburb of Berlin, from 1926 to 1945. The *MPCs* are published in batches, prepared around the time of each Full Moon, and contain the published astrometric observations of minor planets, comets and outer irregular satellites of the giant planets, along with orbits, ephemerides and new namings. The publication schedule from 1947 to 1978 was rather erratic (a number of the earliest *MPC*s are undated), with intervals of six months between successive batches being common. When the MPC moved to Cambridge in 1978, the publication schedule was changed to monthly

(initially, on the first day of the month, changed to the date of Full Moon in October 1981) and, with a few exceptions when staff members were absent, this schedule has been maintained to the present day. The vast increase in printed material prompted the removal of the printed astrometric observations to a new journal, the *Minor Planet Observation Supplement* (*MPS*), in 1997, with the observations being summarized in the *MPC*s. Continuing increases in the amount of printed material led to the removal of most of the orbital data to another new journal, the *Minor Planet Orbit Supplement* (*MPO*), in 2000, with the *MPC*s containing a summary of the new numberings and new identifications. Both the *MPS* and *MPO* were published only as PDFs, available for download from the subscription area of the MPC website, With the current free availability of MPC publications and services, the *MPC*s are now published only in electronic form.

2.5: Efemeridy Malykh Planet

Following the IAU's reassignment of responsibility for minor-planet work following World War II, the Institute for Theoretical Astronomy (ITA, Leningrad/St. Petersburg) was tasked with handling the orbits of the numbered minor planets. The ITA publishes the *Efemeridy Malykh Planet* (*Ephemerides of Minor Planets*, *EMP*), the direct successor to the *Kleine Planeten*. The first edition of the *EMP* was for 1947 and it is still being published. Each volume contains orbital elements and opposition ephemerides for the numbered minor planets. In recent years, the number of numbered minor planets has grown so large that it is not possible to include all the numbered minor planets in the printed volume. Printed publication is now restricted to objects with $H < 13.5$, with data for fainter objects being included in an electronic version.

3: Relevant Astronomical Terms

This section gives brief descriptions of some astronomical terms, mostly related to orbits, that are used in this thesis.

3.1: Definition of Planet/Dwarf Planet/Small Solar System Body

Resolution B5 adopted at the 2006 IAU General Assembly[2] defines the terms planet, dwarf planet and small solar system body.

2 http://www.iau.org/static/resolutions/Resolution_GA26-5-6.pdf

A planet is defined as: A celestial body that (a) is in orbit around the Sun, (b) has sufficient mass for its self-gravity to overcome rigid body forces so that it assumes a hydrostatic equilibrium (nearly round) shape, and (c) has cleared the neighbourhood around its orbit.

A dwarf planet is defined as: A celestial body that (a) is in orbit around the Sun, (b) has sufficient mass for its self-gravity to overcome rigid body forces so that it assumes a hydrostatic equilibrium (nearly round) shape, (c) has not cleared the neighbourhood around its orbit, and (d) is not a satellite.

A small solar system body is defined as: Any celestial body, except satellites, orbiting the Sun that is not a planet or dwarf planet.

3.2: Astronomical Unit

One astronomical unit (AU) is, to a good approximation, the mean distance from the earth to the sun. Until recently, a more formal definition (e.g., Williams, 1997) was that one astronomical unit is the heliocentric distance at which a massless point-source object, moving in a unperturbed circular orbit about the sun, would have a mean daily motion of k radians/day, where k is the Gaussian gravitational constant ≡ 0.01720209895. At the 2012 IAU General Assembly (Beijing, China) the definition of the astronomical unit was modified. An astronomical unit is now exactly the distance 149 597 870 700 metres.

3.3: Aphelion/Perihelion

The closest approach of an object to the sun occurs at perihelion, the furthest approach at aphelion. Perihelion is denoted by q, aphelion by Q.

3.4: Osculating and Proper Elements

Osculating orbital elements are elements describing the orbit of an object that have been computed considering the perturbing effect of bodies other than the sun. This usually includes the major planets (Mercury through Neptune) and the three largest main-belt minor planets. The earth and

moon are treated as separate perturbers if the object is on an orbit that approaches the earth. For non-NEAs, the earth-moon system is treated as a single perturber, located at the barycentre of the earth-moon system. Since the orbital elements will change with time, osculating orbital elements are given for a specific osculating epoch, and are only correct for that instant.

Proper elements are orbital elements from which the effects of the short-term planetary perturbations have been removed.

3.5: Mean-Motion Resonances

A mean-motion resonance (MMR) occurs when the orbital periods of two objects can be expressed as a simple integer fraction, which results in regular gravitational perturbations of each object on the other. MMRs can be stable or unstable. In unstable resonances, the regular gravitational perturbations pump up the orbital eccentricity of one or both objects, to the point that the orbit(s) become planet crossing: when that happens, it is usually only a short time before the object encounters the planet and either hits it or is perturbed away. In a stable resonance, the periodic perturbations are such that they are self-correcting and the objects remain in the resonance. Prime examples of stable MMRs in the solar system are the Hilda minor planets, the Jupiter Trojans, and Neptune and Pluto:

- The Hildas are at the 3:2 resonance[3] with Jupiter, which is located at 3.95 AU: for typical orbital eccentricities of 0.1–0.2, this means that at aphelion low-inclination Hildas can be within 1 AU of Jupiter's orbit, yet they are protected from Jupiter encounters by coming to aphelion at elongations of ± 60° and 180° from Jupiter. A diagram by the author showing the motion of (153) Hilda in a frame rotating with Jupiter is available on the MPC website[4]: the sun is at the centre of the diagram and Jupiter is the white dot on the right. The motion of the minor planet in the period 1900–2100 is shown in red. The minor planet completes 25 orbits of the sun in that period and all the aphelia occur well away from Jupiter.
- The Jupiter Trojans are in 1:1 resonance with Jupiter, at a mean distance of 5.2 AU. There are two groups of Trojans: one orbiting ~60° of the planet and one orbiting ~60°

3 Resonances are expressed here in terms of the inner:outer ratio: for a 3:2 resonance the inner object completes three orbits in the time it takes the outer object to complete two. Some authors express resonances in the reverse order (outer:inner ratio).

4 `http://www.minorplanetcenter.net/iau/plot/00153.gif`

behind. A diagram I made some years ago showing the motion of (588) Achilles (the first Jupiter Trojan discovered) in a frame rotating with Jupiter is available on the MPC website[5]. The motion of the minor planet in the period 1900–2100 is shown in red. The minor planet completes 17 orbits of the sun in that period, but never comes to within ~2.9 AU to Jupiter.

- Neptune and Pluto are protected by a number of resonances, one of which is a 3:2 MMR. Another important factor keeping the two planets apart is a libration of the argument of perihelion of Pluto around 90°, which keeps Pluto's perihelion point well above the plane of the ecliptic. These effects conspire to keep Neptune and Pluto at least 17 AU apart, even though the two orbits approach to within 2.5 AU. An animation I made some years ago that shows the motion of Neptune and Pluto over three Neptunian years is available on the MPC website[6]. In the animation, the moving arrow at right shows the separation between the two objects at each step. The separation never drops below about 17 AU. (An example of a similar, but non-resonant, case is also available[7].)

A prime example of non-stable MMRs are the Kirkwood Gaps in the Main Belt (see Figure 2.7 [p. 43]). A review of the reasons why some MMRs are stable and others unstable is given by Lecar *et al.* (2001).

3.6: Secular Resonances

Secular resonances occur when the precession of two orbits, typically the position of the perihelion or the longitude of the ascending node, is synchronized (Scholl *et al.*, 1989). For minor planets in a secular resonance with a major planet, the minor planet precesses at the same rate as the major planet. Over time, the eccentricity and orbital inclination of the minor planet will be much changed. The three principal secular resonances present in the Main Belt are ν_5, ν_6 and ν_{16} (Williams, 1989). The ν_5 resonance occurs where the rate of precession of an object's longitude of perihelion, $\dot{\varpi}$, matches the rate of precession of Jupiter's longitude of perihelion, $\dot{\varpi}_J$. At the ν_6 resonance, $\dot{\varpi}$ matches $\dot{\varpi}_S$, the rate of precession of the longitude of perihelion of Saturn. At the ν_{16} resonance, the rate of precession of an object's nodes, $\dot{\Omega}$, matches the rate of precession of Jupiter's node, $\dot{\Omega}_J$. The

5 http://www.minorplanetcenter.net/iau/plot/00588.gif
6 http://www.minorplanetcenter.net/iau/anims/Resonant.html
7 http://www.minorplanetcenter.net/iau/anims/NonResonant.html

ν_6 and ν_{16} resonances are responsible for shaping the inner edge of the Main Belt, while all three resonances constrain various high-inclination groups. The approximate locations of the three principal secular resonances, along with the approximate locations of three high-inclination groups are shown in Figure A1.

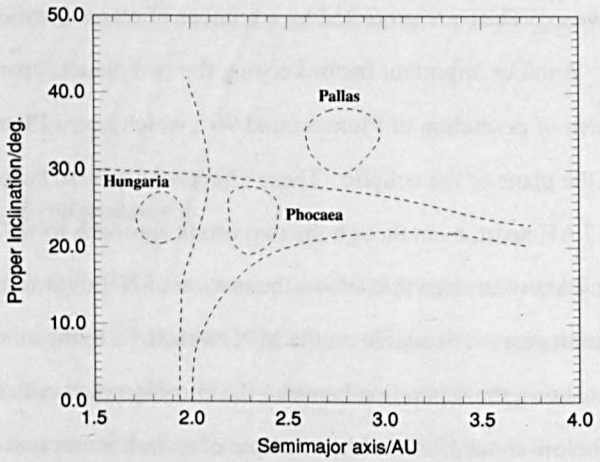

Figure A1: Approximate location of principal secular resonances

3.7: Phase Angle

The phase angle is the angle between the earth and the sun as seen from a third body. In celestial mechanic studies, the phase angle is usually denoted β, while in photometric studies, it is usually denoted α.

Figure A2 shows the phase angle in a system consisting of the sun, Earth and a minor planet. Also shown is the solar elongation, ε, as well as various distances. The distance from the sun to Earth is R, the distance of the minor planet from the sun is r and the distance of the minor planet from Earth is Δ. All three objects lies in the same plane, as a unique plane can be fitted through three non-coincidental points.

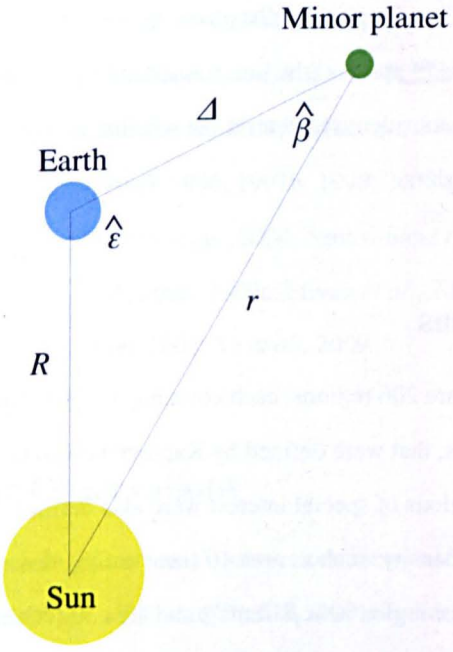

Figure A2: Geometric representation (not to scale) showing phase angle, solar elongation, geocentric distance and heliocentric distances

3.8: Potentially-Hazardous Asteroids (PHAs) and NEAs

Potentially-Hazardous Asteroids (PHAs) are those Near-Earth Asteroids (NEAs) whose orbits approach to within 0.05 AU of the orbit of the earth and whose absolute magnitudes are brighter than $V = 22.0$. There are a number of different definitions in the literature for the various classes of NEAs. Table A3 contains the limits on certain orbital elements that the MPC uses to define the various classes. The defining orbital elements are the perihelion distance, q, the semimajor axis, a, and the aphelion distance, Q.

Table A3: Minor Planet Center definition of NEA classes

Class	q/AU	a/AU	Q/AU
Atira			< 1.0
Aten		< 1.0	$\geqslant 1.0$
Apollo	< 1.0	$\geqslant 1.0$	
Amor	1.0–1.3		

The MPC definitions are known as the "1D definitions". Other groups adopt the "2D definitions", where the value 1.0 in Table A3 is replaced by 0.983 (which is the Earth's perihelion distance) or

1.017 (which is the Earth's aphelion distance). Some even adopt the "3D definitions", where the alignment of the lines of apsides (the line connecting the perihelion and aphelion point) of the minor planet and Earth are considered to deterimine whether on not the minor planet's orbit actually crosses the Earth's orbit.

3.9: Selected Areas

The Selected Areas are 206 regions, each covering about 1° by 1°, spaced around the entire sky at roughly 15° intervals, that were defined by Kapteyn (1906) to assist his studies of galactic structure. An additional 46 regions of special interest were also defined, which were chosen to emphasize variations in stellar density, such as area 10 (near α Cyg, described by Kapteyn as "[e]xtremely rich"), area 19 ("Poor region near β Tauri") and area 30 ("Quick change in density near θ Argus" [now θ Car]). Within each Selected Area (and Special Area), positions, magnitudes and motions (both proper and radial) were to be obtained to as faint a limit as possible, to determine star counts in various directions, in the hopes of determining the structure of the galaxy. At the time Kapteyn made his proposal, the role of interstellar absorption was not appreciated, so the original aim of determining the structure of the galaxy was not successful. The use of Selected Areas was later expanded to studies of extragalactic distributions and published studies of these regions are a rich source of accurate photometry of faint stellar objects. Some Selected Areas have had accurate magnitudes determined for objects fainter than $B = 22$.

4: Sources of Colours

This section lists the individual references for the colours lumped together as the penultimate entry in Table 3.6 [p. 64]: Belskaya *et al.*, 2009; Betzler and Novaes, 2008; Betzler *et al.*, 2010; Blanco and Riccoli, 1999; Buchheim, 2005, 2006; Buchheim and Pray, 2005; Buchheim *et al.*, 2004; Carbognani, 2008; Carbognani *et al.*, 2008; Carvano and Lazzaro, 2010; Chernova *et al.*, 1993; Dahlgren *et al.*, 1998; de Luise *et al.*, 2007; Debehogne and Zappalà, 1980a; Degewij and van Houten, 1979; Denchev, 2000; Doressoundiram *et al.*, 1999; Erikson *et al.*, 1991; Ford *et al.*, 2009; Gary, 2004; Guilbert *et al.*, 2009; Hahn *et al.*, 1989; Hergenrother *et al.*, 2009; Hicks and Collins, 1996; Hicks and Rhoades, 2010; Hicks and Somers, 2010; Hicks and Truong, 2010; Hicks *et al.*, 2004, 2009a, 2009b, 2009c, 2010a, 2010b, 2010c, 2010d, 2010e, 2010f, 2010g, 2010h, 2011a, 2011b; Jewitt, 2005; Jewitt *et al.*, 2007; Juarez *et al.*,

2005; Kamél, 1998; Kitazato *et al.*, 2004; Krugly *et al.*, 2007, 2010; Lagerkvist *et al.*, 1986, 1987, 1992, 1995, 1998; Magnusson and Lagerkvist, 1991; Magnusson *et al.*, 1996; Marciniak *et al.*, 2009; Mottola *et al.*, 1997; Mueller *et al.*, 2007; Neugent and Slivan, 2008; Noll *et al.*, 2006; Pfleiderer *et al.*, 1987; Polishook and Brosch, 2008; Pravec *et al.*, 1995, 1996, 1997b, 1998, 2000a, 2000b, 2002a, 2005, 2006; Romanishin *et al.*, 1997; Rosenbush *et al.*, 2009; Ryan, 2004; Santos-Sanz *et al.*, 2009; Schmude, 1995; Schober *et al.*, 1993, 1994; Shevchenko *et al.*, 2008, 2009a; Slivan *et al.*, 2008, 2009; Snodgrass *et al.*, 2010; Stecher *et al.*, 2008; Warner *et al.*, 2006, 2008; Ye *et al.*, 2009.

5: Sources of Photometric Observations

This section lists the papers from which photometric observations were extracted, as described in section 5.4 [p. 104]: Ahmad, 1954; Aksenov *et al.*, 1987; Angeli *et al.*, 2001; Baker and Warner, 2011; Baker *et al.*, 2011; Baker *et al.*, 2012; Barucci *et al.*, 1985, 1986, 1992, 1994; Belskaya and Dovgopol, 1992; Belskaya *et al.*, 1993; Binzel, 1985; Binzel and Tholen, 1983; Binzel *et al.*, 1987; Birch *et al.*, 1983; Birlan *et al.*, 1996; Borošová, 1991; Buie and Bus, 1992; Bus *et al.*, 1989; Carlsson and Lagerkvist, 1981a, 1981b; Carvano and Lazzaro, 2010; Chernova *et al.*, 1995; Chiorny *et al.*, 2007; De Sanctis *et al.*, 1994; Debehogne and Zappalà, 1980b; Debehogne *et al.*, 1977, 1978a, 1978b, 1982a, 1982b, 1983; Degewij and van Houten, 1979; Degewij *et al.*, 1978a, 1978b; Di Martino, 1984; Di Martino and Cacciatori, 1984a, 1984b; Di Martino *et al.*, 1987a, 1987b, 1994, 1995; Dotto *et al.*, 1992, 1995; Dovgopol *et al.*, 1992; Dunlap and Gehrels, 1969; Dunlap and Taylor, 1979; Dunlap *et al.*, 1973; Erikson *et al.*, 1991; Fornasier *et al.*, 2004, 2007; Franco, 2012; Franco and Sergison, 2011; Franco *et al.*, 2012; French, 1987; Gandolfi *et al.*, 2009; Gehrels, 1967a; Gehrels and Owings, 1962; Groeneveld and Kuiper, 1954; Harris and Young, 1983, 1989; Harris *et al.*, 1984a, 1984b, 1987, 1989a, 1989b, 1992, 1999; Hollis, 1987; Hollis *et al.*, 1997; Jewitt *et al.*, 2007; Karlsson *et al.*, 2009; Kitazato *et al.*, 2004; Krugly *et al.*, 2002, 2007; Lagerkvist, 1981; Lagerkvist and Kamél, 1982; Lagerkvist and Rickman, 1981; Lagerkvist *et al.*, 1987; Lupishko *et al.*, 1980, 1981; Magnusson and Lagerkvist, 1991; Michałowski and Velichko, 1990; Millis *et al.*, 1976; Mohamed *et al.*, 1994a, 1994b, 1995; Mottola *et al.*, 1995; Müller, 1893; Ostro *et al.*, 1984; Perna *et al.*, 2010; Pfleiderer *et al.*, 1987; Polishook and Brosch, 2009; Poutanen *et al.*, 1985; Pravec *et al.*, 1995, 1997a, 1997b, 1998, 2000a, 2000b; Reynoldson *et al.*, 1993; Romon-Martin *et al.*, 2003; Rosenbush *et al.*, 2009; Sather, 1976; Scaltriti and Zappalà, 1975, 1976, 1977; Schmude, 1995; Schober, 1976, 1978, 1979, 1981a, 1981b, 1981c, 1982a, 1982b, 1983a, 1983b, 1987; Schober and Schroll, 1982, 1983, 1985; Schober and Stadler, 1990; Schober and Surdej, 1979;

Schober *et al.*, 1979, 1982, 1988, 1993, 1994; Schuster *et al.*, 1979; Shatzel, 1954; Shevchenko *et al.*, 1992, 1996, 1997, 2003, 2009b; Slivan and Binzel, 1996; Slivan *et al.*, 2003, 2008, 2009; Snodgrass *et al.*, 2010; Stanzel and Schober, 1980; Stephens and Warner, 2004; Surdej and Surdej, 1977; Surdej *et al.* 1983a, 1983b; Taylor *et al.*, 1971; Tedesco *et al.*, 1983a, 1983b; van Houten-Groeneveld and van Houten, 1958; van Houten-Groeneveld *et al.*, 1979; Wamsteker and Sather, 1974; Weidenschilling *et al.*, 1987, 1990; Weissman *et al.*, 2007; Wisniewski *et al.*, 1997; Wolters, 2005 (see also Wolters *et al.*, 2005); Wood and Kuiper, 1963; Zappalà and van Houten-Groeneveld, 1979; Zappalà *et al.*, 1979, 1982, 1983, 1989; Zellner *et al.*, 1975, 1977.

6: Accessing the Thesis Data

There are two methods for accessing the data associated with this thesis. For accessing photometric data on a single object or single group of objects, there are a number of web-accessible query forms that can return the desired data. For accessing photometric data on the entire set of objects, complete data files are available for download from the thesis website. The thesis website is hosted on the MPC website, as much of the data are of use for general MPC operations.

6.1: Web Forms

The web forms are located at `http://www.minorplanetcenter.net/photometry`. Five forms are provided. The first two forms return either the adopted *HG* solution or all the *HG* solutions for a single object, along with the taxonomic classification and colours used in the reductions, as well as albedo and diameter determinations (if available), and links to phase-curve plots. The third form returns the adopted thesis *HG* values and the current MPC *HG* values for a group of objects. The return page has links to the full information for each object. The fourth form returns raw observational data for a single object, either just the corrected magnitudes (along with the Julian Date of observation and the observatory code) or all the data associated with each observation. The fifth form allows quick access to phase-curve plots.

The web forms are designed for small(ish) data requests. Users requiring large amounts of data should download the complete data sets. The web forms output *HG* values and uncertainties to two decimal places. The *HG* values stored in the MySQL databases are stored with four decimal places and, to minimize artifacts in statistical studies, these values are accessible in the complete data sets.

6.2: Complete Data Sets

Some users may prefer to access complete data sets. For convenience in downloading, most of the files are compressed. The compression method used is gzip, as it can cope with files larger than 2 GB. The largest downloadable files as supplied as gzip'ed tar files, as there are multiple files contained in each download file. Some small files are available as plain ASCII (`.TXT`) files. Some of the files are final data sets, some are intermediate files used in the thesis. All the files are accessible from `http://www.minorplanetcenter.net/iau/info/Photometry.html`, with MD5 checksums listed for each file to allow verification that file transfers have been completed without error.

The following final data sets are available:

- `tot_hg.txt.gz`, containing the adopted *HG* solutions.
- `tot_h.txt.gz`, containing all the *HG* solutions.
- `cols_and_tax.txt.gz`, containing the colours and taxonomic data used.
- `albedos.txt.gz`, containing the albedo and diameter results.
- `cdpc.tar.gz`, containing the CMC-14-Derived Photometric Catalogue and the ASTCAT-C catalogue.
- `sdpc.tar.gz`, containing the Sloan-Derived Photometric Catalogue and the ASTCAT-S catalogue.

The following intermediate files are available:

- `ASTROMETRICA.TXT`, a list of observatory codes that used versions of Astrometrica that produced high-quality photometry and the dates when such versions were first used.
- `fitfile.tar.gz`, containing the details of the photometric fits used to correct the observations.
- `corrobs.tar.gz`, containing the raw observational material, in the final extended form of the Standard Format.
- `OBS_CORRECTIONS.TXT`, the values of the observer corrections used by `WORKOUTH`.
- `F51_ONLY.H`, *HG* determinations from Pan-STARRS-1 observations only.
- `F51_ONLY.HG`, adopted *HG* determinations from Pan-STARRS-1 observations only.

- `FASTT_ONLY.H`, *HG* determinations from USNO FASTT observations only.
- `FASTT_ONLY.HG`, adopted *HG* determinations from USNO FASTT observations only.
- `FASTT_ONLY_0001605.H`, *HG* determination of (1605) Milankovitch from USNO FASTT observations only.
- `FASTT_ONLY_0002060.H`, *HG* determinations of (2060) Chiron (= 95P/Chiron) from USNO FASTT observations only.
- `PHOTOMETRY_ONLY.H`, *HG* determinations from photometric observations only.
- `PHOTOMETRY_ONLY.HG`, adopted *HG* determinations from photometric observations only.
- `SDSS_ONLY.H`, *HG* determinations from SDSS observations only.
- `SDSS_ONLY.HG`, adopted *HG* determinations from SDSS observations only.

Note that certain `.H` and `.HG` files are from runs of `WORKOUTH` using version of the program that did not output as much information as the current version.

7: Supplementary and Supporting Information

Included here are sections that were removed from the main body of the text (as was present in earlier versions of this thesis) in order to improve the readability of the main text. Some additional explanations requested by the viva committee are also included here.

7.1: Derivation of the 5 log $(r\Delta)$ term in Equation 2.1

The 5 log $(r\Delta)$ term in Equation 2.1 [p. 13] can be derived by application of the inverse-square nature of light. Knowledge of the logarithmic identities $\log x - \log y = \log (x/y)$ and $\log (x^2) = 2 \log x$ is also required.

The difference between any two magnitudes m_1 and m_2 is given by Equation A7.1 (remembering that brighter intensities are represented by smaller numeric magnitudes), where I_1 and I_2 are the intensities corresponding to m_1 and m_2, respectively:

$$\left.\begin{aligned} m_2 - m_1 &= -2.5 \log I_2 - (-2.5 \log I_1) \\ &= 2.5 \log I_1 - 2.5 \log I_2 \\ &= 2.5 \log (I_1 / I_2) \end{aligned}\right\} \quad \text{(A7.1)}$$

If we set m_1 to be the absolute magnitude H and m_2 to be the V magnitude at a given time, then we can set $I_1 = 1$. The relative intensity I_2 is then given by the product of the reciprocals of the squares of the heliocentric and geocentric distances. The ratio I_1/I_2 is then simply:

$$\left.\begin{aligned} \frac{I_1}{I_2} &= \frac{1}{r^{-2}\Delta^{-2}} \\ &= r^2\Delta^2 \end{aligned}\right\} \quad \text{(A7.2)}$$

Making the appropriate substitutions of Equation A7.2, H and V in Equation A7.1 then leads to:

$$\left.\begin{aligned} V - H &= 2.5 \log (r^2\Delta^2) \\ V &= H + 5 \log (r\Delta) \end{aligned}\right\} \quad \text{(A7.3)}$$

which is the first part of Equation 2.1 [p. 13].

7.2: Goodness of Fit

The goodness of fit, R^2, is a statistical measure of how well a statistical model fits the set of observations used to generate the model. The goodness of fit is quoted as a dimensionless value in the inclusive range 0 to 1. A value of R^2 near 1 indicates that the model fits the data very well, while a value near 0 indicates a very poor fit. The goodness of fit is determined by the following procedure, where x and y are n sets of observed data to be fit, barred quantities represent means and σ is a standard deviation:

$$\left.\begin{aligned} \bar{x} &= (\Sigma x)/n \\ \bar{y} &= (\Sigma y)/n \\ \sigma_{xx} &= \Sigma x^2 - n\bar{x}^2 \\ \sigma_{yy} &= \Sigma y^2 - n\bar{y}^2 \\ \sigma_{xy} &= \Sigma xy - n\bar{x}\bar{y} \\ R^2 &= \sigma_{xy}^2/(\sigma_{xx}\sigma_{yy}) \end{aligned}\right\} \quad \text{(A7.4)}$$

7.3: Examination of 2MASS as a Source Catalogue

A collaborative effort between the University of Massachusetts and Caltech's Infrared Processing and Analysis Center, 2MASS (Skrutskie *et al.*, 2006) was an all-sky infrared survey undertaken using two identical 1.3-m telescopes,. The northern-hemisphere instrument was located on Mt. Hopkins, AZ, and the southern-hemisphere instrument at the Cerro Tololo Inter-American Observatory, Chile. Each telescope was equipped with a three-channel camera, each channel comprising a 256 × 256 array of HgCdTe detectors. Using the three channels, simultaneous observations were made in the three survey bands: J, centred at 1.25 μm; H, 1.65 μm; and K_s, 2.16 μm. The limiting magnitudes in each band were $J \sim 15.8$, $H \sim 15.1$ and $K_s \sim 14.3$. The northern site observed between 1997 June and 2000 December, the southern site observed between 1998 March and February 2001. The 2MASS All-Sky Data Release contains positions and photometry for 470 992 970 point sources, mostly stars, along with 1 647 599 extended sources, mostly galaxies.

Some thought was given to seeing whether it was possible to derive reliable visual colours from the 2MASS infrared colours. It was decided to compare the visual colours of Landolt standard stars to the corresponding 2MASS colours. A complication in converting from infrared to visual colours is interstellar reddening, which is variable across the sky and highly so near the galactic plane and the galactic centre.

7.3.1: Comparison of Landolt and 2MASS Colours

Landolt (1992) presented positions, finder charts and *BVRI* magnitudes for 526 stars located close to the celestial equator. A machine-readable version of these data was downloaded from Vizier. The coordinates in the data file, which are taken from the paper, were semi-accurate, given to a precision of 1^s in α and $1''$ in δ. The *accuracy* of many of the positions was far worse (in some cases due to the star having a high proper motion) and this precluded unambiguous identification of the Landolt stars in the 2MASS catalogue. To obtain better coordinates, the supplied finder charts were used to locate each star in the Google Sky web service. All 526 stars were identified and accurate coordinates were read off the screen. In practice, these "quick and dirty" positions are probably only good to $\pm 1''$, but they are fully sufficient for identification purposes. The number of matches then found to objects in the 2MASS catalogue was 517.

In a later paper, Landolt (2007) presented accurate coordinates, finder charts and *BVRI* magnitudes for 109 stars located at about $\delta = -50°$. As before, the 2MASS catalogue was searched in order to match the Landolt stars to 2MASS stars. The number of matches found was 108.

Various colour-colour plots are shown in Figure A3 (the red lines in each are not a formal best-fit line, but rather a visual guide for the eye).

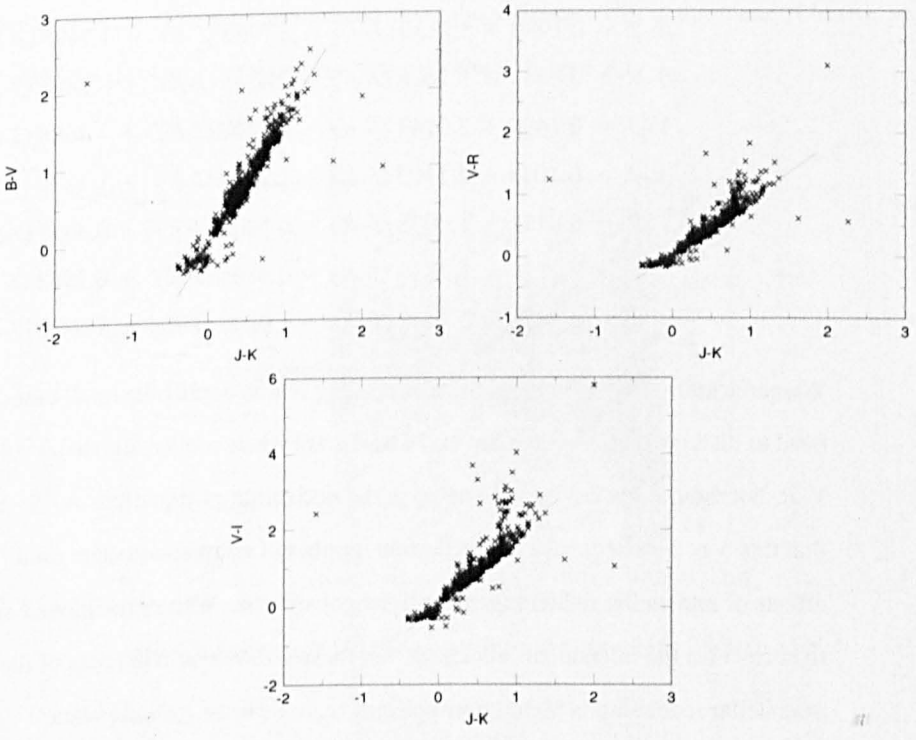

Figure A3: Comparison of 2MASS and Landolt colours

It is clear from Figure A3 that it will not be possible to use 2MASS colours to derive visual colours that are good to better than 0.1 mag.

7.3.2: Re-Examination of Landolt and 2MASS Colours

In a paper detailing a project to determine *HG* parameters, Warner (2007) demonstrated a procedure for converting 2MASS *JHK* magnitudes into *BVRI* using transformation expressions derived from Landolt standard stars. Using 128 of the standard stars, taken from the

loneos.phot list, Warner located each star in the 2MASS catalogue. He then derived expressions relating the *J–K* colour to the *B–J*, *B–V*, *V–J*, *R–J*, *V–R*, *I–J* and *V–I* colours, claiming the expressions represented the *BVRI* magnitudes of the Landolt stars to better than ± 0.080 mag. This paper necessitated a re-examination of the suitability of the 2MASS catalogue for this thesis.

Warner restricted his analysis to stars with $-0.1 < J-K < 1.0$, to avoid excessively blue or red stars. Warner's transformation equations are given below:

$$\left.\begin{aligned}
B-J &= 0.1980 + 5.2150\,(J-K) - 2.7785\,(J-K)^2 + 1.7495\,(J-K)^3 \\
B-V &= 0.0484 + 1.7006\,(J-K) - 0.4535\,(J-K)^2 + 0.2807\,(J-K)^3 \\
V-J &= 0.1496 + 3.5143\,(J-K) - 2.3250\,(J-K)^2 + 1.4688\,(J-K)^3 \\
R-J &= 0.1045 + 2.5105\,(J-K) - 1.7849\,(J-K)^2 + 1.1230\,(J-K)^3 \\
V-R &= 0.0451 + 1.0038\,(J-K) - 0.5401\,(J-K)^2 + 0.3458\,(J-K)^3 \\
I-J &= 0.0724 + 1.2816\,(J-K) - 0.4866\,(J-K)^2 + 0.2963\,(J-K)^3 \\
V-I &= 0.0856 + 2.1652\,(J-K) - 1.6902\,(J-K)^2 + 1.0770\,(J-K)^3
\end{aligned}\right\} \qquad \text{(A7.5)}$$

Warner acknowledged that these equations may not be applicable in all cases. He noted the need to distinguish between giant and dwarf stars when converting visual colours, e.g.. *V–I* to *V–R*, but did not see any need to do so in the derivation of Equations A7.5. Warner suggested that this was a consequence of the limited number of comparison stars used. In addition, the effects of interstellar reddening are still not considered. Warner mentioned some possible ways to correct for the interstellar reddening, but these will not help in areas of the sky where the interstellar reddening is highly non-uniform (e.g., near the galactic plane).

I extracted the *B–V* colour of 31 671 stars from loneos.phot. I then located each of those stars in the 2MASS catalogue, extracted the *J*, *H* and *K* colours and derived *J–K*, *J–H* and *H–K* colours.. The relationship between the *B–V* colours and each of the 2MASS colours is shown in Figure A4.

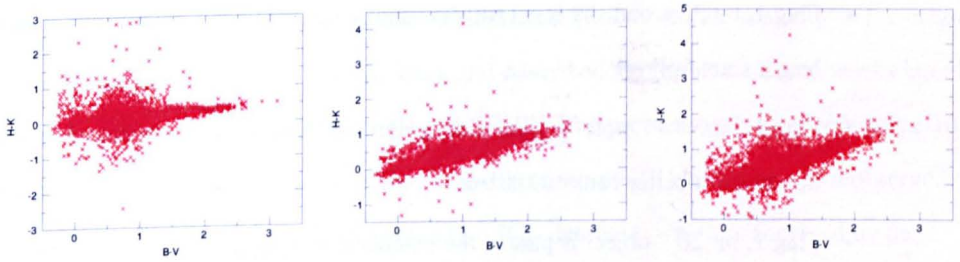

Figure A4: Comparison of B–V and 2MASS colours

In addition, I derived the *V* magnitude for each of the 31 671 stars using the 2MASS *J–K* colour and Equation A7.5. For each star I determined the difference *dV*, in the sense of loneos.phot *V* minus 2MASS-derived *V*, and displayed the results in Figure A5.

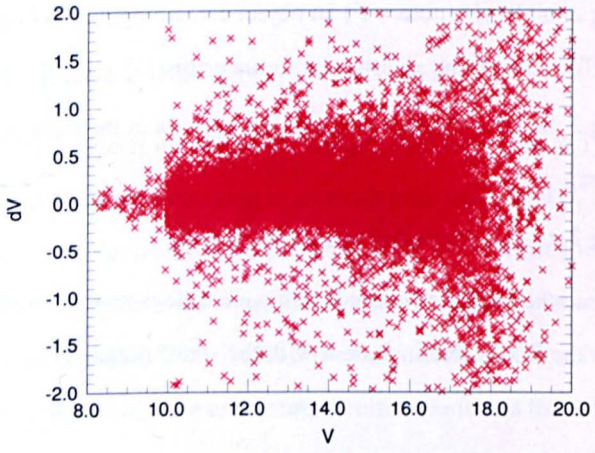

Figure A5: Difference between loneos.phot V and 2MASS-derived V

Figures A4 and A5 confirm my earlier assertion that 2MASS alone is not suitable as a basis for the photometric catalogues needed for this thesis.

7.4: List of SDSS Photometric Flags Examined

The full list of SDSS photometric flags examined was as follows:

- Flag 1, bit 18 – object is saturated;
- Flag 2, bit 11 – object centre is saturated;
- Flag 1, bit 24 – object is too large (it has a radius of more than 4″);

- Flag 1, bit 22 – bad sky level (this is usually caused by the subtraction of the wings of bright stars failing);
- Flag 1, bit 5 – (*, note 'p') position is derived from position of peak pixel, as attempts to determine a better centroid failed;
- Flag 1, bit 20 – object is part of the extended wing of a bright star;
- Flag 2, bit 14 – deblended object may not be real as no peak was found;
- Flag 2, bit 12 – (*, note 'c') an object's centre is very close to at least one interpolated pixel;
- Flag 2, bit 15 – flux measurement for object may be inaccurate as more than 20% of the flux was interpolated;

- Flag 2, bit 8 – (*, note ='i') an object containing interpolated pixels had too few good pixels to determine an estimate for its errors;
- Flag 2, bit 25 – (*, note = 'g') object appears in the right place to be an electronics ghost;
- Flag 2, bit 0 – deblended as moving object.

The entries marked with (*) in the list above are flags that, if set, do not reject the star from inclusion in the SDPC, but include it with the stated note.

7.5: Duplicates in the SDSS DR7 PhotoPrimary Database

While verifying the library routines that access data from the SDPC, I noticed that there were quite a number of cases where there were two SDSS sources within 0.″5 of each other. In all cases, both sources were marked as being PRIMARY objects: this should not occur, as there should be only one PRIMARY object in such a small region of sky. That any such cases were detected while extracting less than 0.0001% of the objects in the SDPC suggested that there were a large number of such duplicates. I was uncertain as to whether the problem was in the CfA's copy of the DR7 data or whether it was present in the original SDSS database. I selected one of the problem cases and used the SDSS website's query tool to search for objects within 1″ of the coordinates: only one object was returned. I then tried a few more of the problem cases: in every case, only one object was returned. I brought the problem to the attention of Bill Wyatt, who maintains the CfA's copy of the

SDSS data. He investigated the matter and agreed that there was some inconsistency in the original SDSS data set. He contacted the SDSS help desk and described the problem. Some weeks later he received a reply, which he forwarded to me (Wyatt, 2009). The problem stemmed from stripe 10 of observing run 752 which had very poor seeing for much of the run. This region was reobserved later in the survey during run 6793. In the final DR7 SQL database, which is accessed by the website's query tool, the objects from run 6793 were given the status PRIMARY, while the objects from run 752 were set to SECONDARY. However, this change was not made in the tsObj files that are available for downloading and that were used to build the CfA's copy of the SDSS data set. It is unclear whether SDSS will fix the status flags within the tsObj files or will simply produce a list of problem cases for placement on the website. For the purposes of this thesis, the duplicated entries are similar enough that I could simply reject the second object of each duplicate pair.

7.6: Format of SDPC Data Files

For speed of access, the SDPC objects are stored in multiple data files arranged by north polar distance, each data file contains the objects lying in a one-degree-wide band of declination. North polar distance is used rather than declination in the filenames as I do not need to handle positive and negative values, which complicate the file names. Each data file contains the objects lying in a one-degree-wide band. The objects in each data file are stored in unformatted form and the data files are arranged as indexed Fortran data files, The unformatted form means that the data associated with each object are stored in the internal machine representation of that data rather than in the human-readable character format. Use of unformatted data means that when reading the data file the computer does not need to translate the human-readable format into its internal representation, thereby speeding up the reading process, and the storage requirements are often less. As an example, consider a formatted numeric value that can be in the range 0 to 5000000. In order to store the maximum allowed value, seven bytes of storage have to be allocated, each byte containing the ASCII representation of one digit. So if I wanted to store 3231583 in formatted form, the seven bytes would contain the values &33, &32, &33, &31, &35, &38 and &33 (each value being the hexadecimal ASCII representation of each character in the string). In the unformatted form, the value 3231583 can be stored in four bytes, the standard allocation for an integer variable in Fortran, as (in little-endian form) &5F, &4F, &31, &00 (some Fortran compilers allow use of a 3-byte integer variable type, but this is not common). The use of indexed Fortran data files means that the

data within each file can be accessed in a random-access fashion. It might appear that use of internal machine representations of data might make portability of the data files an issue, particularly if moving data from a little-endian machine (where the low byte is stored at a lower address) to a big-endian (where the high byte is stored at a lower address) machine. However, decent Fortran compilers have compile-time options allowing run-time conversion of internal-format data transparently from one format to another as the data is being read, so portability of internal-format data is not an issue.

The data for a single entry in the SDPC occupies 64 bytes. The layout of each entry is described in Table A4 [p. 236]. The offset is the number of bytes from the start of the record where each datum begins. The variable types are: Integer (4 bytes); DP (double-precision real, 8 bytes); SP (single-precision real, 4 bytes); and Char*<len> (variable length string).

Table A4: Format of a SDPC entry

Offset	Type	Purpose
0	Integer	Object number within declination band
4	DP	Right Ascension (J2000.0)/deg.
12	DP	Declination (J2000.0)/deg.
20	SP	*U* magnitude
24	SP	Uncertainty in *U* magnitude
28	SP	*B* magnitude
32	SP	Uncertainty in *B* magnitude
36	SP	*V* magnitude
40	SP	Uncertainty in *V* magnitude
44	SP	*R* magnitude
48	SP	Uncertainty in *R* magnitude
52	SP	*I* magnitude
56	SP	Uncertainty in *I* magnitude
60	Char*1	Star/Galaxy flag
61	Char*1	Note
62	Char*2	Unused/Spare

If any magnitudes have uncertainties that are too large (see Section 4.5.2 [p. 78]), the magnitude is replaced by the value 99.999 and the uncertainty by the value 9.999. The notes are as defined in the listing of the examined flags in Section 4.5.2 [p. 78].

The index file for the SDPC contains one entry for each 1°-wide declination band. The format of each entry is as shown in Table A5. The format of the CDPC index file is identical to that of the SDPC.

Table A5: Format of SDPC/CDPC index entries

Offset	Type	Purpose
0	Integer	North Polar Distance for this declination band
4	Integer	Pointer to first object with $0° \leq \alpha < 1°$
8	Integer	Pointer to first object with $1° \leq \alpha < 2°$
....		
1436	Integer	Pointer to first object with $358° \leq \alpha < 359°$
1440	Integer	Pointer to first object with $359° \leq \alpha$
1444	Integer	Pointer to last object + 1

If there are no entries in a given 1°-wide R.A. region, the pointer is set to either zero (if there are no entries with smaller R.A.s) or to one more than the last entry in the previous R.A. region.

The designation scheme for the SDPC is SDPC <dec band> <number in band>, analogous to the scheme used in the 19th century star catalogue *Bonner Durchmusterung*. An example of the designation is SDPC +43 137408, which is the star with $B = 16.832$, $V = 15.645$, $R = 14.990$ and $I = 14.381$ at R.A.$_{J2000.0}$ = 145°.02258 = $09^h40^m05^s.42$, Decl.$_{J2000.0}$ = +43°.49846 = +43°29′54″.5.

7.7: The Guide Star Photometric Catalogue

The Guide Star Photometric Catalogue (GSPC) V2.1 is described by Bucciarelli *et al.* (2001) with the V2.4 version seemingly only described in Vizier[8]. The GSPC is a catalogue of *BVR* photometric sequences intended for use in calibrating the magnitudes given in the Guide Star Catalogue (GSC). The V2.4 catalogue contains sequences for 1780 fields, located near the centres of the photographic plates that were used to construct the GSC and distributed all over the celestial sphere. The sequences were measured from CCD images taken at ten different observatories. Photometric accuracy is claimed to be ± 0.07 mag at mag 19 and astrometric accuracy is claimed to be ± 0″.3 relative and up to ± 3″ absolute. There are 554 007 entries in the V2.4 catalogue.

8 http://vizier.cfa.harvard.edu/viz-bin/VizieR?-source=II/272

A small program (MATCHGSPC24) was written to match the GSPC entries to the SDPC entries. For each entry the GSPC RA and Decl (both in decimal degrees) were extracted. Since there are no SDPC entries above $\delta = +77°$ or below $\delta = -12°$, GSPC objects outside these declination limits could be eliminated immediately from further consideration. For those inside the above limits, a search was made of the SDPC. If one or more SDPC objects were returned, a check was made of the agreement of the *B*, *V* and *R* magnitudes between the two catalogues. A simple addition of the absolute differences in the three magnitude bands was computed and the SDPC object with the lowest total was selected as the correct object. Program output consisted of the GSPC identifier, the GSPC *BVR* magnitudes, the SDPC *BVR* magnitudes, the sum of the absolute differences in the magnitudes and the difference in arcseconds between the positions given in the two catalogues.

A first pass was performed on a small subset of the GSPC using a positional match tolerance of ± 3″. A manual check was then made to ensure that all matches were being found. Some probable matches had been missed, so the tolerance was raised to ± 10″ and a second pass was performed on the entire GSPC. The output file from this second run contained 4122 entries.

7.7.1: Problems in the Guide Star Photometric Catalogue

An examination of the output file immediately showed some problems. Since the SDPC is not an all-sky catalogue, there would be a majority of GSPC fields that had no matches with the SDPC. However, at each declination where there was SDPC coverage, there would be a range of GSPC fields where there should be matches between the two catalogues. For example, GSPC fields N050 through N077 cover $63° \leq \delta \leq 68°$: fields N061 through N070 are in regions covered by the SDPC and should have matches.

Field N061 has 89 entries in the GSPC but only 7 entries in the SDPC. In fields N067 and N069, there are 76 and 63 entries, respectively, in the GSPC and none in the SDPC. An immediate suspicion was that there was an astrometric problem with some of the GSPC fields. This suspicion was strengthened when the output for field X493 was examined: 755 GSPC entries, only 22 SDPC entries with positional offsets of 4″–11″ and bad photometric agreement (difference totals up to 12 mag), indicating that the field was mismatched. Examination of the X493 field in Google Sky indicated that the GSPC positions, while good in δ, required a

correction in α of about +10″. A modification to MATCHGSPC24 was made to allow the specification of R.A. and Decl. offsets that would be applied to the GSPC positions before the matching to the SDPC, as well as restricting the output to a specified field. A run of the modified program, specifying an offset of +10″ in right ascension, on just the X493 field produced 189 matches with consistent positional offsets of ~ 1.5″ and good photometric agreement (most difference totals under 0.6 mag.). Using Google Sky, fields N067 and N069 were examined. Both fields showed small offsets (under 2″) between the GSPC objects and the corresponding stellar objects. Further investigation showed that the failure to find any matches in fields N067 and N069 was due to their falling in gaps in SDPC coverage.

I have demonstrated the ability to detect astrometric errors in the GSPC and to correct them in the matching stage. The complication is that I do not know *a priori* which fields need correction. Although it would be possible to use Google Sky to examine all the fields, locate the problem fields and determine how to correct them, this task would be extremely time-consuming. Therefore, I decided that the amount of work necessary to use the GSPC for this thesis was not worthwhile.

7.8: Format of CDPC Data Files

For speed of access, the CDPC objects are stored in multiple data files arranged by north polar distance, in a similar fashion to the SDPC data. The data for a single entry in the CDPC occupies 40 bytes. The layout of each entry is described in Table A6. The offset is the number of bytes from the start of the record where each datum begins. The variable types are: Integer (4 bytes); DP (double-precision real, 8 bytes); and SP (single-precision real, 4 bytes). The current version of the CDPC does not use the notes entry.

Table A6: Format of a CDPC entry

Offset	Format	Use
0	Integer	Object number within declination band
4	DP	Right Ascension (J2000.0)/deg.
12	DP	Declination (J2000.0)/deg.
20	SP	*B* magnitude
24	SP	*V* magnitude
28	SP	*R* magnitude

32	SP	*I* magnitude
36	Char*4	Notes

The designation scheme for the CDPC is CDPC <dec band> <number in band>, consistent with the form for SDPC designations and analogous to the scheme used in the *Bonner Durchmusterung*. An example of the designation is CDPC +43 327689 (= SDPC +43 137408, used as the example in Appendix 7.6 [p. 235]), which is the star with B = 16.612, V = 15.539, R = 14.940 and I = 14.384 at R.A.$_{J2000.0}$ = 145°.02253 = $09^h40^m05^s.41$, Decl.$_{J2000.0}$ = +43°.49843 = +43°29′54″.4.

7.9: The Procedure for Building the ASTCAT Entries

I decided to write a command file on the MPC machines that would automatically process the objects in a single SDPC/CDPC file (which contains entries in a strip one degree wide in Declination) and produce the corresponding ASTCAT file. This would require a number of steps. Each Declination band was split into regions 0.5 degrees wide in R.A. This was to ensure that not too many objects were extracted by a single request. Using the centre coordinates of each region, a command line was constructed that can run on a CF machine, which would extract the stars from each catalogue in turn to an output file and write that command to a file (called `Unix.com`). Each region generates one line in `Unix.com` for each catalogue that is to be searched. An example of the output for one region is shown in table A7.

Table A7: Sample of command file used to populate ASTCAT-S/-C files

```
$cat -h -c ua1 -r 900,1800 -n 50000 -s r 08:34:09.941 +62:30:00.0 > cat_ua1_001.txt
$cat -h -c ua2 -r 900,1800 -n 50000 -s r 08:34:09.941 +62:30:00.0 > cat_ua2_001.txt
$cat -h -c ub1 -r 900,1800 -n 50000 -s r 08:34:09.941 +62:30:00.0 > cat_ub1_001.txt
$cat -h -c gsc2 -r 900,1800 -n 50000 -s r 08:34:09.941 +62:30:00.0 > cat_gsc2_001.txt
$cat -h -c gsc -r 900,1800 -n 50000 -s r 08:34:09.941 +62:30:00.0 > cat_gsc_001.txt
$cat -h -c gsca -r 900,1800 -n 50000 -s r 08:34:09.941 +62:30:00.0 > cat_gsca_001.txt
$cat -h -c ucac1 -r 900,1800 -n 50000 -s r 08:34:09.941 +62:30:00.0 > cat_ucac1_001.txt
$cat -h -c ucac2 -r 900,1800 -n 50000 -s r 08:34:09.941 +62:30:00.0 > cat_ucac2_001.txt
```

The `-h` flag selects header output, `-c` selects the catalogue from which to extract the stars, `-r` defines the size of the search box in arcseconds, `-n` specifies the maximum number of objects that will be extracted and `-s r` indicates the output is to be sorted by R.A. The file used for building

the CDPC also has the `-mx 0.0,18.5` flag to restrict output to objects with a magnitude brighter than 18.5. The `Unix.com` file was then copied to a CF machine and executed remotely. When all of the output `cat*.txt` files had been generated on the CF machines, they were copied to a MPC machine for further processing. Each output file was read in turn, the data within was decoded and an attempt was made to match each star to a SDPC/CDPC entry.

The command file and the Fortran 95 programs necessary for this job were written and tested on the SDPC and declination band +70°. The test process added the astrometric-catalogue magnitudes to the corresponding ASTCAT-S file created when the SDPC was built. After fixing a couple of minor issues, a batch job was submitted to process declination bands +69° to +60°. A check on the status of the batch job four days later showed that the matching step for +62° was still running after 27 hours(!) of execution time. The batch job was stopped and the matching program was recoded slightly to improve the efficiency of the matching step. The +62° matching step was run interactively as a test and it completed in 4 minutes! Batch jobs were submitted to add the astrometric-catalogue magnitudes to all of the ASTCAT-S and ASTCAT-C files. The addition of the astrometric-catalogue magnitudes is rather CPU and network-I/O intensive, so the jobs were submitted sequentially rather than in parallel.

7.10: Errors in Bowell *et al.* (1989)

It should be noted that there are two errors in the equations given in Bowell *et al.* (1989): the denominator of g_j is given as $\varepsilon_i^2 I_i^2$ in Equation 6.5 [p. 130]; and the numerator of G is given as a_1 in Equation 6.7 [p. 130]. These errors were detected via a rather torturous process. I wrote Fortran 95 code (part of `WORKOUTH`) to implement Equations 6.5 to 6.9 [pp. 130–131] as published. I tested the code using photometric observations of (4) Vesta and solved for both parameters—this produced garbage values for H and G. After repeated checks of the published equations and my code failed to show any reason for the difference, I implemented Equation 6.10 [p. 131], determination of H using an assumed value of G. Using the catalogue slope parameter ($G = 0.32$) as the assumed value of G, the test data produced $H = 3.17 \pm 0.06$, in excellent agreement with the catalogued value of 3.20. The uncertainty in H looked reasonable and suggested that Equations 6.9 [p. 131] were implemented correctly. Renewed comparison of my implementation of Equations 6.5 to 6.8 [p. 131] failed to show any difference with the published equations. Suspecting that there was an error in one or more

of the published expressions, I performed a literature search to try to find a published correction. No published corrections were found[9], although numerous authors—e.g., Pravec *et al.* (1998), Weissmann *et al.* (2007), Shevchenko *et al.* (1992)—claim that they used the published equations to derive *HG* values in their papers. (It is interesting to note that Rock and Hollis (1990) give, without comment, the correct expression for *G*. It appears that they used the expression from *Circular* No. 12 of IAU Commission 20, where it is given correctly.) I contacted Bowell and requested a copy of the Fortran source code that his paper said was available "on request". A copy of the program was received within 48 hours. After spending a few moments examining the structure of the program to figure out what was being calculated and where, I compared the expressions in Bowell's program to the published paper. It took only a few minutes to find the two discrepancies between Bowell's program and his paper. After modifying the expressions in my program to match those in Bowell's program, the test data for (4) Vesta gave $H = 3.20 \pm 0.02$ and $G = 0.30 \pm 0.04$.

7.11: Notes on Specific Photometric Papers

This section contains notes on some of the photometric papers, with comments on the usability of the data and, where possible, identification of the comparison stars used. In the lists of comparison star identifications, catalogue numbers and J2000.0 positions are from the UCAC-2 and, unless stated otherwise, listed magnitudes are extracted from the CDPC unless followed by "*", indicating that the magnitude is taken from SIMBAD. Where notes are made about errors in the APC, the relevant changes have been made in my copy of the data files.

Barucci and Di Martino (1984) give rough B1950.0 coordinates of the comparison stars, but no comparison-star magnitudes. The (123) and (376) data are not usable, the relative magnitudes are extracted from lightcurve plots with the zero point equal to maximum light, but no information relating the zero point to an absolute scale is given. The (437) and (1224) lightcurve plots are relative to the comparison star and so are rereduceable. Table A8 identifies the comparison stars.

Table A8: Comparison star identifications for Barucci and Di Martino (1984)

Star	Publ. B1950.0	Identification	Id. B1950.0	Id. J2000.0	Id. *V*
A	00 04.9 +09 54	201.000290	00 04.7 +09 55	00 07 22.67 +10 09 09.3	12.87
B	00 33.4 +19 12	220.001961	00 33.2 +19 15	00 35 50.84 +19 31 28.5	11.88
C	00 32.0 +18 55	219.001900	00 32.1 +18 52	00 34 43.06 +19 08 02.3	11.85
D	00 02.6 +17 23	216.000312	00 02.9 +17 25	00 05 26.92 +17 42 04.9	10.73

9 Rather late in the preparation of this thesis, note of the error in the expression for *G* appeared in Muinonen *et al.* (2010).

Barucci *et al.* (1985) reported observations made at the Teramo Astronomical Observatory and at the Catania Astrophysical Observatory, but omitted to indicate which observations were made at which site. A similar problem affects Angeli *et al.* (2001), Chiorny *et al.* (2007) and Shevchenko *et al.* (2003). Such observations are indicated on the MPC photometric record as being geocentric (code 500).

Barucci *et al.* (1994) give no information on comparison stars. Non-relative magnitudes that are given are corrected to unit distance, but are not flagged as such in the APC data file. The photometry is apparently relative, but is not flagged as such in the APC data file.

Binzel (1984) does not identify the comparison star used for his 1982 observations of Pallas, but clearly identifies the comparison star for the 1983 observations as SAO 104678, although he omits to mention what magnitude he used for the star. The APC data file appears to contain only a fraction of the observations discussed in the paper, I do not have enough information to rereduce the data.

Birlan *et al.* (1996) give no information on comparison stars. Magnitudes are absolute and are corrected to unit distance. These data were not present on the APC CD-ROM.

Gehrels (1956), in his seminal in-depth study of the phase curve of (20) Massalia, clearly identifies the comparison stars and gives full details of the reduction process for the minor-planet magnitudes. The magnitudes of the comparison stars were determined through comparison with BD +0° 2875. Observed magnitudes of the minor planet on each night were obtained by comparison to two comparison stars: the first comparison was used as a direct comparison; the second comparison was compared with the first comparison, to ensure non-variability, then compared to the minor planet. The observations are fully rereduceable and the comparison stars are identified in Table A9 (all magnitudes are taken from SIMBAD). While rereducing the observations using the modern *V* comparison-star magnitudes from Table A9, I noticed that, in every case, the difference between the magnitude estimates derived from the two comparison stars on one night was greater than the difference found by Gehrels. The greatest difference occurred for the observation on 1955 April 17, where I found a difference of 0.13 mag in the estimates derived from comparison C I and comparison C II, whereas Gehrels' difference was only 0.032 mag. The comparison star magnitudes derived by Gehrels are internally consistent at the ± 0.03-mag level and his magnitude for

comparison star C I differs by only –0.04 mag from the SIMBAD value. This seems to be a clear demonstration that modern magnitudes of many comparison stars are often worse than the magnitudes determined in the past by careful photometric observers. I will use Gehrels' published magnitudes rather than my rereductions.

Table A9: Comparison star identifications for Gehrels (1956)

Published Comparison Star			SIMBAD	
Label	Ident	*V*	Position	*V*
C I	BD +0° 2875	9.139	12 00 24.22 –00 41 30.3	9.18
A I	BD –1° 2639	8.056	12 16 44.09 –02 44 22.4	8.04
A II	BD –1° 2648	9.340	12 19 24.21 –02 13 50.3	9.31
B I	BD –0° 2550	9.769	12 14 10.58 –01 38 31.7	9.71
B II	BD –1° 2633	9.893	12 25 08.67 –02 10 02.7	9.75
C II	BD +0° 2884	10.034	12 02 39.91 –00 23 22.0	10.23
D I	BD +0° 2864	9.963	11 57 24.02 +00 06 49.8	9.98
D II	BD +0° 2861	11.031	11 56 48.98 +00 04 51.3	11.03
E I	BD +1° 2625	10.151	11 54 04.80 +00 20 20.8	10.19

Groeneveld and Kuiper (1954) presented light curves for 12 minor planets, but no information on the comparison stars is given. The zero points of the light-curve plots are given, but no information is provided as to the absolute value of the zero point, so it is not possible to correct the observations.

Müller (1893) gives sufficient information on the comparison stars and the minor-planet observations to allow rereduction of his observations. These observations are not present on the APC CD-ROM. The comparison stars are listed in Table A10: Bayer-designated stars are given first, followed by Flamsteed designations and BD designations. The published *V* values are given in the third column, with the SIMBAD values in the fourth column. Six of the comparison stars used by Müller are (possibly) variable (Samus and Durlevich, 2005): χ Aqr is a semiregular red giant with an amplitude of 0.35 mag.; V2125 Oph is an α^2 Canum Venaticorum variable with an amplitude of 0.04 mag.; NSV 6297 is a variable of unknown type with an amplitude of 0.07 mag.; NSV 487 is a possible variable of unknown type and unknown amplitude; CF Psc is a comparatively long-period pulsating B star with an amplitude of 0.03 mag.; and NSV 8142 is a variable of unknown type with an amplitude of 0.09 mag. The variable nature of most of these can safely be ignored, with the exception of χ Aqr, which is rejected as a comparison star because of its large amplitude.

Table A10: Comparison star identifications for Müller (1893)

Comparison	J2000.0		Publ. *V*	*V*	Note
	R.A.	Decl.			
θ Vir	13 09 56.99	–05 32 20.4	4.46	4.381	
λ Cet	02 59 42.90	+08 54 26.5	4.78	4.701	
π Vir	12 00 52.39	+06 36 51.7	4.63	4.659	
σ Ari	02 51 29.59	+15 04 55.4	5.45	5.514	
χ Aqr	23 16 50.94	–07 43 53.4	5.06	var.	4.75–5.10*V*
11 Vir	12 10 03.42	+05 48 25.2	5.69	5.71	
32 Aqr	22 04 47.42	–00 54 22.8	5.23	5.285	
40 Aur	06 06 35.10	+38 28 57.5	5.22	5.353	
52 Oph	17 35 18.50	–22 02 37.8	6.56	6.478	= V2125 Oph
58 Oph	17 43 25.79	–21 40 59.5	4.84	4.873	
59 Vir	13 16 46.52	+09 25 27.0	5.09	5.22	
60 Cnc	08 55 55.55	+11 37 33.7	5.36	5.452	
74 Vir	13 31 57.88	–06 15 20.9	4.81	4.69	= NSV 6297
78 Aqr	22 54 34.12	–07 12 16.6	6.33	6.194	
80 Vir	13 35 31.30	–05 23 46.3	5.73	5.715	
81 Gem	07 46 07.45	+18 30 36.2	5.17	4.884	
BD –5° 101	00 40 42.37	–04 21 06.6	5.81	5.905	
BD –4° 4376	17 56 47.74	–04 04 54.6	5.41	5.453	
BD –4° 5568	21 54 10.37	–04 16 34.2	5.74	5.716	
BD –1° 179	01 22 34.83	–00 26 58.8	6.59	6.499	= NSV 487
BD –0° 258	01 40 07.02	–00 14 32.3	7.43	7.28	
BD +0° 3529	16 28 33.98	+00 39 54.0	5.61	5.401	
BD +1° 108	00 38 00.55	+02 45 49.1	7.87	7.68	
BD +3° 46	00 26 16.50	+03 49 32.7	7.08	6.86	= CF Psc
BD +10° 2516	13 09 12.44	+10 01 20.9	5.85	5.798	
BD +14° 3179	17 03 07.87	+14 05 31.0	5.08	5.000	= NSV 8142
BD +17° 1191	06 16 23.79	+17 10 53.8	6.48	6.398	
BD +17° 4999	23 53 00.92	+17 53 59.2	6.59	6.582	
BD +17° 5001	23 53 54.23	+17 59 30.3	7.15	7.196	
BD +19° 876	05 15 11.61	+20 03 21.9	7.68	7.72	
BD +19° 893	05 19 14.69	+20 08 04.6	6.05	6.10	
BD +20° 885	05 07 48.40	+20 25 06.2	5.15	5.292	

Scaltriti and Zappalà (1975) gave the designations of the comparison stars used, but omitted mention of what magnitudes they used for those stars. Neither do they give offsets from the comparison stars to the means/maxima/zero-points shown in the plots.

Scaltriti and Zappalà (1976) give the designations and magnitudes of the comparison stars used. These are identified in Table A11 [p. 246], with a reminder that asterisked magnitudes are taken from SIMBAD:

Table A11: Comparison star identifications for Scaltriti and Zappalà (1976)

Star	Publ. *V*	Position	*V*
BD +1° 3301	10.23	16 46 46.13 +01 11 54.4	10.13*
BD +3° 3266	9.50	16 45 56.67 +02 46 37.3	9.45*
BD +3° 3264	9.89	16 45 07.93 +03 12 17.7	9.82*
BD +7° 3181	10.61	16 28 11.03 +06 46 52.2	10.52*
BD +7° 3177	11.01	16 27 05.06 +06 55 18.1	10.98
BD +7° 3157	10.38	16 22 46.98 +06 59 26.6	10.30*
BD −4° 4270	10.42	17 22 44.97 −04 12 39.4	10.18

Comparison star BD +7° 3177 was not present in SIMBAD and there seemed to be no bright star at the coordinates derived from the BD catalogue. I noted the presence of a bright star, without a BD identifier, at an offset of -10^s in R.A. and +3.6′ in Decl. The *V* magnitude of this candidate extracted from the CDPC (*V* = 10.98) was in excellent agreement with the published *V* magnitude (*V* = 11.01), so I adopted the identification with BD +7° 3177 for Table A11.

The comparison stars for Schober (1979) are listed in Table A12.

Table A12: Comparison star identifications for Schober (1979)

Star	Publ. *V*	Position	*V*
CD −23° 17809	9.51	23 15 19.94 −22 27 48.7	9.48*
CD −33° 16158	10.88	23 44 56.14 −33 46 13.6	10.9 *

Schober *et al.* (1979) list comparison star information but do not supply mean magnitudes, magnitudes ranges or amplitudes in tabular form for the minor planets under study. Nightly lightcurves for the three minor planets are provided, supposedly showing the differences minor planet minus comparison star. However, this was not consistent with the labelling of the axes of the plots. In order to figure out what was actually being plotted required examination of the predicted *V* or *B* magnitude at the time of observation with the *V* or *B* magnitude of the comparison star. Because of the confusion caused by the plot labelling, in Table A13 I list the mean differences (minor planet minus comparison star, as intended) that I derived from the lightcurves. Table A14 lists the comparison star identifications (for the two stars published as "uncatalogued", and for BD +12° 82, I include identifications from the Tycho catalogue).

Table A13: Mean differences minor planet minus comparison star from Schober et al. (1979)

Object	Obs. Date	Difference	Object	Obs. Date	Difference
(49)	1977 Nov. 18	–0.27	(88)	1977 Aug. 25	+0.63
	1977 Nov. 19	–0.24		1977 Sept. 24	+0.83
	1977 Nov. 20	–0.21		1977 Oct. 3	+1.21
(92)	1977 Dec. 10	+0.11		1977 Oct. 10	+0.22
	1977 Dec. 14	+0.12		1977 Oct. 11	+0.19
	1977 Dec. 15	+0.08			
	1977 Dec. 16	+0.09			

Table A14: Comparison star identifications for Schober et al. (1979)

Star (Publ. B1950)	Id. B1950.0	Id. J2000.0	Id. *V*	Note
A (03 06 +22 01)	03 06.3 +22 02	03 09 13.99 +22 13 09.5	10.89	TYC 1231-488-1
B (05 19 +17 32)	05 19.4 +17 40	05 22 21.00 +17 42 20.9	10.83	TYC 1300-2203-1
BD +12° 82	00 41.0 +13 05	00 43 38.45 +13 21 22.7	10.21*	TYC 610-984-1
BD +11° 49	00 20.3 +11 49	00 22 53.41 +12 05 52.5	9.51*	
BD +10° 23	00 14.5 +10 56	00 17 04.88 +11 13 07.2	9.04*	
BD +11° 21	00 11.9 +12 06	00 14 32.31 +12 22 55.0	10.10*	B = 10.86*

There were a number of other problems with the Schober *et al.* (1979) paper:

- The published coordinates for comparisons A and B were extremely rough. Neither object was listed in the *Bonner Durchmusterung*, according to the paper's authors. Searches using SIMBAD's coordinate query tool in a 10′-radius around each of the published positions (precessed to J2000.0) produced only one candidate for each comparison star. These candidates are listed in Table A14. The discordance in the B1950.0 position of candidate B is 8′ in Declination, which is large even for a rough position. Examination using Google Sky of the region around the candidate for comparison A showed that identification to be firm. A similar examination of the region around the candidate for comparison B showed a second possible candidate: HD 243083 = BD +17° 916, V = 9.67, J2000 position $05^h22^m54^s.97$ +17°37′57″.2; B1950.0 position $05^h20^m00^s.30$ +17°35′10″.4. While closer in Declination, this candidate was rejected because it is too bright and because it is in the *Bonner Durchmusterung* (a contradiction to the authors' published statement).
- While identifying the comparison stars using SIMBAD, I noticed that BD +12° 82 was not found using the identifier query tool. A quick search showed that stars such as

BD +12° 81 and BD +12° 83 were listed in SIMBAD. To figure out why BD +12° 82 was missing, I extracted the B1855.0 position ($00^h36^m05^s.6$ +12°33'.8) from a digital version of the BD catalogue, precessed the position to J2000.0 ($00^h43^m38^s.9$ +13°21'.5) and used it as input to SIMBAD's coordinate query tool. One object was returned: TYC 610-984-1 with J2000.0 position $00^h43^m38^s.45$ +13°21'22".7. A check of Google Sky showed that this object was the only candidate of that brightness within 15' of the stated position, suggesting that BD +12° 82 = TYC 610-984-1. I adopted this identification in Table A14 and contacted the SIMBAD help desk via e-mail to report the problem. A reply was received within 12 hours (Ochsenbein, 2009) explaining that BD/CD/CPD designations were not yet fully integrated into SIMBAD. A subsequent check showed the BD +12° 82 identifier has since been inserted into the SIMBAD database.

Taylor *et al.* (1971) give rough B1950.0 coordinates for the comparison stars as well as *V* magnitudes and *B–V* colours. The observing locations are missing from the APC file. Identifications for the comparison stars are provided in Table A15 [p. 248].

Table A15: Comparison star identifications for Taylor et al. (1971)

	Publ. B1950.0	Publ. *V*	Identification	B1950.0	J2000.0	*V*
A	04 26.1 +21 02	11.690	223.014884	04 26.1 +21 00	04 29 03.45 +21 06 38.7	11.66
B	04 16.2 +21 11	8.181	223.014141	04 16.1 +21 11	04 19 01.39 +21 17 55.6	8.20*
C	04 11.8 +21 29	11.802	224.013896	04 11.7 +21 30	04 14 38.44 +21 37 26.1	11.75
D	04 04.6 +21 22	11.652	224.013470	04 04.6 +21 24	04 07 35.44 +21 31 39.3	11.75
E	04 01.8 +21 22	11.243	223.013243	04 01.7 +21 21	04 04 40.09 +21 29 05.8	10.87
F	03 56.0 +21 08	12.504	223.012827	03 56.2 +21 13	03 59 11.29 +21 21 56.1	12.45
G	03 52.3 +21 08	11.972	223.012551	03 52.4 +21 08	03 55 17.16 +21 16 14.7	11.93
H	03 49.4 +21 19	9.486	223.012347	03 49.4 +21 19	03 52 18.53 +21 28 17.6	9.57*
I	03 41.8 +20 53	11.718	223.011746	03 41.7 +20 53	03 44 35.92 +21 02 02.4	11.74
J	03 30.2 +21 19	13.492	223.010979	03 29.9 +21 19	03 32 46.97 +21 29 12.1	13.22

The agreement between the published and CDPC/SIMBAD *V* magnitudes is generally within 0.1 mag. For comparison star E there is a discordance of 0.37 mag and for comparison star J a discordance of 0.27 mag. In both cases, the published *B–V* colours (+1.030 and +0.782, respectively) agree well with the CDPC *B–V* colours (+1.17 and +0.74, respectively). The largest B1950.0 positional discordance occurs for comparison star F. No suitable UCAC-2 candidate was

found within 5′ of the published coordinates. A broader search was performed, assuming that either the α or δ was incorrect by a small amount. The given candidate, found at a δ offset of +5′, has a CDPC *B–V* colour of +0.61, which is in broad agreement with the published *B–V* colour, +0.711.

Weidenschilling *et al.* (1987) give reduced maximum and minimum magnitudes from 257 lightcurves of 26 objects. A follow-up paper (Weidenschilling *et al.*, 1990) gives magnitudes derived from 107 lightcurves of 59 objects. Unfortunately, in many cases the quoted magnitude ranges are applied to a range of dates so the mean magnitude cannot be associated with a specific date of observation. Photometric data from this reference can be used only where there is a single date associated with the magnitude range, reducing the counts of useful data points in the two papers from 257 to 86 and from 107 to 33.

Wisniewski (1987) gives single *V* determinations for six NEAs, but fails to document whether the published *V* values are mean or maximum values. A number of the objects observed have amplitudes exceeding 0.2 magnitudes, making the inclusion of these data unwise.

8: Determining Minor-Planet Albedos

The spectrum of a minor planet beyond (i.e., at wavelengths longer than) 5 μm is dominated by thermal emission from the object, while the spectrum below (i.e., at wavelengths shorter than) 2.5 μm is dominated by reflected solar radiation (see, e.g., Lebofsky and Spencer, 1989). The transition from reflected solar radiation to thermal emission occurs between 2.5 and 5 μm, and the wavelength at which this occurs depends on the heliocentric distance, albedo, and other physical properties of the object. A large dark (low albedo) minor planet may appear visually to be the same brightness as a small reflective (high albedo) minor planet. In the thermal-emission region, the large dark object will show much greater emission as it is both warmer and larger than the small object. A minor planet's albedo is determined by combining observations made in the thermal infrared region with observations of the object's visual brightness. A thermal model, which describes how a planetary body responds to solar radiation, is required to relate thermal-emission observations to physical parameters.

Simple thermal models assume a regular geometry (usually a spherical geometry) and idealized values for physical parameters. The refined Standard Thermal Model (STM) of Lebofsky *et al.* (1986) assumes instantaneous equilibrium between the solar insolation and the thermal emission, as well as a non-rotating spherical body. The STM was found to not be a good fit for some small near-Earth minor planets, as it gave albedos that were too high. Such objects are better fit by the Fast Rotating Model (FRM) of Lebofsky and Spencer (1989), which also assumes the insolation/thermal emission balance and a spherical body. Further assumptions are that the object is rotating rapidly, is very cold or has an extremely rock surface, meaning that there is no longitude variation in surface temperature. The variation in surface temperature depends only on the latitude. While appropriate for main-belt objects, the use of the STM and FRM models on irregularly-shaped near-Earth objects can be problematic due to the assumptions inherent in those models. The Near-Earth Asteroid Thermal Model (NEATM, Harris, 1998) made simple modifications to the STM/FRM to handle small near-Earth objects, which were expected to have rockier, less dusty surfaces than main-belt objects. The Night Emission Simulated Thermal Model (NESTM, Wolters and Green, 2009) assumes that the thermal emission on the night side of an object is non-zero.

Thermophysical models make fewer assumptions than simple thermal models, replacing the ideal sphere with detailed shape models and considering detailed physical properties of the surface. Shapes are modelled as a number (typically several thousand) of discrete surface elements and effects such as shadowing and heat conduction are considered. An example of a thermophysical models include and the Advanced Thermophysical Model (ATPM, Rozitis and Green, 2011), which incorporates partial shadowing, scattering, self-heating and infrared re-radiation of absorbed sunlight due to surface roughness.

A full discussion of the methods of albedo determination is outside the scope of this thesis. Details may be found in the papers listed here and the references there-in.

References

Where possible, the papers referenced here are URL-linked to the corresponding ADS entries. This feature works only in those PDF readers that support URL linking. The journal abbreviations adhere to the IAU guidelines (`www.iau.org/science/publications/proceedings_rules/abbreviations/`) and the list of abbreviations given in *Astronomy and Astrophysics Abstracts*. Foreign language titles are given first in their original language, followed by an English translation.

Abazajian *et al.*, 2009 : K. N. Abazajian, J. K. Adelman-McCarthy, M. A. Agüeros, S. S. Allam, C. Allende Prieto, D. An, K. S. J. Anderson, S. F. Anderson, J. Annis, N. A. Bahcall, C. A. L. Bailer-Jones, J. C. Barentine, B. A. Bassett, A. C. Becker, T. C. Beers, E. F. Bell, V. Belokurov, A. A. Berlind, E. F. Berman, M. Bernardi, S. J. Bickerton, D. Bizyaev, J. P. Blakeslee, M. R. Blanton, J. J. Bochanski, W. N. Boroski, H. J. Brewington, J. Brinchmann, J. Brinkmann, R. J. Brunner, T. Budavári, L. N. Carey, S. Carliles, M. A. Carr, F. J. Castander, D. Cinabro, A. J. Connolly, I. Csabai, C. E. Cunha, P. C. Czarapata, J. R. A. Davenport, E. de Haas, B. Dilday, M. Doi, D. J. Eisenstein, M. L. Evans, N. W. Evans, X. Fan, S. D. Friedman, J. A. Frieman, M. Fukugita, B. T. Gänsicke, E. Gates, B. Gillespie, G. Gilmore, B. Gonzalez, C. F. Gonzalez, E. K. Grebel, J. E. Gunn, Z. György, P. B. Hall, P. Harding, F. H. Harris, M. Harvanek, S. L. Hawley, J. J. E. Hayes, T. M. Heckman, J. S. Hendry, G. S. Hennessy, R. B. Hindsley, J. Hoblitt, C. J. Hogan, D. W. Hogg, J. A. Holtzman, J. B. Hyde, S. Ichikawa, T. Ichikawa, M. Im, Ž. Ivezić, S. Jester, L. Jiang, J. A. Johnson, A. M. Jorgensen, M. Jurić, S. M. Kent, R. Kessler, S. J. Kleinman, G. R. Knapp, K. Konishi, R. G. Kron, J. Krzesinski, N. Kuropatkin, H. Lampeitl, S. Lebedeva, M. G. Lee, Y. S. Lee, R. F. Leger, S. Lépine, N. Li, M. Lima, H. Lin, D. C. Long, C. P. Loomis, J. Loveday, R. H. Lupton, E. Magnier, O. Malanushenko, V. Malanushenko, R. Mandelbaum, B. Margon, J. P. Marriner, D. Martínez-Delgado, T. Matsubara, P. M. McGehee, T. A. McKay, A. Meiksin, H. L. Morrison, F. Mullally, J. A. Munn, T. Murphy, T. Nash, A. Nebot, E. H. Neilsen, H. J. Newberg, P. R. Newman, R. C. Nichol, T. Nicins. J. Oravetz, J. P. Ostriker, R. Owen, N. Padmanabhan, K. Pan, C. Park, G. Pauls, J. Peoples, W. J. Percival, J. R. Pier, A. C. Pope, D. Pourbaix, P. A. Price, N. Purger, T. Quinn, M. J. Raddick, P. R. Fiorentin, G. T. Richards, M. W. Richmond, A. G. Riess, H.-W. Rix, C. M. Rockosi, M. Sako, D. J. Schlegel, D. P. Schneider, R.-D. Scholz, M. R. Schreiber, A. D. Schwope, U. Seljak, B. Sesar, E. Sheldon, K. Shimasaku, V. C. Sibley, A. E. Simmons, T. Sivarani, J. A. Smith, M. C. Smith, V. Smolćić, S. A. Snedden, A. Stebbins, M. Steinmetz, C. Stoughton, M. A. Strauss, M. Subba Rao, Y. Suto, A. S. Szalay, I. Szapudi, P. Szkody, M. Tanaka, M. Tegmark, L. F. A. Teodoro, A. R. Thakar, C. A. Tremonti, D. L. Tucker, A. Uomoto, D. E. Vanden Berk, J. Vandenberg, S. Vidrih, M. S. Vogeley, W. Voges, N. P. Vogt, Y. Wadadekar, S. Watters, D. H. Weinberg, A. A. West, S. D. M. White, B. C. Wilhite, A. C. Wonders, B. Yanny, D. R. Yocum, D. G. York, I. Zehavi, S. Zibetti and D. B. Zucker, 2009, "The Seventh Data Release of the Sloan Digital Sky Survey", *Astrophys. J.* **182**, 543–558. [2009ApJS..182..543A]

Ahmad, 1954 : I. I. Ahmad, 1954, "Photometric Studies of Asteroids. IV. The Light-Curves of Ceres, Hebe, Flora, and Kalliope", *Astrophys. J.* **120**, 551–559. [1954ApJ...120..551A]

Angeli *et al.*, 2001 : C. A. Angeli, T. A. Guimarães, D. Lazzaro, R. Duffard, S. Fernández, M. Florczak, T. Mothé-Diniz, J. M. Carvano and A. S. Betzler, 2001, "Rotation Periods for Small Main-Belt Asteroids from CCD Photometry", *Astron. J.* **121**, 2245–2252. [2001AJ....121.2245A]

Aksenov *et al.*, 1987 : A. N. Aksenov, Y. A. Egorov, V. G. Teigel' and G. A. Kharitonova, 1987, "Period of Rotation of Asteroid 4 Vesta", *Sov. Astron. Lett.* **13**, 257–259. [1987SvAL...13..257A]

Argelander, 1837 : F. Argelander, 1837, "Auszug aus einem Schreiben der Herrn Professors Argelander, Directors der Sternwarte in Helsingfors, an den Herausgeber" ["Extract from a Letter from Prof. Argelander, Director of the Helsingfors Observatory, to the Editor"], *Astron. Nachr.* **14**, 203–206. [1837AN.....14..203A]

Argelander, 1855a : F. Argelander, 1855, "Über die Helligkeiten der kleinen Planeten" ["On the Brightness of the Minor Planets"], *Astron. Nachr.* **41**, 337–342. [1855AN.....41..337A]

Argelander, 1855b : F. Argelander, 1855, "Vorschlag zu Beobachtungen über die Helligkeiten der kleinen Planeten" ["Proposals for the Observation of the Brightness of Minor Planets"], *Astron. Nachr.* **42**, 177–186. [1855AN.....42..177A]

Baker and Warner, 2011 : R. E. Baker and B. D. Warner, 2011, "Photometric Observations and Analysis of 604 Tekmessa", *Minor Planet Bull.* **38**, 195–197. [2011MPBu...38..195B]

Baker *et al.*, 2010 : R. E. Baker, V. Benishek, F. Pilcher and D. Higgins, 2010, "Rotation Period and *H-G* Parameters Determination for 1700 Zvezdata: A Collaborative Photometry Project", *Minor Planet Bull.* **37**, 81–83. [2010MPBu...37...81B]

Baker *et al.*, 2011 : R. E. Baker, F. Pilcher and V. Benishek, 2011, "Photometric Observations and Analysis of 1082 Pirola", *Minor Planet Bull.* **38**, 111–114 [2011MPBu...38..111B]

Baker *et al.*, 2012 : R. E. Baker, F. Pilcher and D. A. Klinglesmith III, 2012, "Rotation Period and *H-G* Parameters Determination for 1188 Gothlandia", *Minor Planet Bull.* **39**, 60–63. [2012MPBu...39...60B] Also *Minor Planet Circ.* 79428. [2012MPC..79428...1B]

Barnard, 1895 : E. E. Barnard, 1895, "Micrometrical Determinations of the Diameters of the Minor Planets Ceres (1), Pallas (2), Juno (3) and Vesta (4), Made With the Filar Micrometer of the 36-inch Equatorial of the Lick Observatory, and on the Albedos of those Planets", *Mon. Not. R. Astron. Soc.* **56**, 55–63. [1895MNRAS..56...55B]

Barucci, 2009 : M. A. Barucci, 2009, personal communication, e-mail dated 2009 Jan. 4.

Barucci and Di Martino, 1984 : M. A. Barucci and M. Di Martino, 1984, "Rotational Rates of Very Small Asteroids: 123 Brunhild, 376 Geometria, 437 Rhodia and 1224 Fantasia", *Astron. Astrophys. Suppl.* **57**, 103–106. [1984A&AS...57..103B]

Barucci and Dipaoloantonio, 1983 : M. A. Barucci and A. Dipaoloantonio, 1983, "A Check for the Pole Coordinates of Asteroid 22 Kalliope", *Astron. Astrophys.* **117**, 1–2. [1983A&A...117....1B]

Barucci *et al.*, 1985 : M. A. Barucci, M. Fulchignoni, R. Burchi and V. D'Ambrosio, 1985, "Rotational Properties of Ten Main Belt Asteroids: Analysis of the Results Obtained by Photoelectric Photometry", *Icarus* **61**, 152–162. [1985Icar...61..152B]

Barucci *et al.*, 1986 : M. A. Barucci, D. Bockelee-Morvan, A. Brahic, S. Clairemidi, J. Lecacheux and F. Roques, 1986, "Asteroid Spin Axes: Two Additional Pole Determinations and Theoretical Implications", *Astron. Astrophys.* **163**, 261–268. [1986A&A...163..261B]

Barucci *et al.*, 1992 : M. A. Barucci, M. Di Martino and M. Fulchignoni, 1992, "Rotational Properties of Small Asteroids: Photoelectric Observations", *Astron. J.* **103**, 1679–1686. [1992AJ....103.1679B]

Barucci *et al.*, 1994 : M. A. Barucci, M. Di Martino, E. Dotto, M. Fulchignoni, A. Rotundi and R. Burchi, 1994, "Rotational Properties of Small Asteroids: Photoelectric Observations of 16 Asteroids", *Icarus* **109**, 267–273. [1994Icar..109..267B]

Bauer *et al.*, 2001 : J. M. Bauer, K. J. Meech, T. C. Owen, T. L. Roush and S. E. Dahm, 2001, "Chiron's Spectrum at Outburst", *Bull. Amer. Astron. Soc.* **33**, 1048. [2001DPS....33.1212B]

Behrend 2011 : R. Behrend, 2011, `http://obswww.unige.ch/~behrend/page_cou.html`

Belskaya and Dovgopol, 1992 : I. N. Belskaya and A. N. Dovgopol, 1992, "Asteroids With Unusual Lightcurves: 14 Irene and 51 Nemausa", in *Asteroids, Comets, Meteors 1991*, 45–48. [1992acm..proc...45B]

Belskaya *et al.*, 1993 : I. N. Belskaya, A. N. Dovgopol, A. Erikson, C.-I. Lagerkvist and T. Oja, 1993, "Physical Studies of Asteroids. XXVII. Photoelectric Photometry of Asteroids 14 Irene, 54 Alexandra and 56 Melete", *Astron. Astrophys. Suppl.* **101**, 507–511. [1993A&AS..101..507B]

Belskaya *et al.*, 2009 : I. N. Belskaya, S. Fornasier and Yu. N. Krugly, 2009, "Polarimetry and *BVRI* Photometry of the Potentially Hazardous Near-Earth Asteroid (23187) 2000 PN_9", *Icarus* **201**, 167–171. [2009Icar..201..167B]

Bertin and Arnouts, 1996 : E. Bertin and S. Arnouts, 1996, "SExtractor: Software for Source Extraction", *Astron. Astrophys. Suppl.* **117**, 393–404. [1996A&AS..117..393B]

Beshore, 2007 : E. Beshore, 2007, personal communication, e-mail dated 2007 March 27.

Beshore, 2008 : E. Beshore, 2008, personal communication, e-mail dated 2008 January 23.

Bessell, 1990 : M. S. Bessell, 1990, "*UBVRI* Passbands", *Publ. Astron. Soc. Pac.* **102**, 1181–1199. [1990PASP..102.1181B]

Betzler and Novaes, 2008 : A. S. Betzler and A. B. Novaes, 2008, "Colors of Potentially Hazardous Asteroids 2005 WJ_{56} and 2007 TU_{24}", *Minor Planet Bull.* **35**, 108–109. [2008MPBu...35..108B]

Betzler *et al.*, 2010 : A. S. Betzler, A. B. Novaes, A. C. P. Santos and E. G. Sobral, 2010, "Photometric Observations of the Near-Earth Asteroid 1999 AP_{10}, 2000 TO_{64}, 2000 UJ_1, 2000 XK_{44}, 2001 MZ_7, 2003 QO_{104}, 2005 RQ_6, 2005 WJ_{56} and 2009 UN_3", *Minor Planet Bull.* **37**, 95–97. [2010MPBu...37...95B]

Binzel, 1984 : R. P. Binzel, 1984, "2 Pallas:1982 and 1983 Lightcurves and a New Pole Solution", *Icarus* **59**, 456–461. [1984Icar...59..456B]

Binzel, 1985 : R. P. Binzel, 1985, "Is 1220 Crocus a Precessing, Binary Asteroid?", *Icarus* **63**, 99–108. [1985Icar...63...99B]

Binzel, 1991 : R. P. Binzel, 1991, "The Origins of the Asteroids", *Sci. Am.* **265**, No. 4, 88–94. [1991SciAm.265...88B]

Binzel and Tholen, 1983 : R. P. Binzel and D. J. Tholen, 1983, "The Rotation, Color, Phase Coefficient and Diameter of 1915 Quetzalcoatl", *Icarus* **55**, 495–497. [1983Icar...55..495B]

Binzel *et al.*, 1987 : R. P. Binzel, A. L. Cochran, E. S. Barker, D. J. Tholen, A. Barucci, M. Di Martino, R. Greenberg, S. J. Weidenschilling, C. R. Chapman and D. R. Davis, 1987, "Coordinated Observations of Asteroids 1219 Britta and 1972 Yi Xing", *Icarus* **71**, 148–158. [1987Icar...71..148B]

Birch *et al.*, 1983 : P. V. Birch, E. F. Tedesco, R. C. Taylor, R. P. Binzel, C. Blanco, S. Catalano, P. Hartigan, F. Scaltriti, D. J. Tholen and V. Zappalà, 1983, "Lightcurves and Phase Function of Asteroids 44 Nysa during its 1979 Apparition", *Icarus* **54**, 1–12. [1983Icar...54....1B]

Birlan *et al.*, 1996 : M. Birlan, M. A. Barucci, C. A. Angeli, A. Doressoundiram and M. C. De Sanctis, 1996, "Rotational Properties of Asteroids: CCD Observations of Nine Small Asteroids", *Planet. Space Sci.* **44**, 555–558. [1996P&SS...44..555B]

Blanco and Riccioli, 1999 : C. Blanco and D. Riccioli, 1999, "*V* Lightcurves and *B-V* Colour of Main-Belt Asteroids", in *Evolution and Source Regions of Asteroids and Comets*, 175–184. [1999esra.conf..175B]

Bobrovnikoff, 1929 : N. T. Bobrovnikoff, 1929, "The Spectra of Minor Planets", *Lick Obs. Bull.* **14**, 18–27. [1929LicOB..14...18B]

Bodewits *et al.*, 2011 : D. Bodewits, M. S. Kelley, J.-Y. Li, W. B. Landsman, S. Besse and M. F. A'Hearn, 2011, "Collisional Excavation of Asteroid (596) Scheila", *Astrophys. J.* **733**, L3. [2011ApJ...733L...3B]

Borošová, 1991 : J. Borošová, 1991, "Photometric Observations of 18 Melpomene", *Contrib. Astron. Obs. Skalnate Pleso* **21**, 333–338. [1991CoSka..21..333B]

Bottke *et al.*, 2002 : W. F. Bottke Jr., D. Vokrouhlický, D. P. Rubincam and M. Broz, 2002, "The Effect of Yarkovsky Thermal Forces on the Dynamical Evolution of Asteroids and Meteoroids", in *Asteroids III*, 395–408. [2002aste.conf..395B]

Bottke *et al.*, 2005 : W. F. Bottke Jr., D. D. Durda, D. Nesvorný, R. Jedicke, A. Morbidelli, D. Vokrouhlický and H. F. Levison, 2005, "Linking the Collisional History of the Main Asteroid Belt to its Dynamical Excitation and Depletion", *Icarus* **179**, 63–94. [2005Icar..179...63B]

Bowell and Lumme, 1979 : E. Bowell and K. Lumme, 1979, "Colorimetry and Magnitudes of Asteroids", in *Asteroids*, 132–169. [1979aste.book..132B]

Bowell *et al.*, 1978 : E. Bowell, C. R. Chapman, J. C. Gradie, D. Morrison and B. Zellner, 1978, "Taxonomy of Asteroids", *Icarus* **35**, 313–335. [1978Icar...35..313B]

Bowell *et al.*, 1989 : E. Bowell, B. Hapke, D. Domingue, K. Lumme, J. Peltoniemi and A. W. Harris, 1989, "Application of Photometric Models to Asteroids", in *Asteroids II*, 524–556. [1989aste.conf..524B]

Bowell *et al.*, 1994 : E. Bowell, K. Muinonen and L. H. Wasserman, 1994, "A Public-Domain Asteroid Orbit Database", in *Asteroids, Comets, Meteors 1993*, 477–481. [1994IAUS..160..477B]

Bower, 1924 : E. C. Bower, 1924, "On Provisional Designations of Asteroids", *Astron. Nachr.* **223**, 149. [1924AN....223..149B]

Britt and Consolmagno, 2004 : D. T. Britt and G. J. Consolmagno, 2004, "Meteorite Porosities and Densities: A Review of Trends in the Data", *LPI Sci. Conf. Abstr.* **35**, 2108. [2004LPI....35.2108B]

Britt and Lebofsky, 1997 : D. T. Britt and L. A. Lebofsky, 1997, "Asteroid Compositional Structure and Taxonomy", in *Encyclopedia of Planetary Sciences*, 33–35, Chapman & Hall, London.

Brouwer, 1949 : D. Brouwer, 1949, "Index of Minor Planet Observations", *Minor Planet Circ.* 191. [1949MPC....191...1B]

Brouwer, 1951 : D. Brouwer, 1951, "Secular Variations of the Orbital Elements of Minor Planets", *Astron. J.* **56**, 9–32. [1951AJ.....56....9B]

Bucciarelli *et al.*, 2001 : B. Bucciarelli, J. García Yus, R. Casalegno, M. Postman, B. M. Lasker, C. Sturch, M. G. Lattanzi, B. J. McLean, E. Costa, A. Falasca, R. Le Poole, G. Massone, M. Potter, A. Rosenberg, T. Borgman, J. Doggett, J. Morrison, A. Pizzuti, E. Pompei, D. Rehner, L. Siciliano and D. Wolfe, 2001, "An All-Sky Set of *(B)-V-R* Photometric Calibrators for Schmidt Surveys. GSPC2.1: First Release", *Astron. Astrophys.* **368**, 335–346. [2001A&A...368..335B]

Buchheim, 2005 : R. K. Buchheim, 2005, "Asteroid Photometry Reports from Altamira Observatory—Winter 2004–2005", *Minor Planet Bull.* **32**, 79–80. [2005MPBu...32...79B]

Buchheim, 2006 : R. K. Buchheim, 2006, "Photometry of Asteroids 133 Cyrene, 454 Mathesis, 477 Italia and 2264 Sabrina", *Minor Planet Bull.* **33**, 29–30. [2006MPBu...33...29B]

Buchheim and Pray, 2005 : R. K. Buchheim and D. P. Pray, 2005, "Lightcurve of 755 Quintilla", *Minor Planet Bull.* **32**, 1. [2005MPBu...32....1B]

Buchheim *et al.*, 2004 : R. K. Buchheim, M. Conjat, R. Roy, P. Baudoin and R. Behrend, 2004, "A Photometric Study of 371 Bohemia", *Minor Planet Bull.* **31**, 90–91. [2004MPBu...31...90B]

Buie and Bus, 1992 : M. W. Buie and S. J. Bus, 1992, "Physical Observations of (5145) Pholus", *Icarus* **100**, 288–294. [1992Icar..100..288B]

Bus and Binzel, 2002 : S. J. Bus and R. P. Binzel, 2002, "Phase II of the Small Main-Belt Asteroid Spectroscopic Survey: A Feature-Based Taxonomy", *Icarus* **158**, 146–177. [2002Icar..158..146B]

Bus *et al.*, 1987 : S. J. Bus, E. Bowell and A. W. Harris, 1987, "2060 Chiron: CCD Photometry", *Bull. Amer. Astron. Soc.* **19**, 851. [1987BAAS...19Q.851B]

Bus *et al.*, 1989 : S. J. Bus, E. Bowell, A. W. Harris and A. V. Hewitt, 1989, "2060 Chiron: CCD and Electronographic Photometry", *Icarus* **77**, 223–238. [1989Icar...77..223B]

Bus *et al.*, 2002 : S. J. Bus, F. Vilas and M. A. Barucci, 2002, "Visible-Wavelength Spectroscopy of Asteroids", in *Asteroids III*, 169–182. [2002aste.conf..169B]

Carbognani, 2008 : A. Carbognani, 2008, "Lightcurve Photometry of NEAs 4450 Pan, (170891) 2004 TY_{16}, 2002 RC_{118} and 2007 VD_{12}", *Minor Planet Bull.* **35**, 109–110. [2008MPBu...35..109C]

Carbognani *et al.*, 2008 : A. Carbognani, P. Pravec, Yu. N. Krugly, D. P. Pray, Š. Gajdoš, N. M. Gaftonyuk and I. Slyusarev, 2008, "Lightcurve Photometry and Search for Cometary Activity of NEA 2007 PU_{11}", *Minor Planet Bull.* **35**, 61–62. [2008MPBu...35...61C]

Carlsson and Lagerkvist, 1981a : M. Carlsson and C.-I. Lagerkvist, 1981, "Physical Studies of Asteroids. I : Photoelectric Observations of the Asteroids 38, 218, 268, 344, 485, 683, 690 and 792", *Astron. Astrophys. Suppl.* **44**, 14–22. [1981A&AS...44...15C]

Carlsson and Lagerkvist, 1981b : M. Carlsson and C.-I. Lagerkvist, 1981, "Physical Studies of Asteroids IV: Photoelectric Observations of the Asteroids 47, 95, 431", *Astron. Astrophys. Suppl.* **45**, 1–4. [1981A&AS...45....1C]

Carvano and Lazarro, 2010 : J. M. Carvano and D. Lazzaro, 2010, "Diameter, Geometric Albdeo and Compositional Constraints for (298) Baptistina Through Visible and Mid-Infrared Photometry", *Mon. Not. R. Astron. Soc.* **404**, L31–L34. [2010MNRAS.404L..31C]

Cellino, 2006 : A. Cellino, 2006, "Division III/Commission 15/Working Group Physical Study of Minor Planets", *Trans. Int. Astron. Union, Series B*, **26**, 131–132.[1]

Cellino, 2009 : A. Cellino, 2009, "Commission 15/Physical Studies of Comets and Minor Planets", *Trans. Int. Astron. Union, Series B*, **27**, 168–162.[1]

Chambers, 2006 : K. Chambers, 2006, "Killers and Kabooms—Observing the Transient Universe with Pan-STARRS", `http://online.itp.ucsb.edu/online/grbtu_c06/chambers/pdf/KChambers_KITP.pdf`.

Chapman *et al.*, 1973a : C. R. Chapman, T. B. McCord and T. V. Johnson, 1973, "Asteroid Spectral Reflectivities", *Astron. J.* **78**, 126–140. [1973AJ.....78..126C]

Chapman *et al.*, 1973b : C. R. Chapman, T. B. McCord and C. Pieters, 1973, "Minor Planets and Related Objects. X. Spectrophotometric Study of the Composition of (1685) Toro", *Astron. J.* **78**, 502–505. [1973AJ.....78..502C]

1 The individual IAU Commission and Division reports in the *Trans. Int. Astron. Union* do not seem to be indexed in ADS, so no links can be provided for the two Cellino references.

Chapman *et al.*, 1975 : C. R. Chapman, D. Morrison and B. Zellner, 1975, "Surface Properties of Asteroids–A Synthesis of Polarimetry, Radiometry, and Spectrophotometry", *Icarus* **25**, 104–130. [1975Icar...25..104C]

Chapman *et al.*, 1976 : C. R. Chapman, 1976, "Asteroids as Meteorite Parent-Bodies: The Astronomical Perspective", *Geochim. Cosmochim. Acta* **40**, 701–719. [1976GeCoA..40..701C]

Chernova *et al.*, 1993 : G. P. Chernova, N. X. Minikulov and N. N. Kiselev, 1993, "Photoelectric Photometry of the Asteroid 2078 Nanking", *LPI Contrib.* **810**, 64. [1993LPICo.810...64C]

Chernova *et al.*, 1995 : G. P. Chernova, N. N. Kiselev, Y. N. Krugley, D. F. Lupishko, V. G. Shevchenko, F. P. Velichko and R. A. Mohamed, 1995, "Photometry of Amor Asteroids 1036 Ganymede and 1627 Ivar", *Astron. J.* **110**, 1875–1878. [1995AJ....110.1875C] *[Both the article title and article have incorrect name for (1036) Ganymed]*

Chesley *et al.*, 2003 : S. R. Chesley, S. J. Ostro, D. Vokrouhlický, D. Čapek, J. D. Giorgini, M. C. Nolan, J.-L. Margot, A. A. Hine, L. A. M. Benner and A. B. Chamberlin, 2003, "Direct Detection of the Yarkovsky Effect by Radar Ranging to Asteroid 6489 Golevka", *Science* **302**, 1739–1742. [2003Sci...302.1739C]

Chesley *et al.*, 2010 : S. R. Chesley, J. Baer and D. G. Monet, 2010, "Treatment of Star Catalog Biases in Asteroid Astrometric Observations", *Icarus* **210**, 158–181. [2010Icar..210..158C]

Chiorny *et al.*, 2007 : V. G. Chiorny, V. G. Shevchenko, Yu. N. Krugly, F. P. Velichko and N. M. Gaftonyuk, 2007, "Photometry of Asteroids: Lightcurves of 24 Asteroids Obtained in 1994–2005", *Planet. Space Sci.* **55**, 986–997. [2007P&SS...55..986C]

Chiorny *et al.*, 2011 : V. Chiorny, A. Galád, P. Pravec, P. Kušnirák, K. Hornoch, Š. Gajdoš, L. Kornoš, J. Világi, M. Husárik, Z. Kaňuchová, Z. Krišandová, D. Higgins, D. P. Pray, R. Durkee, R. Dyvig, V. Reddy, J. Oey, F. Marchis and R. D. Stephens, 2011, "Absolute Photometry of Small Main-Belt Asteroids in 2007–2009", *Planet. Space Sci.* **59**, 1482–1489. [2011P&SS...59.1482C]

Chiu, 1980 : L.-T. G. Chiu, 1980, "Classification of Stellar Populations and Luminosity Classes from Accurate Proper Motions", *Astrophys. J. Suppl.* **44**, 31–71. [1980ApJS...44...31C]

Clark *et al.*, 2002 : B. E. Clark, B. Hapke, C. Pieters and D. Britt, 2002, "Asteroid Space Weathering and Regolith Evolution", in *Asteroids III*, 585–599. [2002aste.conf..585C]

Cooney, 2005 : W. R. Cooney, 2005, "Lightcurve Results for Minor Planets 228 Agathe, 297 Caecillia, 744 Aguntina, 1062 Ljuba, 1605 Milankovitch, and 3125 Hay", *Minor Planet Bull.* **32**, 15–16. [2005MPBu...32...15C]

Cousins, 1976 : A. W. J. Cousins, 1976, "*VRI* Standards in the E Regions", *Mem. R. Astron. Soc.* **81**, 25–36. [1976MmRAS..81...25C]

Cunningham, 2002 : C. J. Cunningham, 2002, *The First Asteroid: Ceres 1801–2001*, Star Lab Press.

Curry *et al.*, 1998 : H. M. Curry, K. S. Rumstay, J. R. Webb and E. K. Strobel, 1998, "Photometry of Stars in the Fields of Selected Active Galactic Nuclei", *IAPPP Comm.* **73**, 18–28. [1998IAPPP..73...18C]

Dahlgren and Lagerkvist, 1995 : M. Dahlgren and C.-I. Lagerkvist, 1995, "A Study of Hilda Asteroids", *Astron. Astrophys.* **302**, 907–914. [1995A&A...302..907D]

Dahlgren *et al.*, 1998 : M. Dahlgren, J. F. Lahulla, C.-I. Lagerkvist, J. Lagerros, S. Mottola, A. Erikson, M. Gonano-Beurer and M. di Martino, 1998, "A Study of Hilda Asteroids. V. Lightcurves of 47 Hilda Asteroids", *Icarus* **133**, 247–285. [1998Icar..133..247D]

Dandy *et al.*, 2003 : C. L. Dandy, A. Fitzsimmons and S. J. Collander-Brown, 2003, "Optical Colors of 56 Near-Earth Objects: Trends with Size and Orbit", *Icarus* **163**, 363–373. [2003Icar..163..363D]

Davis *et al.*, 2002 : D. R. Davis, D. D. Durda, F. Marzari, A. Campo Bagatin and R. Gil-Hutton, 2002, "Collisional Evolution of Small-Body Populations", in *Asteroids III*, 545–558. [2002aste.conf..545D]

Dawes, 1851 : W. R. Dawes, 1851, "On a Photometrical Method of Determining the Magnitudes of Telescopic Stars", *Mon. Not. R. Astron. Soc.* **11**, 187–198. [1851MNRAS..11..187D]

de Luise *et al.*, 2007 : F. de Luise, D. Perna, E. Dotto, S. Fornasier, I. N. Belskaya, A. Boattini, G. B. Valsecchi, A. Milani, A. Rossi, M. Lazzarin, P. Paolicchi and M. Fulchignoni, 2007, "Physical Investigation of the Potentially Hazardous Asteroid (144898) 2004 VD_{17}", *Icarus* **191**, 628–635. [2007Icar..191..628D]

De Sanctis *et al.*, 1994 : M. C. De Sanctis, M. A. Barucci, C. A. Angeli, M. Fulchignoni, R. Burchi and P. Angelini, 1994, "Photoelectric and CCD Observations of 10 Asteroids", *Planet. Space Sci.* **42**, 859–864. [1994P&SS...42..859D]

Debehogne and Zappalà, 1980a : H. Debehogne and V. Zappalà, 1980, "Photoelectric Lightcurves and Rotation Period of 308 Polyxo, Obtained at ESO-La Silla in May 1978", *Astron. Astrophys. Suppl.* **39**, 163–165. [1980A&AS...39..163D]

Debehogne and Zappalà, 1980b : H. Debehogne and V. Zappalà, 1980, "Photoelectric Lightcurves of the Asteroids 139 Juewa and 161 Athor, Obtained with the 50 cm Photometric Telescope at ESO, La Silla", *Astron. Astrophys. Suppl.* **42**, 85–89. [1980A&AS...42...85D]

Debehogne *et al.*, 1977 : H. Debehogne, A. Surdej and J. Surdej, 1977, "Photoelectric Lightcurves of Minor Planets 599 Luisa and 128 Nemesis During the 1976 Opposition", *Astron. Astrophys. Suppl.* **30**, 375–379. [1977A&AS...30..375D]

Debehogne *et al.*, 1978a : H. Debehogne, A. Surdej and J. Surdej, 1978, "Photoelectric Lightcurves of the Minor Planets 29 Amphitrite, 121 Hermione and 185 Eunikre", *Astron. Astrophys. Suppl.* **32**, 127–133. [1978A&AS...32..127D]

Debehogne *et al.*, 1978b : H. Debehogne, A. Surdej and J. Surdej, 1978, "Photoelectric Lightcurves and Rotation Period of the Minor Planet 59 Elpis", *Astron. Astrophys. Suppl.* **33**, 1–5. [1978A&AS...33....1D]

Debehogne *et al.*, 1982a : H. Debehogne, G. De Sanctis and V. Zappalà, 1982, "Photoelectric Photometry of Three Dark Asteroids", *Astron. Astrophys.* **108**, 197–200. [1982A&A...108..197D]

Debehogne *et al.*, 1982b : H. Debehogne, C.-I. Lagerkvist and V. Zappalà, 1982, "Physical Studies of Asteroids VIII. Photoelectric Photometry of the Asteroids 42, 48, 93, 105, 145 and 245", *Astron. Astrophys. Suppl.* **50**, 277–281. [1982A&AS...50..277D]

Debehogne *et al.*, 1983 : H. Debehogne, G. De Sanctis and V. Zappalà, 1983, "Photoelectric Photometry of Asteroids 45, 120, 776, 804, 814 and 1982 DV", *Icarus* **55**, 236–244. [1983Icar...55..236D]

Degewij and van Houten, 1979 : J. Degewij and C. J. van Houten, 1979, "Distant Asteroids and Outer Jovian Satellites", in *Asteroids*, 417–435. [1979aste.book..417D]

Degewij *et al.*, 1978a : J. Degewij, J. Gradie and B. Zellner, 1978, "Minor Planets and Related Objects. XXV. *UBV* Photometry of 145 Faint Asteroids", *Astron. J.* **83**, 643–650. [1978AJ.....83..643D]

Degewij *et al.*, 1978b : J. Degewij, L. Lebofsky and M. Lebofsky, 1978, "1978 CA and 1978 DA", *Int. Astron. Union Circular* 3193, 1. [1978IAUC.3193....1D]

Dell'Oro and Cellino, 2008 : A. Dell'Oro and A. Cellino, 2008, "GAIA: An Opportunity for the Physical Studies of Asteroids", *LPI Contrib.* **1405**, 8008. [2008LPICo1405.8008D]

DeMeo *et al.*, 2009 : F. E. DeMeo, R. P. Binzel, S. M. Slivan and S. J. Bus, 2009, "An Extension of the Bus Asteroid Taxonomy into the Near-Infrared", *Icarus* **202**, 160–180. [2009Icar..202..160D]

Denchev, 2000 : P. Denchev, 2000, "Photometry of 11 Asteroids during their 1998 and 1999 Apparitions", *Planet. Space Sci.* **48**, 987–992. [2000P&SS...48..987D]

Deutsch, 1935 : A. N. Deutsch, 1935, "Über das System der Sterngrößen der Kleinen Planeten und ihrer Farbenindizes" ["On the Magnitude System for Minor Planets and their Colour Indices"], *Astron. Nachr.* **256**, 189–196. [1935AN....256..189D]

Di Martino, 1984 : M. Di Martino, 1984, "Physical Studies of Asteroids: Lightcurves and Rotational Periods of Six Asteroids", *Icarus* **60**, 541–546. [1984Icar...60..541D]

Di Martino and Cacciatori, 1984a : M. Di Martino and S. Cacciatori, 1984, "Rotation Periods and Light Curves of the Large Asteroids 409 Aspasia and 423 Diotima", *Astron. Astrophys.* **130**, 206–207. [1984A&A...130..206D]

Di Martino and Cacciatori, 1984b : M. Di Martino and S. Cacciatori, 1984, "Photoelectric Photometry of 14 Asteroids", *Icarus* **60**, 75–82. [1984Icar...60...75D]

Di Martino *et al.*, 1987a : M. Di Martino, V. Zappalà, G. De Sanctis and S. Cacciatori, 1987, "Photoelectric Photometry of 17 Asteroids", *Icarus* **69**, 338–353. [1987Icar...69..338D]

Di Martino *et al.*, 1987b : M. Di Martino, V. Zappalà, J. A. De Campos, H. Debehogne and C.-I. Lagerkvist, 1987, "Rotational Properties and Lightcurves of the Minor Planets 94, 107, 197, 201, 360, 451, 511 and 702", *Astron. Astrophys. Suppl.* **130**, 95–101. [1987A&AS...67...95D]

Di Martino *et al.*, 1994 : M. Di Martino, E. Dotto, M. A. Barucci and A. Rotundi, 1994, "Photoelectric Photometry of Ten Small and Fast Spinning Asteroids", *Icarus* **109**, 210–218. [1994Icar..109..210D]

Di Martino *et al.*, 1995 : M. Di Martino, E. Dotto, A. Cellino, M. A. Barucci and M. Fulchignoni, 1995, "Intermediate Size Asteroids: Photoelectric Photometry of 8 Objects", *Astron. Astrophys. Suppl.* **112**, 1–7. [1995A&AS..112....1D]

Dohnanyi, 1969 : J. S. Dohnanyi, 1969, "Collisional Model of Asteroids and Their Debris", *J. Geophys. Res.* **74**, 2531–2554. [1969JGR....74.2531D]

Doressoundiram *et al.*, 1999 : A. Doressoundiram, P. R. Weissman, M. Fulchignoni, M. A. Barucci, A. Le Bras, F. Colas, J. Lecacheux, M. Birlan, M. Lazzarin, S. Fornasier, C. Barbieri, M. V. Sykes, S. Larson and C. Hergenrother, 1999, "4979 Otawara: Flyby Target of the Rosetta Mission", *Astron. Astrophys.* **352**, 697–702. [1999A&A...352..697D]

Dotto *et al.*, 1992 : E. Dotto, M. A. Barucci, M. Fulchignoni, M. Di Martino, A. Rotundi, R. Burchi and A. Di Paolantonio, 1992, "M-Type Asteroids: Rotational Properties of 16 Objects", *Astron. Astrophys. Suppl.* **95**, 195–211. [1992A&AS...95..195D]

Dotto *et al.*, 1995 : E. Dotto, G. De Angelis, M. Di Martino, M. A. Barucci, M. Fulchignoni, G. De Sanctis and R. Burchi, 1995, "Pole Orientation and Shape of 12 Asteroids", *Icarus* **117**, 313–327. [1995Icar..117..313D]

Dovgopol *et al.*, 1992 : A. N. Dovgopol, Yu. N. Krugly and V. G. Shevchenko, 1992, "Asteroid 126 Velleda: Rotation Period and Magnitude-Phase Curve", *Acta Astron.* **42**, 67–72. [1992AcA....42...67D]

Downes and Shara, 1993 : R. A. Downes and M. M. Shara, 1993, "A Catalog of Cataclysmic Variables", *Publ. Astron. Soc. Pac.* **105**, 127–245. [1993PASP..105..127D]

Dunham *et al.*, 1991 : D. W. Dunham, W. Osborn, G. Williams, J. Brisbin, A. Gada, T. Hirose, P. Maley, H. Povenmire, J. Stamm, J. Thrush, C. Aikman, M. Fletcher, M. Soma and W. Sichao, 1991, "The Sizes and Shapes of (4) Vesta, (216) Kleopatra and (381) Myrrha from Occultations Observed During January 1991", *LPI Contrib.* **765**, 54. [1991LPICo.765...54D]

Dunlap and Gehrels, 1969 : J. L. Dunlap and T. Gehrels, 1969, "Minor Planets. III. Lightcurves of a Trojan Asteroid", *Astron. J.* **74**, 796–803. [1969AJ.....74..796D]

Dunlap and Taylor, 1979 : J. L. Dunlap and R. C. Taylor, 1979, "Minor Planets and Related Objects. XXVII. Lightcurves of 887 Alinda", *Astron. J.* **84**, 269–273. [1979AJ.....84..269D]

Dunlap *et al.*, 1973 : J. L. Dunlap, T. Gehrels and M. L. Howes, 1973, "Minor Planets and Related Objects. IX. Photometry and Polarimetry of (1685) Toro", *Astron. J.* **78**, 491–501. [1973AJ.....78..491D]

Durda and Dermott, 1997 : D. D. Durda and S. F. Dermott, 1997, "The Collisional Evolution of the Asteroid Belt and Its Contribution to the Zodiacal Cloud", *Icarus* **130**, 140–164. [1997Icar..130..140D]

Durda *et al.*, 1998 : D. D. Durda, R. Greenberg and R. Jedicke, 1998, "Collisional Models and Scaling Laws: A New Interpretation of the Shape of the Main-Belt Asteroid Size Distribution", *Icarus* **135**, 431–440. [1998Icar..135..431D]

Dymock and Miles, 2009 : R. Dymock and R. Miles, 2009, "A Method for Determining the *V* Magnitude of Asteroids From CCD Images", *J. Brit. Astron. Assoc.* **119**, 149–155. [2009JBAA..119..149D]

Edmondson, 1952 : F. K. Edmondson, 1952, "Report on the Minor Planet Observing Program at the Goethe Link Observatory, Indiana University", *Minor Planet Circ.* 816–817. [1952MPC....816...2E]

Elst *et al.*, 1996 : E. W. Elst, O. Pizarro, C. Pollas, J. Tichá, M. Tichý, Z. Moravec, W. Offutt and B. G. Marsden, 1996, "Comet P/1996 N2 (Elst-Pizarro)", *IAU Circ.* 6456. [1996IAUC.6456....1E]

Erikson *et al.*, 1991 : A. Erikson, G. Cutispoto, H. Debehogne, G. Hahn, C.-I. Lagerkvist, M. Lindgren and P. Magnusson, 1991, "Physical Studies of Asteroid XXIII: Photometric Observations of the Asteroids 6, 32, 196, 243, 416, 532 and 1580", *Astron. Astrophy. Suppl.* **91**, 259–264. [1991A&AS...91..259E]

Evans *et al.*, 2002 : D. W. Evans, M. J. Irwin and L. Helmer, 2002, "The Carlsberg Meridian Telescope CCD Drift Scan Survey", *Astron. Astrophys.* **395**, 347–356. [2002A&A...395..347E] Also `http://www.ast.cam.ac.uk/~dwe/SRF/cmcl4.html`

Fang *et al.*, 2012 : J. Fang, J.-L. Margot and P. Rojo, 2012, "Orbits, Masses, and Evolution of Main Belt Triple (87) Sylvia", *Astron. J.* **144**, 70. [2012AJ....144...70F]

Ferguson, 1851 : J. Ferguson, 1851, "Observations Made with the Filarmicrometer of the Washington Equatoreal", *Astron. Nachr.* **33**, 183–188. [1851AN.....33..183F]

Ferguson, 1852 : J. Ferguson, 1852, "Results of Observations for Determining the Relative Brightness of the Asteroids made with Washington Equatoreal", *Astron. Nachr.* **34**, 155–158. [1852AN.....34..155.] Also *Astron. J.* **2**, 93–94. [1852AJ.....2...93F]

Fischer, 1941 : H. Fischer, 1941, "Farbmessungen an Kleinen Planeten" ["Colour Measurements of Minor Planets"], *Astron. Nachr.* **272**, 127–147. [1941AN....272..127F]

Ford *et al.*, 2009 : L. Ford, G. Stecher and K. Lorenzen, 2009, "Photometric Measurements of 343 Ostara and Other Asteroids at Hobbs Observatory", *Minor Planet Bull.* **36**, 77. [2009MPBu...36...77F]

Fornasier *et al.*, 2004 : S. Fornasier, E. Dotto, F. Marzari, M. A. Barucci, H. Boehnhardt, O. Hainaut and C. de Bergh, 2004, "Visible Spectroscopic and Photometric Survey of L_5 Trojans: Investigation of Dynamical Families", *Icarus* **172**, 221–232. [2004Icar..172..221F]

Fornasier *et al.*, 2007 : S. Fornasier, E. Dotto, O. Hainaut, F. Marzari, H. Boehnhardt, F. De Luise and M. A. Barucci, 2007, "Visible Spectroscopic and Photometric Survey of Jupiter Trojans: Final Results on Dynamical Families", *Icarus* **190**, 622–642. [2007Icar..190..622F]

Franco, 2012 : L.Franco, 2012, "Lightcurve Photometry and *H-G* Parameters for 1077 Campanula", *Minor Planet Bull.* **39**, 67–69. [2012MPBu...39...67F]

Franco and Sergison, 2011 : L. Franco and D. Sergison, 2011, "Lightcurve Photometry and *H-G* Parameters for 1342 Brabantia", *Minor Planet Bull.* **38**, 132–134. [2011MPBu...38..132F]

Franco *et al.*, 2010 : L. Franco, A. Carbognani, P. Wiggins, B. W. Koehn and R. Schmidt, 2010, "Collaborative Lightcurve Photometry of Near-Earth Asteroid (159402) 1999 AP_{10}", *Minor Planet Bull.* **37**, 83–85. [2010MPBu...37...83F]

Franco *et al.*, 2012 : L. Franco, A. Ferrero and R. I. Durkee, 2012, "Lightcurve Photometry and *H-G* Parameters for 1151 Ithaka", *Minor Planet Bull.* **39**, 47–48. [2012MPBu...39...47F]

Frei and Gunn, 1994 : Z. Frei and J. E. Gunn, 1994, "Generating Colors and *k* Corrections from Existing Catalogue Data", *Astron. J.* **108**, 1476–1485. [1994AJ....108.1476F]

French, 1987 : L. M. French, 1987, "Rotation Properties of Four L_5 Trojan Asteroids from CCD Photometry", *Icarus* **72**, 325–341. [1987Icar...72..325F]

Fukugita *et al.*, 1996 : M. Fukugita, T. Ichikawa, J. E. Gunn, M. Doi, K. Shimasaku and D. P. Schneider, 1996, "The Sloan Digital Sky Survey Photometric System", *Astron. J.* **111**, 1748–1756. [1996AJ....111.1748F]

Gaffey *et al.*, 1989 : M. J. Gaffey, J. F. Bell and D. P. Cruikshank, 1989, "Reflectance Spectroscopy and Asteroid Surface Mineralogy", in *Asteroids II*, 98–127. [1989aste.conf...98G]

Galád *et al.*, 2009 : A. Galád, L. Kronoš and M. Husárik, 2009, "The Very Long Sidereal Period of 1807 Slovakia", *Minor Planet Bull.* **36**, 149–151. [2009MPBu...36..149G]

Gandolfi *et al.*, 2009 : D. Gandolfi, M. Cigna, D. Fulvio and C. Blanco, 2009, "CCD and Photon-Counting Photometric Observations of Asteroids Carried Out at Padova and Catania Observatories", *Planet. Space Sci.* **57**, 1–9. [2009P&SS...57....1G]

Garradd *et al.*, 2008 : G. J. Garradd, G. Sostero, P. Camilleri, E. Guido, C. Jacques and E. Pimentel, 2008, "Comet C/2008 R1 (Garradd)", *IAU Circ.* 8969. [2008IAUC.8969....1G]

Garrett, 1997 : L. Garrett, 1997, "Magnitude Alert Project (MAP)", *Minor Planet Bull.* **24**, 11. [1997MPBu...24...11G]

Gary, 2004 : B. L. Gary, 2004, "CCD Photometry of Asteroid 12753 Povenmire", *Minor Planet Bull.* **31**, 56–57. [2004MPBu...31...56G]

Gauss, 1809 : C. F. Gauss, 1809, *Theoria Motus Corporum Colestium in Sectionibus Conicis Solem Ambientium* [*Theory of the Motion of Celestial Bodies Moving in Conic Sections About the Sun*, English translation by C. H. Davis (1857), reprinted by Dover Publications (1963)].

Gehrels, 1956 : T. Gehrels, 1956, "Photometric Studies of Asteroids: V. The Light-curve and Phase Function of 20 Massalia", *Astrophys. J.* **123**, 331–338. [1956ApJ...123..331G]

Gehrels, 1957 : T. Gehrels, 1957, "Photometric Studies of Asteroids: VI. Photographic Magnitudes", *Astrophys. J.* **125**, 550–570. [1957ApJ...125..550G]

Gehrels, 1967a : T. Gehrels, 1967, "Minor Planets. I. The Rotation of Vesta", *Astron. J.* **72**, 929–938. [1967AJ.....72..929G]

Gehrels, 1967b : T. Gehrels, 1967, "Minor Planets: II. Photographic Magnitudes", *Astron. J.* **72**, 1288–1291. [1967AJ.....72.1288G]

Gehrels, 1970 : T. Gehrels, 1970, "Photometry of Asteroids", in *Surfaces and Interiors of Planets and Satellites*, 317–375. [1970sips.conf..317G]

Gehrels and Gehrels, 1978 : T. Gehrels and N. Gehrels, 1978, "Minor Planets and Related Objects. XXVI. Magnitudes for the Numbered Asteroids", *Astron. J.* **83**, 1660–1674. [1978AJ.....83.1660G]

Gehrels and Owings, 1962 : T. Gehrels and D. Owings, 1962, "Photometric Studies of Asteroids. IX. Additional Light-curves", *Astrophys. J.* **135**, 906–924. [1962ApJ...135..906G]

Gehrels and Taylor, 1977 : T. Gehrels and R. C. Taylor, 1977, "Minor Planets and Related Objects. XXII. Phase functions for (6) Hebe", *Astron. J.* **82**, 229–237. [1977AJ.....82..229G]

Gehrels and Tedesco, 1979 : T. Gehrels and E. F. Tedesco, 1979, "Minor Planets and Related Objects. XXVIII. Asteroids Magnitudes and Phase Relations", *Astron. J.* **84**, 1079–1087. [1979AJ.....84.1079G]

Gibbs *et al.*, 2012 : A. R. Gibbs, H. Sato, W. H. Ryan, E. V. Ryan, P. Birtwhistle, M. Mašek, J. Cerny, J. Ebr, M. Prouza, P. Kubanek, M. Jelínek, T. Vorobjov, G. Hug, E. Guido, N. Howes, G. Sostero and G. V. Williams, 2012, "Comet P/2012 F5 (Gibbs)", *Cent. Bureau Electron. Tel.* 3069. [2012CBET.3069....1G]

Gingerich, 1999 : O. Gingerich, 1999, "Benjamin Apthorp Gould and the Founding of the Astronomical Journal", *Astron. J.* **117**, 1–5. [1999AJ....117....1G]

Gladman *et al.*, 2009 : B. J. Gladman, D. R. Davis, C. Neese, R. Jedicke, G. Williams, J. J. Kavelaars, J.-M. Petit, H. Scholl, M. Holman, B. Warrington, G. Esquerdo and P. Tricarico, 2009, "On the Asteroid Belt's Orbital and Size Distribution", *Icarus* **202**, 104–118. [2009Icar..202..104G]

Gould, 1852 : B. A. Gould, 1852, "On the Symbolic Notation of the Asteroids", *Astron. J.* **2**, 80. [1852AJ.....2...80G]

Gradie and Tedesco, 1982 : J. Gradie and E. Tedesco, 1982, "Compositional Structure of the Asteroid Belt", *Science* **216**, 1405–1407. [1982Sci...216.1405G]

Grav *et al.*, 2011 : T. Grav, A. K. Mainzer, J. Bauer, J. Masiero, T. Spahr, R. S. McMillan, R. Walker, R. Cutri, E. Wright, P. R. M. Eisenhardt, E. Blauvelt, E. DeBaun, D. Elsbury, T. Gautier IV, S. Gomillion, E. Hand and A. Wilkins, 2011, "WISE/NEOWISE Observations of the Jovian Trojans: Preliminary Results", *Astrophys. J.* **742**, 40. [2011ApJ...742...40G]

Grav *et al.*, 2012 : T. Grav, A. K. Mainzer, J. Bauer, J. Masiero, T. Spahr, R. S. McMillan, R. Walker, R. Cutri, E. Wright, P. R. Eisenhardt, E. Blauvelt, E. DeBaun, D. Elsbury, T. Gautier, S. Gomillion, E. Hand and A. Wilkins, 2012, "WISE/NEOWISE Observations of the Hilda Population: Preliminary Results", *Astrophys. J.* **744**, 197. [2012ApJ...744..197G]

Gray, 1999 : B. G. Gray, 1999, "GSC-ACT files and information", `http://www.projectpluto.com/gsc_act.htm`.

Groeneveld and Kuiper, 1954 : I. Groeneveld and G. P. Kuiper, 1954, "Photometric Studies of Asteroids. II", *Astrophys. J.* **120**, 529–546. [1954ApJ...120..529G]

Guido *et al.*, 2011 : E. Guido, R. Ligustri, N. Falla, H. Sato, S. Kurti, G. V. Williams, G. Sostero and C. L. Marsden, 2011, "Minor Planet Observations [H06 RAS Observatory, Mayhill]", *Minor Planet Circ.* 74224. [2011MPC..74224...4G]

Guilbert *et al.*, 2009 : A. Guilbert, M. A. Barucci, R. Brunetto, A. Delsanti, F. Merlin, A. Alvarez-Candal, S. Fornasier, C. de Bergh and G. Sarid, 2009, "A Portrait of Centaur (10199) Chariklo", *Astron. Astrophys.* **501**, 777–784. [2009A&A...501..777G]

Hahn *et al.*, 1989 : G. Hahn, P. Magnusson, A. W. Harris, J. W. Young, L. A. Belkora, N. J. Fico, D. F. Lupishko, V. G. Shevchenko, F. P. Velichko, R. Burchi, G. Ciunci, M. di Martino and H. Debehogne, 1989, "Physical Studies of Apollo-Amor Asteroids: *UBVRI* Photometry of 1036 Ganymed and 1627 Ivar", *Icarus* **78**, 363–381. [1989Icar...78..363H]

Hansen, 1976 : O. L. Hansen, 1976, "Radii and Albedos of 84 Asteroids From Visual and Infrared Photometry", *Astron. J.* **81**, 74–84. [1976AJ.....81...74H]

Harrington, 1883 : W. M. Harrington, 1883, "A Brief Study of Vesta", *Amer. J. Sci.* **126**, 461–464. [1883AmJS..126..461H]

Harris, 1998 : A. W. Harris, 1998, "A Thermal Model for Near-Earth Asteroids", *Icarus* **131**, 291–301. [1998Icar..131..291H]

Harris and Harris, 1997 : A. W. Harris and A. W. Harris, 1997, "On the Revision of Radiometric Albedos and Diameters of Asteroids", *Icarus* **126**, 450–454. [1997Icar..126..450H]

Harris and Lupishko, 1989 : A. W. Harris and D. F. Lupishko, 1989, "Photometric Lightcurve Observations and Reduction Techniques", in *Asteroids II*, 39–53. [1989aste.conf...39H]

Harris and Young, 1983 : A. W. Harris and J. W. Young, 1983, "Asteroid Rotation IV. 1979 Observations", *Icarus* **54**, 59–109. [1983Icar...54...59H]

Harris and Young, 1989 : A. W. Harris and J. W. Young, 1989, "Asteroid Lightcurve Observations from 1979–1981", *Icarus* **81**, 314–364. [1989Icar...81..314H]

Harris *et al.*, 1984a : A. W. Harris, J. W. Young, F. Scaltriti and V. Zappalà, 1984, "Lightcurves and Phase Relations of the Asteroids 82 Alkmene and 444 Gyptis", *Icarus* **57**, 251–258. [1984Icar...57..251H]

Harris *et al.*, 1984b : A. W. Harris, M. Carlsson, J. W. Young and C.-I. Lagerkvist, 1984, "The Lightcurve and Phase Relation of the Asteroid 133 Cyrene", *Icarus* **58**, 377–382. [1984Icar...58..377H]

Harris *et al.*, 1987 : A. W. Harris, J. W. Young, J. Goguen, H. B. Hammel, G. Hahn. E. F. Tedesco and D. J. Tholen, 1987, "Photoelectric Lightcurves of the Asteroid 1862 Apollo", *Icarus* **70**, 246–256. [1987Icar...70..246H]

Harris *et al.*, 1989a : A. W. Harris, J. W. Young, E. Bowell, L. J. Martin, R. L. Millis, M. Poutanen, F. Scaltriti, V. Zappalà, H. J. Schober, H. Debehogne and K. W. Zeigler, 1989, "Photoelectric Observations of Asteroids 3, 24, 60, 261 and 863", *Icarus* **77**, 171–186. [1989Icar...77..171H]

Harris *et al.*, 1989b : A. W. Harris, J. W. Young, L. Contreiras, T. Dockweiler, L. Belkora, H. Salo and W. D. Harris, 1989, "Phase Relations of High Albedo Asteroids: The Unusual Opposition Brightening of 44 Nysa and 64 Angelina", *Icarus* **81**, 365–374. [1989Icar...81..365H]

Harris *et al.*, 1992 : A. W. Harris, J. W. Young, T. Dockweiler, J. Gibson, M. Poutanen and E. Bowell, 1992, "Asteroid Lightcurve Observations from 1981", *Icarus* **95**, 115–147. [1992Icar...95..115H]

Harris *et al.*, 1999 : A. W. Harris, J. W. Young, E. Bowell and D. J. Tholen, 1999, "Asteroid Lightcurve Observations from 1981 to 1983", *Icarus* **142**, 173–201. [1999Icar..142..173H]

Harris *et al.*, 2007 : A. W. Harris, P. Pravec and B. Warner, 2007, `http://www.minorplanetcenter.net/iau/lists/LightcurveDat.html`.

Heiligenstein, 1829 : A. Heiligenstein, 1829, "Schreiben des Herrn A. v. Heiligenstein an den Herausgeber" ["Letter to the Editor From Mr. A. v. Heiligenstein"], *Astron. Nachr.* **7**, 413–416. [1829AN.....7..413V]

Helin *et al.*, 1997 : E. F. Helin, S. H. Pravdo, D. L. Rabinowitz and K. J. Lawrence, 1997, "Near-Earth Asteroid Tracking (NEAT) Program", *Ann. New York Acad. Sci.* **822**, 6–25. [1997NYASA.822....6H]

Henden, 2009 : A. Henden, 2009, "AAVSO Photometry All-Sky Survey (APASS)", `http://www.aavso.org/news/apass.shtml`.

Henden and Honeycutt, 1995 : A. A. Henden and R. K. Honeycutt, 1995, "Secondary Photometric Standards for Northern Nova-Like Cataclysmic Variables", *Publ. Astron. Soc. Pac.* **107**, 324–346. [1995PASP..107..324H]

Henden and Honeycutt, 1997 : A. A. Henden and R. K. Honeycutt, 1997, "Secondary Photometric Standards for Northern Cataclysmic Variables and Related Objects", *Publ. Astron. Soc. Pac.* **109**, 441–460. [1997PASP..109..441H]

Henden and Kaitchuck, 1982 : A. A. Henden and R. H. Kaitchuck, 1982, *Astronomical Photometry*.

Hergenrother *et al.*, 2009 : C. W. Hergenrother, R. J. Whiteley and E. J. Christensen, 2009, "Photometric Observations of Five Near-Earth Asteroids: (31221) 1998 BP_{26}, (96315) 1997 AP_{10}, (164184) 2004 BF_{68}, 2006 VV_2 and 2006 XY_{94}", *Minor Planet Bull.* **36**, 16–18. [2009MPBu...36...16H]

Herget, 1951 : P. Herget, 1951, "Note on Magnitudes", *Minor Planet Circ.* 603. [1951MPC....603...1H]

Herget, 1956 : P. Herget, 1956, "Resumé of Minor Planet Perturbation Computations at the Cincinnati Observatory", *Minor Planet Circ.* 1423–1431. [1956MPC...1423...1H]

Herget, 1971 : P. Herget, 1971, "The Work of the Minor Planet Center", in *Physical Studies of Minor Planets*, 9–12. [1971NASSP.267....9H]

Herschel, 1802 : W. Herschel, 1802, "VIII. Observations on the Two Lately Discovered Celestial Bodies", *Phil. Trans. Roy. Soc.* **92**, 213–232. [1802RSPT...92..213H]

Hewitt and Burbidge, 1993 : A. Hewitt and G. Burbidge, 1993, "A Revised and Updated Catalog of Quasi-Stellar Objects", *Astrophys. J. Suppl.* **87**, 451–947. [1993ApJS...87..451H]

Hicks and Collins, 1996 : M. Hicks and J. Collins, 1996, "1996 JA_1", *Int. Astron. Union Circ.* 6402, 1. [1996IAUC.6402....1S]

Hicks and Rhoades, 2010 : M. Hicks and H. Rhoades, 2010, "The Near-Earth Asteroid 2010 TD_{54}: The Fastest Rotating Natural Body Known in the Solar System?", *Astron. Tel.* 2984. [2010ATel.2984....1H]

Hicks and Somers, 2010 : M. Hicks and J. Somers, 2010, "2007 MK_{13}: A Highly Elongated C-type Potentially Hazardous Asteroid", *Astron. Tel.* 2372. [2010ATel.2372....1H]

Hicks and Truong, 2010 : M. Hicks and T. Truong, 2010, "Broadband Photometry of the Near-Earth Asteroid 66146 (1998 TU_3)", *Astron. Tel.* 2833. [2010ATel.2833....1H]

Hicks *et al.*, 2004 : M. D. Hicks, J. M. Bauer and A. T. Tokunaga, 2004, "(2867) Steins", *Int. Astron. Union Circ.* 8315, 3. [2004IAUC.8315....3H]

Hicks *et al.*, 2009a : M. Hicks, H. Rhoades and J. Summers, 2009, "Broad-Band Photometry of the Potentially Hazardous Asteroid 2002 LV", *Astron. Tel.* 2134. [2009ATel.2134....1H]

Hicks *et al.*, 2009b : M. Hicks, T. Barajas and A. McAuley, 2009, "Broad-Band Photometry of the Potentially Hazardous Asteroid 2009 KC_3", *Astron. Tel.* 2247. [2009ATel.2247....1H]

Hicks *et al.*, 2009c : M. Hicks, J. Somers, T. Barajas, J. Foster, A. McAuley and J. Shitanishi, 2009, "Broad-Band Photometry of the Binary Potentially Hazardous Asteroid 2009 YT_1", *Astron. Tel.* 2289. [2009ATel.2289....1H]

Hicks *et al.*, 2010a : M. Hicks, T. Barajas, J. Somers, J. Shitanishi and D. Mayes, 2010, "217807 (2000 XK_{44}): Broad-Band Photometry of a Slowly Rotating Near-Earth Asteroid", *Astron. Tel.* 2371 [2010ATel.2371....1H]

Hicks *et al.*, 2010b : M. Hicks, T. Barajas and J. Shitanishi, 2010, "Broadband Colors and Rotation Lightcurves of the Potentially Hazardous Asteroid 2009 UN_3", *Astron. Tel.* 2449. [2010ATel.2449....1H]

Hicks *et al.*, 2010c : M. Hicks, K. Lawrence, J. Somers and A. McAuley, 2010, "Optical Characterization of the Potentially Hazardous Asteroid and Planetary Radar Target 4486 Mithra: Evidence for Rotational Variability?", *Astron. Tel.* 2488. [2010ATel.2488....1H]

Hicks *et al.*, 2010d : M. Hicks, J. Somers, J. Foster and A. McAuley, 2010, "Broadband Photometry of the Potentially Hazardous Asteroid 2010 GU_{21}", *Astron. Tel.* 2592. [2010ATel.2592....1H]

Hicks *et al.*, 2010e : M. Hicks, D. Mayes, A. McAuley and J. Foster, 2010, "Broadband Photometry of the Potentially Hazardous Asteroid 1999 MN: Suggestive of YORP and/or Tidal Spin-Up?", *Astron. Tel.* 2706. [2010ATel.2706....1H]

Hicks *et al.*, 2010f : M. Hicks, H. Rhoades, J. Somers, J. Foster, T. Troung and K. Garcia, 2010, "2009 KD_5: Photometric Signature of a Binary Near-Earth Asteroid?", *Astron. Tel.* 2709. [2010ATel.2709....1H]

Hicks *et al.*, 2010g : M. Hicks, T. Truong and J. Somers, 2010, "Broad-Band Photometry of the Near-Earth Asteroid 154029 (2002 CY_{46}): An Unusually Steep Solar Phase Curve and Evidence for Complex Rotation", *Astron. Tel.* 2859. [2010ATel.2859....1H]

Hicks *et al.*, 2010h : M. Hicks, D. Mayes and T. Barajas, 2010, "Broadband Photometry of 2002 VE_{68}, a Quasi-Moon of Venus", *Astron. Tel.* 3073. [2010ATel.3073....1H]

Hicks *et al.*, 2011a : M. Hicks, J. Somers, T. Truong, M. McCormack, S. Teague and H. Rhoades, 2011, "Broadband Photometry of 2011 HP: A Possibly Water-Rich, Low Delta-V Near-Earth Asteroid", *Astron. Tel.* 3419. [2011ATel.3419....1H]

Hicks *et al.*, 2011b : M. Hicks, J. Somers, H. Rhoades, M. McCormack, C. Gerhart, J. Bauer, A. Mainzer, J. Masiero and T. Grav, 2011, "Broadband Photometry of 267494 (2002 VB_9): A Near-Earth Asteroid with Remarkable Solar Phase Behavior", *Astron. Tel.* 3460. [2011ATel.3460....1H]

Hilton, 2002 : J. L. Hilton, 2002, "Asteroid Masses and Densities", in *Asteroids III*, 103–112. [2002aste.conf..103H]

Hilton, 2007 : J. L. Hilton, 2007, "When did the Asteroids become Minor Planets?", `http://www.usno.navy.mil/USNO/astronomical-applications/astronomical-information-center/minor-planets`

Hirayama, 1918 : K. Hirayama, 1918, "Groups of Asteroids Probably of Common Origin", *Astron. J.* **31**, 185–188. [1918AJ.....31..185H]

Høg *et al.*, 2000 : E. Høg, C. Fabricius, V. V. Makarov, S. Urban, T. Corbin, G. Wycoff, U. Bastian, P. Schwekendiek and A. Wicenec, 2000, "The Tycho-2 Catalogue of the 2.5 Million Brightest Stars", *Astron. Astrophys.* **335**, L27–L30. [2000A&A...355L..27H]

Hollis, 1987 : A. J. Hollis, 1987, "Photometric Properties of the Minor Planets: Observations of (4) Vesta in 1985", *J. Brit. Astron. Assoc.* **97**, 350–352. [1987JBAA...97..350H]

Hollis *et al.*, 1997 : A. J. Hollis, C. S. Bembrick, M. Dumont and R. Miles, 1997, "Photometric Properties of the Minor Planets: Observations of (8) Flora in 1984", *J. Brit. Astron. Assoc.* **97**, 220–223. [1987JBAA...97..220H]

Hsieh and Jewitt, 2007 : H. H. Hsieh and D. Jewitt, 2007, "Main Belt Comets", *Bull. Amer. Astron. Soc.* **39**, 227 [2007AAS...210.9803H]

Hsieh *et al.*, 2006 : H. H. Hsieh, D. Jewitt and J. Pittichová, 2006, "Comet P/1999 RE_{70} = (118401)", *IAU Circ.* 8704. [2006IAUC.8704....3H]

Hsieh *et al.*, 2011 : H. Hsieh, L. Denneau and R. Wainscoat, 2011, "Comet P/2006 VW_{139} = (300163) 2006 VW_{139}", *Cent. Bureau Electron. Tel.* 2920. [*This reference is not present in ADS.*]

Hughes and Marsden, 2007 : D. W. Hughes and B. G. Marsden, 2007, "Planet, Asteroid, Minor Planet: A Case Study in Astronomical Nomenclature", *J. Astron. Hist. Herit.* **10**, 21–30. [2007JAHH...10...21H]

Ishiguro *et al.*, 2004 : M. Ishiguro, D. J. Tholen, S. Hasegawa, M. Abe, T. Sekiguchi, S. J. Ostro and M. Kaasalainen, 2004, "Ground-based Observations for the Asteroid Itokawa", *35th COSPAR Scientific Assembly* **35**, 1220. [2004cosp...35.1220I]

Ivezić *et al.*, 2002 : Z. Ivezić, M. Jurić, R. H. Lupton, S. Tabachnik and T. Quinn, 2002, "Asteroids Observed by the Sloan Digital Survey", in *Survey and Other Telescope Technologies and Discoveries, Proceedings of the SPIE* **4836**, 98–103. [2002SPIE.4836...98I]

Jedicke *et al.*, 2002 : R. Jedicke, J. Larsen and T. Spahr, 2002, "Observational Selection Effects in Asteroid Surveys", in *Asteroids III*, 71–87. [2002aste.conf...71J]

Jester *et al.*, 2005 : S. Jester, D. P. Schneider, G. T. Richards, R. F. Green, M. Schmidt, P. B. Hall, M. A. Strauss, D. E. Vanden Berk, C. Stoughton, J. E. Gunn, J. Brinkman, S. M. Kent, J. Allyn Smith, D. L. Tucker and B. Yanny, 2005, "The Sloan Digital Sky Survey View of the Palomar-Green Bright Quasar Survey", *Astron. J.* **130**, 873–895. [2005AJ....130..873J]

Jewitt, 2005 : D. Jewitt, 2005, "A First Look at the Damocloids", *Astron. J.* **129**, 530–538. [2005AJ....129..530J]

Jewitt *et al.*, 2007 : D. Jewitt, N. Peixinho and H. H. Hsieh, 2007, "*U*-Band Photometry of Kuiper Belt Objects", *Astron. J.* **134**, 2046–2053. [2007AJ....134.2046J]

Jewitt, 2012 : D. Jewitt, 2012, "The Active Asteroids", *Astron. J.* **143**, 66. [2012AJ....143...66J]

Johnson, 1853 : M. J. Johnson, 1853, "On the Application of the Heliometer to the Photometry of Stars", Appendix to the *Astronomical Observations Made at the Radcliffe Observatory in the Year 1851.*

Johnson, 1939 : W. A. Johnson, 1939, "Spectrophotometric Study of Three Asteroids", *Bull. Harv. Coll. Obs.* 911, 13–16. [1939BHarO.911...13J]

Johnson, 1965 : H. L. Johnson, 1965, "Interstellar Extinction in the Galaxy", *Astrophys. J.* **141**, 923–942. [1965ApJ...141..923J]

Johnson and Morgan, 1951 : H. L. Johnson and W. W. Morgan, 1951, "On the Color-Magnitude Diagram of the Pleiades", *Astrophys. J.* **114**, 522-543. [1951ApJ...114..522J]

Johnson and Morgan, 1953 : H. L. Johnson and W. W. Morgan, 1953, "Fundamental Stellar Photometry for Standard of Spectral Type on the Revised System of Yerkes Spectral *Atlas*", *Astrophys. J.* **117**, 313–352. [1953ApJ...117..313J]

Juarez *et al.*, 2005 : R. A. Juarez, C. T. Martinez, W. H. Ryan and E. V. Ryan, 2005, "Physical Properties of the Vesta Family Asteroid 2511 Patterson", *Bull. Amer. Astron. Soc.* **37**, 1155. [2005AAS...207.0412J]

Jurić *et al.*, 2002 : M. Jurić, Ž. Ivezić, R. H. Lupton, T. Quinn, S. Tabachnik, X. Fan, J. E. Gunn, G. S. Hennessy, G. R. Knapp, J. A. Munn, J. R. Pier, C. M. Rockosi, D. P. Schneider, J. Brinkmann, I. Csabal and M. Fukugita, 2002, "Comparison of Positions and Magnitudes of Asteroids Observed in the Sloan Digital Sky Survey with those Predicted for Known Asteroids", *Astron. J.* **124**, 1776–1787. [2002AJ....124.1776J]

Kaasalainen and Torppa, 2001 : M. Kaasalainen and J. Torppa, 2001, "Optimization Methods for Asteroid Lightcurve Inversion: I. Shape Determination", *Icarus* **153**, 24–36. [2001Icar..153...24K]

Kaasalainen *et al.*, 2001 : M. Kaasalainen, J. Torrpa and K. Muinonen, 2001, "Optimization Methods for Asteroid Lightcurve Inversion: II. The Complete Inverse Problem", *Icarus* **153**, 37–51. [2001Icar..153...37K]

Kaiser *et al.*, 2002 : N. Kaiser, H. Aussel, B.E. Burke, H. Boesgaard, K. Chambers, M. R. Chun, J. N. Heasley, K.-W. Hodapp, B. Hunt, R. Jedicke, D. Jewitt, R. Kudritzki, G. A. Luppino, M. Maberry, E. Magnier, D. G. Monet, P. M. Onaka, A. J. Pickes, P. H. H. Rhoads, T. Simon, A. Szalay, I. Szapudi, D. J. Tholen, J. L. Tonry, M. Waterson and J. Wick, 2002, "Pan-STARRS: A Large Synoptic Survey Telescope Array", in *Survey and Other Telescope Technologies and Discoveries, Proceedings of the SPIE* **4836**, 154–164. [2002SPIE.4836..154K]

Kamél, 1998 : L. Kamél, 1998, "CCD Photometry of 154 Bertha", *Minor Planet Bull.* **25**, 1–2. [1998MPBu...25....1K]

Kapteyn, 1906 : J. C. Kapteyn, 1906, *Plan of Selected Areas.*

Karlsson *et al.*, 2009 : O. Karlsson, C.-I. Lagerkvist and B. Davidson, 2009, "*(U)BVRI* Photometry of Trojan L_5 Asteroids", *Icarus* **199**, 106–118. [2009Icar..199..106K]

Kirkwood, 1869 : D. Kirkwood, 1869, "On the Nebular Hypothesis and the Approximate Commensurability of the Planetary Periods", *Mon. Not. R. Astron. Soc.* **29**, 96–102. [1869MNRAS..29...96K]

Kitazato *et al.*, 2004 : K. Kitazato, M. Abe, H. Mito, K. Tarusawa, T. Soyano, S. Nishihara and Y. Sarugaku, 2004, "Photometric Behaviour Dependent on Solar Phase Angle and Physical Characteristics of Binary Near-Earth Asterioid (65803) 1996 GT", *Lunar Planet. Sci.* **XXXV**, Abstract #1623. [2004LPI....35.1623K]

Krueger, 1892 : A. Krueger, 1892, "Notiz betr. dir Nummerirung der kleinen Planeten" ["Notice on the Designation of Minor Planets"], *Astron. Nachr.* **130**, 159. [1892AN....130Q.159K]

Krugly *et al.*, 2002 : Y. N. Krugly, I. N. Belskaya, V. G. Shevchenko, V. G. Chiorny, F. P. Velichko, S. Mottola, A. Erikson, G. Hahn, A. Nathues, G. Neukum, N. M. Gaftonyuk and E. Dotto, 2002, "The Near-Earth Objects Follow-up Program IV. CCD Photometry in 1996–1999", *Icarus* **158**, 294–304. [2002Icar..158..294K]

Krugly *et al.*, 2007 : Yu. N. Krugly, C. Maccone, N. M. Gaftonyuk, D. F. Lupishko, V. G. Shevchenko and V. P. Velichko, 2007, "11264 Claudiomaccone: Small Binary Main-Belt Asteroid", *Planet. Space Sci.* **55**, 449–454. [2007P&SS...55..449K]

Krugly *et al.*, 2010 : N. Krugly, R. Behrend, P. Pravec, K. Hornoch, P. Kušnirák, A. Galád, P. Veres, R. Crippa, E. Manzini, M. Audejean, L. Bernasconi, N. Gaftonyuk, B. D. Warner, I. Molotov and L. Elenin, 2010, "(8373) Stephengould", *Cent. Bureau Electron. Tel.* 2193. [2010CBET.2193....1K]

Kuiper *et al.*, 1958 : G. P. Kuiper, Y. Fujita, T. Gehrels, I. Groeneveld, J. Kent, G. Van Biesbroeck and C. J. van Houten, 1958, "Survey of Asteroids", *Astrophys. J. Suppl.* **3**, 289–334. [1958ApJS....3..289K]

Lagerkvist, 1981 : C.-I. Lagerkvist, 1981, "Physical Studies of Asteroids II: Photoelectric Observations of the Asteroids 63, 93, 135 and 409", *Astron. Astrophys. Suppl.* **44**, 345–347. [1981A&AS...44..345L]

Lagerkvist and Kamél, 1982 : C.-I. Lagerkvist and L. Kamél, 1982, "Physical Studies of Asteroids. X. Photoelectric Light Curves of the Asteroids 219 and 512", *Moon Planets* **27**, 463–466. [1982M&P....27..463L]

Lagerkvist and Rickman, 1981 : C.-I. Lagerkvist and H. Rickman, 1981, "Physical Studies of Asteroids V: Photoelectric Observations of the Asteroids 70, 101, 369 and 432", *Astron. Astrophys. Suppl.* **45**, 177–179. [1981A&AS...45..177L]

Lagerkvist *et al.*, 1986 : C.-I. Lagerkvist, G. Hahn, P. Magnusson, H. Rickman and G. Hammarbäck, 1986, "Physical Studies of Asteroids XII: *UBVRI* Observations of M and CMEU Asteroids", in *Asteroids, Comets, Meteors II*, 67–68. [1986acm..proc...67L]

Lagerkvist *et al.*, 1987 : C.-I. Lagerkvist, G. Hahn, P. Magnusson and H. Rickman, 1987, "Physical Studies of Asteroids XVI: Photoelectric Photometry of 17 Asteroids", *Astron. Astrophys. Suppl.* **70**, 21–32. [1987A&AS...70...21L]

Lagerkvist *et al.*, 1992 : C.-I. Lagerkvist, P. Magnusson, H. Debehogne, M. Hoffmann, A. Erikson, A. De Campos and G. Cutispoto, 1992, "Physical Studies of Asteroids. XXV: Photoelectric Photometry of Asteroids Obtained at ESO and Hoher List", *Astron. Astrophys. Suppl.* **95**, 461–470. [1992A&AS...95..461L]

Lagerkvist *et al.*, 1995 : C.-I. Lagerkvist, A. Erikson, H. Debehogne, L. Festin, P. Magnusson, S. Mottola, T. Oja, G. De Angelis, I. N. Belskaya, M. Dahlgren, M. Gonano-Beurer, J. Lagerros, K. Lumme and S. Pohjolainen, 1995, "Physical Studies of Asteroids. XXIX. Photometry and Analysis of 27 Asteroids", *Astron. Astrophys. Suppl.* **113**, 115–129. [1995A&AS..113..115L]

Lagerkvist *et al.*, 1998 : C.-I. Lagerkvist, I. Belskaya, A. Erikson, V. Schevchenko, S. Mottola, V. Chiorny, P. Magnusson, A. Nathues and J. Piironen, 1998, "Physical Studies of Asteroids: XXXIII. The Spin Rate of M-Type Asteroids", *Astron. Astrophys. Suppl.* **131**, 55–62. [1998A&AS..131...55L]

Lagerkvist *et al.*, 2000 : C.-I. Lagerkvist, J. Piironen and A. Erikson, 2000, *Asteroid Photometric Catalogue: Fifth Update*, Uppsala Observatory.

Landolt, 1992 : A. Landolt, 1992, "*UBVRI* Photometric Standard Stars in the Magnitude Range 11.5–16.0 Around the Celestial Equator", *Astron. J.* **104**, 340–371. [1992AJ....104..340L]

Landolt, 2007 : A. Landolt, 2007, "*UBVRI* Photometric Standard Stars Around the Sky at −50° Declination", *Astron. J.* **133**, 2502–2523. [2007AJ....133.2502L]

Larson *et al.*, 2010 : S. Larson, R. Kowalski, H. Sato, K. Yoshimoto and S. Nakano, 2010, "(596) Scheila", *Cent. Bureau Electron. Tel.* 2583, 1. [2010CBET.2583....1L]

Lasker *et al.*, 1990 : B. M. Lasker, C. R. Sturch, B. J. McLean, J. L. Russell, H. Jenkner and M. M. Shara, 1990, "The Guide Star Catalog. I – Astronomical Foundations and Image Processing", *Astron. J.* **99**, 2019–2058. [1990AJ.....99.2019L]

Lasker *et al.*, 2008 : B. M. Lasker, M. G. Lattanzi, B. J. McLean, B. Bucciarelli, R. Drimmel, J. Garcia, G. Greene, F. Guglielmetti, C. Hanley, G. Hawkins, V. G. Laidler, C. Loomis, M. Meakes, R. Mignani, R. Morbidelli, J. Morrison, R. Pannunzio, A. Rosenberg, M. Sarasso, R. L. Smart, A. Spagna, C. R. Sturch, A. Volpicelli, R. L. White, D. Wolfe and A. Zacchei, 2008, "The Second-Generation Guide Star Catalog: Description and Properties", *Astron. J.* **136**, 735–766. [2008AJ....136..735L]

Lazzaro *et al.*, 2004 : D. Lazzaro, C. A. Angeli, J. M. Carvano, T. Mothé-Diniz, R. Duffard and M. Florczak, 2004, "S^3OS^2: The Visible Spectroscopic Survey of 820 Asteroids", *Icarus* **172**, 179–220. [2004Icar..172..179L]

Lebofsky and Spencer, 1989: L. A. Lebofsky and J. R. Spencer, 1989, "Radiometry and Thermal Modeling of Asteroids", in *Asteroids II*, 128–147. [1989aste.conf..128L]

Lebofsky *et al.*, 1986 : L. A. Lebofsky, M. V. Sykes, E. F. Tedesco, G. J. Veeder, D. L. Matson, R. H. Brown, J. C. Gradie, M. A. Feierberg and R. J. Rudy, 1986, "A refined 'standard' thermal model for asteroids based on observations of 1 Ceres and 2 Pallas", *Icarus* **68**, 239–251. [1986Icar...68..239L]

Lecar *et al.*, 2001 : M. Lecar, F. A. Franklin, M. J. Holman and N. J. Murray, 2001, "Chaos in the Solar System", *Annu. Rev. Astron. Astrophys.* **39**, 581–631. [2001ARA&A..39..581L]

Lowry *et al.*, 2007 : S. C. Lowry, A. Fitzsimmons, P. Pravec, D. Vokrouhlický, H. Boehnhardt, P. A. Taylor, J.-L. Margot, A. Galád, M. Irwin, J. Irwin, and P. Kusnirák, 2007, "Direct Detection of the Asteroidal YORP Effect", *Science* **316**, 272–274. [2007Sci...316..272L]

Lumme *et al.*, 1993 : K. Lumme, K. Muinonen, A. W. Harris and E. Bowell, 1993, "A New Three-Parameter Magnitude System for Asteroids", *Bull. Amer. Astron. Soc.* **25**, 1125. [1993DPS....25.3402L]

Lupishko *et al.*, 1980 : D. F. Lupishko, N. N. Kiselev, G. P. Chernova and I. N. Belskaya, 1980, "The Opposition Effect and the Surface Structure of the Asteroid 16 Psyche", *Sov. Astron. Lett.* **6**, 102–104. [1980SvAL....6..102L]

Lupishko *et al.*, 1981 : D. F. Lupishko, F. P. Velichko, F. A. Tupieva and G. P. Chernova, 1981, "Asteroid 354 Eleonora: Orientation of Rotation Axis and *UBV* Photometry", *Sov. Astron. Lett.* **7**, 241–244. [1981SvAL....7..241L]

Magnusson and Lagerkvist, 1991 : P. Magnusson and C.-I. Lagerkvist, 1991, "Physical Studies of Asteroids: XXII. Photoelectric Photometry of the Asteroids 34, 98, 115, 174, 270, 389, 419 and 804", *Astron. Astrophy. Suppl.* **87**, 269–275. [1991A&AS...87..269M]

Magnusson *et al.*, 1996 : P. Magnusson, M. Dahlgren, M. A. Barucci, L. Jorda, R. P. Binzel, S. M. Slivan, C. Blanco, D. Riccioli, B. J. Buratti, F. Colas, J. Berthier, G. De Angelis, M. Di Martino, E. Dotto, J. D. Drummond, U. Fink, M. Hicks, W. Grundy, W. Wisniewski, N. M. Gaftonyuk, E. H. Geyer, T. Bauer, M. Hoffmann, V. Ivanova, B. Komitov, Z. Donchev, P. Denchev, Yu. N. Krugly, F. P. Velichko, V. G. Chiorny, D. F. Lupishko, V. G. Shevchenko, T. Kwiatkowski, A. Kryszczynka, J. F. Lahulla, J. Licandro, O. Mendez, S. Mottola, A. Erikson, S. J. Ostro, P. Pravec, W. Pych, D. J. Tholen, R. Whiteley, W. J. Wild, M. Wolf and L. Šarounová, 1996, "Photometric Observations and Modeling of Asteroid 1620 Geographos", *Icarus* **123**, 227–244. [1996Icar..123..227M]

Mainzer *et al.*, 2011 : A. Mainzer, T. Grav, J. Bauer, J. Masiero, R. S. McMillan, R. M. Cutri, R. Walker, E. Wright, P. Eisenhardt, D. J. Tholen, T. Spahr, R. Jedicke, L. Denneau, E. DeBaun, D. Elsbury, T. Gautier, S. Gomillion, E. Hand, W. Mo, J. Watkins, A. Wilkins, G. L. Bryngelson, A. Del Pino Molina, S. Desai, M. Gómez Camus, S. L. Hidalgo, I. Konstantopoulos, J. A. Larsen, C. Maleszewski, M. A. Malkan, J.-C. Mauduit, B. L. Mullan, E. W. Olszewski, J. Pforr, A. Saro, J. V. Scotti and L. H. Wasserman, 2011, "NEOWISE Observations of Near-Earth Objects: Preliminary Results", *Astrophys. J.* **743**, 156. [2011ApJ...743..156M]

Majewski *et al.*, 1994 : S. R. Majewski, R. G. Kron, D. C. Koo and M. A. Bershady, 1994, "Deep *UBVRI* Photometric Calibration of High-Latitude Fields: SA 57 (1307+30) and Hercules (1720+50)", *Publ. Astron. Soc. Pac.* **106**, 1258–1270. [1994PASP..106.1258M]

Marciniak *et al.*, 2009 : A. Marciniak, T. Michałowski, R. Hirsch, R. Behrend, L. Bernasconi, P. Descamps, F. Colas. K. Sobkowiak, K. Kamiński, A. Kryszcyńska, T. Kwiatkowski, M. Polińska, R. Rudawska, S. Fauvaud, G. Santacana, A. Bruno, M. Fauvaud, J.-P. Teng-Chien-Yu and A. Peyrot, 2009, "Photometry and Models of Selected Main Belt Asteroids: VII. 350 Ornamenta, 771 Libera and 984 Gretia", *Astron. Astrophys.* **508**, 1503–1507. [2009A&A...508.1503M]

Marsden, 1980 : B. G. Marsden, 1980, "The Minor Planet Center", *Celest. Mech.* **22**, 63–71. [1980CeMec..22...63M]

Marsden, 1985 : B. G. Marsden, 1985, "Notes from the IAU General Assembly", *Minor Planet Circ.* 10193–10194. [1985MPC..10193...1M]

Marsden, 1993 : B. G. Marsden, 1993, "Periodic Comet Shoemaker-Levy 9 (1993e)", *IAU Circ.* 5893, 1. [1993IAUC.5893....1M]

Marsden, 1996 : B. G. Marsden, 1996, "Searches for Planets and Comets", *Astron. Soc. Pac. Conf. Proc.* **107**, 193–207. [1996ASPC..107..193M]

Marsden *et al.*, 1994 : B. G. Marsden, D. W. E. Green and G. V. Williams, 1994, "MPC and ICQ Databases", in *Asteroids, Comets, Meteors 1993*, 489–494. [1994IAUS..160..489M]

Masi *et al.*, 2008 : G. Masi, S. Foglia and R. P. Binzel, 2008, "Search and Confirmation of V-type Asteroids Beyond 2.5 AU Using Sloan Digital Sky Survey Colors", *LPI Contrib.* **1405**, 8065. [2008LPICo1405.8065M]

Masiero *et al.*, 2011 : J. R. Masiero, A. K. Mainzer, T. Grav, J. M. Bauer, R. M. Cutri, J. Dailey, P. R. M. Eisenhardt, R. S. McMillan, T. B. Spahr, M. F. Skrutskie, D. Tholen, R. G. Walker, E. L. Wright, E. DeBaun, D. Elsbury, T. Gautier IV, S. Gomillion and A. Wilkins, 2011, "Main Belt Asteroids with WISE/NEOWISE. I. Preliminary Albedos and Diameters", *Astrophys. J.* **741**, 68 [2011ApJ...741...68M]

Matson *et al.*, 1986 : D. L. Matson, G. J. Veeder, L. A. Lebofsky, E. F. Tedesco and R. G. Walker, 1986, "The IRAS Asteroid and Comet Survey", *Bull. Amer. Astron. Soc.* **18**, 790. [1986BAAS...18Q.790M]

McCord and Chapman, 1975a : T. B. McCord and C. R. Chapman, 1975a, "Asteroids: Spectral Reflectance and Color Characteristics", *Astrophys. J.* **195**, 553–562. [1975ApJ...195..553M]

McCord and Chapman, 1975b : T. B. McCord and C. R. Chapman, 1975b, "Asteroids: Spectral Reflectance and Color Characteristics. II", *Astrophys. J.* **197**, 781–790. [1975ApJ...197..781M]

Meyer and Raab, 1995 : E. Meyer and H. Raab, 1995, "CCD Astrometry", *CCD Astronomy* **2**, No. 1, 20–22. [1995CCDA....2...20M]

Michałowski and Velichko, 1990 : T. Michałowski and F. P. Velichko, 1990, "Photoelectric Photometry, Parameters of Rotation and Shapes of Asteroids 22 Kalliope and 79 Eurynome", *Acta Astron.* **40**, 321–332. [1990AcA....40..321M]

Miller *et al.*, 1995 : J. K. Miller, P. J. Antreasian, J. Georgini, W. M. Owen, B. G. Williams and D. K. Yeomans, 1995, "Determination of Eros Physical Parameters for Near Earth Asteroid Rendezvous Orbit Phase Navigation", *NASA STI/Recon Tech. Rep. N*, 75266. [1995STIN...0075266M]

Millis *et al.*, 1976 : R. L. Millis, E. Bowell and D. T. Thompson, 1976, "*UBV* Photometry of Asteroid 433 Eros", *Icarus* **28**, 53–67. [1976Icar...28...53M]

Misselt, 1996 : K. A. Misselt, 1996, "Secondary Photometric Standards in Selected Northern Dwarf-Nova Fields", *Publ. Astron. Soc. Pac.* **108**, 146–165. [1996PASP..108..146M]

Mohamed *et al.*, 1994a : R. A. Mohamed, V. G. Chiorny, A. N. Dovgopol and V. G. Shevcheno, 1994, "Photometry of five asteroids: 189 Phthia, 220 Stephania, 289 Nenetta, 312 Pierretta and 626 Notburga", *Astron. Astrophys. Suppl.* **108**, 69–72. [1994A&AS..108...69M]

Mohamed *et al.*, 1994b : R. A. Mohamed, Y. N. Krugly and F. P. Velichko, 1994, "Photometry of two Mars-Crossing Asteroids 2078 Nanking and 2204 Lyyli", *Planet. Space Sci.* **42**, 341–343. [1994P&SS...42..341M]

Mohamed *et al.*, 1995 : R. A. Mohamed, Y. N. Krugly and D. F. Lupishko, 1995, "Light Curves and Rotation Periods of Asteroids 371 Bohemia, 426 Hippo, 480 Hansa and 735 Marghanna", *Astron. J.* **109**, 1877–1879. [1995AJ....109.1877M]

Monet *et al.*, 1996 : D. Monet, A. Bird, B. Canzian, H. Harris, N. Reid, A. Rhodes, S. Sell, H. Ables, C. Dahn, H. Guetter, A. Henden, S, Leggett, H. Levison, C. Luginbuhl, J. Martini, A. Monet, J. Pier, B. Riepe, R. Stone, F. Vrba and R. Walker, 1996, "The PMM USNO-A1.0 Catalogue", `http://vizier.u-strasbg.fr/vizier/VizieR/pmm/usnol.htx`.

Monet *et al.*, 1998 : D. Monet, A. Bird, B. Canzian, C. Dahn, H. Guetter, H. Harris, A. Henden, S. Levine, C. Luginbuhl, A. K. B. Monet, A. Rhodes, B. Riepe, S. Sell, R. Stone, F. Vrba and R. Walker, 1998, "The PMM USNO-A2.0 Catalogue", `http://vizier.u-strasbg.fr/vizier/VizieR/pmm/usno2.htx`.

Monet *et al.*, 2003 : D. G. Monet, S. E. Levine, B. Canzian, H. D. Ables, A. R. Bird, C. C. Dahn, H. H. Guetter, H. C. Harris, A. A. Henden, S. K.Leggett, H. F. Levison, C. B. Luginbuhl, J. Martini, A. K. B. Monet, J. A. Munn, J. R. Pier, A. R. Rhodes, B. Riepe, S. Sell, R. C. Stone, F. J. Vrba, R. L. Walker, G. Westerhout, R. J. Brucato, I. N. Reid, W. Schoening, M. Hartley, M. A. Read and S. B. Tritton, 2003; "The USNO-B Catalog", *Astron. J.* **125**, 984–993. [2003AJ....125..984M]

Moons and Morbidelli, 1995 : M. Moons and A. Morbidelli, 1995, "Secular Resonances in Mean Motion Commensurabilities: The 4/1, 3/1, 5/2 and 7/3 Cases", *Icarus* **114**, 33–50. [1995Icar..114...33M]

Morgan *et al.*, 1992 : D. H. Morgan, S. B. Tritton, A. Savage, M. Hartley and R. D. Cannon, 1992, "Current and Future Programmes with the UK Schmidt Telescope", in *Digitised Optical Sky Surveys*, 11–22. [1992ASSL..174...11M]

Moro and Munari, 2000 : D. Moro and U. Munari, 2000, "The Asiago Database on Photometric System (ADPS): I. Census Parameters for 167 Photometric Systems", *Astron. Astrophys. Suppl.* **147**, 361–628. [2000A&AS..147..361M]

Mottola *et al.*, 1995 : S. Mottola, G. de Angelis, M. di Martino, A. Erikson, G. Hahn and G. Neukum, 1995, "The Near-Earth Objects Follow-Up Program: First Results", *Icarus* **117**, 62–70. [1995Icar..117...62M]

Mottola *et al.*, 1997 : S. Mottola, A. Erikson, A. W. Harris, G. Hahn, G. Neukum, M. W. Buie, W. D. Sears, A. W. Harris, D. J. Tholen, R. Whiteley, P. Magnusson, J. Piironen, T. Kwiatkowski, W. Borczyk, E. S. Howell, M. D. Hicks, R. Fevig, Yu. N. Krugly, F. P. Velichko, V. G. Chiorny, N. M. Gaftonyuk, M. Di Martino, P. Pravec, L. Šarounová, M. Wolf, W. Worman, J. K. Davies, H.-J. Schober and W. Pych, 1997, "Physical Model of Near-Earth Asteroid 6489 Golevka (1991 JX) From Optical and Infrared Observations", *Astron. J.* **114**, 1234–1245. [1997AJ....114.1234M]

Mueller *et al.*, 2007 : M. Mueller, A. W. Harris and A. Fitzsimmons, 2007, "Size, Albedo and Taxonomic Type of Potential Spacecraft Target Asteroid (10302) 1989 ML", *Icarus* **187**, 611–615. [2007Icar..187..611M]

Muinonen, 1994 : K. Muinonen, 1994, "Coherent Backscattering by Solar System Dust Particles", in *Asteroids, Comets, Meteors 1993*, 271–296. [1994IAUS..160..271M]

Muinonen *et al.*, 2010 : K. Muinonen, I. N. Belskaya, A. Cellino, M. Delbò, A.-C. Levasseur-Regourd, A. Penttilä and E. F. Tedesco, 2010, "A Three-Parameter Magnitude Phase Function for Asteroids", *Icarus* **209**, 542–555. [2010Icar..209..542M]

Müller, 1886 : G. Müller, 1886, "Beobachtungen über den Einfluss der Phase auf dir Lichtstärke kleiner Planeten" ["Observation of the Influence of Phase on the Brightness of Minor Planets"], *Astron. Nachr.* **114**, 177–196. [1886AN....114..177M]

Müller, 1888 : G. Müller, 1888, "H. M. Parkhurst, Photometric Observations of Asteroids", *Vierteljahrschrift Astron. Ges.* **23**, 297–308. [1888VAG....23..297M]

Müller, 1893 : G. Müller, 1893, "Helligkeitbestimmungen des grossen Planeten und einiger Asteroiden" ["Brightness Measurements of the Major Planets and some Asteroids"], *Publ. Astrophys. Obs. Potsdam* **8**, 198–389. [1893POPot..30..198M]

Müller, 1897 : G. Müller, 1897, *Die Photometrie der Gestirne* [*Stellar Photometry*], Engelmann, Leipzig.

Neugent and Slivan, 2008 : K. F. Neugent and S. M. Slivan, 2008, "Rotation Periods and *H* Magnitudes of Two Koronis Family Members", *Minor Planet Bull.* **35**, 116–118. [2008MPBu...35..116N]

Noll *et al.*, 2006 : K. S. Noll, H. F. Levison, W. M. Grundy and D. C. Stephens, 2006, "Discovery of a Binary Centaur", *Icarus* **184**, 611–618. [2006Icar..184..611N]

Nomen *et al.*, 2010 : J. Nomen, P. Birtwhistle, R. Holmes, S. Foglia and J. V. Scotti, 2010, "Comet P/2010 R2 (La Sagra)", *Cent. Bureau Electron. Tel.* 2459. [2010CBET.2459....1N]

Nugent *et al.*, 2012 : C. R. Nugent, A. Mainzer, J. Masiero, T. Grav and J. Bauer, 2012, "The Yarkovsky Drift's Influence on NEAs: Trends and Predictions with NEOWISE Measurements", *Astron. J.* **144**, 75. [2012AJ....144...75N]

Ochsenbein, 2009 : F. Ochsenbein, 2009, personal communication, e-mail dated 2009 Sept. 18.

Ochsenbein *et al.*, 2000 : F. Ochsenbein, P. Bauer and J. Marcout, 2000, "The Vizier Database of Astronomical Catalogues", *Astron. Astrophys. Suppl.* **143**, 23–32. [2000A&AS..143...23O]

Oke, 1974 : J. B. Oke, 1974, "Absolute Spectral Energy Distributions for White Dwarfs", *Astrophys. J. Suppl.* **236**, 21–35. [1974ApJS...27...21O]

Orton *et al.*, 2009 : G. S. Orton, L. Fletcher, A. Wesley, P. Yanamandra-Fisher, B. Fisher, O. Mousis, W. Golisch, I. de Pater, F. Marchis, P. Kalas, M. Fitzgerald, J. Graham, M. Wong, J. Rogers, T. Momary, A. Sanchez-Lavega, H. Hammel and A. Simon-Miller, 2009, "First Observations of the 2009 Collision in Jupiter's Atmosphere", *AAS/Division for Planetary Sciences Meeting Abstracts* **#41**, #10.01. [2009DPS....41.1001O]

Ostro *et al.*, 1984 : S. J. Ostro, A. W. Harris, D. B. Campbell, I. I. Shapiro and J. W. Young, 1984, "Radar and Photoelectric Observations of Asteroid 2100 Ra-Shalom", *Icarus* **60**, 391–403. [1984Icar...60..391O]

Oszkiewicz *et al.*, 2011 : D. A. Oszkiewicz, K. Muinonen, E. Bowell, D. Trilling, A. Penttilä, T. Pieniluoma, L. H. Wasserman and M.-T. Enga, 2011, "Online Multi-Parameter Phase-Curve Fitting and Application to a Large Corpus of Asteroid Photometric Data", *J. Quant. Spectrosc. Radiat. Trans.* **112**, 1919–1929. [2011JQSRT.112.1919O]

Oszkiewicz *et al.*, 2012 : D. A. Oszkiewicz, E. Bowell, L. H. Wasserman, K. Muinonen, A. Penttilä, T. Pieniluoma, D. E. Trilling and C. A. Thomas, 2012, "Asteroid Taxonomic Signatures from Photometric Phase cCrves", *Icarus* **219**, 283–296. [2012Icar..219..283O]

Parker *et al.*, 2008 : A. Parker, Ž. Ivezić, M. Jurić, R. Lupton, M. D. Sekora and A. Kowalski, 2008, "The Size Distributions of Asteroid Families in the SDSS Moving Object Catalog 4", *Icarus* **198**, 138–155. [2008Icar..198..138P]

Parkhurst, 1889 : H. M. Parkhurst, 1889, "Photometric Observations of Asteroids", *Astron. J.* **9**, 127. [1889AJ.....9..127P]

Parkhurst, 1890 : H. M. Parkhurst, 1890, "Photometric Observations of Asteroids", *Ann. Harv. Coll. Obs.* **18**, 29–72. [1890AnHar..18...29P]

Parkhurst, 1893 : H. M. Parkhurst, 1893, "Photometric Observations of Asteroids", *Ann. Harv. Coll. Obs.* **29**, 65–78. [1893AnHar..29...65P]

Parley, 2008 : N. R. Parley, 2008, *Serendipitous Asteroid Survey Using SuperWASP*, PhD Thesis, Open University.

Patry, 1958 : A. Patry, 1958, "Identification: (864) Aase = (1078) Mentha", *Minor Planet Circ.* 1763. [1958MPC...1763...1P]

Paulson *et al.*, 2006 : D. B. Paulson, J. C. Allred, R. B. Anderson, S. L. Hawley, W. Cochran and S. Yelda, 2006, "Optical Spectroscopy of a Flare on Barnard's Star", *Publ. Astron. Soc. Pac.* **118**, 227–235. [2006PASP..118..227P]

Perna *et al.*, 2010 : D. Perna, M. A. Barucci, S. Fornasier, F. E. DeMeo, A. Alvarez-Candal, F. Merlin, E. Dotto, A. Doressoundiram and C. de Bergh, 2010, "Colors and Taxonomy of Centaurs and Trans-Neptunian Objects", *Astron. Astrophys.* **510**, A53. [2010A&A...510A..53P]

Pfleiderer *et al.*, 1987 : J. Pfleiderer, M. Pfleiderer and A. Hanslmeier, 1987, "Photoelectric Five-Colour Photometry of the Asteroids 16 Psyche, 201 Penelope and 702 Alauda", *Astron. Astrophys. Suppl.* **69**, 117–122. [1987A&AS...69..117P]

Pickering, 1879 : E. C. Pickering, 1879, "Stellar Magnitudes", *Astron. Nachr.* **95**, 29–32. [1879AN.....95...29P] Also *Mon. Not. R. Astron. Soc.* **39**, 391–393 [1879MNRAS..39..391P] and *Nature* **20**, 14–15. [1879Natur..20...14P]

Pickering, 1893 : E. C. Pickering, 1893, "Comparison of Results Obtained from the Photometric Observations of Asteroids by Parkhurst and Müller", *Ann. Harv. Coll. Obs.* **29**, 225–227. [1893AnHar..29..225P]

Pickering, 1909 : E. C. Pickering, 1909, "A Standard Scale of Photographic Magnitude", *Harvard Coll. Obs. Circ.* 150. [1909HarCi.150....1P]

Pickering, 1911 : E. C. Pickering, 1911, "Photometric Observations of Asteroids", *Harv. Coll. Obs. Circ.* 169. [1911HarCi.169....1P]

Pickering and Wendell, 1890 : E. C. Pickering and O. C. Wendell, 1890, "Results of Observations with the Meridian Photometer During the Years 1882–88", *Ann. Harv. Coll. Obs.* **24**. [1890AnHar..24....1P]

Pickering *et al.*, 1881 : E. C. Pickering, L. Boss, S. W. Burnham, A. Hall, W. Harkness, E. S. Holden, S. Newcomb, C. H. F. Peters, O. Stone and C. A. Young, 1881, "Report of the Committee on Standards of Stellar Magnitude", *Obser.* **4**, 327–329. [1881Obs.....4..327P]

Pickering *et al.*, 1884 : E. C. Pickering, A. Searle and O. C. Wendell, 1884, "Observations with the Meridian Photometer During the Years 1879–82", *Ann. Harv. Coll. Obs.* **14**. [1884AnHar..14.....P]

Pickering *et al.*, 1885 : E. C. Pickering, L. Boss, S. W. Burnham, A. Hall, W. Harkness, E. S. Holden, S. Newcomb, C. H. F. Peters, O. Stone and C. A. Young, 1885, "Second Report of the Committee on Standards of Stellar Magnitudes", *Obser.* **8**, 51–52. [1885Obs.....8...51P]

Piironen *et al.*, 1998 : J. Piironen, C.-I. Lagerkvist, A. Erikson, T. Oja, P. Magnusson, L. Festin, A. Nathues, M. Gaul and F. Velichko, 1998, "Physical Studies of Asteroids XXXII. Rotation Periods and *UBVRI*-Colours for Selected Asteroids", *Astron. Astrophys. Suppl.* **128**, 525–540. [1998A&AS..128..525P]

Piironen *et al.*, 2001 : J. Piironen, C.-I. Lagerkvist, J. Torppa, M. Kaasalainen and B. Warner, 2001, "Standard Asteroid Photometric Catalogue", *Bull. Amer. Astron. Soc.* **33**, 1562. [2001DPS....33.5812P]

Pogson, 1856 : N. Pogson, 1856, "Magnitudes of Thirty-Six of the Minor Planets for the First Day of Each Month of the Year 1857", *Mon. Not. R. Astron. Soc.* **17**, 12–15. [1856MNRAS..17...12P]

Pogson, 1857 : N. Pogson, 1857, "Magnitudes of Forty of the Minor Planets, for the First Day of Each Month in the Year 1858", *Mon. Not. R. Astron. Soc.* **18**, 47–49. [1857MNRAS..18...47P] Also *Astron. Nachr.* **47**, 289–292. [1858AN.....47..289P]

Pogson, 1859 : N. Pogson, 1859, "Magnitudes of Forty-Eight of the Minor Planets for the First Day of Each Month in the Year 1859", *Mon. Not. R. Astron. Soc.* **19**, 80–81. [1859MNRAS..19...80P]

Pogson, 1860 : N. Pogson, 1860, "Magnitude Constants for Fifty-Seven of the Minor Planets", *Mon. Not. R. Astron. Soc.* **21**, 33–35. [1860MNRAS..21...33P]

Polishook and Brosch, 2008 : D. Polishook and N. Brosch, 2008, "Photometry of Aten Asteroids—More Than a Handful of Binaries", *Icarus* **194**, 111–124. [2008Icar..194..111P]

Polishook and Brosch, 2009 : D. Polishook and N. Brosch, 2009, "Photometry and Spin Rate Distribution of Small-Sized Main Belt Asteroids", *Icarus* **199**, 319–332. [2009Icar..199..319P]

Poutanen *et al.*, 1985 : M. Poutanen, E. Bowell, L. J. Martin and D. T. Thompson, 1985, "Photoelectric Photometry of Asteroid 69 Hesperia", *Astron. Astrophys. Suppl.* **61**, 291–297. [1985A&AS...61..291P]

Pratchett and Wood, 1976 : B. Pratchett and R. Wood, 1976, "The 1974 Type I Supernova in NGC 4414", *Mon. Not. R. Astr. Soc.* **175**, 595–603. [1976MNRAS.175..595P]

Pravdo *et al.*, 1999 : S. H. Pravdo, D. L. Rabinowitz, E. F. Helin, K. J. Lawrence, R. J. Bambery, C. C. Clark, S. L. Groom, S. Levin, J. Lorre, S. B. Shaklan, P. Kervin, J. A. Africano, P. Sydney and V. Soohoo, 1999, "The Near-Earth Asteroid Tracking (NEAT) Program: An Automated System for Telescope Control, Wide-Field Imaging, and Object Detection", *Astron. J.* **117**, 1616–1633. [1999AJ....117.1616P]

Pravec *et al.*, 1995 : P. Pravec, M. Wolf, M. Varady and P. Bárta, 1995, "CCD Photometry of 6 Near-Earth Asteroids", *Earth, Moon Planets* **71**, 177–187. [1995EM&P...71..177P]

Pravec *et al.*, 1996 : P. Pravec, L. Šarounová and M. Wolf, 1996, "Lightcurves of 7 Near-Earth Asteroids", *Icarus* **124**, 471–482. [1996Icar..124..471P]

Pravec *et al.*, 1997a : P. Pravec, M. Wolf, L. Šarounová, A. W. Harris and J. K. Davies, 1997, "Spin Vector, Shape and Size of the Amor Asteroid (6053) 1993 BW_3", *Icarus* **127**, 441–451. [1997Icar..127..441P]

Pravec *et al.*, 1997b : P. Pravec, M. Wolf, L. Šarounová, S. Mottola, A. Erikson, G. Hahn, A. W. Harris, A. W. Harris and J. W. Young, 1997, "The Near-Earth Objects Follow-Up Program: II. Results for 8 Asteroids from 1982 to 1995", *Icarus* **130**, 275–286. [1997Icar..130..275P]

Pravec *et al.*, 1998 : P. Pravec, M. Wolf and L. Šarounová, 1998, "Lightcurves of 26 Near-Earth Asteroids", *Icarus* **136**, 124–153. [1998Icar..136..124P]

Pravec *et al.*, 2000a : P. Pravec, C. Hergenrother, R. Whiteley, L. Šarounová, P. Kušnirák and M. Wolf, 2000, "Fast Rotating Asteroids 1999 TY_2, 1999 SF_{10} and 1998 WB_2", *Icarus* **147**, 477–486. [2000Icar..147..477P]

Pravec *et al.*, 2000b : P. Pravec, P. Kušnirák, M. Hicks, B. Holliday and B. Warner, 2000, "2000 DP_{107}", *Int. Astron. Union Circ.* 7504, 3. [2000IAUC.7504....3P]

Pravec *et al.*, 2002a : P. Pravec, P. Kušnirák, L. Šarounová, A. W. Harris, R. P. Binzel and A. S. Rivkin, 2002, "Large Coherent Asteroid 2001 OE_{84}", in *Proceedings of Asteroids, Comets, Meteors (ACM 2002)*, 743–745. [2002ESASP.500..743P]

Pravec *et al.*, 2002b : P. Pravec, A. W. Harris and T. Michałowski, 2002, "Asteroid Rotations", in *Asteroids III*, 113–122. [2002aste.conf..113P]

Pravec *et al.*, 2005 : P. Pravec, A. W. Harris, P. Scheirich, P. Kušnirák, L. Šarounová, C. W. Hergenrother, S. Mottola, M. D. Hicks, G. Masi, Yu. N. Krugly, V. G. Shevchenko, M. C. Nolan, E. S. Howell, M. Kaasalainen, A. Galád, P. Brown, D. R. DeGraff, J. V. Lambert, W. R. Cooney Jr. and S. Foglia, 2005, "Tumbling Asteroids", *Icarus* **173**, 108–131. [2005Icar..173..108P]

Pravec *et al.*, 2006 : P. Pravec, P. Scheirich, P. Kušnirák, L. Šarounová, S. Mottola, G. Hahn, P. Brown, G. Esquerdo, N. Kaiser, Z. Krzeminski, D. P. Pray, B. D. Warner, A. W. Harris, M. C. Nolan, E. S. Howell, L. A. M. Benner, J.-L. Margot, A. Galád, W. Holliday, M. D. Hicks, Yu. N. Krugly, D. Tholen, R. J. Whiteley, F. Marchis, D. R. DeGraff, A. Grauer, S. Larson, F. P. Velichko, W. R. Cooney Jr., R. Stephens, J. Zhu, K. Kirsch, R. Dyvig. L. Snyder, V. Reddy, S. Moore, Š. Gajdoš, J. Világi, G. Masi, D. Higgins, G. Funkhouser, B. Knight, S. Slivan, R. Behrend, M. Grenon, G. Burki, R. Roy, C. Demeautis, D. Matter, N. Waelchli, Y. Revaz, A. Klotz, M. Rieugné, P. Thierry, V. Cotrez, L. Brunetto and G. Kober, 2006, "Photometric Survey of Binary Near-Earth Asteroids", *Icarus* **181**, 63–93. [2006Icar..181...63P]

Pravec *et al.*, 2012 : P. Pravec, A. W. Harris, P. Kušnirak, A. Galád and K. Hornoch, 2012, "Absolute Magnitudes of Asteroids and a Revision of Asteroid Albedo Estimates From NEOWISE Thermal Observations", *Icarus* **221**, 365–387. [2012Icar..221..365P]

Prialnik and Rosenberg, 2009 : D. Prialnik and E. D. Rosenberg, 2009, "Can Ice Survive in Main-Belt Comets? Long-term Evolution Models of Comet 133P/Elst-Pizarro", *Mon. Not. R. Astron. Soc.* **399**, L79–L83. [2009MNRAS.399L..79P]

Read *et al.*, 2005 : M. T. Read, T. H. Bressi, T. Gehrels, J. V. Scotti, and E. J. Christensen, 2005, "Comet P/2005 U1 (Read)", *IAU Circ.* 8624. [2005IAUC.8624....1R]

Recht, 1934 : A. Recht, 1934, "Magnitudes and Color Indices of Asteroids", *Astron. J.* **44**, 25–32. [1934AJ.....44...25R]

Reynoldson *et al.*, 1993 : G. Reynoldson, P. Thacker, A. Ericson and T. Oja, 1993, "Photoelectric Photometry of Asteroid 4 Vesta", *Minor Planet. Bull.* **20**, 11–13. [1993MPBu...20...11R]

Rock and Hollis, 1990 : J. W. Rock and A. J. Hollis, 1990, "Photometric Properties of the Minor Planets: Observations of (4) Vesta between 1972 and 1988", *J. Brit. Astron. Assoc.* **100**, 17–22. [1990JBAA..100...17R]

Romanishin *et al.*, 1997 : W. Romanishin, S. C. Tegler, J. Levine and N. Butler, 1997, "*BVR* Photometry of Centaur Objects 1995 GO, 1993 HA_2 and 5145 Pholus", *Astron. J.* **113**, 1893–1898. [1997AJ....113.1893R]

Romon-Martin *et al.*, 2003 : J. Romon-Martin, C. Delahodde, M. A. Barucci, C. de Bergh and N. Peixinho, 2003, "Photometric and spectroscopic observations of (2060) Chiron at the ESO Very Large Telescope", *Astron. Astrophys.* **400**, 369–373. [2003A&A...400..369R]

Rosenbush *et al.*, 2009 : V. K. Rosenbush, V. G. Shevchenko, N. K. Kiselev, A. V. Sergeev, N. K. Shakhovskoy, F. P. Velichko, S. V. Kolesnikov and N. V. Karpov, 2009, "Polarization and Brightness Opposition Effects for the E-Type Asteroid 44 Nysa", *Icarus* **201**, 655–665. [2009Icar..201..655R]

Rozitis and Green, 2011 : B. Rozitis and S. F. Green, 2011, "Directional Characteristics of Thermal-Infrared Beaming from Atmosphereless Planetary Surfaces–A New Thermophysical Model", *Mon. Not. R. Astron. Soc.* **415**, 2042–2062. [2011MNRAS.415.2042R]

Rubincam, 2000 : D. P. Rubincam, 2000, "Radiative Spin-up and Spin-down of Small Asteroids", *Icarus* **148**, 2–11. [2000Icar..148....2R]

Russell *et al.*, 1990 : J. L. Russell, B. M. Lasker, B. J. McLean, C. R. Sturch and H. Jenkner, 1990, "The Guide Star Catalog. II – Photometric and Astrometric Models and Solutions", *Astron. J.* **99**, 2059–2081. [1990AJ.....99.2059R]

Ryan, 2004 : W. H. Ryan, 2004, "Photometry of Minor Planet 6897 Tabei", *Minor Planet Bull.* **31**, 73–74. [2004MPBu...31...73R]

Samus and Durlevich, 2005 : N. N. Samus and O. V. Durlevich, 2005, *General Catalogue of Variable Stars*, `http://www.sai.msu.su/groups/cluster/gcvs/gcvs/index.htm`.

Santos-Sanz *et al.*, 2009 : P. Santos-Sanz, J. L. Ortiz, L. Barrera and H. Boehnhardt, 2009, "New *BVRI* Photometry Results on Kuiper Belt Objects from the ESO VLT", *Astron. Astrophys.* **494**, 693–706. [2009A&A...494..693S]

Sather, 1976 : R. E. Sather, 1976, "Minor Planet and Related Objects. XIX. Shape and Pole Orientation of (39) Laetitia", *Astron. J.* **81**, 67–73. [1976AJ.....81...67S]

Scaltriti and Zappalà, 1975 : F. Scaltriti and V. Zappalà, 1975, "A Photometric Study of the Minor Planet 15 Eunomia", *Astron. Astrophys. Suppl.* **19**, 249–255. [1975A&AS...19..249S]

Scaltriti and Zappalà, 1976 : F. Scaltriti and V. Zappalà, 1976, "A Photometric Study of the Minor Planets 192 Nausikaa and 79 Eurynome", *Astron. Astrophys. Suppl.* **23**, 167–179. [1976A&AS...23..167S]

Scaltriti and Zappalà, 1977 : F. Scaltriti and V. Zappalà, 1977, "Photoelectric photometry of the Minor Planets 41 Daphne and 129 Antigone", *Astron. Astrophys.* **56**, 7–11. [1977A&A....56....7S]

Schmude, 1995 : R. W. Schmude Jr., 1995, "Wideband Photometry of the Minor Planet 8 Flora", *I.A.P.P.P. Comm.* **61**, 48–49. [1995IAPPP..61...48S]

Schober, 1976 : H. J. Schober, 1976, "Photoelectric Photometry of the Minor Planet 32 Pomona: Composite Light Curve and the Synodic Period of Rotation", *Astron. Astrophys.* **53**, 115–119. [1976A&A....53..115S]

Schober, 1978 : H. J. Schober, 1978, "Photometric Variations of the Minor Planets 55 Pandora and 173 Ino During the Opposition in 1977: Light Curves and Rotation Periods", *Astron. Astrophys. Suppl.* **34**, 377–381. [1978A&AS...34..377S]

Schober, 1979 : H. J. Schober, 1979, "387 Aquitania and 776 Berberica: Two Slowly Spinning Asteroids with Rotation Periods of Nearly One Day?", *Astron. Astrophys. Suppl.* **38**, 91–99. [1979A&AS...38...91S]

Schober, 1981a : H. J. Schober, 1981, "Rotation Period of 234 Barbara, a Further Slowly Spinning Asteroid", *Astron. Astrophys.* **96**, 302–305. [1981A&A....96..302S]

Schober, 1981b : H. J. Schober, 1981, "Rotational Properties and Lightcurves of the Asteroids 679 Pax and 796 Sarita", *Astron. Astrophys.* **99**, 199–201. [1981A&A....99..199S]

Schober, 1981c : H. J. Schober, 1981, "Photoelectric Photometry of the Asteroids 404 Arsinoe and 628 Christine", *Astron. Astrophys.* **100**, 311–313. [1981A&A...100..311S]

Schober, 1982a : H. J. Schober, 1982, "Quadruple Extrema in the Complex Lightcurve of the Asteroid 37 Fides?", *Astron. Astrophys.* **105**, 419–421. [1982A&A...105..419S]

Schober, 1982b : H. J. Schober, 1982, "A Revised Rotation Period for the Asteroid 164 Eva", *Astron. Astrophys. Suppl.* **48**, 57–62. [1982A&AS...48...57S]

Schober, 1983a : H. J. Schober, 1983, "Rotation Periods and Lightcurves of the Asteroids 136 Austria and 238 Hypatia", *Astron. Astrophys.* **117**, 362–364. [1983A&A...117..362S]

Schober, 1983b : H. J. Schober, 1983, "The Large C-Type Asteroids 146 Lucina and 410 Chloris, and the Small S-Type Asteroids 152 Atala and 631 Philippina: Rotation Periods and Lightcurves", *Astron. Astrophys. Suppl.* **53**, 71–75. [1983A&AS...53...71S]

Schober, 1987 : H. J. Schober, 1987, "Rotation and Variability of the Large C-Type Asteroid 375 Ursula", *Astron. Astrophys.* **183**, 151–155. [1987A&A...183..151S]

Schober and Schroll, 1982 : H. J. Schober and A. Schroll, 1982, "The Asteroids 36 Atalante and 48 Doris: Rotation, *UBV*-Photometry and Lightcurves", *Astron. Astrophys.* **107**, 402–405. [1982A&A...107..402S]

Schober and Schroll, 1983 : H. J. Schober and A. Schroll, 1983, "Rotation Properties of the High-Numbered Asteroids 1236 Thais and 1317 Silvretta", *Astron. Astrophys.* **120**, 106–108. [1983A&A...120..106S]

Schober and Schroll, 1985 : H. J. Schober and A. Schroll, 1985, "The Asteroid 476 Hedwig: Lightcurve, Rotation Period and *UBV*-Photometry", *Astron. Astrophys. Suppl.* **62**, 187–189. [1985A&AS...62..187S]

Schober and Stadler, 1990 : H. J. Schober and M. Stadler, 1990, "Lightcurve of the Small S-Type Asteroid 714 Ulula: Large Amplitude and Short Period", *Astron. Astrophys.* **230**, 233–237. [1990A&A...230..233S]

Schober and Surdej, 1979 : H. J. Schober and J. Surdej, 1979, "*UBV* Photometry of the Asteroids 9 Metis, 87 Sylvia and 247 Eukrate During their Oppositions in 1989 with Respect to Lightcurves", *Astron. Astrophys. Suppl.* **38**, 269–274. [1979A&AS...38..269S].

Schober *et al.*, 1979 : H. J. Schober, F. Scaltriti and V. Zappalà, 1979, "Photoelectric Photometry and Rotation Periods of Three Large and Dark Asteroids: 49 Pales, 88 Thisbe and 92 Undina", *Astron. Astrophys. Suppl.* **36**, 1–8. [1979A&AS...36....1S]

Schober *et al.*, 1982 : H. J. Schober, J. Surdej, A. W. Harris and J. W. Young, 1982, "The Six-Day Rotation Period of 1689 Floris-Jan: A New Record Among Slowly Rotating Asteroids", *Astron. Astrophys.* **115**, 257–262. [1982A&A...115..257S]

Schober *et al.*, 1988 : H. J. Schober, M. Di Martino and A. Cellino, 1988, "165 Loreley, One of the Last Large "Unknown" Asteroids", *Astron. Astrophys.* **197**, 327–330. [1988A&A...197..327S]

Schober *et al.*, 1993 : H. J. Schober, A. Erikson, G. Hahn and C.-I. Lagerkvist, 1993, "Physical Studies of Asteroids: XXVI. Rotation Periods and Photoelectric Photometry of Asteroids 323, 350, 852, 1021 and 1866", *Astron. Astrophys. Suppl.* **101**, 499–505. [1993A&AS..101..485B]

Schober *et al.*, 1994 : H. J. Schober, A. Erikson, G. Hahn, C.-I. Lagerkvist, R. Albrecht, W. Ornig, A. Schroll and M. Stadler, 1994, "Physical Studies of Asteroids: XXVIII. Lightcurves and Photoelectric Photometry of Asteroids 2, 14, 51, 105, 181, 238, 258, 369, 377, 416, 487, 626, 679, 1048 and 2183", *Astron. Astrophys. Suppl.* **105**, 281–300. [1994A&AS..105..281S]

Scholl *et al.*, 1989 : H. Scholl, C. Froeschlé, H. Kinoshita, M. Yoshikawa and J. G. Williams, 1989, "Secular Resonances", in *Asteroids II*, 845–861. [1989aste.conf..845S]

Schuster *et al.*, 1979 : H. E. Schuster, A. Surdej and J. Surdej, 1979, "Photoelectric Observations of Two Unusual Asteroids: 1978 CA and 1978 DA", *Astron. Astrophys Suppl.* **37**, 483–486. [1979A&AS...37..483S]

Schulz *et al.*, 2012 : R. Schulz, H. Sierks, M. Küppers and A. Accomazzo, 2012, "Rosetta Fly-by at Asteroid (21) Lutetia: An Overview", *Planet. Space Sci.* **66**, 2–8. [2012P&SS...66....2S]

Scotti and Larsen, 2009 : J. V. Scotti and J. A. Larsen, 2009, personal communication, e-mail dated 2009 Feb. 5.

Searle, 1889 : A. Searle, 1889, "The Zodiacal Light", *Ann. Harv. Coll. Obs.* **19**, 165–245. [1889AnHar..19..165S]

Sesar *et al.*, 2011 : B. Sesar, J. S. Stuart, Ž. Ivezić, D. P. Morgan, A. C. Becker and P. Woźniak, 2011, "Exploring the Variable Sky with LINEAR. I. Photometric Recalibration with the Sloan Digital Sky Survey", *Astron. J.* **142**, 190. [2011AJ....142..190S]

Shatzel, 1954 : A. V. Shatzel, 1954, "Photometric Studies of Asteroids. III The Light-curve of 44 Nysa", *Astrophys. J.* **120**, 547–550. [1954ApJ...120..547S]

Sheppard, 2010 : S. S. Sheppard, 2010, "The Colors of Extreme Outer Solar System Objects", *Astron. J.* **139**, 1394–1405. [2010AJ....139.1394S]

Shevchenko, 1997 : V. G. Shevchenko, 1997, "Analysis of Asteroid Brightness–Phase Relations", *Sol. Sys. Res.* **31**, 246–254. [1997SoSyR..31..219S]

Shevchenko *et al.*, 1992 : V. G. Shevchenko, V. G. Chiornij, Yu. N. Krugly, D. F. Lupishko, R. A. Mohamed, F. P. Velichko, T. Michałowski, V. V. Avramchuk and A. N. Dovgopol, 1992, "Photometry of Seventeen Asteroids", *Icarus* **100**, 295–306. [1992Icar..100..295S]

Shevchenko *et al.*, 1996 : V. G. Shevchenko, V. G. Chiorny, A. V. Kalashnikov, Y. N. Krugly, R. A. Mohamed and F. P. Velichko, 1996, "Magnitude-Phase Dependences for Three Asteroids", *Astron. Astrophys. Suppl.* **115**, 475–479. [1996A&AS..115..475S]

Shevchenko *et al.*, 1997 : V. G. Shevchenko, I. N. Belskaya, V. G. Chiorny, J. Piironen, A. Erikson, G. Neukum and R. Mohamed, 1997, "Asteroid Observations at Low Phase Angles. I. 50 Virginia, 91 Aegina and 102 Miriam", *Planet. Space Sci.* **45**, 1615–1623. [1997P&SS...45.1615S]

Shevchenko *et al.*, 2003 : V. G. Shevchenko, Yu. N. Krugly, V. G. Chiorny, I. N. Belskaya and N. M. Gaftonyuk, 2003, "Rotation and Photometric Properties of E-Type Asteroids", *Planet. Space Sci.* **51**, 525–532. [2003P&SS...51..525S]

Shevchenko *et al.*, 2008 : V. G. Shevchenko, V. G. Chiorny, N. M. Gaftonyuk, Yu. N. Krugly, I. N. Belskaya, I. A. Tereschenko, F. P. Velichko, 2008, "Asteroid Observations at Low Phase Angles. III. Brightness Behavior of Dark Asteroids", *Icarus* **196**, 601–611. [2008Icar..196..601S]

Shevchenko *et al.*, 2009a : V. G. Shevchenko, Yu. N. Krugly, I. N. Belskaya, V. G. Chiorny, N. M. Gaftonyuk, I. G. Slyusarev, A. Tereschenko, Z. Donchev, V. Ivanova, G. Borisov, M. A. Ibrahimov, A. L. Marshalkina and I. E. Molotov, 2009, "Do Trojan Asteroids Have the Brightness Opposition Effect?", *40th Lunar and Planetary Science Conference* 1391. [2009LPI....40.1391S]

Shevchenko *et al.*, 2009b : V. G. Shevchenko, N. Tungalag, V. G. Chiorny, N. M. Gaftonyuk, Y. N. Krugly, A. W. Harris and J. W. Young, 2009, "CCD-Photometry and Pole Coordinates for Eight Asteroids", *Planet. Space Sci.* **57**, 1514–1520. [2009P&SS...57.1514S]

Skiff, 2000a : B. A. Skiff, 2000, "Photometry of Stars in the Field of BI Andromedae", *Int. Bull. Var. Stars* 4889. [2000IBVS.4889....1S]

Skiff, 2000b : B. A. Skiff, 2000, "Photometry of Stars in the Field of AF Cygni and AW Cygni", *Int. Bull. Var. Stars* 4890. [2000IBVS.4890....1S]

Skiff, 2000c : B. A. Skiff, 2000, "Photometry of Stars in the Field of BF Cygni", *Int. Bull. Var. Stars* 4891. [2000IBVS.4891....1S]

Skiff, 2000d : B. A. Skiff, 2000, "Photometry of Stars in the Field of CI Cygni", *Int. Bull. Var. Stars* 4892. [2000IBVS.4892....1S]

Skiff, 2000e : B. A. Skiff, 2000, "Photometry of Stars in the Field of AP Pegasi", *Int. Bull. Var. Stars* 4893. [2000IBVS.4893....1S]

Skiff, 2000f : B. A. Skiff, 2000, "Photometry of Stars in the Field of CQ Tauri", *Int. Bull. Var. Stars* 4894. [2000IBVS.4894....1S]

Skiff, 2012 : B. A. Skiff, personal communication, e-mail dated 2012 June 21.

Skiff and Williams, 1997 : B. A. Skiff and G. V. Williams, 1997, "Identification of Dahlmark Variables: I", *Int. Bull. Var. Stars* 4448. [1997IBVS.4448....1S]

Skrutskie *et al.*, 2006 : M. F. Skrutskie, R. M. Cutri, R. Stiening, M. D. Weinberg, S. Schneider, J. M. Carpenter, C. Beichman, R. Capps, T. Chester, J. Elias, J. Huchra, J. Liebert, C. Lonsdale, D. G. Monet, S. Price, P. Seitzer, T. Jarrett, J. D. Kirkpatrick, J. Gizis, E. Howard, T. Evans, J. Fowler, L. Fullmer, R. Hurt, R. Light, E. L. Kopan, K. A. Marsh, H. L. McCallon, R. Tam, S. Van Dyk and S. Wheelock, 2006, "The Two Micron Sky Survey (2MASS)", *Astron. J.* **131**, 1163–1183. [2006AJ....131.1163S]

Slivan and Binzel, 1996 : S. M. Slivan and R. P. Binzel, 1996, "Forty-Eight New Rotation Lightcurves of 12 Koronis Family Asteroids", *Icarus* **124**, 452–470. [1996Icar..124..452S]

Slivan *et al.*, 2003 : S. M. Slivan, R. P. Binzel, L. D. Crespo de Silva, M. Kaasalainen, M. M. Lyndaker and M. Krčo, 2003, "Spin Vectors in the Koronis Family: Comprehensive Results From Two Independent Analyses of 213 Rotation Lightcurves", *Icarus* **162**, 285–307. [2003Icar..162..285S]

Slivan *et al.*, 2008 : S. M. Slivan, R. P. Binzel, S. C. Boroumand, M. W. Pan, C. M. Simpson, J. T. Tanabe, R. M. Villastrigo, L. L. Yen, R. P. Ditteon, D. P. Pray and R. D. Stephens, 2008, "Rotation Rates in the Koronis Family, Complete to H≈11.2", *Icarus* **195**, 226–276. [2008Icar..195..226S]

Slivan *et al.*, 2009 : S. M. Slivan, R. P. Binzel, M. Kaasalainen, A. N. Hock, A. J. Klesman, L. J. Eckelman and R. D. Stephens, 2009, "Spin Vectors in the Koronis Family II. Additional Clustered Spins, and One Stray", *Icarus* **200**, 514–530. [2009Icar..200..514S]

Snodgrass *et al.*, 2010 : C. Snodgrass, B. Carry, C. Dumas and O. Hainaut, 2010, "Characterisation of Candidate Members of (136108) Haumea's Family", *Astron. Astrophys.* **511**, A72. [2010A&A...511A..72S]

Spahr, 1998 : T. B. Spahr, 1998, *Determining the Orbital Element and Absolute Magnitude Distribution of Main Belt Asteroids*, PhD thesis, University of Florida. [1998PhDT.....20S]

Spahr and Williams, 2009 : T. B. Spahr and G. V. Williams, 2009, "Minor Planet Center Activities in the Next Generation of Search Programs", submitted to 2009 IAA Planetary Defense Conference proceedings.

Stampfer, 1851 : S. Stampfer, 1851, "Über die kleinen Planeten zwischen Mars und Jupiter" ["On the Minor Planets Between Mars and Jupiter"], *Sitzungs. Wiener Akad. Wissenschaften* **7**, 756–776. [1851SKAWM...7..756S]

Standish and Hellings, 1989 : E. M. Standish and R. W. Hellings, 1989, "A Determination of the Masses of Ceres, Pallas, and Vesta From Their Perturbations Upon the Orbit of Mars", *Icarus* **80**, 326–333. [1989Icar...80..326S]

Stanzel and Schober, 1980 : R. Stanzel and H. J. Schober, 1980, "The Asteroids 118 Peitho and 952 Caia: Rotation Periods and Lightcurves from Photoelectric Observations", *Astron. Astrophys. Suppl.* **39**, 3–5. [1980A&AS...39....3S]

Stecher *et al.*, 2008 : G. Stecher, L. Ford, K. Lorenzen and S. Ulrich, 2008, "Photometric Measurements of 1084 Tamariwa at Hobbs Observatory", *Minor Planet Bull.* **35**, 76–77. [2008MPBu...35...76S]

Stephens and Warner, 2004 : R. D. Stephens and B. D. Warner, 2004, "Lightcurve Analysis of Koronis Family Asteroid 1635 Bohrmann", *Minor Planet Bull.* **31**, 3–4. [2004MPBu...31....3S]

Stephens *et al.*, 2010 : R. D. Stephens, B. D. Warner and A. W. Harris, 2010, "A Proposed Standard for Reporting Asteroid Lightcurve Data", *Bull. Amer. Astron. Soc.* **42**, 1035. [2010DPS....42.3914S]

Stevenson *et al.*, 2012 : R. Stevenson, E. A. Kramer, J. M. Bauer, J. R. Masiero and A. K. Mainzer, 2012, "Characterization of Active Main Belt Object P/2012 F5 (Gibbs): A Possible Impacted Asteroid", *Astrophys. J.* **759**, 142. [2012ApJ...759..142S]

Stokes *et al.*, 2000 : G. H. Stokes, J. B. Evans, H. E. M. Viggh, F. C. Shelly and E. C. Pearce, 2000, "Lincoln Near-Earth Asteroid Program (LINEAR)", *Icarus* **148**, 21–28. [2000Icar..148...21S]

Stone, 2000 : R. C. Stone, 2000, "Accurate FASTT Positions and Magnitudes of Asteroid: 1997–1999 Observations", *Astron. J.* **120**, 2708–2720. [2000AJ....120.2708S]

Struve, 1837 : F. G. W. Struve, 1837, *Stellarum duplicum et multiplicum mensurae micrometricae* [*Micrometric Measures of Double and Multiple Stars*].

Stuart, 2008 : J. S. Stuart, 2008, personal communication, e-mail dated 2008 Nov. 13.

Stuart, 2009 : J. S. Stuart, 2009, personal communication, e-mail dated 2009 May 22.

Stuart, 2012 : J. S. Stuart, 2012, personal communication, e-mail dated 2012 Feb. 10.

Suntzeff *et al.*, 1988 : N. B. Suntzeff, R. P. Kraft and T. D. Kinman, 1988, "Spectroscopy and Photometry of Giant Stars in NGC 2419 and Other Metal-Poor Halo Clusters", *Astron. J.* **95**, 91–105. [1988AJ.....95...91S]

Surdej and Surdej, 1977 : A. Surdej and J. Surdej, 1977, "Rotation Period and Photoelectric Lightcurves of Asteroid 471 Papagena", *Astron. Astrophys. Suppl.* **30**, 121–124. [1977A&AS...30..121S]

Surdej *et al.*, 1983a : J. Surdej, A. Surdej and B. Louis, 1983, "*UBV* Photometry of the Minor Planets 86 Semele, 521 Brixia, 53 Kalypso and 113 Amalthea", *Astron. Astrophys. Suppl.* **52**, 203–211. [1983A&AS...52..203S]

Surdej *et al.*, 1983b : J. Surdej, B. Louis, N. Cramer, F. Rufener, C. Waelkens, R. Barbier and P. V. Birch, 1983, "Photoelectric Lightcurves and Rotation Period of the Minor Planet 201 Penelope", *Astron. Astrophys. Suppl.* **54**, 371–378. [1983A&AS...54..371S]

Sykes *et al.*, 2000 : M. V. Sykes, R, M. Cutri, J. W. Fowler, D. J. Tholen, M. F. Skrutskie, S. Price and E. F. Tedesco, 2000, "The 2MASS Asteroid and Comet Survey", *Icarus* **146**, 161–175. [2000Icar..146..161S]

Taylor *et al.*, 1971 : R. C. Taylor, T. Gehrels and A. B. Silvester, 1971, "Minor Planets and Related Object: VI. Asteroid (110) Lydia", *Astron. J.* **76**, 141–146. [1971AJ.....76..141T]

Tedesco, 1975 : E. Tedesco, 1975, "*UBV* Mean Colors", EAR-A-5-DDR-UBV-MEAN-VALUES-V1.2. [2005PDSS...30.....T]

Tedesco and Marsden, 1986 : E. Tedesco and B. G. Marsden, 1986, "Magnitude Parameters For The Numbered Minor Planets", *Minor Planet Circ.* 11095–11108. [1986MPC..11095...2T]

Tedesco *et al.*, 1983a : E. F. Tedesco, R. C. Taylor, J. Drummond, D. Harwood, I. Nickoloff, F. Scaltriti, H. J. Schober and V. Zappalà, 1983, "Worldwide Photometry and Lightcurve Observations of 1 Ceres", *Icarus* **54**, 23–29. [1983Icar...54...23T]

Tedesco *et al.*, 1983b : E. F. Tedesco, R. C. Taylor, J. Drummond, D. Harweood, I. Nickoloff, F. Scaltriti and V. Zappalà, 1983, "Worldwide Photometry and Lightcurve Observations of 16 Psyche during the 1975–1976 Apparition", *Icarus* **54**, 30–37. [1983Icar...54...30T]

Tedesco *et al.*, 1990 : E. Tedesco, B. G. Marsden and G. V. Williams, 1990, "Magnitude Parameters For The Numbered Minor Planets", *Minor Planet Circ.* 17256–17273. [1990MPC..17256...2T]

Tedesco *et al.*, 1992 : E. F. Tedesco, G. J. Veeder, J. W. Fowler and J. R. Chillemi, 1992, "The IRAS Minor Planet Survey", Phillipps Lab., Hanscom AFB, PL-TR-92-2049. [1992imps.rept.....T]

Tedesco *et al.*, 1996 : E. Tedesco, G. V. Williams, D. J. Tholen and A. W. Harris, 1996, "Magnitude Parameters For The Numbered Minor Planets", *Minor Planet Circ.* 28103–28116. [1996MPC..28103...1T]

Tedesco *et al.*, 2002 : E. F. Tedesco, P. V. Noah, M. Noah and S. D. Price, 2002, "The Supplemental IRAS Minor Planet Survey", *Astron. J.* **123**, 1056–1085. [2002AJ....123.1056T]

Tholen, 1984 : D. J. Tholen, 1984, *Asteroid Taxonomy from Cluster Analysis of Photometry*, PhD Thesis, University of Arizona. [1984PhDT.....3T]

Tholen and Barucci, 1989 : D. J. Tholen and M. A. Barucci, 1989, "Asteroid Taxonomy", in *Asteroids II*, 298–315. [1989aste.conf..298T]

Tholen *et al.*, 1988 : D. J. Tholen, W. K. Hartmann, D. P. Cruikshank, S. Lilly, E. Bowell and A. Hewitt, 1988, "(2060) Chiron", *Int. Astron. Union Circ.* 4554, 2. [1988IAUC.4554....2T]

Thomas *et al.*, 2011 : C. A. Thomas, D. E. Trilling, J. P. Emery, M. Mueller, J. L. Hora, L. A. M. Benner, B. Bhattacharya, W. F. Bottke, S. Chesley, M. Delbó, G. Fazio, A. W. Harris, A. Mainzer, M. Mommert, A. Morbidelli, B. Penprase, H. A. Smith, T. B. Spahr and J. A. Stansberry, 2011, "ExploreNEOs. V. Average Albedo by Taxonomic Complex in the Near-Earth Asteroid Population", *Astron. J.* **142**, 85 [2011AJ....142...85T]

Trilling *et al.*, 2007 : D. E. Trilling, B. Bhattacharya, M. Blaylock, J. A. Stansberry, M. V. Sykes and L. H. Wasserman, 2007, "The Spitzer Asteroid Catalog: Albedos and Diameters of 35,000 Asteroids", *Bull. Amer. Astron. Soc.* **39**, 484. [2007DPS....39.3515T]

Trilling *et al.*, 2010 : D. E. Trilling, M. Mueller, J. L. Hora, A. W. Harris, B. Bhattacharya, W. F. Bottke, S. Chesley, M. Delbo, J. P. Emery, G. Fazio, A. Mainzer, B. Penprase, H. A. Smith, T. B. Spahr, J. A. Stansberry and C. A. Thomas, 2010, "ExploreNEOs. I. Description and First Results from the Warm Spitzer Near-Earth Object Survey", *Astron. J.* **140**, 770–784. [2010AJ....140..770T]

Tyson, 2002 : J. A. Tyson, 2002, "Large Synoptic Survey Telescope: Overview", in *Survey and Other Telescope Technologies and Discoveries, Proceedings of the SPIE* **4836**, 10–20. [2002SPIE.4836...10T]

Urban *et al.*, 1997 : S. Urban, T. Corbin and G. Wycoff, 1997, "The ACT Reference Catalogue", *Bull. Amer. Astron. Soc.* **29**, 1306. [1997AAS...191.5707U]

Usui *et al.*, 2011 : F. Usui, D. Kuroda, T. G. Müller, S. Hasegawa, M. Ishiguro, T. Ootsubo, D. Ishihara, H. Kataza, S. Takita, S. Oyabu, M. Ueno, H. Matsuhara and T. Onaka, 2011, "Asteroid Catalog Using Akari: AKARI/IRC Mid-Infrared Asteroid Survey", *Publ. Astron. Soc. Japan* **63**, 1117–1138. [2011PASJ...63.1117U]

van Houten *et al.*, 1970 : C. J. van Houten, I. van Houten-Groeneveld, P. Herget and T. Gehrels, 1970, "The Palomar-Leiden Survey of Faint Minor Planets", *Astron. Astrophys. Suppl.* **2**, 339–448. [1970A&AS....2..339V]

van Houten-Groeneveld and van Houten, 1958 : I. van Houten-Groeneveld and C. J. van Houten, 1958, "Photometric Studies of Asteroids. VII", *Astrophys. J.* **127**, 253–273. [1958ApJ...127..253V]

van Houten-Groeneveld *et al.*, 1979 : I. van Houten-Groeneveld, C. J. van Houten and V. Zappalà, 1979, "Photoelectric Observations of Seven Asteroids", *Astron. Astrophys. Suppl.* **35**, 223–232. [1979A&AS...35..223V]

Veverka *et al.*, 1994 : J. Veverka, M. Belton, K. Klaasen and C. Chapman, 1994, "Galileo's Encounter with 951 Gaspra: Overview", *Icarus* **107**, 2–17. [1994Icar..107....2V]

Veverka *et al.*, 1999 : J. Veverka, P. Thomas, A. Harch, B. Clark, J. F. Bell, B. Carcich, J. Joseph, S. Murchie, N. Izenberg, C. Chapman, W. Merline, M. Malin, L. McFadden and M. Robinson, 1999, "NEAR Encounter with Asteroid 253 Mathilde: Overview", *Icarus* **140**, 3–16. [1999Icar..140....3V]

Vogel, 1874 : H. C. Vogel, 1874, *Untersuchungen ueber die Spectra der Planeten* [*Investigation of Planetary Spectra*], 23–24, Wilhelm Engelmann, Leipzig.

Vokrouhlický *et al.*, 2003 : D. Vokrouhlický, D. Nesvorný and W. F. Bottke, 2003, "The Vector Alignments of Asteroid Spins by Thermal Torques", *Nature* **425**, 147–151. [2003Natur.425..147V]

Wainscoat *et al.*, 2012 : R. Wainscoat, R., H. Hsieh, L. Denneau, D. J. Tholen, M. Micheli, G. T. Elliott, H. Sato, L. Buzzi, H. DeVore, S. Foglia, T. Vorobjov, R. Holmes and G. V. Williams, 2012, "Comet P/2012 T1 (PANSTARRS)", *Cent. Bureau Electron. Tel.* 3252. [2012CBET.3252....1W]

Wamstecker and Sather, 1974 : W. Wamstecker and R. E. Sather, 1974, "Minor Planets and Related Objects: XVII. Five-Color Photometry of Four Asteroids", *Astron. J.* **79**, 1465–1470. [1974AJ.....79.1465W]

Warner, 2005 : B. D. Warner, 2005, *A Practical Guide to Lightcurve Photometry and Analysis*, 2nd edition.

Warner, 2007 : B. Warner, 2007, "Initial Results From a Dedicated *H-G* Project", *Minor Planet Bull.* **34**, 113–119. [2007MPBu...34..113W]

Warner *et al.*, 2006 : B. D. Warner, C. Jacques, E. Pimentel, G. Crawford, R. Behrend, A. Klotz, R. Stoss, J. Nomen and S. Sanchez, 2006, "Analysis of the Lightcurve of 1992 UY_4", *Minor Planet Bull.* **33**, 20–21. [2006MPBu...33...20W]

Warner *et al.*, 2008 : B. D. Warner, A. W. Harris, P. Pravec, R. D. Stephens, D. P. Pray, W. R. Cooney Jr., J. Gross, D. Terrell, Š. Gajdoš, A. Galád and Y. Krugly, 2008, "1453 Fennia: A Hungaria Binary", *Minor Planet Bull.* **35**, 73–74. [2008MPBu...35...73W]

Warner *et al.*, 2009 : B. D. Warner, A. W. Harris and P. Pravec, 2009, "The Asteroid Lightcurve Database", *Icarus* **202**, 134–146. [2009Icar..202..134W]

Warner *et al.*, 2011 : B. D. Warner, B. A. Skiff and K. McLelland, 2011, "Lightcurve Analysis of the Near-Earth Asteroid (154029) 2002 CY_{46}", *Minor Planet Bull.* **38**, 32–33. [2011MPBu....38...32W]

Warner, 2012a : B. D. Warner, 2012, "Asteroid Lightcurve Analysis at the Palmer Divide Observatory: 2011 September–December", *Minor Planet Bull.* **39**, 69–80. [2012MPBu...39...69W]

Warner, 2012b : B. D. Warner, 2012, "Asteroid Lightcurve Analysis at the Palmer Divide Observatory: 2011 December–2012 March", *Minor Planet Bull.* **39**, 158–167. [2012MPBu...39..158W]

Watson, 1940 : F. G. Watson, 1940, "Colors and Magnitudes of Asteroids", *Bull. Harv. Coll. Obs.* 913, 3–4. [1940BHarO.913....3W]

Weidenschilling *et al.*, 1987 : S. J. Weidenschilling, C. R. Chapman, D. R. Davis, R. Greenberg, D. H. Levy and S. Vail, 1987, "Photometric Geodesy of Main-Belt Asteroids I. Lightcurves of 26 Large, Rapid Rotators", *Icarus* **70**, 191–245. [1987Icar...70..191W]

Weidenschilling *et al.*, 1990 : S. J. Weidenschilling, C. R. Chapman, D. R. Davis, R. Greenberg, D. H. Levy, R. P. Binzel, S. M. Vail, M. Magee and D. Spaute, 1990, "Photometric Geodesy of Main-Belt Asteroids III: Additional Lightcurves", *Icarus* **86**, 402–447. [1990Icar...86..402W]

Weissman *et al.*, 2007 : P. R. Weissman, S. C. Lowry and Y.-J. Choi, 2007, "Photometric Observations of Rosetta Target Asteroid 2867 Steins", *Astron. Astrophys.* **466**, 737–742. [2007A&A...466..737W]

Williams, 1979 : J. G. Williams, 1979, "III. Proper Elements and Family Memberships of the Asteroids", in *Asteroids*, 1040–1063. [1979aste.book.1040W]

Williams, 1989 : J. G. Williams, 1989, "Asteroid Family Identifications and Proper Elements", in *Asteroids II*, 1034–1072. [1989aste.conf.1034W]

Williams, 1992 : G .V. Williams, 1992, "The Mass of (1) Ceres From Perturbations on (348) May", in *Asteroids, Comets, Meteors 1991*, 641–643. [1992acm..proc..641W]

Williams, 1997 : G. V. Williams, 1997, "Astronomical Unit", in *Encyclopedia of Planetary Sciences*, 48 & 50–51, Chapman & Hall, London.

Williams, 2012a : G. V. Williams, 2012, "Yearly Breakdown of Observations", `http://www.minorplanetcenter.net/iau/special/CountObsByYear.txt`, examined 2012 May 29.

Williams, 2012b : G V. Williams, 2012, "Correcting the Astrophotometry: A Status Report", `http://www.lpi.usra.edu/meetings/acm2012/pdf/6168.pdf`

Wisniewski, 1987 : W. Z. Wisniewski, 1987, "Photometry of Six Radar Target Asteroids", *Icarus* **70**, 566–572. [1987Icar...70..566W]

Wisniewski *et al.*, 1997 : W. Z. Wisniewski, T. M. Michałowski, A. W. Harris and R. S. McMillan, 1997, "Photometric Observations of 125 Asteroids", *Icarus* **126**, 395–449. [1997Icar..126..395W]

Wolf, 1892 : M. Wolf, 1892, "Photographische Aufnahmen von kleinen Planeten" ["Photographic Images of Minor Planets"], *Astron. Nachr.* **129**, 337–342. [1892AN....129..337W]

Wolters, 2005 : S. D. Wolters, 2005, *Thermal Infrared and Optical Observations of Near-Earth Asteroids*, PhD thesis, Open University.

Wolters and Green, 2009 : S. D. Wolters and S. F. Green, 2009, "Investigation of systematic bias in radiometric diameter determination of near-Earth asteroids: the night emission simulated thermal model (NESTM)", *Mon. Not. R. Astron. Soc.* **400**, 204–218. [2009MNRAS.400..204W]

Wolters *et al.*, 2005 : S. D. Wolters, S. F. Green, N. McBride and J. K. Davies, 2005, "Optical and Thermal Infrared Observations of Six Near-Earth Asteroids in 2002", *Icarus* **175**, 92–110. [2005Icar..175...92W]

Wood and Kuiper, 1963 : H. J. Wood and G. P. Kuiper, 1963, "Photometric Studies of Asteroids", *Astrophys. J.* **137**, 1279–1285. [1963ApJ...137.1279W]

Wyatt, 2009 : W. Wyatt, 2009, personal communication, e-mail dated 2009 Sept. 15.

Ye *et al.*, 2009 : Q. Ye, L. Shi, W.-H. Ip and H.-C. Lin, 2009, "Multi-Color Photometry of 1998 BE_7", *Minor Planet Bull.* **36**, 41–42. [2009MPBu...36...41Y]

Yeomans *et al.*, 2000 : D. K. Yeomans, P. G. Antreasian, J.-P. Barriot, S. R. Chesley, D. W. Dunham, R. W. Farquhar, J. D. Giorgini, C. E. Helfrich, A. S. Konopliv, J. V. McAdams, J. K. Miller, W. M. Owen, D. J. Scheeres, P. C. Thomas, J. Veverka and B. G. Williams, 2000, "Radio Science Results During the NEAR-Shoemaker Spacecraft Rendezvous with Eros", *Science* **289**, 2085–2088. [2000Sci...289.2085Y]

Zach, 1801a : F. Zach, 1801, "Über einen zwischen Mars und Jupiter längst vermutheten, nun wahrscheinlich entdeckten neuen Hauptplaneten unseres Sonnen-Systems" ["Regarding a New Primary Planet of our Solar System Long Suspected Between Mars and Jupiter and Now Likely Discovered"], *Mon. Corr.* **3**, 592–623. [1801MCBEH...3..592Z] Translations from Cunningham (2002).

Zach, 1801b : F. Zach, 1801, "Fortgesetzte Nachrichten über den längst vermutheten neuen Haupt-Planeten unseres Sonnen-Systems" ["Continued Reports about the Long-Suspected New Primary Planet of our Solar System"], *Mon. Corr.* **4**, 558–582. [1801MCBEH...4..558Z] Translations from Cunningham (2002).

Zach, 1802 : F. Zach, 1802, "Fortgesetzte Nachrichten über den zwischen Mars und Jupiter richtig vermutheten nun wirklich entdeckten neuen Haupt-Planeten unseres Sonnen-Systems: Ceres Ferdinandea" ["Continued Reports Regarding the New Primary Planet of our Solar System Correctly Suspected Between Mars and Jupiter and now Finally Discovered: Ceres Ferdinandia"], *Mon. Corr.* **5**, 170–184. [1802MCBEH...5..170Z] Translations from Cunningham (2002).

Zacharias *et al.*, 2000 : N. Zacharias, S. E. Urban, M. I. Zacharias, D. M. Hall, G. L. Wycoff, T. J. Rafferty, M. E. Germain, E. R. Holdenried, J. W. Pohlman, F. S. Gauss, D. G. Monet and L. Winter, 2000, "The First US Naval Observatory CCD Astrograph Catalogue", *Astron. J.* **120**, 2131–2147. [2000AJ....120.2131Z]

Zacharias *et al.*, 2004a : N. Zacharias, S. E. Urban, M. I. Zacharias, G. L. Wycoff, D. M. Hall, D. G. Monet and T. J. Rafferty, 2004, "The Second US Naval Observatory CCD Astrograph Catalog (UCAC2)", *Astron. J.* **127**, 3043–3059. [2004AJ....127.3043Z]

Zacharias *et al.*, 2004b : N. Zacharias, D. G. Monet, S. E. Levine, S. E. Urban, R. Gaume and G. L. Wycoff, 2004, "The Naval Observatory Merged Astrometric Dataset (NOMAD)", *Bull. Amer. Astron. Soc.* **36**, 1418. [2004AAS...205.4815Z] See also `http://www.nofs.navy.mil/nomad/`.

Zacharias *et al.*, 2009 : N. Zacharias, C. Finch, T. Girard, N. Hambly, G. Wycoff, M. I. Zacharias, D. Castillo, T. Corbin, M. DiVittorio, S. Dutta, R. Gaume, S. Gauss, M. Germain, D. Hall, W. Hartkopf, D. Hsu, E. Holdenried, V. Makarov, M. Martines, B. Mason, D. Monet, T. Rafferty, A. Rhodes, T. Siemers, D. Smith, T. Tilleman, S. Urban, G. Wieder, L. Winter and A. Young, 2009, "The Third US Naval Observatory CCD Astrograph Catalog (UCAC3)", *Astron. J.* **139**, 2184–2199. [2010AJ....139.2184Z]

Zappalà and van Houten-Groeneveld, 1979 : V. Zappalà and I. van Houten-Groeneveld, 1979, "Pole Coordinates of the Asteroids 9 Metis, 22 Kalliope and 44 Nysa", *Icarus* **40**, 289–296. [1979Icar...40..289Z]

Zappalà *et al.*, 1979 : V. Zappalà, I. van Houten-Groeneveld and C. J. van Houten, 1979, "Rotation Period and Phase Curve of the Asteroids 349 Dembowska and 354 Eleonora", *Astron. Astrophys. Suppl.* **35**, 213–221. [1979A&AS...35..213Z]

Zappalà *et al.*, 1982 : V. Zappalà, F. Scaltriti, C.-I. Lagerkvist, H. Rickman and A. W. Harris, 1982, "Photoelectric Photometry of Asteroids 33 Polyhymnia and 386 Siegena", *Icarus* **52**, 196–201. [1982Icar...52..196Z]

Zappalà *et al.*, 1983 : V. Zappalà, F. Scaltriti and M. Di Martino, 1983, "Photoelectric Photometry of 21 Asteroids", *Icarus* **56**, 325–344. [1983Icar...56..325Z]

Zappalà *et al.*, 1989 : V. Zappalà, M. Di Martino, A. Cellino, P. Farinella, G. de Sanctis and W. Ferreri, 1989, "Rotational Properties of Outer Belt Asteroids", *Icarus* **82**, 354–368. [1989Icar...82..354Z]

Zellner, 1973 : B. Zellner, 1973, "Polarimetric Albedos of Asteroids", *Bull. Amer. Astron. Soc.* **5**, 388. [1973BAAS....5..388Z]

Zellner and Gradie, 1976 : B. Zellner and J. Gradie, 1976, "Minor Planets and Related Objects. XX. Polarimetric Evidence for the Albedos and Compositions of 94 Asteroids", *Astron. J.* **81**, 262–280. [1976AJ.....81..262Z]

Zellner *et al.*, 1975 : B. Zellner, W. Z. Wisniewski, L. Andersson and E. Bowell, 1975, "Minor Planets and Related Objects. XVIII. *UBV* Photometry and Surface Composition", *Astron. J.* **80**, 986–995. [1975AJ.....80..986Z]

Zellner *et al.*, 1977 : B. Zellner, L. Anderson and J. Gradie, 1977, "*UBV* Photometry of Small and Distant Asteroids", *Icarus* **31**, 447–455. [1977Icar...31..447Z]

Zellner *et al.*, 1985 : B. Zellner, D. J. Tholen and E. F. Tedesco, 1985, "The Eight-Color Asteroid Survey: Results for 589 Minor Planets", *Icarus* **61**, 355–416. [1985Icar...61..355Z]